RIGA TECHNICAL UNIVERSITY

Davide Ceradini

DEVELOPMENT OF SCALABLE SYNTHESIS FOR SELECTED PROTEASE uPA INHIBITORS

Doctoral Thesis

RTU Press
Riga 2023

RIGA TECHNICAL UNIVERSITY
Faculty of Materials Science and Applied Chemistry
Institute of Technology of Organic Chemistry

Davide Ceradini
Doctoral study program "Chemistry"

DEVELOPMENT OF SCALABLE SYNTHESIS FOR SELECTED SERINE PROTEASE uPA INHIBITORS

Doctoral Thesis

Supervisor
principal investigator *Dr. chem.*
KIRILL SHUBIN

Supervisor
professor *Dr. chem.*
AIGARS JIRGENSONS

Rīga 2023

Ceradini, D. Development of scalable synthesis for selected serine protease uPA inhibitors. Doctoral Thesis. Riga: RTU press, 2023. 252 p.

Published in accordance with the decision of the Promotion Council "RTU P-01" of Protocol No 04030-9.1/35.

This project has received funding from the European Union's Horizon 2020 research and innovation program under the Marie Skłodowska-Curie Initial Training Network (ITN) "ITDED3" (H2020-MSCA-ITN-2017) grant agreement no. 765608.

DOCTORAL THESIS PROPOSED TO
RIGA TECHNICAL UNIVERSITY FOR THE PROMOTION
TO THE SCIENTIFIC DEGREE OF DOCTOR OF SCIENCES

To be granted the scientific degree of Doctor of Sciences (*Ph.D.*), the present Doctoral Thesis will be defended at a public session on 13th April 2023 at the Faculty of Materials Science and Applied Chemistry of Riga Technical University, Paula Valdena Street 3, Room 272

OFFICIAL REVIEWERS

Dr. chem. Aiva Plotniece,
Latvian Institute of Organic Synthesis, Latvia

Dr. Jurgen Joossens,
University of Antwerp, Belgium

Dr. chem. Gints Šmits
Latvian Institute of Organic Synthesis, Latvia

DECLARATION OF ACADEMIC INTEGRITY

I hereby declare that the Doctoral Thesis submitted for the review to Riga Technical University for the promotion to the scientific degree of Doctor of Sciences (Ph. D.) is my own. I confirm that this Doctoral Thesis has not been submitted to any other university for the promotion to other scientific degree.

Davide Ceradini ……. (signature)

Date…….

The Doctoral thesis has been written in English. It consists of an introduction, literature review, results and discussion, experimental part, conclusion, 16 figures, 83 schemes, 45 tables, and 4 appendices. The total number of pages is 181 excluding appendices. The bibliography contains 133 titles.

ANNOTATION

Development of scalable synthesis for selected serine protease uPA inhibitors. Ceradini D., supervisor Prof. *Dr. Chem*. Jirgensons A. and *Dr. Chem.* Shubin K. Doctoral thesis, 252 pages, 16 figures, 45 tables, 83 schemes, 133 references, 4 appendices. In English

DRY EYE DISEASE, α-AMINOPHOSPHONATES, BIRUM-OLEKSYSZYN, YTTRIUM CATALYSIS, DESIGN OF EXPERIMENT, CHIRAL CARBAMATES

Dry eye disease (DED) is a widespread illness, with a prevalence ranging from 8.7 to 30.1 % of the population. Due to a limited number of therapies present on the market, development of new drugs is highly desirable. α-Aminophosphonate UAMC-00050, is a perspective lead compound for the treatment of DED. However, upscale of medicinal chemistry route for its preparation met with several problems: poor yields for some of the steps, hazardous reagents, and suboptimal environmental footprint. This doctoral thesis discuss the optimization of a multigram synthesis of UAMC-00050. In the update synthetic route, environmental unfriendly solvents were excluded and hazardous reagents were replaced with safer alternatives, more efficient in terms of atom economy. Every step was carefully studied to improve the yield and design of experiment (DoE) was used to find the optimum conditions in the last reaction. Yttrium triflate was discovered as an efficient green catalyst for the synthesis of a key intermediate through a one-pot three-component Birum–Oleksyszyn reaction. To reduce the process mass intensity, flash chromatography purifications of intermediates were substituted with alternative techniques (extraction, crystallization, antisolvent precipitation). The overall yield was increased from 3 % in the medicinal chemistry route to 22 % in the process development route. The optimized protocol was applied, with the necessary changes, for the preparation of the close analogues of UAMC-00050: UAMC-0004206 (a backup compound for UAMC-00050) and UAMC-0004207 (a compound that will be tested as proof of concept for the activity of α-amino-4-chlorophenolphosphonates). Finally, a series of chiral carbamates were prepared to test a diastereoselective Birum-Oleksyszyn reaction promoted by yttrium triflate. Various new α-aminophosphonates were synthesized with dr up to 75:25.

ANOTĀCIJA

Mērogojamas sintēzes izstrāde izvēlētiem serīna proteāzes uPA inhibitoriem. Ceradini D., vadītājs Prof. Dr. Chem. Jirgensons A. un Dr. Chem. Šubins K. Promocijas darbs, 253 lapas, 16 attēli, 45 tabulas, 83 shēmas, 133 atsauces, 4 pielikumi.

SAUSĀS ACS SINDROMS, α-AMINOFOSFONĀTI, BIRUM-OLEKSYSZYN, ITRIJA KATALĪZE, EKSPERIMENTA IZSTRĀDE, HIRĀLIE KARBAMĀTI

Sausās acs sindroms (SAS) ir plaši izplatīta slimība, kas sastopama no 8,7 līdz 30,1 % iedzīvotāju. Tā kā komerciāli ir ierobežoti daudzi terapijas veidi, jaunu zāļu izstrāde joprojām ir ļoti aktuāla. SAS ārstēšanai viena no perspektīvākajām vielām ir svinu saturošs savienojums α-aminofosfonāts UAMC-00050. Tomēr sintēzes mērogošana savienojuma iegūšanai saskarās ar vairākām problēmām: zemu iznākumu dažos sintēzes posms, bīstamiem reaģentiem un kaitīgu ietekmi uz vidi. Šajā promocijas darbā apskatīta UAMC-00050 lielapjoma sintēzes optimizācija. Optimizētajā sintēzes metodikā tika izslēgti videi kaitīgi šķīdinātāji, un bīstamie reaģenti aizstāti ar drošākām alternatīvām, kas ir efektīvāki atomu ekonomijas ziņā. Rūpīgi tika izpētīts katras sintēzes stadijas iznākums un pēdējās stadijas optimālāko apstākļus atrašanai tika izmantota eksperimenta dizaina (DoE) metodika. Kā efektīvs zaļais katalizators galvenā starpprodukta iegūšanai viena-trauka trīskomponentu (Birum - Oleksyszyn) reakcijā tika atrasts itrija triflāts. Lai samazinātu procesa masas intensitāti, starpproduktu attīrīšanu ar kolonu hromatogrāfiju aizstāja ar alternatīvām metodēm: ekstrakciju, kristalizāciju, izgulsnēšanu ar pretšķīdinātāju. Kopējais iznākums palielināts no 3 % medicīnas ķīmijas ceļā līdz 22 % procesu ķīmijas izstrādes ceļā. Nepieciešamības gadījumā veicot izmaiņas, optimizētā metodoloģija izmantota arī UAMC-00050 tuvu analogu iegūšanai: UAMC-0004206 (UAMC-00050 rezerves savienojums) un UAMC-0004207 (savienojums, kas tiks pārbaudīts kā α-amino-4-hlorfenolfosfonātu aktivitātes koncepta pierādījums). Visbeidzot tika iegūta virkne hirālu karbamātu, lai pārbaudītu itrija triflāta katalizētu diastereoselektīvo Biruma-Oleksišina reakciju. Tika iegūti dažādi jauni α-aminofosfonāti ar diastereomēru attiecību līdz 75:25.

Abbreviations

ABNO	9-Azabicyclo[3.3.1]nonane *N*-oxyl
ABP	Activity based probe
Ac	Acetyl
AN	Area normalized
BINOL	1,1′-Bi-2-naphthol
Boc	*tert*-Butyloxycarbonyl
Bpy	2,2′-Bipyridine
Bn	Benzyl
Bu	Butyl
Bz	Benzoyl
CAN	Ceric ammonium nitrate
Cbz	Benzyl carbamate
CD	Cluster of differentiation
cPent	cyclopentyl
CV	Column volume
Cy	cyclohexyl
DABCO	1,4-Diazabicyclo[2.2.2]octane
DBAD	Di-*tert*-butyl azodicarboxylate
DBED	*N*,*N*′-Dibenzylethylenediamine
DCM	Dichloromethane
DED	Dry eye disease
DIPEA	*N*,*N*-Diisopropylethylamine
DMAP	4-Dimethylaminopyridine
DMF	Dimethylformamide
DMP	Dess-Martin periodinane
DMSO	Dimethyl sulfoxide
DyPB	Dysprosium potassium BINOL complex
EDG	Electron donating group
Et	Ethyl
EWG	Electron withdrawing group
FDA	Food and Drug Administration
FMOC	Fluorenylmethyloxycarbonyl
GdPB	Gadolinium potassium BINOL complex
HPA	Heteropoly acid
HPLC	High Performance Liquid Chromatography
iPr	*iso*-Propyl
IS	Internal standard

LC-MS	Liquid Chromatography Mass Spectrometry
LMB	Lanthanoid metal BINOL complex
LLB	Lanthanoid lithium BINOL complex
LSB	Lanthanoid sodium BINOL complex
LPB	Lanthanoid potassium BINOL complex
m-CPBA	*meta*-Chloroperoxybenzoic acid
Me	Methyl
^{MeO}bpy	4-4′-Dimethoxy-2-2′-bipyridine
MCF7	Michigan Cancer Foundation-7
MMP	Matrix metalloproteinase
MTBE	Methyl *tert*-butyl ether
MS	Molecular sieve
NBS	*N*-Bromosuccinimide
NMI	1-Methylimidazole
NMP	*N*-Methyl-2-pyrrolidone
NMR	Nuclear magnetic resonance
NTf_2	Bistriflymide
OTf	Triflate
PIDA	Phenyliodine(III) diacetate
PIPO	Polymer-immobilized TEMPO derivative
PMA	Phosphomolybdic acid
PMI	Process mass intensity
Ph	Phenyl
Pr	Propyl
PrPB	Praseodymium potassium BINOL complex
PTC	Phase transfer catalyst
RP	Reverse phase
RSM	Response surface model
SmPB	Samarium potassium BINOL complex
STT	Spinning tube-in-tube
TADDOL	α,α,α',α'-Tetraaryl-2,2-disubstituted 1,3-dioxolane-4,5-dimethanol
TBHP	*tert*-Butyl hydroperoxide
TBOx	Tethered bis(8-quinolinolato)
TEA	Triethylamine
TEMPO	(2,2,6,6-Tetramethylpiperidin-1-yl)oxyl
TFA	Trifluoroacetic acid
TFAA	Trifluoroacetic anhydride
THF	Tetrahydrofuran
TNF-α	Tumor necrosis factor

TNT	Trititanate nanotube
TOF	Turnover frequency
TRIP	3,3′-Bis(2,4,6-triisopropylphenyl)-1,1′-binaphthyl-2,2′-diyl hydrogenphosphate
UAMC	University of Antwerp medicinal chemistry
uPA	Urokinase plasminogen activator
YbPB	Ytterbium potassium BINOL complex
ZIF	Zeolitic imidazolate framework

Contents

1 INTRODUCTION 12
1.1 Actuality of the topic 13
1.2 Aims and objective 14
1.2.1 Overall goal of the thesis 14
1.2.2 Task of the thesis 15
1.2.3 Scientific significance and novelty 15
1.2.4 Practical significance 16
1.2.5 Main thesis to defend 16
1.2.6 Structure and volume of the thesis 17
1.2.7 Approbation of the thesis 17
2 LITERATURE REVIEW 19
2.1 One-pot preparation of α-aminophosphonates 19
2.1.1 Metal salts, oxides and heteropolymetalates as catalyst for the one-pot three-component preparation of α-aminophosphonates 20
2.1.2 Two-component synthesis of α-aminophosphonates from aminals 28
2.1.3 Selection of Lewis acids and additives for the improvement of the Birum-Oleksyszyn step 29
2.2 Enantioselective synthesis of α-aminophosphonates 29
2.2.1 Catalysis by chiral metal complexes 30
2.2.2 Catalysis by chiral phosphoric acids 37
2.2.3 Catalysis by Cinchona alkaloids and Cinchona-derived organocatalysts 40
2.2.4 Catalysis by chiral thioureas 44
2.2.5 Catalysis by proline derivatives 47
2.2.6 Synthesis with chiral auxiliaries 47
2.2.7 Selection of stereoselective protocol for the preparation of UAMC-00050 53
2.3 Green Chemistry approach to the synthesis of the key aldehyde 53
2.3.1 Oxidation with O_2 or Air 54
2.3.2 Oxidation with H_2O_2 58
2.3.3 Synthesis of aldehydes promoted by NaClO 61
2.3.4 Selection of oxidation protocol for the optimization of the route to UAMC-0005064
3 RESULTS AND DISCUSSION 65
3.1 Process Development UAMC-00050 66

3.1.1 Preparation of triaryl phosphite 3 66
3.1.2 Boc-Protection of the amine group in aniline 4 67
3.1.3 Preparation of aldehyde 7 68
3.1.4 Birum-Oleksyszyn reaction 70
3.1.5 *N*-Boc deprotection of intermediate 9 81
3.1.6 Guanylation of intermediate 178 82
3.1.7 Purification of UAMC-00050 88
3.1.8 Process development route to UAMC-00050 92
3.1.9 Scope of $Y(OTf)_3$-catalyzed Birum-Oleksyszyn reaction 93
3.1.10 Yttrium-catalyzed Birum-Oleksyszyn reaction for the preparation of phosphonolactones 96
3.2 Activity-based probe and α-aminophosphonates selectivity 98
3.3 Process optimization and preparation of UAMC-0004206 100
3.3.1 Route selection of UAMC-0004206 100
3.3.2 Birum-Oleksyszyn synthesis of intermediate 160 101
3.3.3 *N*-Boc deprotection of intermediate 193 104
3.3.4 Guanylation of intermediate 194 and 195 105
3.3.5 *N*-Boc deprotection of intermediate 196 107
3.3.6 Salt exchange of intermediate 197 108
3.4 Process development of UAMC-0004207 109
3.4.1 Route selection for UAMC-0004207 109
3.4.2 Birum-Oleksyszyn reaction 110
3.4.3 *N*-Boc deprotection of intermediate 206 113
3.4.4 Guanylation of intermediate 212 114
3.4.5 *N*-Boc deprotection of guanidine 209 116
3.5 Stereoselective preparation of UAMC-00050 117
3.5.1 Separation of enantiomers, screening of conditions and scale-up 117
3.5.2 Enantiomers 1 and 2 *in vitro* test on uPA enzyme 121
3.5.3 Catalysis of Birum-Oleksyszyn reaction with a chiral metal complex 122
3.5.4 Diastereoselective synthesis of α-aminophosphonates 123
4 EXPERIMENTAL PART 141
4.1 General information 141
4.2 Compounds synthesized for the preparation of UAMC-00050 141

4.3 Compounds prepared for the scope Birum-Oleksyszyn reaction 147
4.4 Compounds synthesized for the preparation of UAMC-0004206 158
4.5 Compounds synthesized for the preparation of UAMC-0004207 160
4.6 Compounds prepared for the stereoselective synthesis of α-aminophosphonates 163
5 CONCLUSIONS 167
6 REFERENCES 170
7 Appendix I 181
8 Appendix II 235
9 Appendix III 245
10 Appendix IV 249

1 INTRODUCTION

Dry eye disease (DED) also known as *keratoconjunctivitis sicca* is a multifactorial disease of the ocular surface[1] that affects hundreds of millions of people around the world.[2] Risk factors for the development of DED include advanced age, female sex, hormonal imbalance, autoimmune disease, abnormal corneal innervation, vitamin deficiency, environmental stress, contact lens use, infection, medication use, and ophthalmic surgery.[3] The disease is characterized by a dry, gritty, or burning feeling in the eye, as well as excessive tearing and photosensitivity.[4] DED is an inflammatory disease that involves both metabolic and immune dysregulation. An increasing osmolarity in the tear film can induce oxidative conditions at the ocular surface which activates a pathological cascade. Recently, a new biologically active α-aminophosphonate, (UAMC-00050, product **1**, Scheme 1.1) was developed at the University of Antwerp as a drug lead for the treatment of DED.[5,6] The molecule is a peptidic diphenyl phosphonate serine protease inhibitor which forms a covalent bond with the serine side chain hydroxyl group, at the active site of an enzyme. The selectivity profile of this type of compounds is usually enforced by incorporating peptidic tails. In contrast, Joossens *et al.* demonstrated that a potent and selective inhibition can also be achieved with small, non-peptidic diphenyl phosphonates. The diarylphosphonate UAMC-00050 shows good inhibitory activity against urokinase plasminogen activator (uPA) and other trypsin-like serine proteases, which are involved in eye diseases. Animals treated with UAMC‑00050 displayed a significant reduction in ocular surface damage after evaluation with sodium fluorescein, compared to untreated, vehicle-treated, and cyclosporine-treated animals. The concentrations of IL1α and TNFα were also significantly reduced in tear fluid from UAMC-00050 treated rats. Additionally, the inflammatory cell infiltration in the palpebral conjunctiva (CD3 and CD45), was substantially reduced. An accumulation of pro-MMP9 and a decrease in active MMP9 were found in tear fluid from animals treated with UAMC−00050, suggesting that trypsin‑like serine proteases play a role in activating MMP9 in ocular inflammation in this animal model. The medicinal chemistry route for the preparation of UAMC-00050 starts from the commercially available 4-aminophenethyl alcohol (**4**). After the protection of the amine with Boc_2O in the presence of triethylamine (TEA), alcohol **6** is oxidized to aldehyde **7** with Dess-Martin periodinane (DMP). The molecule's core (**9**) is built by a one-pot three-component Birum-Oleksyszyn reaction between aldehyde **6**, benzyl carbamate (**8**) and phosphite **3**, using copper triflate as a catalyst.[7–9] Triarylphosphite **3** was prepared from paracetamol (**2**) and used as a crude product. Then the Boc group was removed in TFA/DCM (1:1 v/v) to generate salt **9**. The guanidine moiety was inserted using *N*,*N*′-di-Boc-1*H*-pyrazole-1-carboxamidine (**10**), the two Boc groups were removed with TFA/DCM 1:1 v/v and the trifluoroacetate counterion was ion exchanged with chloride after stirring compound **12** with a DOWEX 1X8 Cl resin to get **1** (Scheme 1.1).[6]

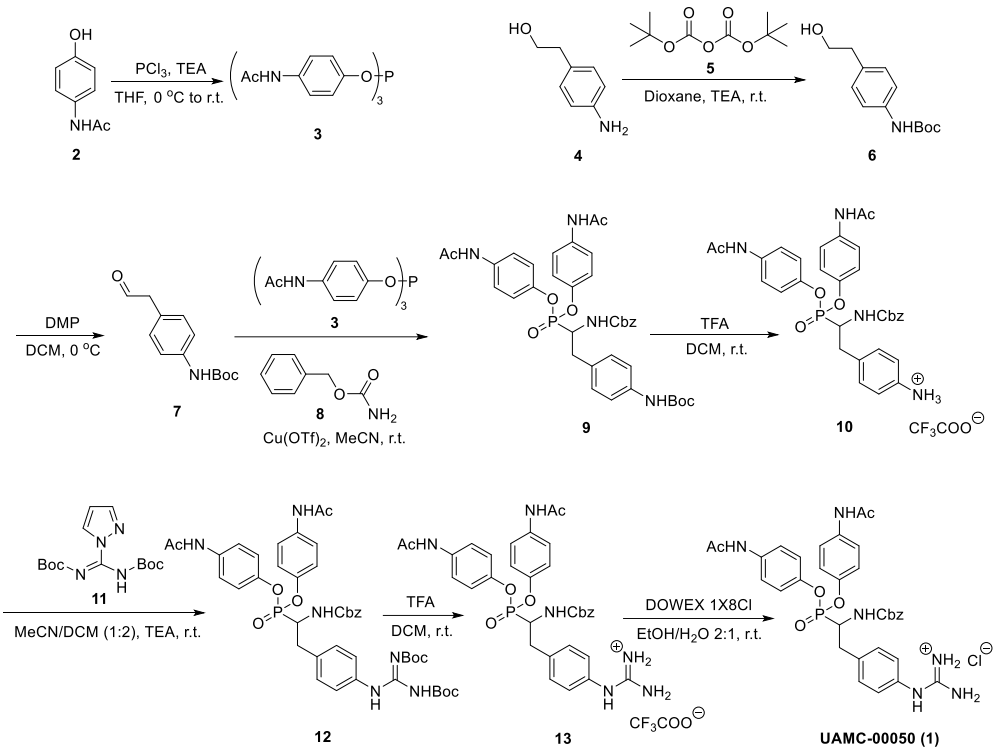

Scheme 1.1. Medicinal chemistry route of UAMC-00050

1.1 Actuality of the topic

DED, as a combination of symptoms and signs, has an overall prevalence ranging from 8.7 to 30.1 %.[2] The incidence of DED has also been reported growing, in a Caucasian population, aged between 48 and 91 years, 13.3 % of individuals developed symptomatic DED over 5 years and 21.6 % over 10 years.[10] Artificial tears are the most common treatment for DED patients, however, despite providing immediate relief, they do not possess any anti-inflammatory properties. On the other hand, topical application on the eye surface of cyclosporine A (Restasis) showed a reduction of the inflammatory signs in the eye, however, some patients show incomplete response to cyclosporine A or significant side effects. Corticosteroids are also used to decrease inflammation of the eye surface, but they can be employed only for a short amount of time due to their several adverse effects. Recently, the small molecule Lifitegrast (Xiidra) was approved by FDA for the treatment of *keratoconjunctivitis sicca.* The new compound showed promising results in randomized clinical trials. With just one drug developed exclusively for DED, there is a necessity

for further studies to find an alternative to Lifitegrast which may possess a better efficacy in the treatment of DED. Serine proteases play a role in the development of DED signs and symptoms by promoting inflammatory protein expression and have a direct influence on the degradation of extracellular matrix component. Investigation and development of serine protease inhibitors represent a good change to provide and efficient alternative to patients with DED.

1.2 Aims and objective

1.2.1 Overall goal of the thesis

The main goal of this thesis is to develop a scalable synthesis of the α-aminophosphonate UAMC-00050. The new route must provide the final material with a higher yield than the medicinal chemistry route, which suffers from a poor overall yield (3 %). In particular, to develop a practical synthesis of UAMC-00050, the Birum-Oleksyszyn step represented a bottleneck for the overall yield and purity of the final material. Optimization work was necessary to prepare phosphite **3** due to its high reactivity with oxygen and water. Purity of **3** was important to curb the generation of side products in the Birum-Oleksyszyn step. For the preparation of aldehyde **7,** we seek to remove the Dess-Martin periodinane (DMP) as oxidizing agent due to its low atom economy and its oxidant sensitiveness.[11] To reduce the costs, alternatives to *N*,*N*′-di-Boc-1*H*-pyrazole-1-carboxamidine (**11**) were explored for the formation of guanidine moiety in compound **12**. To lower the process mass intensity (PMI), alternatives to flash chromatography in the purification of the intermediates were developed. As a secondary goal, we aimed to provide 3 - 5 g of the α-aminophosphonates UAMC-0004206 (**14**) which was planned to be used as a follow-up inhibitor of UAMC-00050 and UAMC-0004207 (**15**) which was used to investigate the activity of 4-chloro-substituted-phosphonate derivatives (Figure 1.1). Furthermore, we aimed to perform the separation of the two enantiomers of UAMC-00050 (**1**) to determine the biological activity of the isomers. As a part of this endeavor we attempted to develop a new enantioselective and diastereoselective method for the synthesis of α-aminophosphonates.

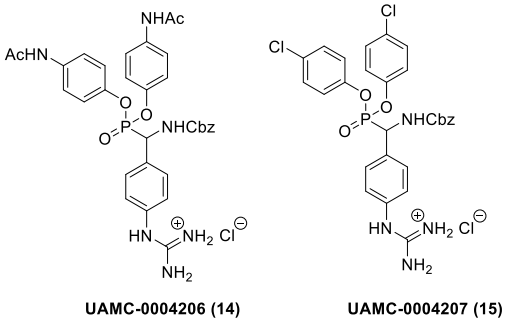

Figure 1.1. Structure of UAMC-0004206 and UAMC-0004207

1.2.2 Task of the thesis

The thesis' task can be summarized in the following points:

1. Develop a new synthetic route for the preparation of UAMC-00050 considering, overall yield, safety, environmental footprint, and cost. Target purity > 98 %.

2. Provide 2 - 5 grams of selected α-aminophosphonates UAMC-0004206 (**14**) and UAMC-0004207 (**15**). Target purity > 95 %.

3. Separate two enantiomers of UAMC-00050 in order to understand if the two stereoisomers possess different inhibitory activity against uPA.

4. Investigate enantioselective or diastereoselective synthesis of α-aminophosphonates which can be later applied to the preparation of UAMC-00050.

1.2.3 Scientific significance and novelty

In this work, a new optimized route for the preparation of UAMC-00050 was developed. The overall yield was increased from 3 to 22 %. Dichloromethane (DCM) was completely removed from the process. The Anelli-Montanari protocol with NaClO/TEMPO was successfully used as an alternative to DMP for oxidation of the alcohol, increasing the safety and the atom economy of the process. A large part of our work was spent on the optimization of the Birum-Oleksyszyn step. After a screen of catalyst yttrium triflate, employed for the first time in this reaction, was found to provide a higher yield than was then further increased using trifluoroacetic anhydride (TFAA) as an additive and the mixture of THF/MeCN 1:1 v/v as reaction medium. The expensive reagent,

N,*N*′-Di-Boc-1*H*-pyrazole-1-carboxamidine was substituted with the cheaper cyanamide for the guanylation reaction and a design of experiment approach was used to find the optimum conditions. α-Aminophosphonates UAMC-0004206 (**14**) and UAMC-0004207 (**15**) were prepared for the first time using a combination of the newly developed route and the old medicinal chemistry route of UAMC-00050. The two enantiomers of UAMC-00050 were isolated and tested, and a 10-fold difference in activity was found between the two enantiomers. Finally, stereoselective synthesis of α-aminophosphonates employing chiral carbamates was investigated. The highest enantioselectivity reached for the product **16** synthesis was modest (Figure 1.2).

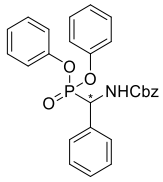

16

Figure 1.2. Structure of model compound **16** used to test the efficacy of the stereoselective preparation of α-aminophosphonate with chiral carbamate.

1.2.4 Practical significance

The work provided a new protocol for the preparation of UAMC-00050 which can be safely and easily reproduced to prepare several grams of the drug substance in a short time. The process represents also a good starting point for a multigram upscale and GMP production. Newly prepared α-aminophosphonates UAMC-0004206 and UAMC-0004207 were tested *in vitro*, both compounds showed a better selectivity against uPA, *versus* Cat G, trypsin, thrombin, and tryptase. The two enantiomers of UAMC-00050 were separated and tested in vitro. Since the using enantiopure UAMC-00050 did not increase dramatically the activity it was decided to proceed with the development of UAMC-00050 as a racemic mixture.

1.2.5 Main thesis to defend

The newly developed route to UAMC-00050 is more effective in terms of yield, it is safer and has a lower impact on the environment. The reduced solvent and silica consumption, and the lower cost of the reagents made the new process cheaper than the medicinal chemistry route.

1.2.6 Structure and volume of the thesis

The thesis comprises five main chapters: introduction, literature review, result and discussion, conclusion, and experimental part. In the introduction, we state the nature of the disease, the discovery and biological properties of UAMC-00050, the problems of the medicinal chemistry route and the necessity of a stereoselective preparation of UAMC-00050. The literature review is divided into three parts. In the first two parts, we report examples of the Birum-Oleksyszyn reaction and the catalytic oxidation of the alcohol while in the third part we report a series of strategies to obtain chiral α-aminophosphonates. The results and discussion represent chapter 3, which is divided in five sections. 3.1 Process optimization of UAMC-00050, 3.2 activity-based probes, 3.3 process optimization of UAMC-0004206, 3.4 process optimization of UAMC-0004207 and 3.5 stereoselective preparation of UAMC-00050. The thesis has been written in English and it consists of 252 pages, 45 tables, 83 schemes, 16 figures, 133 references, and 3 appendices.

1.2.7 Approbation of the thesis

The results of the present thesis are discussed in 4 scientific papers and 3 international conferences

Articles:

1. Ceradini, D., Shubin, K. One-pot synthesis of α-aminophosphonates by yttrium-catalyzed Birum–Oleksyszyn reaction *RSC Adv*., **2021**, 11, 39147-39152. doi.org/10.1039/D1RA07718J

2. Ceradini, D., Shubin, K. New methods for the synthesis of phosphono-δ-lactones (microreview). *Chem Heterocycl Comp*, **2021**, 57, 1167-1169. doi.org/10.1007/s10593-021-03038-7

3. Ceradini, D., Cacivkins, P., Ramos-Llorca, A., Shubin, K. Improved Synthesis of the Selected Serine Protease uPA Inhibitor UAMC-00050, a Lead Compound for the Treatment of Dry Eye Disease. *OPRD*, **2022**, 26, 10, 2937-2946. doi.org/10.1021/acs.oprd.2c00244

4. Ramos-Llorca, A.; Decraecker, L.; Cacheux, V. M. Y.; Zeiburlina, I.; De bruyn, M.; Battut, L.; Moreno-Cinos, C.; Ceradini, D.; Espinosa, E.; Dietrich, G.; Berg, M.; De Meester, I.; Van Der Veken, P.; Boeckxstaens, G.; Lambeir, A.-M.; Denadai-Souza, A.; Augustyns, K. Chemically Diverse Activity-Based Probes with Unexpected Inhibitory Mechanisms Targeting Trypsin-like Serine Proteases. *Frontiers in Chemistry*, **2023**, 10. doi.org/10.3389/fchem.2022.1089959 (*in press*)

Conferences:

1. Ceradini, D. Process optimization of the synthesis of UAMC-00050, a novel uPA inhibitor. *XXVI EFMC International Symposium on Medicinal Chemistry (EFMC-ISMC 2021).* Online August 29th – September 2nd **2021**.

2. Ceradini, D. Process optimization of the synthesis of UAMC-00050, a novel uPA inhibitor. *12th Paul Walden Symposium on Organic Chemistry.* Online, 28-29th October **2021.**

3. Ceradini, D. Upscaling of lead compounds from WP1 and enantioselective synthesis of the serine protease inhibitor UAMC-00050. *Symposium DRY EYE DISEASE IT-DED³ Consortium Meeting*. Paris, France, 2nd-3rd December **2021**.

2 LITERATURE REVIEW

2.1 One-pot preparation of α-aminophosphonates

In general, there are several strategies for the synthesis of α-aminophosphonates. Extensive reviews on the preparation of α-aminophosphonates were written by Varga *et al.*[12], Shastri *et al.*[13] and Sravya *et al.*[14] with a focus on the Kabachnik-Fields reaction while Macarie and coworkers[15] published a review focusing on the synthesis of α-aminophosphonates with ultrasonic irradiation. Herein we have summarized a brief description of four common reactions to access α-aminophosphonates (Scheme 2.1). In the Michaelis-Arbuzov reaction, the α-aminophosphonates are formed after a reaction between alkyl halides **17** and a trivalent phosphorous ester **18**.[16] In the Pudovik reaction the α-aminophosphonate **19** is generated from an imine **20** and a phosphite diester **18**.[17] The Kabachnik-Fields reaction involves a one-pot three-component reaction between an aldehyde **21**, an amine **22** and a phosphite diester **18**.[18] When a carbamate **23** reacts with an aldehyde **21** and a phosphite triester **24** the reaction is named Birum-Oleksyszyn.[9] Nowadays the one-pot three-component condensation between aldehyde, amine and phosphite, catalyzed by acid (Kabachnik-Fields or Birum-Oleksyszyn), is the most common synthetic method for α-aminophosphonates due to the simplicity and the general good yield.[19] The use of a Lewis acid, as the catalyst, instead of a Brønsted acids was reported for the first time in 1973 by Birum.[8] Unfortunately, only a few papers described the synthesis of diaryl esters of α-aminophosphonates, since dialkyl esters are more frequently used. The advantage of Lewis acids is to allow the use of acid-sensitive functional groups, that otherwise would be degraded in the typical conditions with glacial acetic acid. In the next sections, we will report a series of reactions that were considered during the process development to find a better catalyst for the preparation of the UAMC-00050 intermediate **9**.

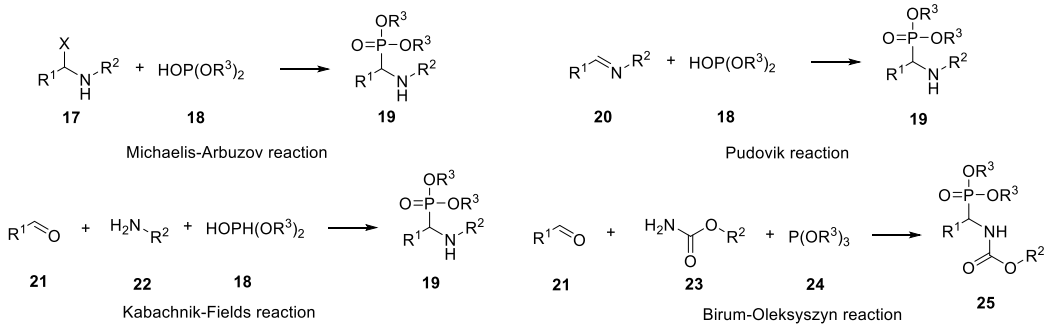

Scheme 2.1. Four different pathways to access the structure of α-aminophosphonates

2.1.1 Metal salts, oxides and heteropolymetalates as catalyst for the one-pot three-component preparation of α-aminophosphonates

α-Aminophosphonates were prepared in good yields using a Lewis acid catalyzed Birum–Oleksyszyn reaction.[9] The method presented by Van der Veken *et al.* allows to enlarge the scope of the reaction since aldehydes **21** with acid-labile groups can be used for the synthesis of α-aminophosphonates **19**, for all the substrates triphenyl phosphite **26** and carbamates, **23** are used (Scheme 2.2). Several Lewis acids were tested as catalysts for the reaction, in all cases, a 10 mol% of one of the following $TiCl_4$, $ZnCl_2$, $SnCl_4$, BF_3-Et_2O, or $Cu(OTf)_2$ was used. The yields obtained from these reactions are significantly higher compared to those obtained using the usual protocol (heating in acetic acid), and the 12 reported synthetic protocols provided product **27** yields between 68 % and 94 %. The lower yield (68 %) was obtained when *N*-Boc-4-aminobenzaldehyde was used in combination with 10 mol% of $Cu(OTf)_2$ and benzyl carbamate.

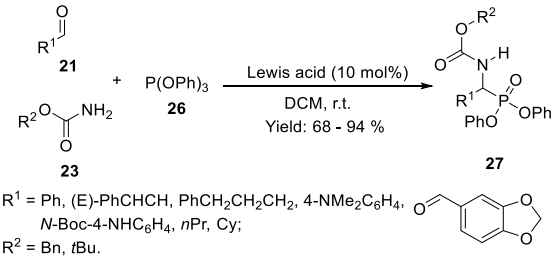

Scheme 2.2. One-pot three-component synthesis of α-aminophosphonates, catalyzed by 10 mol% of the selected Lewis acid

An efficient preparation of α-aminophosphonates by the one-pot condensation of aldehydes **21**, amines **22**, and dialkyl phosphites **18** using catalytic amounts of ytterbium (III) chloride under mild conditions was reported by Xu *et al*. (Scheme 2.3).[20] On the model reaction between benzaldehyde, aniline, and diethyl phosphite nine different catalysts (10 mol% load) were tested in acetonitrile at room temperature with a reaction time of 24 h. Results indicated $YbCl_3$ as the best catalyst, providing the corresponding α-aminophosphonates **19** with an excellent yield of 99 %. The activity of other catalysts was inversely proportional to the atomic radius of the lanthanide ion, following the order: $YCl_3 > GdCl_3 \sim SmCl_3 > NdCl_3 \sim ErCl_3 > LaCl_3$. For $YbCl_3$, it was possible to decrease the catalyst loading to 5 mol%, maintaining an excellent yield of α-aminophosphonate (93 %). With no further improvement, the authors tested the catalyst on a panel of different aldehydes, amines and phosphites. In almost all cases, the corresponding product **19** was obtained in moderate to excellent yields. In the case of *p*-nitrobenzaldehyde, the corresponding product was obtained with a lower yield (28 %). When diphenyl phosphite was used in combination with benzaldehyde and aniline the corresponding product was obtained with a 98 % yield. The authors claimed that the reason for the unsatisfactory results might lie in the competitive coordination of NO_2 with

lanthanide cation. Furthermore, the reaction involving steric bulky amine such as *tert*-butylamine led to the corresponding product in a relatively lower yield (68 %).

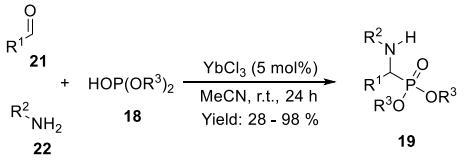

R^1 = Ph, 4-MeC_6H_4, 4-$NO_2C_6H_4$, PhCHCH;
R^2 = *n*Hex, *n*Bu, *t*Bu, Ph, Bn, 4-ClC_6H_4; R^3 = Et, *i*Pr, Ph

Scheme 2.3. One-pot three-component synthesis of α-aminophosphonates, catalyzed by $YbCl_3$

Commercially available magnesium perchlorate was reported as an extremely efficient catalyst for the synthesis of α-aminophosphonates by Bhagat and collaborators.[21] The magnesium salt was found to be superior, compared to other metal perchlorates and metal triflates, in the model reaction of 4-methoxybenzaldehyde, 2,4-dinitroaniline, and dimethylphosphite. The counter anion was pivotal in the reaction outcome, among several magnesium salts (*e.g.* $Mg(ClO_4)_2$, $MgSO_4$, $MgCl_2$, $MgBr_2$, MgI_2, $Mg(OTf)_2$). Between these salts, magnesium perchlorate outperformed all the others. The selected catalyst was tested with several aldehydes **21**, amines **22** and dialkyl phosphites **18** or trialkylphosphites **24** (Scheme 2.4). In all cases, the yield of product **19** was obtained with excellent values. Furthermore, the reaction scope demonstrated that the catalyst was compatible with various functional groups such as Cl, OMe, NO_2, OH, NMe_2, CN, and CO_2Me with no interferences by competitive complex formation with the catalyst. When the catalyst was used to promote the reaction between 4-methoxybenzaldehyde, aniline and diphenyl phosphite the corresponding product was obtained with a yield of 98 %.

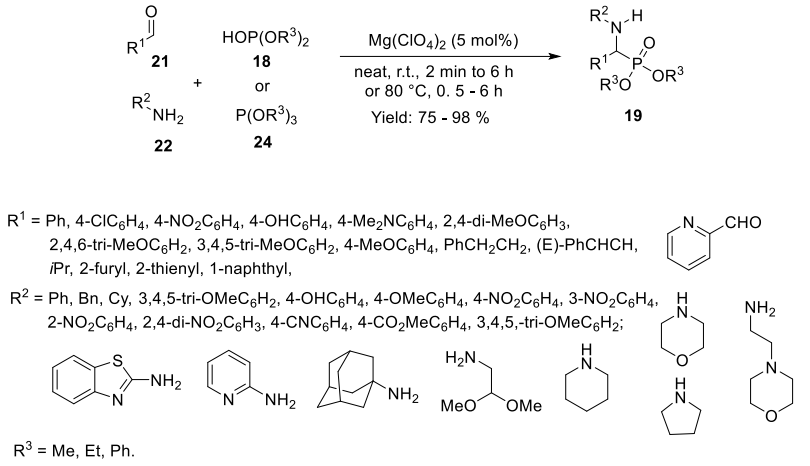

Scheme 2.4. One-pot three-component synthesis of α-aminophosphonates, catalyzed by $Mg(ClO_4)_2$

From the same group, it was later reported that among several zirconium compounds, $ZrOCl_2 \cdot 8H_2O$ was found to be very effective in promoting the one-pot three-component preparation of α-aminophosphonates **19**, between aldehydes **21**, amines **22** and phosphites **18, 24** (Scheme 2.5).[22] Similar to the previous work (Scheme 2.4) the optimal zirconium catalyst was found testing a panel of Zr(IV) Lewis acids on the model reaction between 4-methoxybenzaldehyde, 4-nitroaniline and dimethyl phosphite. The best results were obtained by using 10 mol% of $ZrOCl_2 \cdot 8H_2O$ or $ZrO(ClO_4)_2 \cdot 6H_2O$ at room temperature, yields after 30 minutes are reported to be respectively 92 and 98 %. The reaction was performed under neat conditions, the use of solvents like DCM, MeCN and THF required longer times (2 - 8 h) to afford comparable yields. The compound $ZrOCl_2 \cdot 8H_2O$ was selected for further studies. On the same model reaction a series of phosphites were tested, the authors reported that the reactions were faster with dialkyl/diaryl phosphites **18** than with trialkyl/triaryl phosphites **24**. Next, the generality of the reaction was tested on a panel of aldehydes and amines, dimethyl and diethyl phosphite were selected as phosphites due to their better activity. From the scope of the reaction, the catalyst was found compatible with various functional groups such as Cl, OMe, NO_2, OH, NMe_2, CN, and CO_2Me that do not interfere by competitive complex formation with the metal. The corresponding α-aminophosphonate **19** was obtained with good to excellent yields (70 - 96 %) for all the substrates.

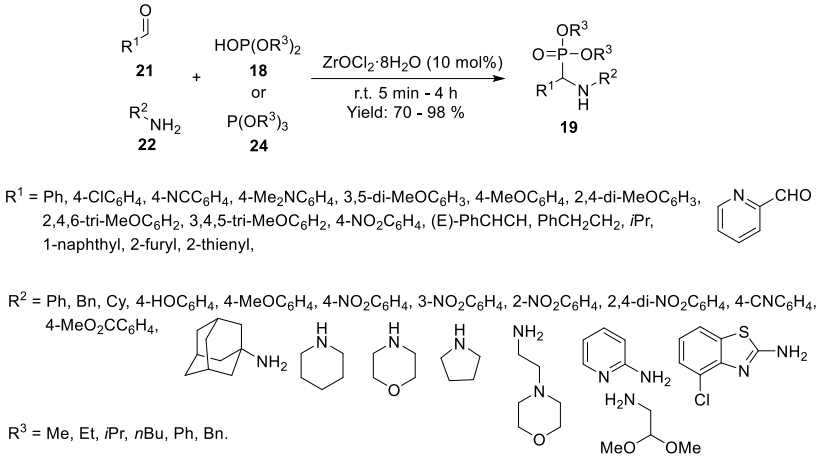

Scheme 2.5. One-pot three-component synthesis of α-aminophosphonates, catalyzed by $ZrOCl_2 \cdot 8H_2O$

Inspired by the work of Bhagat *et al.* with $ZrOCl_2 \cdot 8H_2O$ (Scheme 2.5), Li and coworkers successfully employed $HfCl_4$ as catalyst for the preparation of α-aminophosphonate **19** from aldehydes **21**, amines **22** and phosphites **18**.[23] The authors using the model reaction between benzaldehyde, aniline and dimethylphosphite tested a series of catalyst in EtOH at room temperature (Scheme 2.6). $HfCl_4$ was found superior to $ZrOCl_2 \cdot 8H_2O$, the desired product was obtained with a higher yield (98 vs 91 %) in a shorter time (6 vs 12 h). The high yield was maintained at 98 % even when the catalyst load was lowered to 2 mol%. The reaction time was lowered to 30 minutes when the model reaction was run at 60 °C. Last, the authors tested various solvents and among them, EtOH provided the higher yield of product **19**. With the optimized reaction conditions, a diversity of α-aminophosphonates was synthesized. The reactions with both arylaldehydes and arylamines afforded the corresponding α-aminophosphonates in good to excellent yield (82 - 98 %). Compared to the reactions promoted by Zr(IV) salts, the $HfCl_4$-catalyzed formation of α-aminophosphonates is faster, cleaner and requires a lower amount of catalyst (2 mol %).

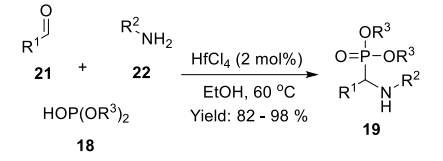

R^1 = Ph, 4-MeOC$_6$H$_4$, 4-MeC$_6$H$_4$, Cy, *n*Pe, *sec*-Bu, 2-furyl;
R^2 = Ph, 4-MeOC$_6$H$_4$, 4-NCC$_6$H$_4$ Bn, Cy;
R^3 = Me, Et, Ph;

Scheme 2.6. One-pot three-component synthesis of α-aminophosphonates, catalyzed by $HfCl_4$

Yan and Qi, reported the preparation of α-(thiophosphorylamino)-substituted benzyl-phosphonate **30** from *O*,*O*-diethyl or *O*-ethyl-*O*-phenyl phosphoroamidothioate **28**, substituted benzaldehydes **29**, and triphenyl phosphite **26** (Scheme 2.7).[24] The reaction was promoted by 50 mol% of $BF_3{\cdot}Et_2O$ and happened in a short time. The mixture was kept at room temperature for 20 minutes and then warmed up to 80 °C for 15 minutes. The scope of the catalyst was tested on 14 different aldehydes and 2 phosphoroamidothioates and the products were obtained with moderate to good yield (34 - 85 %). The lower yield was obtained when 4-NMe_2 substituted benzaldehyde was used, probably due to complexation between the NMe_2-nitrogen and the catalyst.

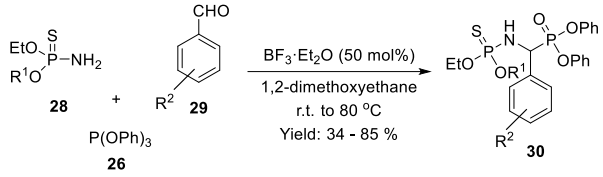

R^1 = Et, Ph;
R^2 = H, 4-Me, 4-F, 4-Cl, 2-Cl, 4-Br, 2-Br, 3-Br, 4-NO_2, 3-NO_2, 4-OMe, 3-OMe, 4-N$(CH_3)_2$, 4-OH,

Scheme 2.7. One-pot three-component synthesis of α-aminophosphonates, catalyzed by $BF_3{\cdot}Et_2O$

With the aim to prepare new antimicrobial agents, a series of α-aminophosphonates containing pyridine moiety **32** were prepared by Abdel-Megeed *et al.*[25] The products were prepared with a one-pot reaction between nicotinaldehyde **31**, triphenyl phosphite **26** and a series of arylamines **22** (*i.e.* aniline, 4-chloroaniline, 4-hydroxyaniline, 4-anisidine, and 4-toluidine) (Scheme 2.8). The transformation was catalyzed by $TiCl_4$ 10 mol% and was performed in DCM at room temperature for 24 - 32 h. The crude products obtained were purified by crystallization from ethanol to give the corresponding α-aminophosphonates with good to excellent yields (78 - 89 %).

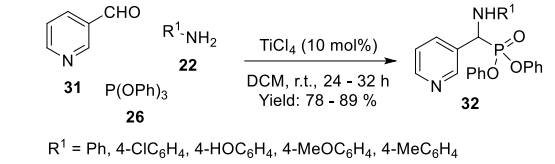

Scheme 2.8. One-pot three-component synthesis of α-aminophosphonates, catalyzed by $TiCl_4$

Aminoquinazoline derivatives are an important class of heterocyclic compounds, which showed a broad variety of biological activity profiles. Awad *et al.* incorporate the quinazoline moiety in a series of α-aminophosphonates in order to prepare a series of compounds with antimicrobial and anticancer activities.[26] The molecules were prepared from a one-pot coupling between 4-hydrazino-quinazoline **33**, triphenyl phosphite **26** and a series of benzaldehydes **29** (Scheme 2.9). The reaction was performed in DCM at room temperature and catalyzed by 10 mol% of anhydrous $ZnCl_2$. Product **34** was isolated after 49 - 54 h and with all four aldehydes, it was obtained with good to excellent yields (81 - 94 %). The prepared compounds were able to inhibit the growth of gram-positive and negative bacteria and fungi at low concentrations. Furthermore, the α-amino-phosphonates showed significant cytotoxicity against the breast cancer line (MCF7).

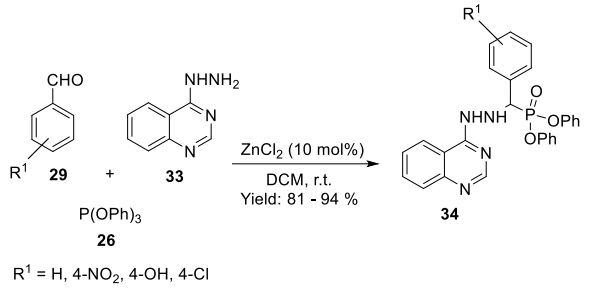

Scheme 2.9. One-pot three-component synthesis of α-aminophosphonates, catalyzed by $ZnCl_2$

With the aim to invent a new method for the one-pot three-component preparation of α-aminophosphonates **36** from benzaldehydes **29**, anilines **35**, and phosphites **18**, Arigala *et al.* investigate the ability of $Zn(OAc)_2 \cdot 2H_2O$ to promote the Kabachnik-Fields reaction (Scheme 2.10).[27] Initially, the catalyst was tested with the coupling between *p*-hydroxybenzaldehyde, 2,4-dichloroaniline, and dimethyl phosphite under solvent-free conditions at 50 °C. The corresponding α-aminophosphonate was obtained with a 94 % yield. Any attempt to lower the catalyst load resulted in a lower yield of the desired product, even after a prolonged reaction time. In order to assess the effect of the solvent the reaction was tested at 50 °C with THF, dioxane, toluene, MeCN, DCM and EtOH. In all cases, the desired product was obtained with a lower yield compared to solvent-free conditions. With the optimization concluded, the generality of the reaction was tested with several substituted benzaldehydes, anilines and diester phosphites. In all cases, the product

was obtained with excellent yields (85 - 94 %). From the authors, it was noted that benzaldehydes containing electron-donating or electron-withdrawing functional groups at different positions, did not show any remarkable difference in the yields of product.

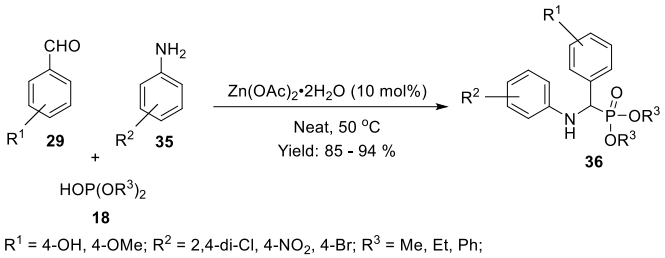

Scheme 2.10. One-pot three-component synthesis of α-aminophosphonates, catalyzed by $Zn(OAc)_2 \cdot 2H_2O$

Organylselanyl α-aminophosphonates **38** were prepared from selenide amines **37**, aldehydes **21** and phosphites **18** by Vogt and collaborators (Scheme 2.11).[28] The authors, using the model reaction between 1-(phenylselanyl)propan-2-amine, *ortho*-tolualdehyde and dimethyl phosphite started to screen the best reaction conditions. SiO_2 (200 mg/mmol substrate) tested at 60 °C led to the corresponding α-aminophosphonates in 48 % yield, rising the temperature to 100 °C and 130 °C provided **38** respectively with 73 and 70 % yield. Hence, 100 °C was selected as the optimal temperature and the investigation was moved to different Lewis acids, keeping the catalyst load of 200 mg/mmol substrate. $FeCl_3$ and $NbCl_5$ showed low efficiencies while $ZnCl_2$, $CeCl_3 \cdot 7H_2O$, $InCl_3$, and $\{NH_4[NbO(C_2O_4)_2(H_2O)] \cdot nH_2O\}$ gave moderate yields. An improvement in terms of yield (81 %) was noted when niobic acid ($Nb_2O_5 \cdot nH_2O$) was used as the catalyst and 90 % of the product was obtained with 2.0 equivalents of dimethylphosphite. An increase in the catalyst load did not improve the yield, while a decrease in the amount led to a decrease in product yield. With the optimal condition in hand, the authors tested the scope of the protocol on several amines, aldehydes and phosphites. Aldehydes with *ortho* substituent on the aryl group, such as methyl, chloride, or fluoride, gave satisfactory yields (75 - 90 %). When the reaction was carried out with 3,5-dimethoxybenzaldehyde, the yield decreased (48 and 65 %), and several byproducts were formed. Cyclohexanecarboxaldehyde also gave the product with good yields (74 and 90 %). When dibutylphosphite was used, the reaction did not take place, while diphenyl phosphite (48 - 86 %) reacted less efficiently than dimethylphosphite. The reaction, also proceeded well with different aryl groups in the selenide amine component. The recyclability of the catalyst was also tested, niobic acid was recycled 3 times without any pretreatment, and gave a comparable amount of product.

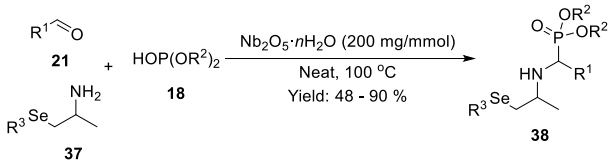

R^1 = 2-MeC_6H_4, 2-FC_6H_4, 2-ClC_6H_4, 3,5-di-MeOC_6H_4, Cy; R^2 = Me, Ph;
R^3 = Ph, 4-MeOC_6H_4, 4-FC_6H_4.

Scheme 2.11. One-pot three-component synthesis of α-aminophosphonates, catalyzed by $Nb_2O_5{\cdot}nH_2O$

The use of heteropoly acids (HPAs) has recently gained great attention in organic synthesis. Among several HPAs, phosphomolybdic acid (PMA, $H_3PMo_{12}O_{40}$) is one of the less expensive and commercially available solid acid catalysts. Reddy and collaborators used PMA to promote the preparation of α-aminophosphonates **40** derived from 2-cyclopropylpyrimidin-4-carbaldehyde **39**, anilines **22** and phosphites **18** (Scheme 2.12). Using the model reaction between 2-cyclopropylpyrimidin-4-carbaldehyde, aniline, and diphenyl phosphite the authors started to screen different catalysts. Common Lewis acids ($AlCl_3$, $FeCl_3$, $ZnCl_2$) and solid acids (Amberlyst-15, cellulose sulfuric acid, Al_2O_3-SiO_2) afforded the desired product with moderate yield (60 - 75 %). Among all the catalysts the best conversion was obtained with $H_3PMo_{12}O_{40}$ (90 %) in toluene. No change was observed when the catalyst load was decreased from 20 mol% to 0.5 mol% Four solvents were screened and among methanol, toluene, acetonitrile and dichloromethane, the best results (95 %) were obtained with DCM. With the optimized protocol in hand, the authors tested the PMA on a panel of anilines, benzothiazolamines and phosphites. In all the cases, excellent yields were obtained with all the substrates (87 - 96 %). The reaction worked well also with benzo-[d]thiazol5-amine and benzo[d]thiazol-6-amine. Finally, the reusability of the phosphomolybdic acid catalyst was examined. After each run, the product was filtered, the solvent was evaporated, and the catalyst residue was washed with dichloromethane and then reused. For the reaction of 2-cyclopropylpyrimidin-4-carbaldehyde, aniline, and diphenyl phosphite the corresponding product's yield was 95 %, 93 %, 92 %, and 90 % over four cycles.

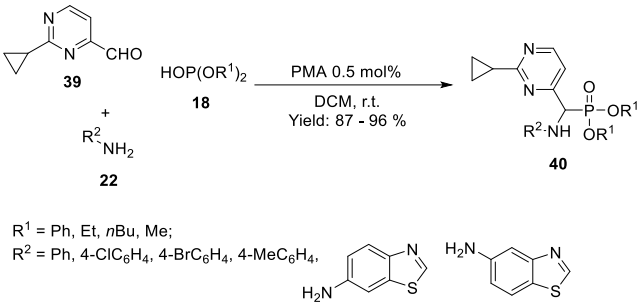

Scheme 2.12. One-pot three-component synthesis of α-aminophosphonates, catalyzed by phosphomolybdic acid (PMA, $H_3PMo_{12}O_{40}$)

2.1.2 Two-component synthesis of α-aminophosphonates from aminals

α-Aminophosphonates **43** were prepared from aminals **41** and various phosphorous compounds **42** (Scheme 2.13). The protocol proposed by Dmitriev and coworkers employed the use of anhydrides like acetic anhydride (Ac_2O) and trifluoroacetic anhydride (TFAA) in excess or in a catalytic amount to promote the conversion. Initially, the Ac_2O and the mixture Ac_2O/AcCl 4:1 v/v were used in large excess as solvent and reagent.[29] In the first screen, under the same conditions, the mixture of Ac_2O/AcCl (4:1 v/v) performed much better, providing the corresponding product with double yield, compared to Ac_2O alone. The scope of the reaction promoted by Ac_2O/AcCl 4:1 v/v was tested both with aromatic and aliphatic aldehydes. For both classes of substrates, the product was obtained with comparable yields ranging from 53 to 76 %. In a second study,[30] TFAA was used to promote the reaction between alkylphosphonous acids **42** and aminals **41** in toluene or DCM at room temperature. The optimal amount of TFAA was tested, among four different values (*i.e.* 0.5, 0.8 1.0 and 1.5 equiv.), 1.0 equivalents of TFAA provided the highest yield of product. In one case 59 % with 1.0 equiv. vs 14 % with 0.5 equiv.

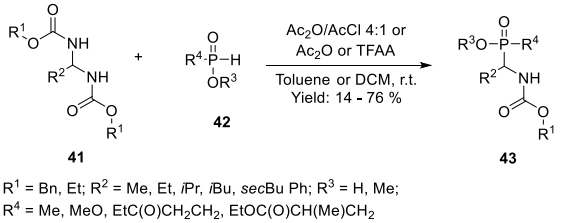

Scheme 2.13. Preparation of α-aminophosphonates from aminals

2.1.3 Selection of Lewis acids and additives for the improvement of the Birum-Oleksyszyn step

In Sections 2.1.1 and 2.1.2 are reviewed several protocols for the one-pot three-component preparation of α-aminophosphonates and the two-component synthesis of α-aminophosphonates from aminals. The published data shows, that many Lewis-acidic metals are capable of catalyzing the desired reaction. At the same time, there's no clear correlation between the catalyst nature and the success of the transformation for a given set of starting materials. Hence, the best use of this data is to create a panel of catalysts for subsequent screening. In order to find a better catalyst for our substrate, we decided to investigate the protocol using only commercially available Lewis acids with a particular focus on chloride and triflates. Furthermore, TFAA was selected as an additive to promote the reaction between side products and byproducts generated during the reaction.

2.2 Enantioselective synthesis of α-aminophosphonates

Chiral phosphonic acids are already established molecules in the pharmaceutical world. Drugs like Fosfomycin (**44**),[31] known for its antibacterial activity, have been used for the treatment of lower urinary tract infections, and Alafosfalin (**45**),[32] is capable to inhibit the biosynthesis of bacterial cell walls (Figure 2.1). Proteins often show enantioselectivity towards their binding partners, and the biological activity of α-aminophosphonate might be related to their absolute configurations.[33] Furthermore, the FDA issued guidelines and policies in 1992 concerning the development of chiral compounds. These rules require the researchers to investigate any biological effect of the various enantiomers/diastereoisomers during the early phase of drug discovery and development.[34] Therefore the development of the enantioselective synthesis of α-aminophosphonates has drawn significant attention in recent years. Several extensive reviews on the enantioselective or diastereoselective synthesis of α-aminophosphonates were published.[35–39] Herein we report a survey of various approaches to their stereoselective synthesis, as well as state-of-the-art catalysts and chiral auxiliaries, which can be used for the stereoselective preparation of chiral UAMC-00050.

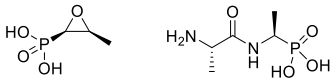

Fosfomycin (**44**) Alafosfalin (**45**)

Figure 2.1. Structure of Alafosfalin (**44**) and Fosfomycin (**45**)

2.2.1 Catalysis by chiral metal complexes

Enantioselective preparation of α-aminophosphonates **47** or **50** from imines **46** or ketimines **48** and phosphites **18** or **49** was successfully achieved by Nazish *et al.* using a chiral complex of titanium (Scheme 2.14).[40] The metal was bound to a series of ligands derived from chiral (1R,2R)-(-)-1,2-diaminocyclohexane and salicylaldehyde. Two molecules of derived imines were then tethered with oligoethylene glycol, to form the circular ligand **51**. Using the reaction between *N*-benzyl-1-phenylmethanimine and dimethylphosphite authors investigated several titanium sources and different lengths of ligand's ethylene glycol chain. The best yield of **47** was obtained with $Ti(OiPr)_4$ as the metal source and when the ethylene glycol chain in the ligand was composed of 5 units of ethylene glycol. With the catalyst in hand, the authors started to screen the catalyst load and the metal/ligand ratio and found that the best results were achieved with 5 mol% loadings and a metal/ligand = 2:1 ratio. The *N*-benzyl-1-phenylmethanimine and dimethylphosphite provided the best yield and second best enantiomeric excess (ee) when compared with diethyl, diphenyl and dibenzyl phosphites. Various solvents were also tested, proving the superiority of toluene compared to DCM, $CHCl_3$, and THF. Regarding temperature, the authors reported a significant drop in yield when the reaction was carried out at 0 °C and - 10 °C. Knowing the optimal conditions, the scope of the reaction was assessed. Various imines were tested, and all substrates provided the corresponding product in good yield (82 - 92 %) and excellent ee (92 - 98 %). The enantioselective protocol was also applicable to a panel of isatin-derived ketimines **48**. During a screen of additives, it was found, that 4 Å MS helped to reach high values of optical purity. Six different ketimines provided the product **50** in good yield (84 - 88 %) with moderate to excellent enantiomeric excess (46 - > 99 %).

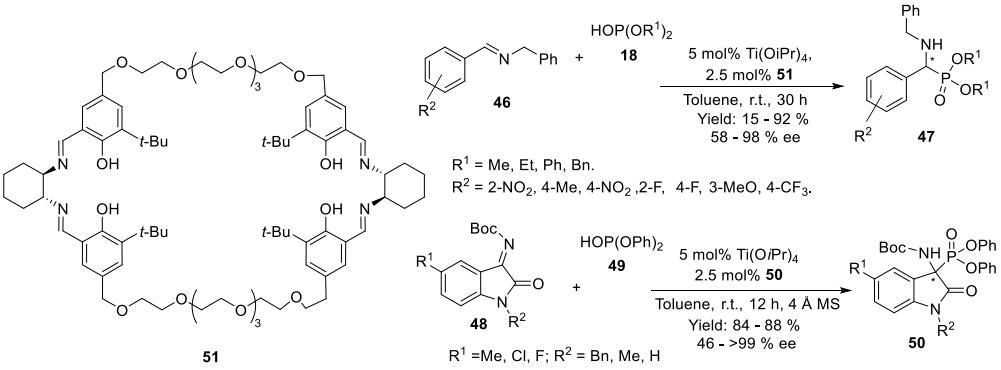

Scheme 2.14. Enantioselective synthesis of α-aminophosphonates, catalyzed by titanium complex with chiral ligand **51**

Preparation of optically pure α-aminophosphonates **54** with a one-pot three-component reaction of aldehydes **21**, *p*-anisidine (**52**), and diarylphosphites **18**, catalyzed by a zinc (II)

bis(imidazoline)'s complex was achieved by Ohara and coworkers (Scheme 2.15).[41] The investigation started from a model reaction between benzaldehyde, *p*-anisidine, and diphenylphosphite using 10 mol% of a Lewis acid and 10 mol% of ligand **55**. Metal salts like $AlCl_3$, $Sc(OTf)_3$, and $Mg(OTf)_2$ afforded an almost racemic product. In contrast, $Zn(OTf)_2$ afforded the desired product in a good yield and 45 % ee, the enantioselectivity increased to 53 % when the reaction was carried out at - 50 °C instead of - 20 °C. Investigation of counterion in the zinc salt revealed, that enantioselectivity can be increased to 59 % with $Zn(NTf_2)_2$ instead of $Zn(OTf)_2$. The last part of the reaction optimization included the screening of ligands. Among six different bis-imidazolines, **56** provided the best reaction outcome with an enantiomeric excess of 90 %, when bis(*ortho*-methoxyphenyl)phosphite was used instead of diphenyl phosphite. With the optimal conditions in hand, the scope of the reaction was tested on a panel of aldehydes. The reaction with different substituted benzaldehydes afforded the corresponding product with a good enantio-selectivity. Reactions with *ortho*-substituted aldehydes provided a lower enantiomeric excess. α,β-Unsaturated aldehydes gave the product in good yield and enantioselectivity, while 3-methylbutanal yielded a poor 31 % ee. The stereo outcome of the preparation of α-aminophosphonate from cyclohexanecarbaldehyde was increased from 45 to 61 % ee by a slow addition of phosphite. Finally, authors were able to generate an optically active α-aminophosphoric acid **54**, without a loss of enantioselectivity, after deprotection of the *p*-methoxyphenyl with NBS and conversion of the phosphonate to phosphoric acid after treatment with HBr/AcOH and propylene oxide.

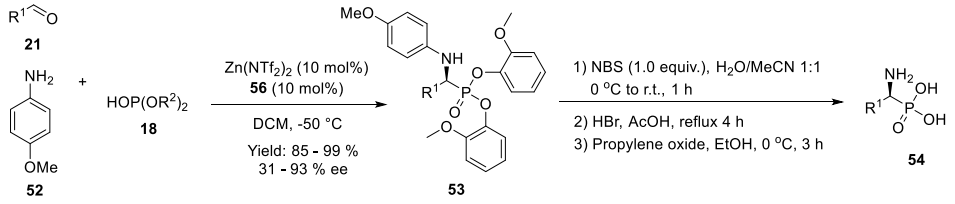

R^1 = Ph, 4-MeC_6H_4, 2-MeOC_6H_4, 3-MeOC_6H_4, 4-MeOC_6H_4, 4-HOC_6H_4, 4-ClC_6H_4, 4-MeO$_2$CC_6H_4, 2-naphthyl, 2-thienyl, 2-furyl, 2-benzofuryl, (E)-PhCHCH, PhCC-, *i*Bu-, Cy; R^2 = Ph, 2-MeOC_6H_4.

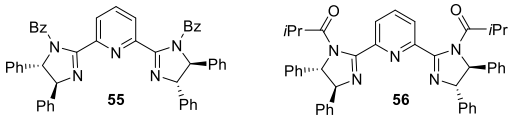

Scheme 2.15. Enantioselective synthesis of α-aminophosphonates, catalyzed by zinc chiral complex **56**

Zhou *et al.* reported a three-component Kabachnik-Fields reaction between aldehydes **21**, 2-aminophenol (**57**), and diphenyl phosphite (**49**) using a chiral catalytic complex of a bis-*N*-oxide **59a,b** and **60a-c** with scandium (III).[42] Corresponding α-aminophosphonate **58** was obtained in a good yield and a good enantiomeric excess (Scheme 2.16). The investigation started with the three-

component reaction between benzaldehyde, 2-aminophenol (**57**), and diphenyl phosphite (**49**), catalyzed by a Sc(III)-complex (molar ratio of ligand/$Sc(OTf)_3$ 2:1) in THF. Among the five tested ligands, authors found, that the chiral backbone of the bis-*N*-oxide significantly impacted the enantioselectivity. **60a** (derived from *L*-Ramiprol) provided the best ee (84 %) when compared with **59a** (derived from *L*-proline, 25 % ee) or **59b** (derived from *L*-pipecolic acid, 63 % ee). The steric effect of the amide moiety was also important to the ee, with decreasing of the steric hindrance enantioselectivity also decreased, **60b** (41 %) and **60c** (0 %). Interesting results were obtained using Lewis acid different than $Sc(OTf)_3$. For all other salts (*e.g.* $Y(OTf)_3$, $La(OTf)_3$, $Sm(OTf)_3$, $Yb(OTf)_3$) complexed with **60a,** the product was obtained with lower ee and with the opposite configuration of the stereocenter. With the optimized conditions in hand (5 mol% bis-*N*-oxide/Sc(III) complex in THF at - 20 °C) the scope of the reaction was tested on 13 different aldehydes **21** with 2-aminophenol (**57**), and diphenyl phosphite (**49**). For all substrates, the corresponding α-aminophosphonates **58** were obtained in good to excellent yields (73 - 94 %) and high enantioselectivity (81 - 87 % ee).

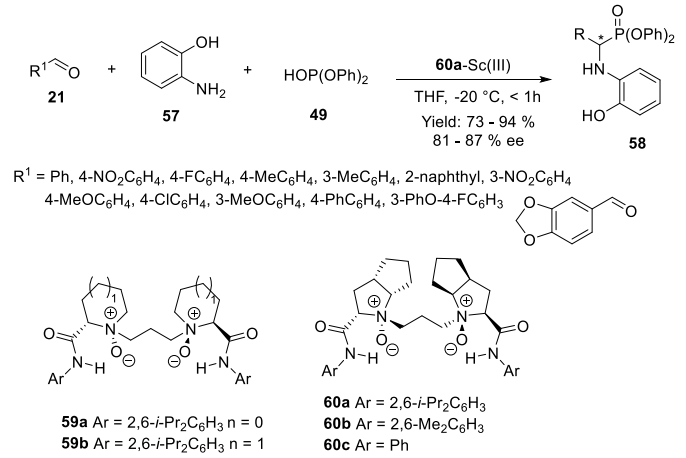

Scheme 2.16. Enantioselective synthesis of α-aminophosphonates, catalyzed by scandium chiral complex **60a**

Abell and his coworker Yamamoto developed a chiral catalyst based on a chiral tethered bis-8-quinoline (TBOxH) ligand and Et_2AlCl as the aluminum source.[43] The complex **64**, which provides good enantioselectivity for the synthesis of chiral hydroxyphosphonates, was also tested for the preparation of chiral α-aminophosphonates **63** (Scheme 2.17). Four imines **61** were screened as substrates in the reaction with di(2,2,2-trifluoroethyl)phosphite (**62**), only *N*-diphenyl phosphinoyl imines could provide an optimal yield (95 %) and enantioselectivity (96 %). The methodology was tested on various substrates providing the corresponding α-aminophosphonates **63** in excellent yield (85 - 98 %) and optical purity (88 - 98 % ee). The catalyst, which already possesses the

advantage to be used with a small loading (0.5 or 1 mol%), was found to be compatible with a variety of functional groups and heterocycles. Furthermore, the authors reported also the high recyclability of the catalyst.

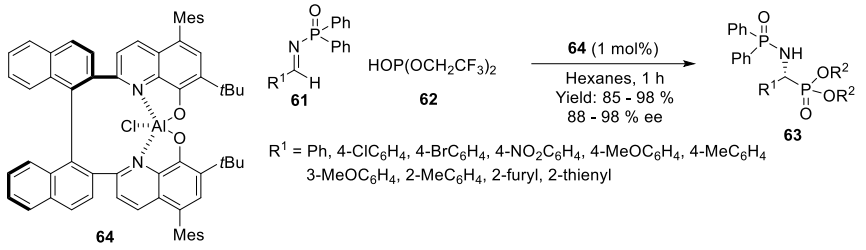

Scheme 2.17. Enantioselective synthesis of α-aminophosphonates, catalyzed by aluminum chiral complex **64**

Another enantioselective route for α-aminophosphonates synthesis, catalyzed by a chiral aluminum complex, was investigated by Saito *et al.* First, they developed a chiral trigonal-bipyramidal aluminum (salalen) complex **68** which proved to be efficient for the preparation of optically active α-hydroxyphosphonate.[44] The reaction was optimized to be run in THF at -15 °C with a catalyst loading of 10 mol%. Interested in exploring the reaction's scope, the authors started to investigate the chiral complex's applicability in a stereoselective synthesis of enantiomerically pure α-aminophosphonates **66** (Scheme 2.18).[45] The asymmetric hydrophosphonylation with dimethylphosphite (**65**) was carried out on a series of imines **20**, where the *N*-moiety was functionalized with a removable protecting group, opening up possibilities for further functionalization of the chiral substrate. In the first set, all reactions were run at room temperature. *N*-Methoxy- and *N*-(dimethylamino)-aldimines did not show any reactivity, while *N*-tert-butoxycarbonyl and *N*-4-toluenesufonyl-aldimines were poorly reactive and with modest enantioselectivity. Aldimines bearing a noncoordinating group (*e.g.* benzyl and *p*-methoxybenzyl groups) were found to be suitable substrates for the reaction, providing the product in good yield and enantiomeric excess. In contrast, the bulkier diphenylmethyl group provided a lower yield and enantioselectivity. Among all the *N*-protecting groups, phenyl provided the best results with almost quantitative yield and 60 % ee which rose to 75 % ee when the reaction was run at -15 °C. From the good results of the phenyl group, the authors started to investigate substituted benzenes as an *N*-protecting group. The introduction of a *p*-methoxy substituent on the aryl ring improved the ee to 78 % while a *p*-bromo substituent decreased the ee to 31 %. Finally, the 4-methoxy-3-methylphenyl provided the highest enantiomeric excess (87 %). Anodic oxidation was then successfully employed for the deprotection of the nitrogen to provide phosphonate **67** without any loss of chirality. The scope also included various aldehyde moieties, electron withdrawing group (EWG) in *para*-position improved the ee to 95 % while electron donating group (EDG) in *para*-position decreased it to 85 %. Heteroaromatic aldimines were also tested: reaction with 2-thienyl

aldimine proceeded with a high 84 % ee while the reaction with 2-furyl aldimine provided a moderate 63 % ee.

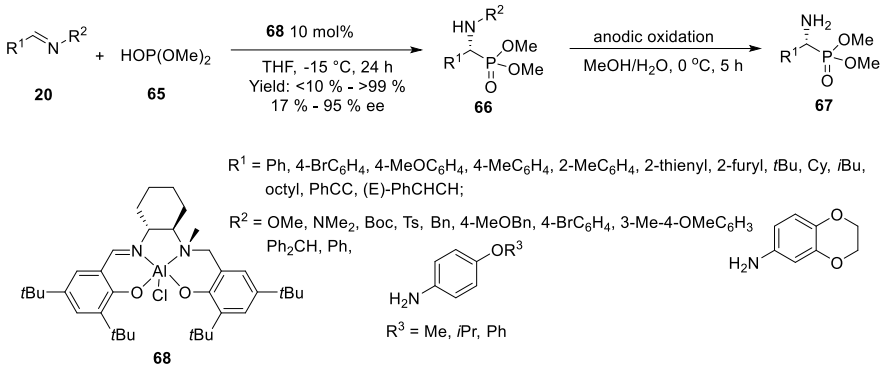

Scheme 2.18. Enantioselective synthesis of α-aminophosphonates, catalyzed by salalen derivative aluminum chiral complex **68**

In 1995, it was reported for the first time the use of a lanthanoid-metal-BINOL heterobimetallic complexes (LMB, **69**) for the synthesis of optically pure α-aminophosphonates **66** from imines and dimethylphosphite (**65**) (Scheme 2.19).[46] The reaction between isopropyl-di-4-anisylmethylimine and dimethylphosphite was selected as a model for the test of various catalysts and conditions. Lanthanum-sodium-BINOL (LSB) was initially tested with 100 mol% loading in THF at 60 °C and 20 mol% loading in THF at room temperature. Using heating and a stoichiometric amount of the catalyst helped to achieve a higher yield (47 %) and a moderate 69 % ee compare with a catalytic amount of LSB. A 20 mol% loading of lanthanum-potassium-BINOL (LPB) at room temperature in THF provided the α-aminophosphonates **66** with a low yield (27 %) but a much higher optical purity (71 %) compared to previous conditions. Changing the reaction medium to a mixture of toluene/THF (7:1 v/v) allowed to increase the yield to 62 % even when the reaction was carried out at room temperature. Enantioselectivity (96 %) and yield (70 %) were both improved when 10 mol% loading of LPB were used with a longer reaction time (96 h). Other BINOL complexes like lanthanum-lithium-BINOL (LLB), gadolinium-potassium-BINOL (GdPB) and praseodymium-potassium-BINOL (PrPB) failed to provide better results than LPB. In general, all complexes were tested on seven different imines providing the corresponding α-aminophosphonates with yields from 38 to 96 %.

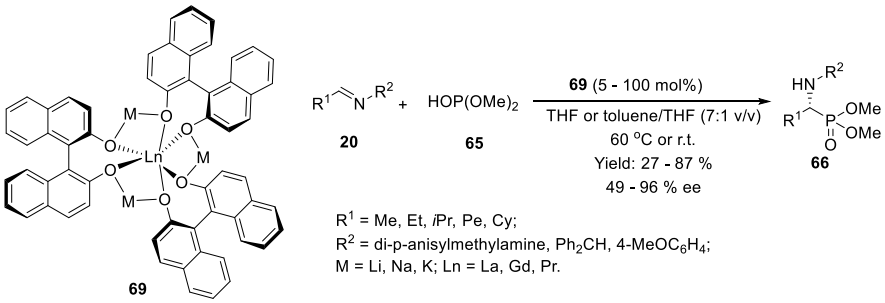

Scheme 2.19. Enantioselective synthesis of α-aminophosphonates, catalyzed by lanthanum-BINOL complex **69**; (*R*)-LMB = (*R*)-lanthanoid-metal-BINOL

An enantioselective synthesis of the biologically active compounds 4-thiazolidinylphosphonates **71** from dihydrothiazoles **70** and phosphites **18** was reported by Gröger *et al.*[47] 2,2,5,5-Tetramethyl-2,5-dihydrothiazole was reacted with dimethylphosphite in THF in the presence of a chiral titanium and lanthanoid complex (20 mol%) (Scheme 2.20). Regarding titanium compounds, when (-)-(R,R)-TADDOL was used as a ligand it provided better enantiomeric excess (46 %) compared with (*R*)-(+)-binaphthol (29 %) and *L*-(+)-diisopropyltartrate (45 %). As previously reported, the use of a lanthanoid-potassium-BINOL complex proved to be efficient in the preparation of optically pure α-aminophosphonates. LPB in toluene/THF (7:1) at room temperature provided the phosphonate **71** in 53 % yield with 61 % ee, while running the reaction at 50 °C gave comparable results in terms of yield (55 %) and ee (64 %), but with a shorter reaction time, 50 h instead of 144 h. During a screening of metals, (praseodymium, samarium, gadolinium, dysprosium and ytterbium) the higher ee of the target phosphonate was obtained with ytterbium-potassium-BINOL (YbPB) (96 % at 50 °C and 98 % at room temperature). It was possible to decrease the loading of YbPB from 20 to 5 mol% maintaining the same enantioselectivity (95 %) with yields respectively 80 and 63 %. Due to its high molecular weight, employing 5 mol% of Yb-complex on an industrial scale might present some problems. Hence, Schlemminger *et al.* started investigating a new and more efficient method for the enantioselective synthesis of 4-thiazolidinylphosphonate **71**.[48] The authors were pleased to find that the optically pure 4-thiazolidinylphosphonates can be generated, from **70** with high enantioselectivity and high conversion when cyclic phosphites are used instead of dimethylphosphite. Modifications on the imine moiety have been reported to have only a little effect on the reaction outcome. The amount of the (*S*)-YbPB catalyst was then reduced stepwise from 20 mol% to 0.1 mol%, and the authors were able to reach a catalyst loading of 2.5 mol% without suppression of yields and optical purity. Then, the focus was moved to the molar ratio of the cyclic phosphite. 5.0, 2.5 and 1.0 equivalents of phosphite were used in the hydrophosphonylation. The experiment indicates that a surplus of phosphite is necessary for maintaining the high yield, but the reaction can be run with 2.5 equivalents without any loss in performance. In summary, the best conditions were: 2.5 mol% of (*S*)-YbPB, 2.5 equivalents of

phosphite at 50 °C in toluene/THF (7:1 v/v) with a reaction time of 48 h. The almost quantitative yields have highlighted the potential of cyclic phosphites over acyclic phosphites in a stereoselective generation of chiral α-aminophosphonates.

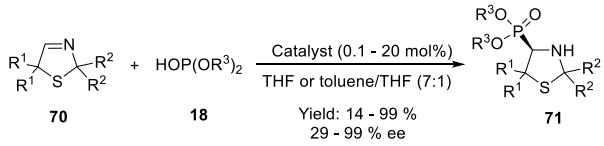

Catalyst.: Ti(Oi-Pr)$_2$(L-dipt), Ti(Oi-Pr)$_2$(L-dipt), Ti(Oi-Pr)$_2$(TAD), Ti(Oi-Pr)$_2$(BIN), (*R*)-LaPB, (*R*)-PrPB, (*R*)-SmPB, (*R*)-GdPB, (*R*)-DyPB, (*R*)-YbPB, (*S*)-YbPB;
R^1 = H, CH_3, -$(CH_2)_5$-; R^2 = CH_3, -$(CH_2)_4$-;
R^3 = Me, -$(CH_2)_3$-, -CH_2-$C(CH_3)_2$-CH_2-, -CH_2-CH=CH-CH_2-

Scheme 2.20. Enantioselective synthesis of α-aminophosphonates, catalyzed by titanium chiral complex and lanthanum-BINOL complex; *L*-dipt = *L*-(+)-diisopropyltartrate, TAD = (-)-(*R*,*R*)-TADDOL; BIN = (*R*)-(+)-binaphthol

Simple chiral catalyst systems are highly desirable when chemists want to synthetize enantiopure compounds. With this concept in mind, Lim and coworkers developed a chiral metal catalyst simply based on a derivative of proline **75** and manganese bromide.[49] The preparation of α-hydroxyphosphonate through the reaction of benzaldehyde with diethylphosphite (**73**) in the presence of lithium carbonate as the base was used to screen a series of manganese source and proline derivatives. Among six different ligands, the modified hydroxyproline **74** was able to provide an enantioselectivity of 28 % in combination with $Mn(OAc)_2$ as a manganese source. The enantiomeric excess was rapidly increased to 71 % when $MnBr_2$ was used as a manganese source. Anhydrous THF was proved to be the optimal solvent compared to anhydrous acetonitrile, DMF, 1,4-dioxane and DCM. Lastly, four bases (*i.e.* K_2CO_3, *n*-BuLi, LiHMDS, and TEA) were screened but none of them was able to raise the ee above 71 %. The optimized reaction conditions were used on a panel of imines **72** in combination with diethylphosphite **73** (Scheme 2.21). The corresponding α-aminophosphonates **74** were prepared with good yields (63 - 72 %) and moderate enantiomeric excess (45 - 71 %). The lowest yield and ee were obtained when 4-NO_2-benzaldehyde was used.

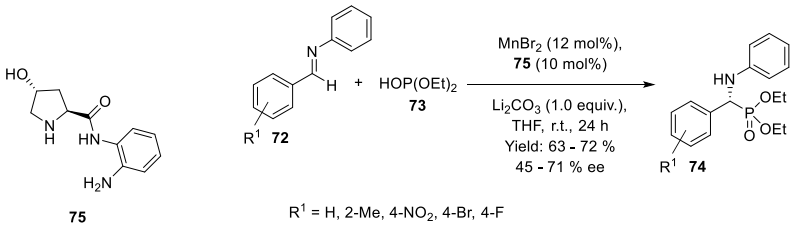

R^1 = H, 2-Me, 4-NO_2, 4-Br, 4-F

Scheme 2.21. Enantioselective synthesis of α-aminophosphonates, catalyzed by proline-manganese chiral catalyst **75**

2.2.2 Catalysis by chiral phosphoric acids

In the last few years, metal-free catalysis has drawn the attention of scientists, due to an increased interest in green chemistry approaches for the preparation of organic compounds. For example, a series of chiral Brønsted acids derived from (*R*)-BINOL were used by Akiyama and coworkers for the metal-free enantioselective synthesis of α-aminophosphonate **19** from imines and phosphites **18** or **24**.[50] The authors performed a hydrophosphonylation reaction on the *N*-benzylidene *para*-anisidine, with diethylphosphite in the presence of the **76e** (10 mol%), in toluene at room temperature (Scheme 2.22). The corresponding product **19** was obtained in 99 % yield with 43 % ee. Using diisopropyl phosphite as a nucleophile the ee was increased to 52 % and the aldimine derived from cinnamaldehyde provided the product with 84 % ee. Other catalysts, used with 10 mol% loading, provided lower yield and optical purity. During the investigation of the reaction's scope, it was noted by the authors, that the use of trialkyl phosphite **24** as a nucleophile decreased the yield and the enantiomeric excess (to 3 % ee), which suggests that OH group of the dialkyl phosphite plays a pivotal role in the outcome of the reaction. It was also noted that the presence of an *ortho*-hydroxyl group in R^2 decreased the enantioselectivity, from 84 to 39 % ee.

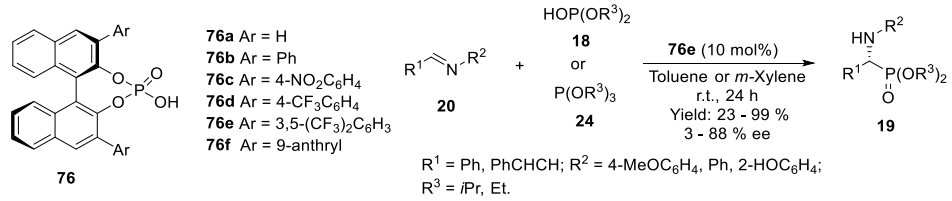

Scheme 2.22. Enantioselective synthesis of α-aminophosphonates, catalyzed by chiral BINOL acids **76a-f**

Xu *et al.*[33] inspired by the work of Akiyama synthesized an analogous axially chiral phosphonic acid catalyst **76e**, by changing the bulky 3,3' aryl substituent with a 4-fluorophenyl group **79**. It was tested on the reaction between phosphites **18** and imines **77** proving that the structure of the substrate and the catalyst strongly influence the yield and the enantiomeric excess and that this class of catalysts is well suited for cinnamaldehyde-derived imines. Considering this, the authors screened a series of solvents (MeCN, DCM, toluene and xylene), on a model reaction of the imine derived from cinnamaldehyde and 2-methyl-aniline, and diisopropyl phosphite, catalyzed by 10 mol% loading of catalyst **79** at room temperature (Scheme 2.23). A higher enantiomeric excess was obtained when the reaction was run in xylene (62 %). The effect of temperature was also investigated: reactions run at - 40 °C, 0 °C and 50 °C provided only a small difference in enantiomeric excess (68 %, 65 % and 58 %, respectively). For this reason, room temperature was chosen as a parameter for a scope screening. In total 16 different α-aminophosphonates **78** were prepared with yields between 30 % and 65 % and enantioselectivity between 8 and 62 % ee. As shown in Akiyama's work, diisopropyl phosphite afforded higher enantioselectivity when

compared with triisopropyl phosphite, proving that the OH moiety plays an important role in the reaction outcome. Better ee was also achieved with diisopropyl phosphite compared to other nucleophiles: $HPO(OEt)_2$, $HPO(OnPr)_2$, and $HOP(OnBu)_2$. Regarding the imine, electron-donating substituent such as the methyl group on the aryl ring seems to have a positive influence on ee. To summarize, catalyst **79** was screened for 16 different substrates with general lower enantioselectivity compared to catalyst **76e**, thus highlighting the importance of a bulky substituted on the 3,3' positions of the BINOL core.

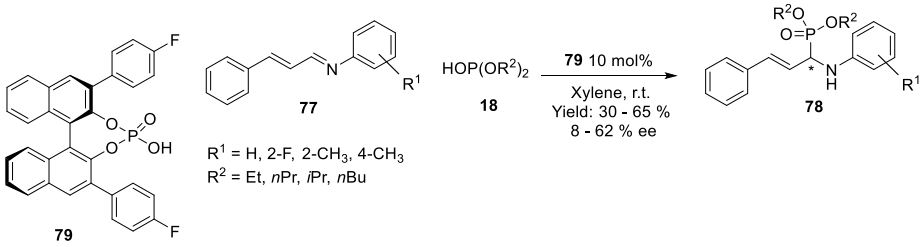

Scheme 2.23. Enantioselective synthesis of α-aminophosphonates, catalyzed by chiral-BINOL acids **79**

Gutierrez and colleagues synthesized a series of chiral biphenyl-2,2'-diyl phosphates from commercially available phenols.[51] The concept resembles the catalyst used by Akiyama and Wu. Two chiral phosphonic acids (**83** and **84**) and a phosphoramidothioate (**85**) were tested for the hydrophosphonylation with diisopropyl phosphite **81** of *N*-benzylidene-2-methoxyaniline **80** in *m*-xylene at r.t. (Scheme 2.24). Despite a good yield (89 %) and the modest optical purity (37 %) of product **82** when catalyst **83** was used, all the other catalysts (**84** and **85**) showed poor conversion (24 and 10 %) and enantioselectivity (13 % for both). A better outcome for **83** can be attributed to the positive contribution of the two chlorine atoms.

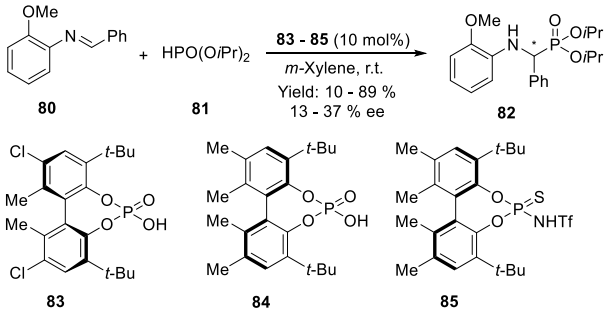

Scheme 2.24. Enantioselective synthesis of α-aminophosphonates, catalyzed by chiral phosphoric acids **83 - 85**

Cheng and coworkers successfully used chiral phosphoric acids for the synthesis of optical pure α-aminophosphonates from α-branched aldehydes.[52] In a previous work, reported by the same group, (*S*)-3,3′-bis(2,4,6-triisopropylphenyl)-1,1′-binaphthyl-2,2′-diyl hydrogenphosphate (TRIP) **89** was used to perform a highly enantioselective reductive amination of α-branched aldehydes by dynamic kinetic resolution.[53] This approach was then used in combination with an enantioselective three-component Kabachnik–Fields reaction for the synthesis of β-branched α-aminophosphonates **88** from aldehydes **86**, *p*-anisidine (**52**) and di(3-penthyl)phosphite (**87**). A model reaction between 2-cyclopentyl-2-phenylacetaldehyde, *p*-anisidine and di(3-penthyl)phosphite catalyzed by **89**, in cyclohexane at 50 °C, provided the desired product with good diastereoselectivity (16:1 dr) but with moderate enantioselectivity (66 % ee) (Scheme 2.25). A catalyst screening highlighted that **90** was able to provide the α-aminophosphonate **88** in good yield (86 %) with both high dr (16:1) and excellent er (96:4); on the other hand, **91** provided the desired product with a 37 % yield, a dr of 15:1 and an er of 80:20, pointing out that bulky substitutes on the binaphthyl phosphonate are required for high enantioselectivity. With the optimized condition in hand, the reaction scope was tested on a panel of 15 different substrates. Yields of **88** were maintained at a high level independently of the electronic nature of the aryl group in the aldehyde, but the enantioselectivity was slightly lower when aryl substituents were present in *ortho* or *meta*-position. A steric effect of the aldehyde substituents was also investigated, where bulky alkyl groups (*e.g.* isopropyl, cyclohexyl) significantly increase the diastereoselectivity and the enantioselectivity of the final product.

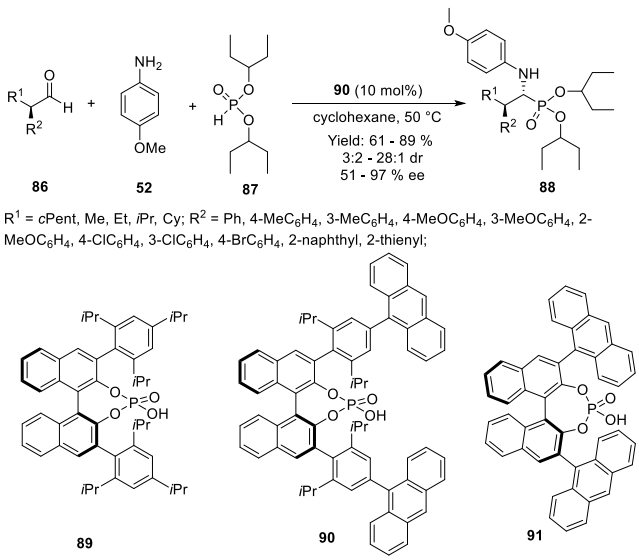

Scheme 2.25. Enantioselective synthesis of α-aminophosphonates, catalyzed by chiral phosphoric acids **89 - 91**

2.2.3 Catalysis by Cinchona alkaloids and Cinchona-derived organocatalysts

The enantioselective synthesis of α-aminophosphonates **93**, through hydrophosphonylation of an imine substrate **92** with disubstituted-phosphite **18** was successfully performed by Nakamura and coworkers using various Cinchona alkaloids as organic catalysts (Scheme 2.26).[54] A series of imines **92**, derived from benzaldehyde were initially reacted with diethylphosphite in the presence of 10 mol% of quinine. *N*-4-Methoxyphenyl- and *N*-2-pyridylmethyl- imines did not provide any product, while *N*-phenylsulfonyl-, *N*-4-tolylsulfonyl-, and *N*-(2-nitrophenylsulfonyl)- imines gave the product with a good conversion (62 - 68 %) but a poor optical purity (30 - 39 % ee). Hydrophosphonylation of *N*-(2-pyridylsulfony)-, *N*-(6-methyl-2-pyridylsulfonyl)-, and *N*-(2-quinolylsulfonyl) imines afforded corresponding products in good to excellent yields (70 - 98 %) and good enantioselectivity (51 - 65 % ee). Having selected the *N*-(2-pyridylsulfonyl)- and *N*-(6-methyl-2-pyridylsulfonyl)- imines as the best substrates, the authors started to investigate reaction conditions for the more reactive diphenyl phosphite. In the case of *N*-(6-methyl-2-pyridylsulfonyl)-imine the enantiomeric excess increased from 64 to 71 % while with *N*-(2-pyridylsulfony)-imine the ee slightly decreased from 65 to 61 %. A significant improvement was achieved in the coupling between *N*-(6-methyl-2-pyridylsulfonyl)-imine and diphenyl phosphite when the reaction was carried out at - 40 °C: the product was obtained in almost quantitative yield with 92 % ee. With hydroquinine and hydroquinidine, at - 40 °C, the product was obtained with comparable yields and optical purity compared to quinine while, at - 78 °C, the optical purity improved to 97 % and 98 % ee. Acetylquinine was also tested at - 40 °C, but yield and ee were considerably lower (50 % and 36 % respectively) compared to other Cinchona alkaloids. From the initial screening, it was clear that *N*-(heteroarenesulfonyl)imines afforded the α-aminophosphonate in good yield and optical purities while for *N*-(arenesulfonyl)imines the results were far from good. With that in mind, the authors prepared a series of imines **94** derived from 6-methylpyridine-2-sulfonamide and various aromatic aldehydes. Imines were reacted with diphenyl phosphite (**49**) in the presence of a Cinchona catalyst (*e.g.* quinine, hydroquinine and hydroquinidine) (Scheme 2.27). All substrates provided the corresponding product **95** in excellent yields (95 - > 99 %) and optical purity was obtained in the range from 83 % to 99 % (after crystallization from hexane/ethyl acetate).

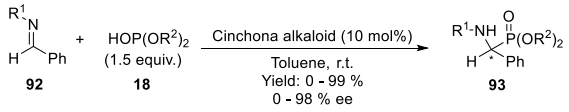

R^1 = 4-$MeOC_6H_4$, 2-$PyCH_2$, $PhSO_2$, 4-$TolSO_2$, 2-$NO_2C_6H_4SO_2$, 2-$PySO_2$, 6-Me-2-$PySO_2$, 2-QuinolylSO_2;
R^2 = Et, Ph.

Scheme 2.26. Enantioselective synthesis of α-aminophosphonates from aldimines, catalyzed by Cinchona alkaloids

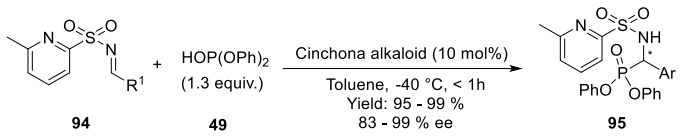

R^1= Ph, 4-Tolyl, 4-$MeOC_6H_4$, 2-$MeOC_6H_4$, 3-$MeOC_6H_4$, 4-ClC_6H_4, 1-naphthyl, 2-naphthyl, (E)-PhCHCH.

Scheme 2.27. Optimized enantioselective synthesis of α-aminophosphonates from aldimines, catalyzed by Cinchona alkaloids

After discovering an enantioselective hydrophosphonylation of aldimines, Nakamura and coworkers focused on the investigation of an enantioselective hydrophosphonylation with phosphite (**18**) of ketimine **96**, which proved to be more challenging due to the lower reactivity of the substrate.[55] Corresponding α-aminophosphonates **97** were obtained from a series of ketimines, derived from acetophenone, treated with diphenyl phosphite (3.0 equiv.) in the presence of 10 mol% of Cinchona alkaloids and 1.0 equivalents of K_2CO_3 (Scheme 2.28). In general, *N*-sulfonylketimines showed a better conversion and enantioselectivity compared to other substrates, 2,4,6-trimethylphenyl group in the substrate was found to provide the highest yield of 78 % and an ee of 59 %, using quinine as a chiral catalyst. The enantioselectivity was improved using Na_2CO_3 instead of K_2CO_3 (86 % instead of 59 %). Finally, an excellent optical purity was reached when hydroquinine and hydroquinidine were used at - 20 °C with the enantiomeric excess in the product of 97 % and 92 %, respectively. With the optimized condition in hand, the protocol was tested on a variety of *N*-2,4,6-trimethylphenylketimines **98**. The corresponding products **99** were obtained by treating **97** with 3.0 equivalents of diphenyl phosphite (**18**), in the presence of 10 mol% of hydroquinine or hydroquinidine and 1.0 equivalents of Na_2CO_3 in toluene at - 20 °C (Scheme 2.29). In general, α-aminophosphonates **99** were obtained with excellent yields (86 - 99 %) and ee (82 - 97 %). Only one substrate (R^1 = $PhCH_2CH_2$) provided a moderate optical purity giving 55 % ee with hydroquinine and 52 % ee with hydroquinidine. A further advantage of the developed methodology was the possibility to cleave 2,4,6-trimethylbenzenesulfonyl group with trifluoroacetic acid (TFA)/anisole at room temperature, providing an unprotected amino group for further modifications of the chiral pure α-aminophosphonate **100**.

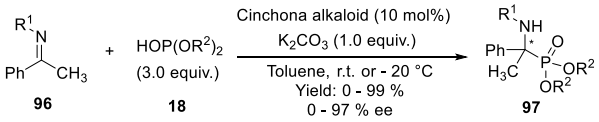

R^1 = CH_3CO, $P(O)Ph_2$, $P(O)(2\text{-thienyl})_2$, 4-$MeC_6H_4SO_2$, 2,4,6-tri-Me-$C_6H_2SO_2$, 4-MeO-$C_6H_4SO_2$, 4-Br-$C_6H_4SO_2$, 4-$CF_3C_6H_4SO_2$, 2,3,5,6-tetra-Me-$C_6H_1SO_2$; R^2 = Ph, Et, Bn

Scheme 2.28. Enantioselective synthesis of α-aminophosphonates from ketimines, catalyzed by Cinchona alkaloids

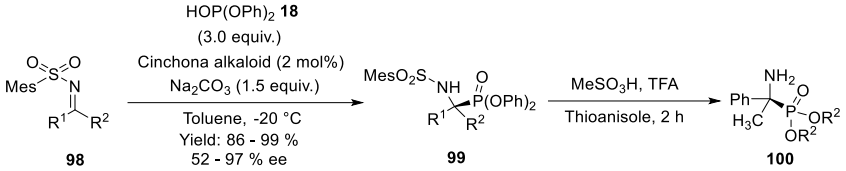

R^1 = Ph, *p*-tolyl, *p*-MeO-Ph, *p*-Cl-Ph, *p*-Br-Ph, *p*-F-Ph, *m*-Cl-Ph, *m*-Br-Ph, 2-naphthyl, $PhCH_2CH_2$, Cy;
R^2 = Me, Et; $R^1 + R^2$ = 1-indanone

Scheme 2.29. Optimized enantioselective synthesis of α-aminophosphonates from ketimines, catalyzed by Cinchona alkaloids

Cinchona alkaloids have been successfully used in the asymmetric aza-Henry reactions of imines.[56] Pettersen *et al.* explored the same organocatalyst for the asymmetric hydro-phosphonylation of imines **20**.[57] The authors started to prepare α-aminophosphonates **101** by treating the imine with diethylphosphite (**73**), in the presence of 10 mol% of quinine **102b** in toluene at room temperature (Scheme 2.30). Comparison of various catalysts (**102 - 104**) showed that the free hydroxy group in the catalyst plays a key role in this transformation because using the ester derivative **102a** and the carbamate derivative **103** provided a lower efficiency with conversions below 10 %. On the other hand, quinine **102b** and quinidine **104** afforded quantitative conversion of the starting material but only moderate enantioselectivity. The optical purity of the α-aminophosphonates was improved by swapping the *N*-tosyl imine of benzaldehyde with *N*-Boc imine of benzaldehyde, which increased ee from 48 to 68 %. As a final step of the reaction optimization, toluene was substituted with xylene further improving the ee to 80 % with quinine (**102b**) as the catalyst. With the reaction protocol in hand, the authors investigated the reaction scope on a panel of 9 different *N*-Boc imines. Substrates with both EDG (-Me, -OMe) and EWG (-Cl) on the aromatic ring gave the corresponding product in good yield with a reaction time of 48 - 72 h at 20 °C. Methyl and methoxy-substituted imines gave a higher enantiomeric excess (78 - 88 %) compared to 3-pyridinyl- and *para*-chloro-substituted imines, 48 % and 77 % ee, respectively, highlighting the role of the electronic effect in the reaction's enantioselectivity. The optical purity of the final material was increased by running the reaction at - 20 °C with a long reaction time, up to 7 days. Under these conditions, ee reached 98 %.

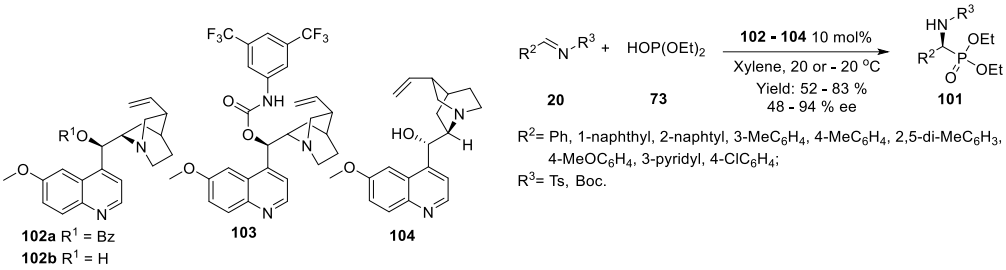

Scheme 2.30. Enantioselective synthesis of α-aminophosphonates, catalyzed by Cinchona-derived alkaloids

Cinchona alkaloid-based chiral phase transfer catalyst (PTC), was used by Li *et al.* for the stereoselective preparation of α-aminophosphonates **106** from imines **105** after the addition of phosphite **18**.[58] Using the addition of diethylphosphite to 1-(4-chlorophenyl)*N*-(6-methoxy-benzo[d]thiazol-2-yl) methanimine **105** as a model reaction, the PTC **107a** was used in combination with different bases (*i.e.* Li_2CO_3, Na_2CO_3, and K_2CO_3) in toluene (Scheme 2.31). Similar yields (90 - 95 %) and similar ee (55 - 50 %) were obtained respectively for Na_2CO_3 and K_2CO_3. However, trace of product was obtained with Na_2CO_3 when the temperature was lowered to - 20 °C. On the other hand, with K_2CO_3, at - 20 °C, the enantiomeric excess was raised to 65 %. The temperature was then further decreased to - 30 and - 40 °C, in both cases the final product was isolated with 70 % ee. With the optimized temperature and base, several chiral PTC were tested, among them, the quinine derivative containing 3,5-bis(trifluoromethyl) benzyl group **107b** showed the highest ee (96 %). Last, several aprotic solvents (*i.e.* DCM, xylene, and THF) were evaluated as an alternative to toluene. Pleasantly, with xylene, the desired α-aminophosphonate was obtained with an excellent > 99 % ee. With the proper reaction conditions in hand, the method was tested with various imines and phosphites. In all cases excellent yields (84 - 96 %) and excellent ee (84 - 99 %) were obtained, and no differences were noted with EWG or EDG on the benzylic ring of the aldehyde. Poor yields and ee were obtained when benzimidazole imine was subjected to this asymmetric catalytic reaction. The authors suspected that the poor outcome was due to weakly basic benzimidazole moiety which suppressesed the catalytic activity haltering the formation of a hydrogen bond in the transition state.

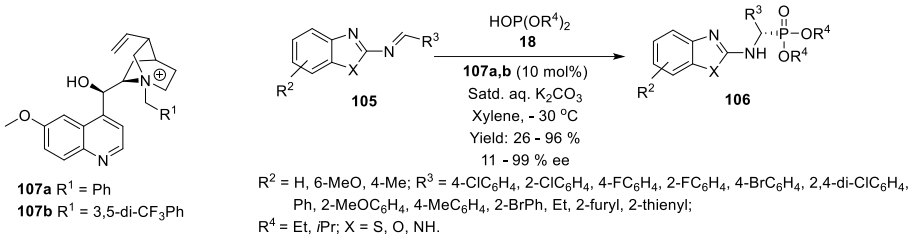

Scheme 2.31. Enantioselective synthesis of α-aminophosphonates, catalyzed by Cinchona alkaloid-based chiral phase transfer catalyst **107a,b**

2.2.4 Catalysis by chiral thioureas

Chiral thioureas have been used as catalysts for the enantioselective hydrophosphonylation with disubstituted-phosphites **18** of *N*-benzyl imines **108** for the preparation of α-aminophosphonates **109**.[59] Preliminary studies of the addition of dimethyl phosphite to *N*-benzyl-1-phenylmethanimine with catalyst **110** loading of 10 mol% at room temperature provided the corresponding product **109** with 77 % ee (Scheme 2.32). The authors investigated the effect of phosphite on the reaction outcome. Diphenyl phosphite and bis-(2,2,2-trifluoroethyl) phosphite provided the target product with a moderate enantioselectivity and a short reaction time (1 h), but the newly formed chiral centers were found to be configurationally unstable. Electron-poor phosphites provide a much more stable products but with longer reaction times. The excellent optical purity (93 % ee) was reached with phosphite bearing *ortho*-nitrobenzyl group as a substituent. The phosphite was then selected for the screening of imines. The excellent optical purity was obtained with almost all imines with ee ranging from 90 to 98 %. Only imines bearing an alkenyl side chain (3-methyl-2-butenyl), or a pyrrole derivative provided a relative low ee (81 - 82 %). The final product successfully underwent global deprotection under hydrogenolytic conditions. Obtained α-aminophosphonates were converted into α-aminophosphonic acids **54** after hydrogenation with 20 mol% Pd/C without loss of optical purity.

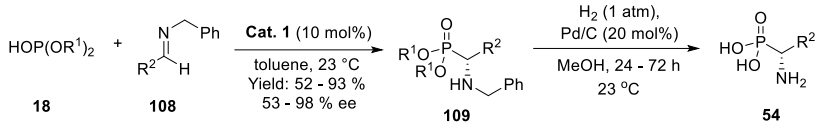

R^1 = Ph, 2,2,2-trifluoroethyl, 2-cyanoethyl, 2-chloroethyl, 2-methoxyethyl, 4-NO_2Bn, 2-NO_2Bn;
R^2 = Ph, 3-pentyl, *i*Pr, *t*Bu, *i*Bu, 4-FC_6H_4, 4-$MeOC_6H_4$, 4-$MeCO_2C_6H_4$, 2-MeC_6H_4 2-ClC_6H_4, 3-ClC_6H_4, 4-ClC_6H_4, 2-naphthyl, 3-pyridyl, 2-furyl, 2-thienyl, 2-pyrrolyl

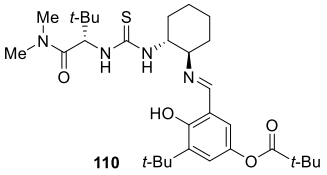

Scheme 2.32. Enantioselective synthesis of α-aminophosphonates, catalyzed by chiral thiourea **110**

Alternatively, Kumar and coworkers were interested in the enantioselective addition of phosphites **18** to a *N*-Boc ketimine **48** to construct oxindole motifs bearing both a phosphorous and nitrogen atom at the C3 position **50** (Scheme 2.33).[60] The authors investigated the catalytic activity of a series of Cinchona alkaloids (*e.g.* cinchonine, cinchonidine, quinine and quinidine), in analogous reactions to those reported previously. The target product was obtained after treatment of **48** with **18** in the presence of 20 mol% of alkaloids in THF at room temperature. The desired products were obtained in good yields (80 - 85 %) but with moderate to low enantioselectivity (28 - 46 % ee). Next, catalytic activity was assessed of 9-thiourea derivatives of Cinchona alkaloids and, among all, **111** was capable to provide both a good yield (79 %) and good enantioselectivity (73 % ee). Further reaction optimizations were carried out by screening of solvents: EtOAc (75 % ee) with a slight increase in enantioselectivity, provided to be superior compared to THF (73 % ee). Running the reaction in EtOAc at - 30 °C improved the enantioselectivity, reaching the value of 94 %. Using the optimized conditions, various derivatives of *N*-Boc ketimines and diphenyl phosphite were tested. Corresponding α-aminophosphonates were obtained in good yields (71 - 82 %), and good to excellent enantiomeric excess (71 - 94 %) when all the substrates reacted with diphenyl phosphite. Other phosphites were also investigated but provided lower yields and ee: dibenzyl phosphite provided the corresponding product with 79 % yield but only 12 % ee while diethylphosphite did not react with the substrate.

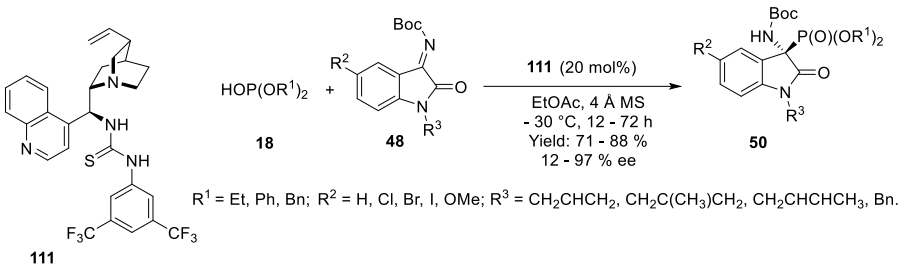

Scheme 2.33. Enantioselective synthesis of α-aminophosphonates from indolyl-3-imines, catalyzed by a chiral thiourea **111**

Chiral α-aminophosphonates **19** were prepared from amides **112** through enantioselective reductive functionalization.[61] The amides were first *in situ* converted, in an Ir-catalyzed cycle to the corresponding imines, and then the α-aminophosphonates were obtained by adding phosphite **18** in the presence of the selected organocatalyst. The authors screened a panel of organocatalysts (four chiral phosphonic acids and five chiral thiourea derivatives) using the reaction between *N*-benzyl isobutyramide and di-(2-nitrobenzyl)phosphite as a model. Chiral thiourea **113** was found to enable the preparation of the desired α-aminophosphonates in 69 % yield and 90 % ee. The transformation was achieved by treating the amide with 0.1 mol% of $[Ir(COE)_2Cl]_2$ and 2.0 equivalents of Et_2SiH_2 in toluene at room temperature, then a solution of phosphite and chiral catalyst (10 mol%) in Et_2O was added at 0 °C (Scheme 2.34). With this one-pot protocol, the authors converted a variety of amides to the corresponding α-aminophosphonates in good yields (59 - 88 %) and excellent enantioselectivities (81 - 98 %). The lower values of yield (14 - 58 %) and enantiomeric excess (40 - 79 %) were obtained when R^3 was represented by a benzyl or methyl group and when R^1 was represented by a methyl group.

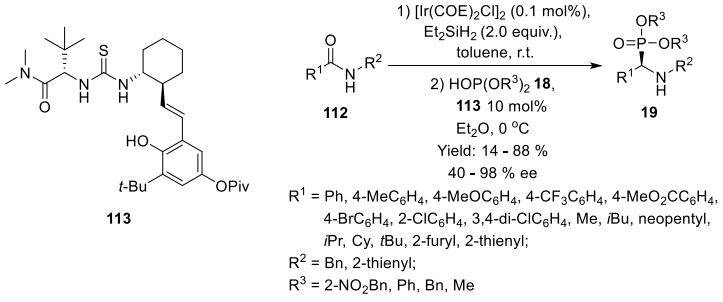

Scheme 2.34. Enantioselective synthesis of α-aminophosphonates from amides, through enantioselective reductive functionalization

2.2.5 Catalysis by proline derivatives

Thorat *et al.* successfully used chiral proline derivatives for the enantioselective one-pot synthesis of α-aminophosphonates **115** between aldehydes **29**, anilines **35**, and triethylphosphite (**114**).[62] A panel of eight organocatalysts derived from proline were initially tested on the model reaction between benzaldehyde, aniline and triethylphosphite. The reaction was carried out in EtOH and promoted by 1.0 equivalents of AcOH in the presence of 10 mol% of chiral additive (Scheme 2.35). Catalyst **116** which gave the best enantioselectivity (81 %), compared to other catalysts (29 to 68 %), was selected for the reaction optimizations, starting from the solvent effect. In water, the target product was obtained with a poor yield (46 %) and 34 % ee. Solvents such as DMF, and DMSO provided α-aminophosphonates in good yield (72 and 78 %) and (71 and 72 %) ee, while DCM and chloroform gave the product in moderate yields (45 and 47 %) and (37 and 41 %) ee. From the solvent screen, it was clear that ethanol, used to test the chiral additive, was the best medium for the reaction. With the interest to further improve the ee, the author increased the load of chiral additive, 12 mol% of catalyst was able to provide the product with 89 % ee while a 15 mol% yielded 87 % ee. With the best conditions in hand, the authors investigated the scope of the reaction. With 20 different combinations of aldehydes **29** and anilines, **35** in all cases corresponding products **115** were obtained in good yields and enantiomeric excesses. It is noteworthy to mention that a higher enantioselectivity was achieved when both aldehyde and amine were bearing electron-withdrawing substituents.

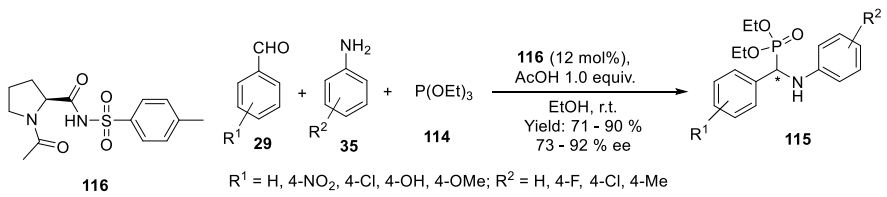

Scheme 2.35. Enantioselective synthesis of α-aminophosphonates, catalyzed by chiral proline derivative **116**

2.2.6 Synthesis with chiral auxiliaries

Chen *et al.* reported in 2008 an asymmetric procedure for the synthesis of α-aminophosphonates **118** using *N-tert*-butylsulfinamide as a chiral auxiliary.[63] Sulfinimines **117** were reacted with dialkyl phosphites **18** in the presence of 5.0 equivalents of K_2CO_3 in Et_2O at room temperature (Scheme 2.36). The authors reported that the reaction outcome was affected by the nature of the alkyl substituent of the phosphite; in fact, diisopropyl phosphite provided very poor results (yields 0 - 18 %) but, on the other hand, dimethylphosphite and diethylphosphite provided excellent de values (85 - > 95 %). The presence of an EWG on the aldehyde was able to accelerate the reaction but the product was obtained, in general, with a lower de.

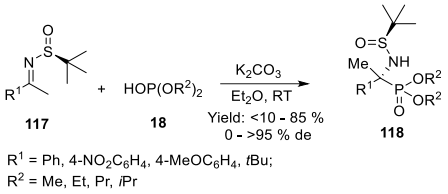

Scheme 2.36. Diastereoselective synthesis of α-aminophosphonates, promoted by *N-tert*-butyl-sulfinamide as chiral auxiliary

Similar to the previous example, *N-tert*-butylsulfinamide **119** was successfully used as a chiral auxiliary for the diastereoselective synthesis of unsaturated α-aminophosphonates **120** after reaction with phosphites **18**.[64] The research started with the investigation of the appropriate base for the model reaction between chiral (*R*)-*N-tert*-butylsulfinyl trifluoromethyl vinylketimine and diethylphosphite in DCM at room temperature. Bases, like Na_2CO_3, K_2CO_3, and DBU failed to promote the reaction, however, with Cs_2CO_3 the α-aminophosphonates were obtained with 80 % yield and 86:14 dr. The solvent screening highlighted that with acetonitrile, tetrahydrofuran and ethyl ether the desired product was not observed, while in toluene the desired product was obtained with a yield of 84 % and 82:18 dr, after 12 h. Taking into account slightly higher diastereoselectivity, DCM was selected as the optimal reaction medium. The reaction optimization was then focused on the effect of phosphites. Dimethylphosphite provided the corresponding product in 83 % yield with 84:16 dr while diphenyl phosphite did not give any product. Further screening of the bases revealed that Rb_2CO_3 was able to promote the addition of diphenyl phosphite to the chiral sulfinylimine with excellent yield (95 %) and excellent dr (90:10). For testing the scope of the reaction, ketimines **119** with various aromatic substituents at the β-position (which proven to be excellent substrates for this reaction) were reacted with diphenyl phosphite in DCM at room temperature in the presence of 1.0 equivalents of Rb_2CO_3 (Scheme 2.37). Corresponding products **120** were obtained with good yields (73 - 88 %) and excellent diastereomeric ratio (89:11 - 98:2). Only perfluoropropyl-substituted ketimine ($R^1 = C_3F_7$) failed to produce the expected product.

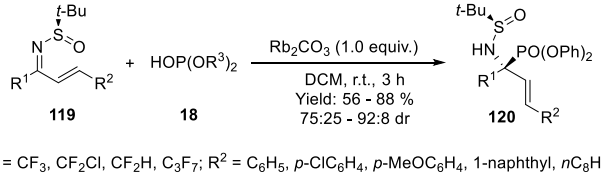

Scheme 2.37. Diastereoselective synthesis of α-aminophosphonates, promoted by *N-tert*-butyl-sulfinamide as a chiral auxiliary

Kaur *et al.* proposed the use of *N*-phosphonyl auxiliary as the pathway to access α-amino-phosphonates **122**.[65] Hydrophosphonylation proceeds with the addition of diethylphosphite (**73**) as a nucleophile to chiral imines **121** in the presence of a strong base, such as LiHDMS, which was selected among other bases (*e.g.* NaHMDS, KHMDS, LDA, *n*-BuLi and *t*-BuLi) that failed to provide good diastereoselectivity (Scheme 2.38). The authors screened also the effect of substituent on the nitrogen of the *N*-phosphonyl auxiliary (R^2), the *N*-*iso*-propyl derivative showed the best yield (97 %) with excellent diastereoselectivity (99:1) while chiral auxiliaries with *iso*-butyl and *neo*-pentyl groups did not exhibit any diastereoselectivity. With the optimized conditions, the method was tested on a variety of imines **121**, and the overall excellent results showed that substituents on the phenyl rings of the aldehyde moiety have no significant effect on both yield and diastereoselectivity. Next, the auxiliary group in α-aminophosphonates was easily deprotected after treatment with 4 N HCl in MeOH and the amine functionalized with benzyl chloroformate (CbzCl), in order to generate product **123**.

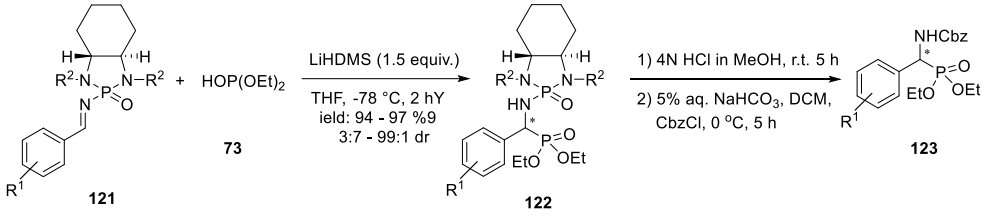

R^1 = H, *2*-Cl, *2*-F, 2-Br, 2-Me, 4-F, 4-Br, 4-Me, 4-MeO
R^2 = Bn, *i*Bu, neo-Pentyl, CH_2-1-Naphtyl, *c*pent, *i*Pr

Scheme 2.38. Diastereoselective synthesis of α-aminophosphonates, promoted by *N*-phosphonyl chiral auxiliaries

As previously reported (Section 2.2.3), Cinchona alkaloids were applied as catalysts in the asymmetric synthesis of α-aminophosphonates. Boratyński and a coworker used Cinchona alkaloids as a chiral auxiliary for the starting imine **124**.[66] The hydroxy group in the quinine molecule was converted to NH_2 which formed an imine with *para*-chloro-benzaldehyde. This substrate was then converted to a chiral phosphonate **125** after a reaction with diethyl phosphite (**73**) in toluene at 90 °C in the presence of 2.5 equivalents of K_2CO_3 (Scheme 2.39). Initial screening of the reaction conditions showed that, in order to achieve a good conversion, it was necessary to use a base like K_2CO_3, heating (90 °C) and a long reaction time (5 days) to obtain 60 % of the product as a single diastereoisomer (NMR assay). It is worth mentioning that when dimethyl phosphite was used instead of diethyl phosphite only a complex mixture was obtained with a trace of the desired product.

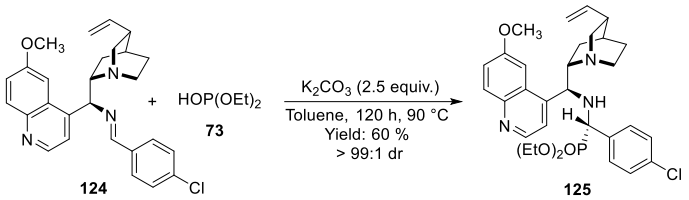

Scheme 2.39. Diastereoselective synthesis of α-aminophosphonates, promoted by Cinchona alkaloid chiral auxiliary

An uncatalyzed one-pot, three-component synthesis of α-aminophosphonates **127, 128** from chiral amines **126** was developed by Tibhe *et al.*[67,68] The target product was obtained as a mixture of two diastereomers with a predominance of the (*R*,*S*)-diastereomers **127**, in reactions of aliphatic and aromatic aldehydes **21** with dimethylphosphite (**65**) and chiral (*S*)-α-methylamines (Scheme 2.40). It was reported that steric hindrance was not a problem for the yield since isobutyraldehyde and pivalaldehyde afforded the corresponding product with excellent yield. (*S*)-α-Ethylbenzylamine provided similar results to (*S*)-α-methylbenzylamine. Swapping the phenyl to 1-naphthyl on the α-position of the chiral amine did not improve diastereoselectivity. On the other side (*S*)-3,3-dimethyl-2-butylamine provided better diastereoselectivity, on a panel of different aldehydes with a diastereomeric ratio up to 93:07. The methodology was developed using microwave irradiation as a heating source, and the protocol allows shorter reaction time (12 minutes) compared to the 5 - 8 h in the classical method.

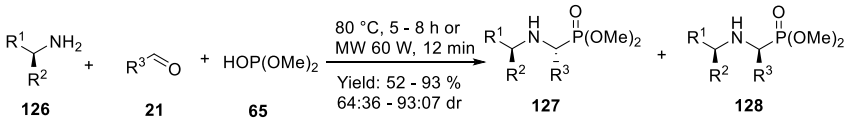

R^1 = Ph, 1-naphthyl, *t*Bu; R^2 = Me, Et; R^3= Ph, 4-ClC_6H_4, 4-MeOC_6H_4, *i*Bu, *i*Pr, *t*Bu.

Scheme 2.40. Diastereoselective uncatalyzed synthesis of α-aminophosphonates, promoted by chiral amines as reaction components

Magnesium dodecyl sulfate was used as a catalyst for a three-component one-pot reaction between (*S*)-α-methylbenzylamine (**129**), diphenyl phosphite (**49**) and an aldehyde (**21**) (*i.e.* benzaldehyde, octanal and cyclohexanecarboxaldehyde) in water at room temperature (Scheme 2.41).[69] This model reaction was used to study the effect of the catalyst on the yield of the corresponding α-aminophosphonates (**130** and **131**). Magnesium, aluminum, calcium, and sodium dodecyl sulfates were tested, and the best yield was achieved with 0.1 equivalents of magnesium dodecyl sulfate. Organic solvents like DCM and THF were also tested but both afforded a lower yield than water. Finally, the authors reported that the use of diethylphosphite, in a moderate excess (2.0 equiv.), was able to increase the yield from 89 to 97 %. On the other hand, when used in combination with (*S*)-α-methylbenzylamine (**129**), provided a lower yield (53 %) compared to the

reaction with triethylphosphite (77 %). However, using diphenyl phosphite, with 1.0 equivalents of triethylamine as an additive increased the product yield to 77 %, and even higher yields were obtained with sparteine and triisopropylamine (87 and 80 %, respectively). For all experiments, the diastereoselectivity remains the same 76:24 dr. In a similar work, (*S*)-α-methylbenzylamine (**129**) and (*R*)-α-methylbenzylamine (**132**) were used to prepare corresponding α-aminophosphonates (**134** and **135**).[70] The transformation was achieved by reacting the 1.0 equivalents of amine with 1.0 equivalents of 5-hydroxymethylfurfural (**133**) and 1.5 equivalents of diethylphosphite with the presence of 5 mol% of I_2 at 50 °C (Scheme 2.42). The products were obtained in good yields (70 and 72 %) and a dr in accordance with similar experiments: 77:23 for **134** and 78:22 for **135**.

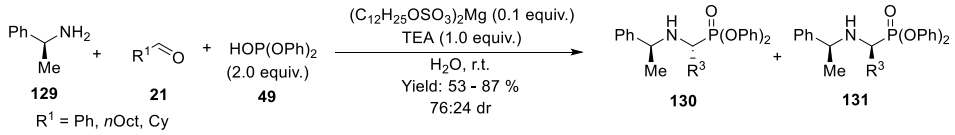

Scheme 2.41. Diastereoselective synthesis of α-aminophosphonates, catalyzed by magnesium dodecyl sulfate

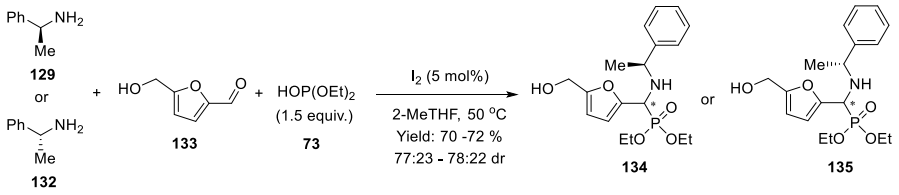

Scheme 2.42. Diastereoselective synthesis of α-aminophosphonates, catalyzed by I_2

Likewise, Bedolla-Medrano *et al.* reported the diastereoselective preparation of α-aminophosphonates **138** and **139** generated from the chiral (*S*)-α-methylbenzylamine (**129**), benzaldehyde (**136**) and dimethyl or diethylphosphite **18** using catalytic amount (10 mol%) of phenylphosphonic acid (**137**) under solvent-free conditions (Scheme 2.43).[71] The catalyst was selected from five different phosphorous acids (*e.g.* diphenyl phosphinic acid, diphenyl phosphite, phenylphosphinic acid, propylphosphonic acid and phenylphosphonic acid). The protocol was tested both with dimethylphosphite and diethylphosphite. The diastereoselectivity of the target products **138** and **139** was reported as follows: dr of 76:24 for dimethylphosphite and 80:20 for diethylphosphite.

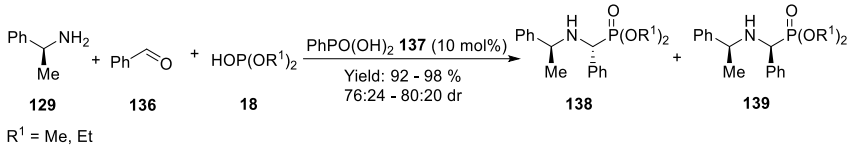

Scheme 2.43. Diastereoselective synthesis of α-aminophosphonates from chiral amines, catalyzed by phosphorous acid

Another kind of chiral α-aminophosphonates **141** and **142** were prepared by Todorov and coworkers during the development of a molecule with cytotoxic properties against several malignant cell lines (HT-29, MDA-MB-231, HepG2 and HeLa).[72] The compound was obtained, with a yield of 34 % and the diastereoisomeric ratio of 60:40 after a reaction between a chiral amine **140**, benzaldehyde (**136**) and dimethylphosphite (**65**) in methanol at 65 - 70 °C in the presence of 2.7 equivalents of triethylamine (Scheme 2.44).

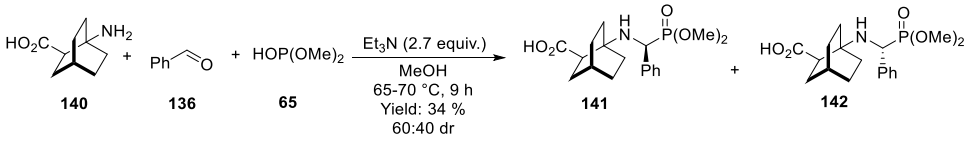

Scheme 2.24. Diastereoselective synthesis of α-aminophosphonates from chiral amines catalyzed by triethylamine as an additive

Chiral carbamates were used for the first time as chiral auxiliaries by Oshikawa *et al.*[73] The optical active nitrogen compounds **146** and **147** were prepared from (-)-menthol (**143**) and camphor derivative **144**, then the carbamate was reacted with aldehyde **21** and triarylphosphite **24** according to the Oleksyszyn's method, using an excess of AcOH to promote the reaction. After the formation of the target α-aminophosphonate, the carbamate bond was cleaved with concentrated hydrochloric acid and the phosphonate esters **146** and **147** were converted to phosphonic acid **54** after the reaction with propylene oxide (Scheme 2.45). Obtained ee was assessed by optical rotation. (-)-Menthyl carbamate **146** provided corresponding α-aminophosphonates **148** in yield between 45 and 54 % and ee between 8 and 42 %. The highest ee was obtained when benzaldehyde was used while the lowest was obtained with acetaldehyde. The use of tri(*o*-methylphenyl)phosphite showed little effect on the enantioselectivity compared to triphenylphosphite. A carbamate derived from camphor derivative **144** provided comparable yields (45 - 51 %) of α-aminophosphonates **149** with respect to (-)-menthyl carbamate, but a lower overall ee, ranging from 13 to 25 %. Also in this case benzaldehyde provided better results compared to acetaldehyde. A second study of asymmetric synthesis of α-aminophosphonates using carbamates as chiral auxiliaries was performed by Chung and collaborators.[74] Similar to the Oshikawa's work, carbamate was generated from (-)-menthol and a series of derivatives of (1S)-(+)-10-camphorsulfonic acid **144**. Chiral carbamates were reacted with an aldehyde **21** and disubstituted phosphite **18** in acetyl chloride at 0 °C to generate

corresponding α-aminophosphonates **149** (Scheme 2.45). In the first screening camphor-sulfonamide-based chiral auxiliaries provided better results (96.4 - > 99 % de) compared with (-)-menthyl carbamate **146** (14 %). The best results among camphor derivatives were achieved with a bulky R^1 = -CH_2-SO_2-N(cyclohexyl)$_2$ which was selected for the following screening of aldehydes. Four aldehydes provided good results in terms of yield (75 - 79 %) and dr (> 99 %) except for cyclohexanecarbaldehyde, which dr was 56 %. This lower result might be attributed to a higher rotational freedom on the C_α-alkyl bond in its *N*-acylimine or iminium ion intermediate.

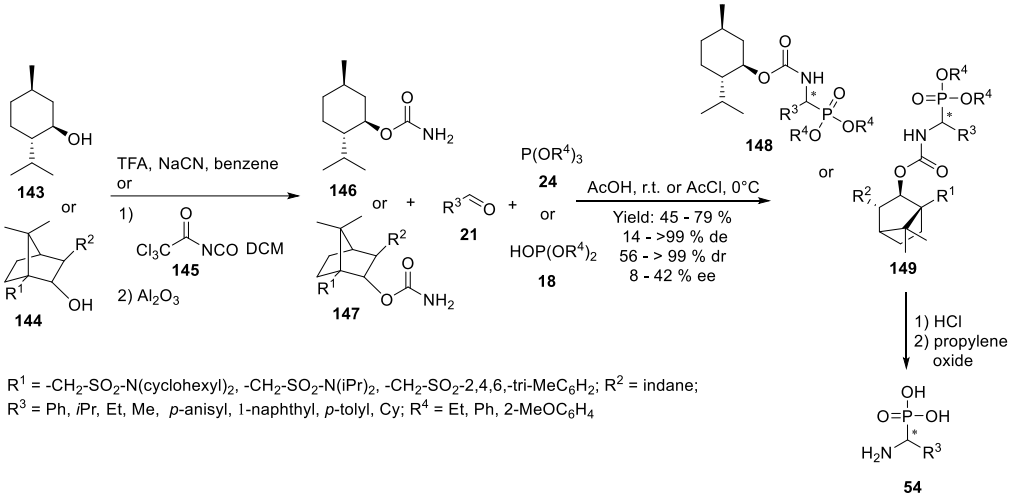

Scheme 2.45. Diastereoselective synthesis of α-aminophosphonates from chiral carbamates, catalyzed by acetic acid or acetyl chloride

2.2.7 Selection of stereoselective protocol for the preparation of UAMC-00050

In section 2.2 we describe different strategies for the stereoselective preparation of α-aminophosphonates. We decided to begin our investigation with the most simple methods. The *L*-proline complex was found to be an interesting starting point for the one-pot three-component enantioselective synthesis of α-aminophosphonates. On the other hand, the chiral carbamate strategy was selected to test the diastereoselective synthesis of α-aminophosphonates.

2.3 Green Chemistry approach to the synthesis of the key aldehyde

According to the principles of green chemistry, every reaction in a chemical process should aim for the best atom economy which is calculated as the total mass of the desired product divided by the mass of the reactants.[75] According to medicinal chemistry research, preparation of the key aldehyde **7** in the current synthetic route is carried out by oxidation of the corresponding primary alcohol **6** with (DMP). Under these reaction conditions, the achieved atom economy is 36 %. DMP

also presents some concerns regarding its safety since it is a high energy molecule. Dallaston *et al.* reported that this hypervalent iodonium compound underwent an exothermic decomposition with onset temperatures of 116 °C.[11] Decompositions were highly exothermic and the oxidant was flagged by Yoshida correlations.[76] With views of a potential scale up and process development of UAMC-00050 an alternative to DMP was required to find a safer and more efficient synthetic method for the preparation of aldehyde (**7**). Preferably, those methods should not include the use of other hypervalent iodonium derivatives and use cheaper oxidants.

In the past decades, several reviews have collected methods for selective catalytic oxidation of primary alcohols to aldehydes. Parmeggiani *et al.*[77] reported a series of reactions using oxygen as a primary oxidant in the presence of transition metal as a catalyst. Wertz et al,[78] on the other hand, focused the review on a series of reactions catalyzed by nitroxides instead of transition metals. Heravi et al,[79] reported the catalytic preparation of aldehydes with hydrogen peroxide as a primary oxidant. Herein we review a series of published reaction protocols that could be useful for the preparation of UAMC-00050 intermediate **7** including its further upscale.

2.3.1 Oxidation with O_2 or Air

Assal *et al.* reported the synthesis of catalytic zinc oxide-manganese carbonate nanoparticles via a facile and straightforward coprecipitation procedure.[80] The ZnOx–$MnCO_3$ catalyst, used in 1.0 mol% loading exhibited excellent performance and selectivity in the aerobic oxidation of 1-phenylethanol, where 100 % conversion and more than 99 % product selectivity were obtained in 5 minutes with superior specific activity (48 $mmol \cdot g^{-1} \cdot h^{-1}$) and 390.6 turnover frequency (TOF). The scope of the oxidation process was extended to different types of alcohols **150**. Various primary, benzylic, aliphatic, allylic, and heteroaromatic alcohols were selectively oxidized into their corresponding aldehydes **151** with 100 % conversion without overoxidation to the carboxylic acids under base-free conditions (Scheme 2.46). This catalytic system offers several advantages including complete alcohol conversions, extremely high specific activities, and selectivity towards target products in extremely short reaction times by using an eco-friendly, low-cost, and reusable heterogeneous catalyst.

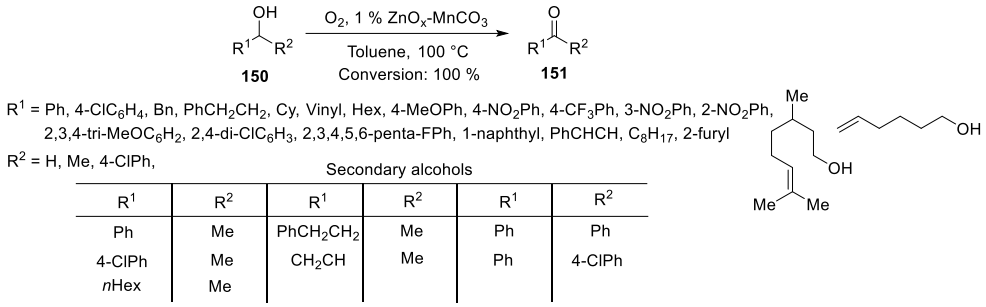

Secondary alcohols

R^1	R^2	R^1	R^2	R^1	R^2
Ph	Me	$PhCH_2CH_2$	Me	Ph	Ph
4-ClPh	Me	CH_2CH	Me	Ph	4-ClPh
*n*Hex	Me				

Scheme 2.46. Aldehyde synthesis by aerobic oxidation catalyzed by zinc oxide nanoparticles doped with manganese carbonate

Kim *et al.*[81] reported that the combination of (2,2,6,6-tetramethylpiperidin-1-yl)oxyl (TEMPO) (10 mol%)/Ceric ammonium nitrate (CAN) (10 - 20 mol%) can be used for the effective oxidation of most of the benzyl, benzylic, and allylic alcohols **152** into their corresponding carbonyl compounds **153**. The authors also reported that steric hindrance has been observed with some substituted allylic systems and aliphatic alcohols, such as cyclohexanols, which showed no reactivity towards the oxidative process. The new protocol was tested on 6 substrates (Scheme 2.47). Reflux in MeCN was fundamental to achieving decent yields. Primary benzyl alcohol reacts quite fast (2.5 h) while substituted allylic alcohols gave the product good yields with a relatively longer reaction time.

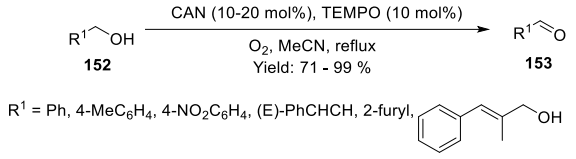

Scheme 2.47. Aldehyde synthesis promoted by O_2 and catalyzed by CAN/TEMPO

Hoover and coworkers developed a protocol that allows the selective oxidation of alcohols **152** to aldehydes **153** using copper catalysis and air as the primary oxidant (Scheme 2.48).[82,83] The authors began the study with conditions screening for the oxidation of (*E*)-4-hexen-1-ol. Both Cu (I) and Cu (II) were tested, where $CuBr_2$ and CuBr were the most effective catalysts for a small-scale process, but the reaction would occasionally form insoluble precipitates and fail to reach complete conversion of the starting material even after 24 h. On the other side $[Cu(MeCN)_4]OTf$ afforded the corresponding aldehyde in quantitative yield. TEMPO and di-*tert*-butyl azodicarboxylate (DBAD) were the two cocatalysts tested during the screen. DBAD was discarded after the failure to convert all the starting material. Among the two bases tested *N*-methylimidazole (NMI) was found superior to KO*t*Bu. 2,2′-Bipyridine (bpy, **154**) was selected as the ligand for copper. Finally, five different solvent systems were tested (DMF, $MeCN/H_2O$, $PhCF_3$, toluene,

MeCN) and pure MeCN was able to provide the highest yield of the target product. The new protocol was tested on 35 different alcohols, in most cases, the product was obtained with moderate to excellent yield (72 - > 98 %). In the case of 2-(2,2-dimethyl-1,3-dioxolan-4-yl)ethan-1-ol and 3-(methylthio)propan-1-ol poor yields were recorded, 47 and 25 % respectively. This behavior is due to the fact that the phenethyl alcohol overoxidized while phenol-containing molecules inhibited the catalyst providing no conversion.

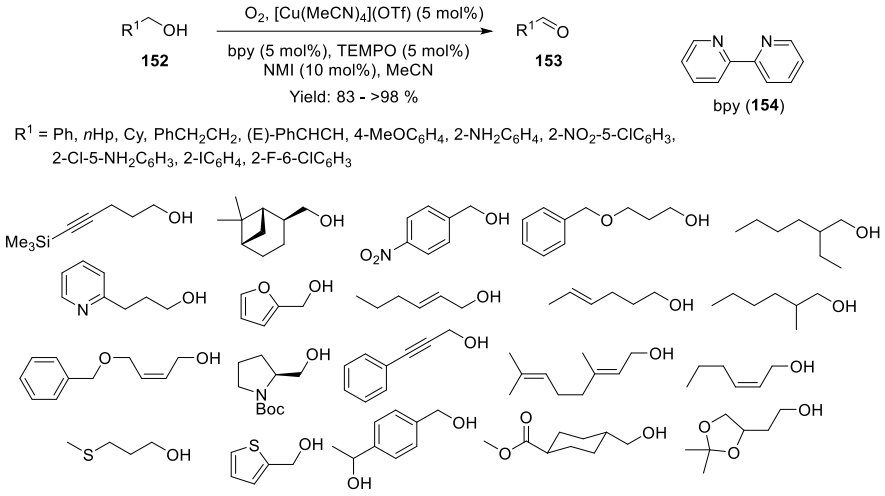

Scheme 2.48. Aldehyde synthesis catalyzed by copper-bpy complex, TEMPO and NMI

A copper (I)/9-azabicyclo[3.3.1]nonane *N*-Oxyl (ABNO)/O_2 method for the selective oxidation of alcohols **152** to aldehydes **153** was developed by Steves *et al.*[84] (Scheme 2.49). To improve the copper (I)/TEMPO/O_2 protocol, the authors decided to exchange the TEMPO with the more reactive ABNO (**156**). Oxidation of cyclohexanemethanol to cyclohexanecarbaldehyde was selected as a model reaction. First, the ligand type was tested, and numerous mono- and bidentate nitrogen ligands were evaluated in combination with CuOTf/ABNO. The highest yield was obtained with ^{MeO}bpy (**155**) and the focus was moved to the screening of the copper source. $Cu(MeCN)_4OTf$ proved to be superior compared to CuBr, $CuBr_2$ and CuI. A higher yield was obtained when the load of ABNO was decreased from 5 mol% to 1 mol%. NMI was found to be superior to 4-dimethylaminopyridine (DMAP) as an additive. With the best conditions in hand, the protocol was tested on a panel of various alcohol substrates. In all cases, excellent yields were obtained and the methodology proved to be compatible with various functional groups, including ethers, thioethers, heterocycles, amides, alkenes, and alkynes. A slower reaction rate was observed with 3-hydroxymethylindole and the highly electron-deficient 4-chloro-2-nitrobenzyl alcohol where it was necessary to heat the reaction to 50 °C.

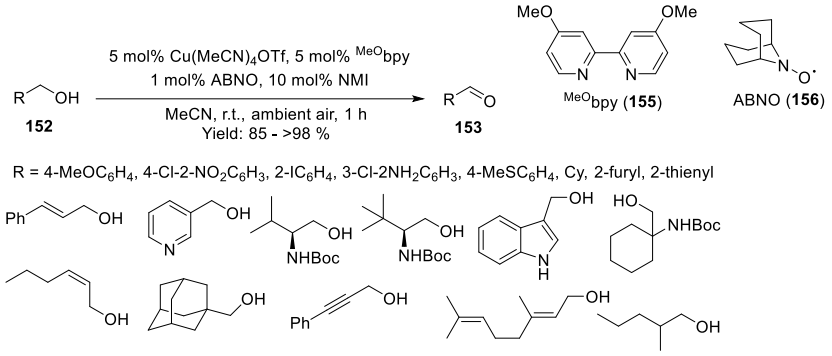

Scheme 2.49. Aldehyde synthesis by oxidation with Cu(I)/ABNO/O_2 system

Xu *et al.* developed copper-catalyzed aerobic oxidation of alcohols **152** to aldehydes **153** without using TEMPO[85] (Scheme 2.50). Recently the catalytic enzymatic reactivity of tyrosinase was mimicked by $[Cu(MeCN)_4]PF_6$ complex with a *N*,*N*'-di-*tert*-butyl-ethylenediamine.[86] The same complex was tested for the oxidation of 1-octanol to the corresponding aldehyde. No significant conversion was noticed in the presence of 4 mol% $[Cu(MeCN)_4]PF_6$ and 5 mol% of *N*,*N*'-di-*tert*-butyl-ethylenediamine, which prompted further screening of reaction conditions. In particular, the effect of a nitrogen base on the reaction was assessed. While strong Brønsted bases, such as DBU, 1,4-diazabicyclo[2.2.2]octane (DABCO), or *N*,*N*-diisopropylethylamine (DIPEA), were ineffective, heterocyclic bases, such as pyridine, NMI, or DMAP, had a positive effect on the reaction. DMAP provided the highest yield (92 %). The reaction can also work with air instead of oxygen but the complete conversion required a longer time to be achieved. The optimized conditions were tested on a panel of primary alcohols. The protocol tolerates several functional groups including silyl, ester, carbamate, alkenes, alkyl halides, and nitro groups.

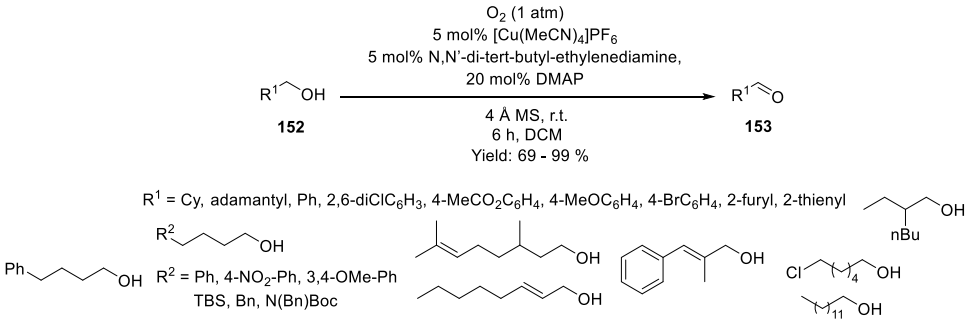

Scheme 2.50. Aldehyde synthesis by aerobic oxidation catalyzed by Cu(I)/DBED/DMAP

2.3.2 Oxidation with H_2O_2

A zinc-catalyzed oxidation of benzyl alcohols by hydrogen peroxide was developed by Wu.[87] A series of zinc salts ($ZnBr_2$, ZnI_2, ZnF_2, $Zn(OTf)_2$, $Zn(OAc)_2$, $Zn(TFA)_2$, $Zn(CN)_2$) were tested in the oxidation of benzyl alcohols by 4.0 equivalents of H_2O_2. $ZnBr_2$ was selected as the best salt with 64 % conversion, and the author tested five commonly used ligands, where pyridine-2,6-dicarboxylate (**157**) showed the highest efficiency: conversion reached 100 % and when the reaction was carried out in THF instead of MeOH yield of the aldehyde raised from 61 % to 91 %. The generality of the methodology was tested on 14 various substrates **152** providing corresponding aldehydes **153** in good to excellent yields (77 - 97 %). Moderate yields were obtained in the preparation of *para*-methoxy-benzaldehyde (65 %) and furfuraldehyde (53 %) (Scheme 2.51).

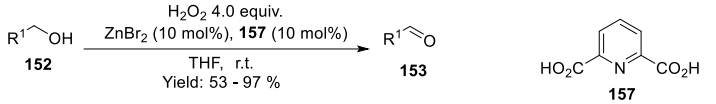

R^1 = 3-MeC_6H_4, 4-*i*-PrC_6H_4, 4-$MeOC_6H_4$, 1-naphthyl, 2-naphthyl, 2-ClC_6H_4, 4-ClC_6H_4, 3-ClC_6H_4, 2-FC_6H_4, 3-FC_6H_4, 4-$CF_3C_6H_4$, 3-CNC_6H_4, 2-furyl, 3-furyl

Scheme 2.51. Aldehyde synthesis by oxidation with H_2O_2 catalyzed by $ZnBr_2$ in the presence of pyridine-2,6-dicarboxylic acid (**157**) as a ligand

Syiemlieh and coworkers used a copper complex $[CuZn(bz)_3(bpy)_2]PF_6$, instead, which could be prepared from commercially available starting materials. With this catalyst loading 0.7 mol%, it could mediate the oxidation of alcohols **152** to aldehydes **153** in the presence of 2.0 equivalents of hydrogen peroxide at 70 °C (Scheme 2.52).[88] An initial screening on the oxidation of benzyl alcohol to benzaldehyde showed that employing solvent-free conditions can provide a higher yield (75 %) compared to other reaction mediums (*e.g.* toluene, benzene, DCM, MeCN, xylene, EtOAc, hexane). The optimized conditions were tested on 14 various alcohols and the corresponding aldehyde was obtained in general with high yields (75 - 98 %). Only stearyl alcohol afforded the corresponding aldehyde with a poor result (22 %). Any further oxidation to carboxylic acids was not noted and the catalyst can be reused without loss of activity over five cycles.

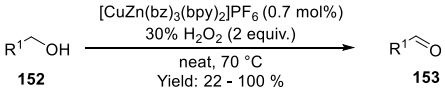

R^1 = Ph, 4-$MeOC_6H_4$, 2-MeC_6H_4, 3-MeC_6H_4, 4-MeC_6H_4, 3-ClC_6H_4, 4-$NO_2C_6H_4$, (*E*)-PhCHCH, 3,4,5-tri-$OMeC_6H_2$, *n*Pr, *n*Bu, $C_{18}H_{37}$, 2-furyl, 2-thienyl

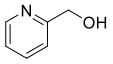

Scheme 2.52. Aldehyde synthesis by oxidation with H_2O_2 catalyzed by Copper-Zinc complex

Wagh *et al.* developed a protocol for the oxidations of alcohols **152** to aldehydes **153** using hydrogen peroxide as oxidant and lactic acid as solvent and oxidation promoter.[89] The authors

started to test the H_2O_2/lactic acid combination on the oxidation of benzyl alcohol and the reaction was carried out at 30 °C (Scheme 2.53). Initially, the required excess of H_2O_2 was investigated, and it was found that a complete conversion can be achieved with only 1.07 equivalents. Any further increase led to an overoxidation to the acid side product. Reaction media other than lactic acid (*e.g.*, MeCN, EtOAc, MeOH, $CHCl_3$) failed to provide complete conversion. The authors also investigated other oxidants such as *m*-CPBA and TBHP, that provided only 77 % and 66 % conversions in 7 h, while benzoyl peroxide showed only 58 % conversion of benzyl alcohol. Finally, several reaction temperatures were also tested, the conversion at 15 °C, 20 °C, and 25 °C was 43 %, 61 %, and 89 % respectively. Only at 35 °C a complete conversion was reached but with a decrease in selectivity. The generality of the protocol under optimized reaction conditions was tested by using various primary aromatic benzyl alcohols bearing electron-donating and withdrawing groups. Corresponding aldehydes were obtained in excellent yields (87 - 97 %). The lower results were recorded with the aliphatic alcohol *n*-BuOH and *i*-PrOH, 81 % and 80 %, respectively.

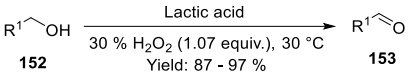

R^1 = Ph, 4-MeC_6H_4, 4-$MeOC_6H_4$, 4-ClC_6H_4, 4-BrC_6H_4, 4-FC_6H_4, 4-CNC_6H_4, 4-$NO_2C_6H_4$, 4-OHC_6H_4, 4-$CO_2HC_6H_4$, 3-OHC_6H_4, 3-MeOPh, (E)-PhCHCH, 2-furyl, 2-thienyl

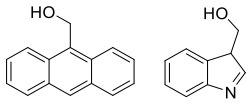

Scheme 2.53. Aldehyde synthesis by oxidation with H_2O_2, promoted by lactic acid

A cobalt zeolitic imidazolate framework (ZIF-9@ Zeolite) was synthesized by Hashemian and collaborators from cobalt (II) nitrate, benzylimidazole and zeolite.[90] The ZIF-9@ Zeolite was tested as a catalyst for the selective conversion of benzyl alcohols (**158**) to benzaldehydes (**29**) with H_2O_2 (Scheme 2.54). Using the model reaction with benzyl alcohol, the authors screened several solvents. Among nine solvents and one mixture (H_2O, DCM, MeCN, *n*-hexane, MeOH, $CHCl_3$, EtOH, DMF, toluene and MeCN/H_2O 1:1 v/v) the best yield (98 %), was obtained when the reaction was carried out in the water. Then, with the best solvent in hand, the focus was moved to the reaction temperature. From 25 °C the temperature was sequentially increased to 40, 60, and 80 °C. The conversion was found to increase with the increasing temperature, and the highest catalyst activity was achieved at 80 °C. The optimized protocol was tested on 14 various substrates. Excellent yields were obtained in all the cases, regardless of the presence of an EWG or an EDG. Finally, the recyclability of the catalyst was tested over four cycles showing a decrease in yield from 5 to 10 % at each cycle.

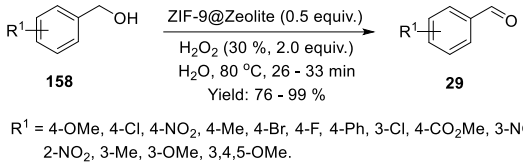

Scheme 2.54. Aldehyde synthesis by oxidation with H_2O_2 catalyzed by ZIF-9@ Zeolite

Aluminum chloride was used to promote the oxidation of benzyl alcohols **158** or phenethyl alcohol (**159**) to benzaldehydes **29** or phenylacetaldehyde (**160**) with hydrogen peroxide (Scheme 2.55).[91] Using the oxidation of benzyl alcohol to benzaldehyde as a model reaction, first, an excess of H_2O_2 was optimized. It was found that 3.0 equivalents of H_2O_2 (25 - 30 % aq. solution) was necessary for a complete conversion of the substrate in MeCN at 45 °C in 2 h. The optimum amount of $AlCl_3$, required for the complete conversion, was 4.5 equivalents. With the optimized conditions in hand, the scope of the reaction was investigated. Benzyl alcohol was transformed into benzaldehyde with a conversion of 92 %. Benzyl alcohol derivatives such as 2-methyl benzyl alcohol and 3-methyl benzyl alcohol were oxidized with 95 and 99 % conversion, respectively. In the case of 2-methyl benzyl alcohol, it was observed a 2:1 ratio between the aldehyde and the carboxylic acid, while 2-phenylethanol was selectively converted to the aldehyde but with a poor yield of 9 %.

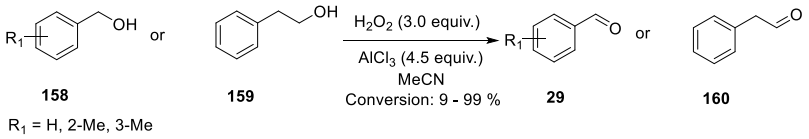

Scheme 2.55. Aldehyde synthesis by oxidation with H_2O_2 catalyzed by $AlCl_3$

Moriyama *et al.* developed halide-catalyzed selective oxidation of benzyl alcohols **158** to benzaldehydes **29** using hydrogen peroxide as the primary oxidant (Scheme 2.56).[92] The investigation began using the model reaction of oxidation of 5-nonanol to the corresponding ketone. Solvents, and metal bromide catalysts were screened. The reaction was initially tested in MeCN/H_2O (9:1 v/v), EtOAc/H_2O (9:1 v/v) and DCM/H_2O (9:1 v/v), the best results were obtained when the reaction was carried out in DCM/H_2O and any different medium or ratio led to a lower yield. KBr proved to be superior to other metal halides like LiBr, NaBr, $CaBr_2$, KCl, KI. Decreasing the amount of KBr to 0.1 equivalents leads to a decrease in yield. Lower yields were obtained when the Brønsted acid $PhSO_3H$ additive was changed to other compounds including $MeSO_3H$, $(PhO)_2P(O)OH$, *p*-NO_2-$PhSO_3H$, TFA. Under the optimized conditions, the method provided a very selective conversion of benzyl alcohols **158** to benzaldehydes **29**. The addition of 0.1 equivalents of TEMPO was found pivotal to avoid the overoxidation to carboxylic acid. The H_2O_2/KBr/$PhSO_3H$/TEMPO method was tested on five substrates providing corresponding aldehydes with excellent yields.

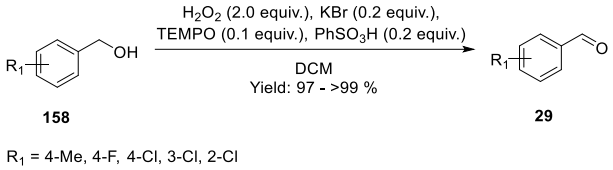

Scheme 2.56. Aldehyde synthesis by oxidation with H_2O_2 catalyzed by KBr/TEMPO/$PhSO_3H$ system

2.3.3 Synthesis of aldehydes promoted by NaClO

Since its discovery,[93] oxidation of primary alcohols to aldehydes with NaClO in aq. biphasic systems gained a lot of attention due to the simplicity, safety, and high efficiency of the process. Modern variations of the transformation include a continuous process for the oxidation of alcohol **152** to aldehyde **153** which was accomplished by Hampton *et al.*[94] The authors employed a spinning tube-in-tube (STT) reactor, that was fed with an organic solution of the substrate, TEMPO (0.01 mol%) and *n*Bu_4NBr (0.05 mol%) in toluene or DCM, and an aqueous solution of bleach diluted with a saturated aqueous solution of sodium bicarbonate (1:1, pH = 8.5). The reactor was cooled at 0 °C and the residence time was kept between 27 seconds and 172 seconds (Scheme 2.57). The methodology was tested on six different substrates, in all the cases the corresponding aldehyde was obtained with good to excellent yield (76 - 99 %) except for the phenethyl alcohol at 0 °C that provided only an 11 % of aldehyde but when the temperature was raised to 25 °C the aldehyde was obtained with 70 % yield. The continuous process provided better yields of aldehyde products and increased the reaction rates compared to the batch process. Also, it provides a basis for a reliable upscale of this reaction.

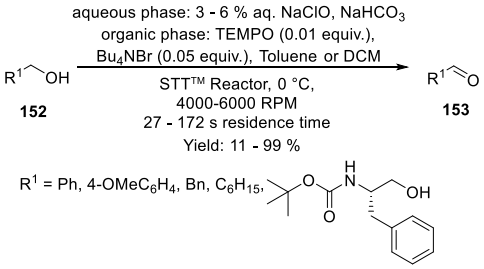

Scheme 2.57. Aldehyde continuous synthesis in STT reactor by oxidation with NaClO catalyzed by TEMPO and Bu_4NBr

Dong and coworkers developed chemoselective oxidation of alcohols **152** to aldehydes **153** using NaClO as the primary oxidant and morpholinone nitroxide **161** as an analogue of TEMPO (Scheme 2.58).[95] The catalyst was prepared in 2 steps starting from the cheap 1-amino-2-methylpropan-2-ol. The protocol was tested on 16 examples of benzyl alcohols, containing EDG or EWG, and both provided excellent yields (81 - 91 %). Only secondary alcohols did not react, making the protocol chemoselective for primary alcohols.

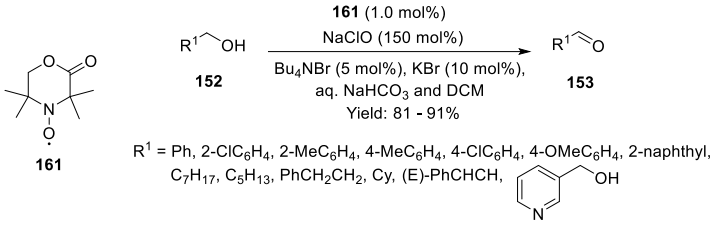

Scheme 2.58. Aldehyde synthesis by oxidation with NaClO, catalyzed by morpholinone nitroxide **161**

Wang *et al.* reported the preparation and the use of a novel solid-phase catalyst for the conversion of alcohols **152** to aldehydes **153** consisting of TEMPO-functionalized multiwalled carbon nanotubes (MWNTs) (Scheme 2.59).[96] Commercially available carbon nanotubes were treated with concentrated nitric acid to create carboxylic acid groups directly on the surface of MWNTs. Oxidized MWNTs were converted to corresponding acyl chlorides and coupled with 4-hydroxy-2,2,6,6-tetramethylpiperidine-1oxyl (HO-TEMPO). The TEMPO loading on the nanotubes was calculated to be 0.74 mmol/g. Oxidation of benzyl alcohol to the corresponding aldehyde was achieved with 1.25 equivalents of NaClO as the primary oxidant, 0.1 equivalents of KBr as a co-catalyst and 1.6 equivalents of $KHCO_3$ as a base to keep the pH at 9.1. The complete conversion was reached after 5 minutes when MWNTs with lower loading of TEMPO was used (0.21 mmol/g of TEMPO), only 60 % conversion was reached in the same amount of time. The methodology was tested on a panel of alcohols. In all cases, complete conversion was reached in 5 minutes, proving that the electronic properties of the substituent on the benzene rings have a negligible influence on the reactivity in the case of primary benzylic alcohols. After the completion of the oxidation, the catalysts were separated from the reaction mixture by filtration, thoroughly washed with water and DCM, and then reused in the next run under the same conditions. Catalysts were recycled for six consecutive reactions without any loss in catalytic activity and only after the seventh run, the activity of catalysts decreased to a certain extent.

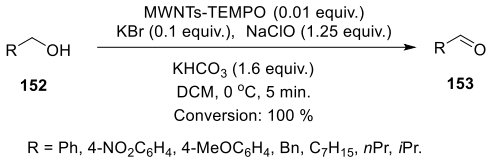

Scheme 2.59. Aldehyde synthesis by oxidation with NaClO, catalyzed by TEMPO-MWNTs

A polymer-immobilized TEMPO-derivative (PIPO) was used by Hinzmann and collaborators for the selective oxidation of alcohols **152** to aldehydes **153** (Scheme 2.60).[97] The study aimed to perform aldehydes synthesis in alternative solvents than DCM, commonly used for TEMPO oxidations. The authors first optimized the TEMPO/NaClO oxidation of *n*-octan-1-ol in DCM at 0 °C to have a benchmark system. Solid $NaClO{\cdot}5H_2O$ was used instead of bleach (15 % aq. solution) and phase transfer catalysts (PTC) (*i.e*. acetylcholine hydrochloride, Bu_4NCl) or salts like $NaHSO_4$ were tested as additives. In the case of PTC the reaction did not proceed, instead, in the presence of $NaHSO_4$ 95 % of the alcohol was consumed, with a small (6 %) overoxidation to the acid. The optimal amount of TEMPO was found to be 0.25 mol% and for the $NaClO{\cdot}5H_2O$ 1.1 equivalents was sufficient for a complete conversion. Screening of solvents, in order to replace DCM, showed that when using EtOAc, MTBE, and 2-Me-THF as organic solvents nearly no conversion of *n*-octan-1-ol takes place. On the other hand, the reaction proceeded in various liquid aliphatic nitriles. In particular, *n*-octanenitrile and *i*-butyronitrile turned out to be highly suitable. The solvent screen was repeated using PIPO as the catalyst. *n*-Butyronitrile and *n*-octanenitrile provided the best conversion with the lowest amount of acid. *n*-Butyronitrile was selected for the scope of the reaction since it is relatively easy to remove under a vacuum. The reaction protocol was tested on 11 substrates. Primary alcohols with electron-withdrawing groups such as a nitro group were rapidly converted into the corresponding aldehydes with high selectivity. In contrast, oxidation is much slower when using alcohols substituted with an EDG such as methoxy group. Yields were generally good, except for cyclohexylmethanol which was obtained with a 58 % yield only.

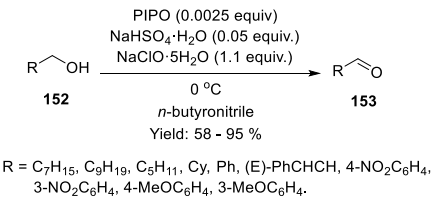

Scheme 2.60. Aldehyde synthesis by oxidation with NaClO, catalyzed by polymer-immobilized TEMPO-derivative (PIPO)

2.3.4 Selection of oxidation protocol for the optimization of the route to UAMC-00050

In Section 2.3 we reported a series of green approaches to the preparation of aldehydes. The approaches were divided into three categories depending on the primary oxidant (*i.e.* Air or O_2, H_2O_2 and NaClO). For our improvement of the synthetic route to UAMC-00050 we selected all three oxidants. Regarding the choice of the catalyst, as for the Birum-Oleksyszyn reaction, we selected a catalyst that can be easily purchased and that does not require any tedious preparation.

3 RESULTS AND DISCUSSION

As shown in the literature review, there are several strategies to implement the synthesis of UAMC-00050, in particular: the aldehyde can be prepared under more safe and green conditions, and the yield of the Birum-Oleksyszyn reaction can be increased after a catalyst screen. The optimized conditions for UAMC-00050 can be later applied for the preparation of the backup compound UAMC-0004206 and the proof-of-concept compound UAMC-0004207. In the literature review were also reported several methods for the stereoselective synthesis of α-amino-phosphonates. In this work, we reported our most important results which can be divided into the following groups.

1) We have optimized every single step of the medicinal chemistry preparation of UAMC-00050, the chlorinate solvent DCM was removed, and hazardous or expensive reagents were replaced with safer or cheaper alternatives, more efficient in terms of atom economy. Every reaction step was optimized to reach a higher yield and DoE was used to reach the optimum conditions in the last step. In all the intermediates, the flash chromatography separations (if required) were replaced with other purification techniques, (*e.g.* silica pad filtration, slurry, or crystallization). The overall yield was increased from 3 % of the medicinal chemistry route to 22 % of the process development route. The yttrium triflate catalyzed Birum-Oleksyszyn reaction was used to prepare a series of α-aminophosphonates which will serve as building blocks for assisting the serine proteases inhibitors research at the University of Antwerp. Lastly, the optimized conditions for the preparation of intermediate **9** were tested for synthesizing a phosphonolactone.

2) The optimized condition for UAMC-00050, with some adjustments, was adapted for the preparation of UAMC-0004206 and UAMC-0004207. The conditions for the Birum-Oleksyszyn reaction were employed without major modifications. In order to simplify the purification of the final compound we prepared the Boc-protected guanidine intermediated from the selected aniline salt using *N*,*N*′-di-Boc-1*H*-pyrazole-1-carboxamidine as a reagent. Due to the limited demand for material, we decided to keep, if necessary, chlorinated solvents and flash chromatography, to achieve a pure final material in a short time.

3) Two enantiomers of UAMC-00050 separated and tested *in vitro*. A series of attempts were made to develop a stereospecific preparation of the α-aminophosphonate. Chiral complexes of Lewis acid and proline were tested for an enantioselective Birum-Oleksyszyn reaction. (*S*)-(-)-1-Phenylethylamine was used to investigate how the reaction conditions (*e.g.* solvents, additives, temperature) affect the diastereoselectivity of the one-pot three-component preparation of α-aminophosphonates. A panel of chiral carbamates were prepared and tested on the Birum-Oleksyszyn reaction. (*R*)-1-(3,5-Bis(trifluoromethyl)phenyl)ethyl carbamate was able to provide an enantiomeric excess of 28 % on the model α-aminophosphonate **16**.

3.1 Process Development UAMC-00050

3.1.1 Preparation of triaryl phosphite 3

The medicinal chemistry research conditions for the preparation of phosphite **3**, were upscaled after minor changes (Scheme 3.1).[5] For this synthesis, 3.0 equivalents of paracetamol (**2**) were dissolved in anhydrous THF in the presence of 3.0 equivalents of triethylamine (TEA) and reacted with 1.0 equivalents of PCl_3. Triethylammonium chloride was filtered off, and the product was obtained as a white foam after removing THF under reduced pressure. The reaction was fast, and we were able to decrease the reaction time from 105 minutes to 60 minutes, where longer times led to reduced product purity. The instability of the triaryl phosphite **3** makes it difficult to separate from the main impurities (diarylphosphite **162** and paracetamol (**2**)) by chromatographic separation, precipitation or crystallization. Therefore, particular attention was paid to optimizing the reaction conditions in order to achieve a higher conversion with the minimum amount of side products. The presence of water in the starting material was found to be the main reason for the decreased purity of product **3**. This is because it can decompose highly reactive PCl_3 to H_3PO_3 and HCl, changing the reagent's ratio, therefore, increasing the amount of **2** and **162**. Moreover, it can also hydrolyze the triaryl phosphite **3** with the formation of paracetamol (**2**) and diarylphosphite **162**. Careful drying of the starting phenol **2** under vacuum (20-25 °C, 5 mbar) for at least 24 h significantly improved the conversion. The water content in paracetamol after drying was 0.030 % (Karl Fisher titration). Once the reaction was completed, the product was separated from triethylammonium chloride by filtration of the mixture under Argon flow, in order to minimize contact between product **3** and the atmospheric moisture. To avoid thermal decomposition of **3**, THF was then removed in vacuo at room temperature, as at a higher temperature (*i.e.* 40 °C in the water bath) product **3** was obtained with a decreased quality. Once the product was obtained in a solid form, it was kept in a vacuum (20-25 °C, 5 mbar) for 6 h, until a 10 % wt (^{1}H NMR assay) of residual THF was reached. Any longer drying time (*i.e.* 24, 48 h) led to slow decomposition of **3** to **162** and **2**. These improvements allowed us to get a final product with a 90 % area normalized (AN) by HPLC. The major impurities were represented by diaryl phosphite **162** and paracetamol (**2**).

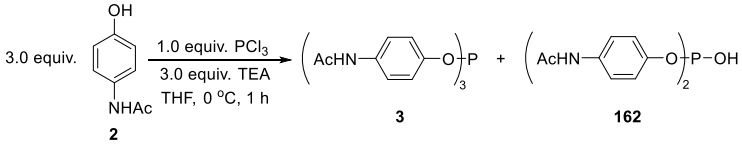

Scheme 3.1. Preparation of **3**, 3.0 equiv. of paracetamol (**2**) are reacted with 1.0 equiv. of PCl_3 in THF in the presence of 3.0 equiv. of TEA at 0 °C

3.1.2 Boc-Protection of the amine group in aniline 4

To enable selective oxidation of alcohol moiety in intermediate **6**, amino group protection was required. It was achieved, using 1.1 equivalents of di-*tert*-butyl dicarbonate (**5**) in the presence of 1.0 equivalents of triethylamine in dioxane (Scheme 3.2).[5] After acidification of the crude reaction mixture with 2 N aq. HCl, the product was extracted with EtOAc and purified with flash chromatography (Table 3.1, entry 1). We decided to explore a more green alternative to dioxane and remove the triethylamine from the reaction to avoid the acid wash. The standard reaction protocol reported in the literature, which uses the more green EtOAc as a reaction medium and does not require a base, was successfully used in our process development.[98] Compound **4** was treated with 1.1 equivalents of di-*tert*-butyl decarbonate (**5**) in EtOAc for 16 h at room temperature (Table 3.1, entry 2). Any attempt to speed up the reaction with a catalytic amount of DMAP provided only a complex reaction mixture.[99] The purified product **6** was obtained from the reaction mixture after a silica pad filtration. After completion of the reaction, the solution of the crude material was diluted with 0.5 volumes of heptane, poured on the silica pad (SiO_2/**6** = 15:1 w/w) and washed with a mixture of heptane/ethyl acetate (1:2 v/v) (Solvent/**6** = 28:1 w/v) (Table 3.1, entry 3). Unfortunately, the filtration was insufficient to remove all the side products and the final product carried a visible yellow color as an indication of the presence of impurities. Refluxing the crude material in ethyl acetate (EtOAc/**6** = 2:1 v/w) in the presence of activated charcoal (charcoal/**6** = 0.5:1 w/w) before the silica pad filtration, was able to provide a colorless material with 99 % AN by HPLC (Table 3.1, entry 4). Further investigation of the reaction revealed that the yellow impurities were present only when **6** was prepared using 4-aminophenethyl alcohol (**4**) from a specific provider. Therefore, changing the purity of the starting material has allowed us to avoid the charcoal treatment and reduce the amount of silica required in the filter pad, from 15.0 w/w to 8.3 w/w obtaining alcohol **6** (99 % AN by HPLC) on a 73 mmol scale (Table 3.1, entry 5). In a later improvement, after the reaction, crude **6** was purified by crystallization. Among 7 different conditions (Table 3.2) the mixture of MeCN/MTBE 1:1 v/v (solvent/**5** = 1.5:1) was found able to provide the crystalline product **6** with 99 % AN by HPLC and 98 % yield (Table 3.1, entry 6).

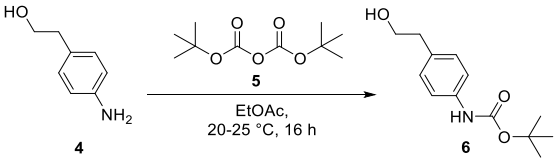

Scheme 3.2. Boc-protection of the amine **4**

Table 3.1

Optimization steps of the Boc protection conditions

Entry	Scale (mmol)	Solvent	Method of purification	Purity (%)	Yield (%)
1[a]	37.00	Dioxane	Flash chromatography	99	99
2	37.00	EtOAc	Flash chromatography	99	99
3	37.00	EtOAc	Pad of Silica (SiO_2/**6** = 15:1 w/w)	79	95
4	19.00	EtOAc	Active charcoal reflux (charcoal/**6** = 0.5:1 w/w; 77 °C) then pad of Silica (SiO_2/**6** = 15:1 w/w)	99	99
5	73.00	EtOAc	Pad of Silica (SiO_2/**6** = 15:1 w/w)	99	99
6	73.00	EtOAc	Crystallization MTBE/MeCN 1:1 v/v (solvent/**6** = 1.5:1)	99	98

[a]1.0 equiv. of TEA as additive.

Table 3.2

Screening of solvents for the crystallization of compound **6**

Entry	Solvent (Solvent/6; v/w)	Wash (Solvent/6; v/w)	Purity (%)	Yield (%)
1	MeCN (2.5:1)	MeCN (1.25:1)	99	74
2	EtOAc (2.5:1)	EtOAc (1.25:1)	99	38
3	MeCN (2.5:1)	No	99	75
4	MeCN (2.0:1)	No	99	73
5	MeCN/MTBE 2:1 v/v (2.5:1)	No	99	70
6	MeCN/MTBE 1:1 v/v (2.5:1)	No	99	97
7	MeCN/MTBE 1:1 v/v (1.5:1)	Heptane (5:1)	99	98

3.1.3 Preparation of aldehyde 7

According to the medicinal chemistry procedure, alcohol **6** was converted to aldehyde **7**, with 1.5 equivalents of DMP in DCM at - 78 °C to 23 °C for 3 h. The reaction mixture was then quenched, and the crude product was purified by flash chromatography. In our research, we decided to avoid the use of DMP and DCM in favor of more green and safe reagents. For instance, (2,2,6,6-tetramethylpiperidin-1-yl)oxyl (TEMPO) is widely used for the catalytic oxidation of alcohols.[100,101] In our first attempt, we used the (bpy)CuI/TEMPO-catalyzed aerobic oxidation,[83] which, however, failed to provide conversion of substrate **6**. Hydrogen peroxide with $AlCl_3$[91] or KBr/TEMPO/pTsOH[92] was also unsuccessful for the preparation of **7**. On the other hand, using 1.5 equivalents of sodium hypochlorite (NaClO) in the presence of a catalytic amount of TEMPO, KBr and $n$$Bu_4$NBr provided a 69 % conversion of substrate **6** with a good atom economy (66 %) (Scheme 3.3) (Table 3.3, entry 1).[94,95] An increase of the equivalents of NaClO (1.8 equiv.) allowed us to achieve a complete conversion (**6** < 1% ^{1}H NMR assay) in 120 minutes. Initially the equivalents of NaClO were reaised to 2.0 then decreased to 1.8 without losing the complete conversion. Since the transformation of alcohol **6** to aldehyde **7** is a fast process, we achieved

complete conversion even when the reaction was quenched after 15 minutes (Table 3.3, entries 2 and 3). Unfortunately, despite the complete consumption of alcohol **6**, a poor yield (31 %) was obtained on a 4.22 mmol scale (Table 3.3, entry 4). The final material showed a modest presence of carboxylic acid **163** which is the main impurity in the process. As reported by Anelli *et al*.,[102] the presence of nBu$_4$NBr catalyzes the aldehyde oxidation to acid **163**. After removing the quaternary salt from the original protocol, the yield was increased to 59 % (Table 3.3, entry 5). To make the reaction more efficient, we decreased the amount of the catalysts (*i.e.* KBr, TEMPO) and the reaction time. The yield was increased to 71 % when NaClO (1.7 equiv.), KBr (0.1 equiv.) and TEMPO (0.01 equiv.) were used with a reaction time of 30 minutes (Table 3.3, entry 6). After upscaling the reaction to 37 mmol we noted a drop in yield to 60 % due to an overoxidation (Table 3.3, entry 7) that was fixed by further reducing the amount of NaClO to 1.6 equivalents and the reaction time to 15 minutes, which allowed us to get a 66 % yield (Table 3.3, entry 8).

As required for a multigram scale synthesis we investigated different methods for the isolation of **7** rather than flash chromatography purification. Analogous to compound **6,** we used a silica pad to purify the crude, but it failed to provide aldehyde **7** with an acceptable purity (52 % AN by HPLC). On the other hand, the bisulfite adduct protocol provided aldehyde **7** with a 99 % AN by HPLC (Scheme 3.3).[103] The crude material was dissolved in 96 % EtOH and a saturated aq. solution of $NaHSO_3$ was added dropwise. The mixture was stirred for 2 h at 20-25 °C and 1 h at 0 °C, then the bisulfite adduct **164** was filtered and washed with cold 96 % EtOH. The aldehyde **7** was regenerated by dissolving compound **164** in water, followed by the addition of 2.2 equivalents of Na_2CO_3 and extraction with EtOAc to provide product **7**. When the bisulfite adduct purification method was applied to a 73 mmol scale preparation of **7**, a decrease in yield (59 %) was observed (Table 3.3, entry 9). A careful examination of the mother liquor indicated the leading cause of a drop in yield: it was attributable to the formation of adduct **164** rather than to the catalytic oxidation process. Extending the reaction time of the crude aldehyde with $NaHSO_3$ from 2 h to 16 h allowed us to completely convert crude **7** to **164**. The bisulfite derivative was then converted back to aldehyde, obtaining **7** in 71 % yield from alcohol **6**, with 99.2 % AN by HPLC (Table 3.3, entry 10). After the optimization, the Anelli-Montanari protocol proved to be superior to the DMP oxidation. No chromatographic separation was required in the process. Moreover, the yield was increased from 65 % to 71 % and the atom economy was enhanced from 33 % to 66 %.

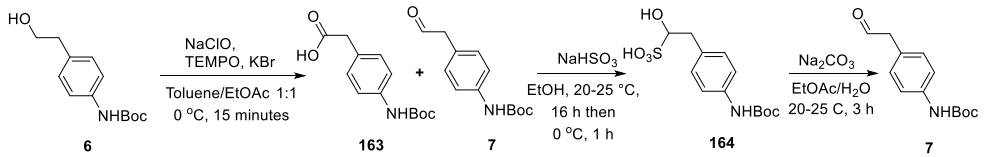

Scheme 3.3. Preparation of **7** by oxidation of **6**, and purification through adduct **164**

Table 3.3

Optimization for the aldehyde **7** synthesis

Entry[a]	Scale (mmol)	NaClO (equiv.)[b]	TEMPO (equiv.)	Time (min)	Conversion (%)	Bisulfite adduct[c]	Yield[d] (%)
1[e]	0.42	1.5	0.05	120	69	-	N/A[f]
2[e]	0.42	1.8	0.05	120	100	-	N/A[f]
3[e]	0.42	1.8	0.05	15	100	-	N/A[f]
4[e]	4.22	1.8	0.05	15	100	2 h (20-25 °C)	31
5	4.22	1.7	0.05	60	100	2 h (20-25 °C)	59
6	4.22	1.7	0.01	30	100	2 h (20-25 °C)	71
7	37.00	1.7	0.01	30	100	2 h (20-25 °C)	60
8	37.00	1.6	0.01	15	100	2 h (20-25 °C)	66
9	73.00	1.6	0.01	15	100	2 h (20-25 °C)	59
10	73.00	1.6	0.01	15	100	16 h (20-25 °C)	71

[a]0.1 Equiv. of KBr; [b]NaClO concentration 11-15%; [c]Additionally stirred 1 h at 0 °C before filtration; [d]Isolated yield; [e]0.05 equiv. of nBu$_4$NBr; [f]100 % conversion.

3.1.4 Birum-Oleksyszyn reaction

3.1.4.1 The complexity of the transformation

The one-pot three-component reaction between the aldehyde **7**, the phosphite **3** and the benzyl carbamate (**8**) is a pivotal step for the preparation of compound **1**. This reaction is the straightest way to build molecular complexity and reach the final target **1**. Unfortunately, we noted a lack of reproducibility for this reaction on a gram scale. The reaction suffered from a poor yield (11 %) and a low selectivity towards the target product. Moreover, the presence of impurities in the crude material made the purification a challenging step. Our investigation began with understanding the nature of the main side products noted in the reaction mixture (Scheme 3.4). Water, promoted by the Lewis acid, was able to hydrolyze product **9** to monoaryl derivative **170** and triaryl phosphite **3** to the diarylphosphite **162.** We speculate that partial removal of the NH-protecting group in aldehyde **7** generates unprotected **165**, which then polymerizes to **166**. The highly reactive imine **167** reacts with the second equivalent of benzyl carbamate to form aminal **168**, a more stable compound that in the presence of a Brønsted or a Lewis acid can also be converted to the reactive cation **169** which can react with **3** and generate **9**. Partial removal of the Boc group from product **9** lead to the generation of side product **171**.

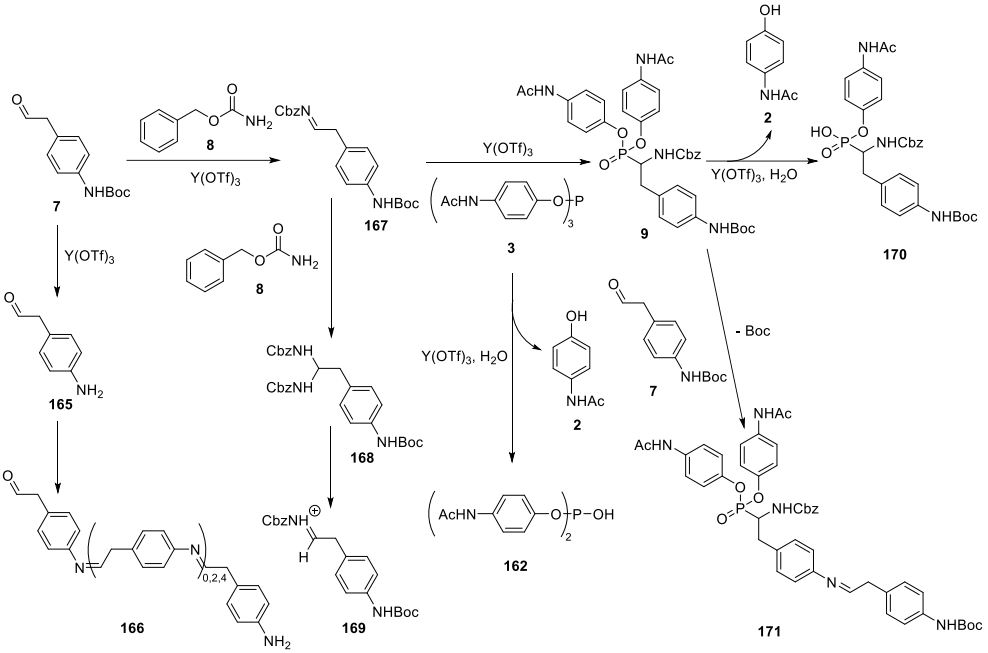

Scheme 3.4. Proposed side reactions for the Birum-Oleksyszyn step

3.1.4.2 Screening of Lewis acid in the Birum-Oleksyszyn reaction

As depicted in Scheme 3.4, improving the overall efficiency of the synthesis of α-aminophosphonate **9** requires the simultaneous promotion of imine formation, Birum-Oleksyszyn reaction, and suppression of unwanted hydrolysis and Boc group removal. A series of acidic catalysts were screened, using an equimolar ratio (1:1:1) of aldehyde **7**, benzyl carbamate (**8**), and phosphite **3** with 10 mol% loads of the catalyst in MeCN. The reaction was carried out at room temperature for 4 h.[5] The isolated yields and the ratio between product **9** and side product **170** are reported in Table 3.4. Due to the fact that hydrolysis of phosphodiesters can be promoted by Lewis acids,[104,105] the ratio of **9** and **170** is used as an extra parameter to understand the catalyst efficiency in this side reaction. In particular, paracetamol-containing phosphonate esters are much more sensitive to the presence of water compared to their alkyl analogues. The screening began by using AcOH as a solvent, no product was obtained since a complete decomposition of starting materials occurred (Table 3.4, entry 1). On the other hand, the Brønsted acid, TfOH, despite a low yield (13 %) provided much better stability of compound **9** toward the hydrolysis, ratio 82:18 (Table 3.4, entry 6). Lewis acids like $TiCl_4$, $Mg(OTf)_2$, and $SnCl_4$ are the catalyst with lower selectivity, in which a reaction of up to half of the product **9** was hydrolyzed (Table 3.4, entries 2, 7, and 14). On

the other hand, LiOTf provided the best compatibility with product **9** and the lowest degree of hydrolysis (85:15), but only a moderate yield of 15% (Table 3.4, entry 9). Two elements of group 1 and group 2, represented by catalysts LiOTf and $Mg(OTf)_2$, provided a low yield of product **9** (15 % and 14 %, respectively), but different selectivity, relatively high for lithium (85:15) (Table 3.4, entry 9) and moderate for magnesium (50:50) (Table 3.4, entry 7). A similar selectivity (74:26 - 76:24) was registered for all the salts of bismuth. However, a large difference was noted between the yield obtained from the three catalysts 13 % for $BiCl_3$, 19 % for $Bi(NO_3)_3 \cdot 5H_2O$, and 31 % for $Bi(OTf)_3$ (Table 3.4, entries 5, 12, and 17). Among four chloride salts, group 4 elements represented by catalysts $TiCl_4$ and $ZrCl_4$ ensured the same low yield of product **9** (8 %) but differed in selectivity (44:56 and 81:19, respectively) (Table 3.4, entries 2 and 3). At the same time, $SnCl_4$ and $ZnCl_2$ afforded product **9** with the same yield (22 %), but the selectivity of $SnCl_4$ was much lower (57:43 vs. 81:19 for $ZnCl_2$) (Table 3.4, entries 14 and 15). The poor performance of $TiCl_4$ and $SnCl_4$ can be explained by their hydrolysis with the formation of HCl under the reaction conditions, leading to decomposition. $FeCl_3$ was reported as an excellent catalyst for the synthesis of α-aminophosphonates from alkyl phosphites,[106] but, in the case of triaryl phosphite **3**, it was able to provide the product **9** in only 15 % yield with 68:32 selectivity (Table 3.4, entry 8). Furthermore, we speculated that the strong black-brown color of the reaction mixture, noted with strong Lewis acids (*i.e.* $TiCl_4$ and $BF_3 \bullet Et_2O$), might be due to the formation of side product **170**. The polymer can arise from the removal of Boc protecting group from **7** and the subsequent reaction of amine **165** and aldehyde **7** (Scheme 3.4). Less strong Lewis acids (*i.e.* $Mg(OTf)_2$ and LiOTf) generated a less colored reaction mixture, hence less polymer **166**, however, most of aldehyde **7** was left unreacted providing poor conversion of the starting materials. An interesting comparison can be made between elements of group 3: $Y(OTf)_3$ provided the highest yield (42 %) and a good selectivity (80:20) of product **9** (Table 3.4, entry 18), $Sc(OTf)_3$ showed a similar selectivity (81:19) but afforded much lower yield (16%) of product **9** (Table 3.4, entry 10). $Yb(OTf)_3$ and $La(OTf)_3$ ensured the formation of product **9** in 20 and 25 % yield with a selectivity of 67:33 and 69:31, respectively (Table 3.4, entries 13 and 16). The group of best performing catalysts includes $ZnCl_2$, $La(OTf)_3$, $Bi(OTf)_3$, and $Y(OTf)_3$. On the scale of 4.3 mmol of target compound **9**, the best performance was achieved with $Y(OTf)_3$, which provided the highest yield (42 %), almost four times higher than in the case of $Cu(OTf)_2$ (11 %) (Table 3.4, entry 4). With $Y(OTf)_3$, the stability of the paracetamol diester group was also one of the highest - only 20 % of diester was hydrolyzed. Furthermore, the reaction mixture possessed a pale yellow color as indication of a scarce formation of polymer **166** and other colored impurities.

Table 3.4

Lewis acid screening for the Birum-Oleksyszyn reaction

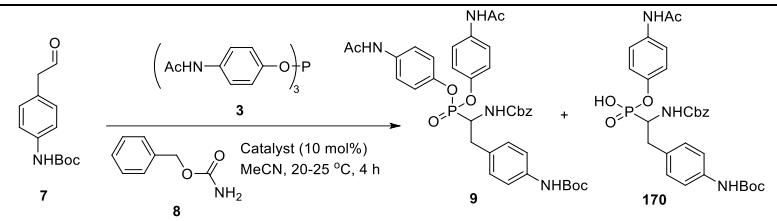

Entry	Catalyst	Yield[b] (%)	Ratio 9/170	Entry	Catalyst	Yield[b] (%)	Ratio[c] 9/170
1	AcOH[d]	0	N/A	10	$Sc(OTf)_3$	16	81:19
2	$TiCl_4$	8	44:56	11	$Et_2O–BF_3$	16	76:24
3	$ZrCl_4$	8	81:19	12	$Bi(NO_3)_3·5H_2O$	19	76:24
4	$Cu(OTf)_2$	11	76:24	13	$Yb(OTf)_3$	20	67:33
5	$BiCl_3$	13	74:26	14	$SnCl_4$	22	57:43
6	TfOH	13	82:18	15	$ZnCl_2$	22	81:19
7	$Mg(OTf)_2$	14	50:50	16	$La(OTf)_3$	25	69:31
8	$FeCl_3$	15	68:32	17	$Bi(OTf)_3$	31	76:24
9	LiOTf	15	85:15	18	$Y(OTf)_3$	42	80:20

[a]Reaction conditions: 1.0 equiv. of aldehyde **7**, 1.0 equiv. of phosphite **3**, 1.0 equiv. of benzyl carbamate (**8**) and 10 mol% of Lewis acid, MeCN, 20-25 °C, 4 h; [b] Isolated yield; [c]Selectivity Calculated as the ratio of HPLC areas; [d]AcOH as solvent.

In order to investigate side reactions, we converted the one-pot Birum-Oleksyszyn reaction into a two-step reaction. First, 1.0 equivalent of aldehyde **7** was reacted with 2.0 equivalents of benzyl carbamate (**8**) in the presence of 10 mol% of $Y(OTf)_3$. The resulting aminal **168** proved to be bench-stable and easily isolable. The aminal **168** was then reacted with phosphite **3** in the presence of 10 mol% of $Y(OTf)_3$ (Scheme 3.5). Instead of isolating product **9** and calculating the yield, we used an internal standard (IS, *i.e.* naphthalene) to facilitate the reaction monitoring. After 4 h, HPLC assay with IS showed only a 63 % (**9**/IS = 0.79) (Table 3.5, entry 2) amount of α-aminophosphonate **9** compared to that obtained in three-component Birum-Oleksyszyn reaction (**9**/IS = 1.26) (Table 3.5, entry 5). According to these data, it can be concluded that aminal **168** can react with phosphite **3**, but is less reactive than imine **167**. Therefore, a one-pot three-component reaction with in situ formations of imine is a preferable strategy for the synthesis of aryl α-aminophosphonates.

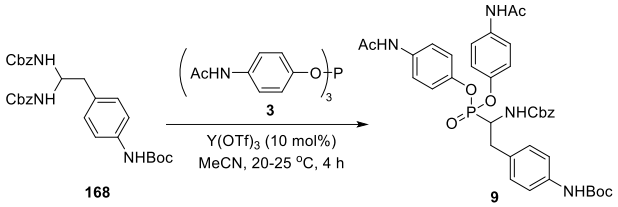

Scheme 3.5. Synthesis of product **9** from aminal **168**, catalyzed by $Y(OTf)_3$

Table 3.5

Comparison of values calculated as a ratio of the chromatographic concentration of product and naphthalene as internal standard

Entry	Two component reaction between 3 and 168; ratio 9/IS	Entry	Three component reaction between 7, 8, and 3; ratio 9/IS
1	0.94 (2 h)	4	1.05 (2 h)
2	0.79 (4 h)	5	1.26 (4 h)
3	0.74 (6 h)	6	1.21 (6 h)

3.1.4.3 Screening of reaction conditions in the Birum-Oleksyszyn reaction

With a good catalyst in hand, our attention moved to selecting a suitable solvent media. While running the reaction in acetonitrile it was observed the formation of a precipitate, which was identified later as aminal **168**. We then started to investigate a new medium for the α-aminophosphonate preparation, assuring the homogeneity of the reaction mixture. MeCN, THF, acetone, and MeCN/THF mixture were selected for their ability to dissolve starting materials. Two alcohols (EtOH and *i*PrOH) were tested to see the effect of protic solvents on the reaction outcome. Dioxane and Toluene were tested to see the effect of a reaction medium incapable to completely dissolve starting materials. The screen of solvents (Table 3.6), highlighted acetone and the mixture THF/MeCN (1:1 v/v) as the mediums capable of providing the best ratio of **9**/IS, respectively 1.47 (8 h), 1.51 (4 h) (Table 3.6, entries 3 and 4). A good yield obtained in THF/MeCN (1:1 v/v) mixture can be explained due to the capability of THF to dissolve all components of the reaction including aminal **168** and, therefore, enhance its reactivity. In protic solvents, like EtOH and *i*PrOH, only traces of the product were detected and the triaryl phosphite was completely hydrolyzed to paracetamol (Table 3.6, entries 7 and 8). Despite a good outcome, acetone was discarded due to its reactivity with phosphite **3**.[107,108] Other solvents like, THF, dioxane, and toluene provided a low ratio product **9**/IS, respectively 0.88 (4 h), 0.06 (8 h), and 0.76 (8 h) (Table 3.6, entries 2, 5, and 6). The mixture MeCN/THF (1:1 v/v) was selected as the reaction medium.

Table 3.6

Solvent screen for the Birum-Oleksyszyn reaction

Entry	Solvent	Ratio 9/IS at 4 h	Ratio 9/IS at 8 h
1	MeCN	1.26	1.17
2	THF	0.88	0.88
3	MeCN/THF 1:1 v/v	1.51	1.34
4	acetone	1.39	1.47
5	dioxane	0.21	0.76
6	toluene	0.04	0.06
7	EtOH	N/A	N/A
8	*i*PrOH	0.04	0.03

The attention was then turned to the reaction concentration. From the initial 0.07 M, the concentration was increased to 0.17 M improving the product **9**/IS ratio from 1.51 to 1.55 (Table 3.7, entry 3), while at 0.30 M **9**/IS was 1.46 (Table 3.7, entry 4). Another factor noted while changing the concentration was a different percentage of monoaryl ester **170** compared with product **9** and side product **171**, which increased linearly with the molarity of the reaction solution going from 18 % at 0.07 M to 23 % at 0.17 M and 36 % at 0.30 M (Table 3.7, entries 2 - 4). The optimized condition, MeCN/THF (1:1 v/v) and 0.17 M were tested on a 4.3 mmol scale, and product **9** was isolated with a yield of 45 %. A series of anhydrides were then screened, since they promote the reaction between aminals and alkylphosphonous acids, as shown in the literature.[29,30,109,110] In our case, we aimed to promote the reaction between aminal **168** and diarylphosphite **162**. The screening was performed with the addition of 1.0 equivalents of anhydride to the reaction mixture. Both acetic and trifluoroacetic anhydrides increased the **9**/IS ratio: using acetic anhydride we allowed it to reach 1.62 (Table 3.7, entry 5) while TFAA gave 1.80 (Table 3.7, entry 6). In both experiments, we noted a decrease in the product IS ratio after 4 h. Lower equivalents of TFAA (0.2 equiv.) lead to a lower **9**/IS ratio (1.69) and an increase of monoaryl ester **170** (39.1 %) (Table 3.7, entry 7). Other anhydrides like, succinic anhydride, and di-*tert*-butyl dicarbonate failed to increase the **9**/IS ratio (Table 3.7, entries 8 and 9). Dehydrating agents, such as 1.0 equivalents of trimethyl orthoformate (TMOF) and molecular sieves 4 Å (MS 4Å/**7** = 2:1 w/w), were tested in combination with 1.0 equivalents of TFAA. A lower yield has been noted in both experiments in contrast to using TFAA alone (Table 3.7, entries 10 and 11). In Figure 3.1 is reported the kinetic profile of the condition in entry 6. It can be seen that the product curve reaches a maximum at 4 h, then is start to decrease due to the decomposition of the product. Conditions in entry 6 provided the best **9**/IS ratio, this methodology was then tested on a 4.3 mmol scale and the α-aminophosphonate **9** was isolated, after flash chromatography, with a 52% yield.

Table 3.7

Screening of Birum-Oleksyszyn reaction conditions

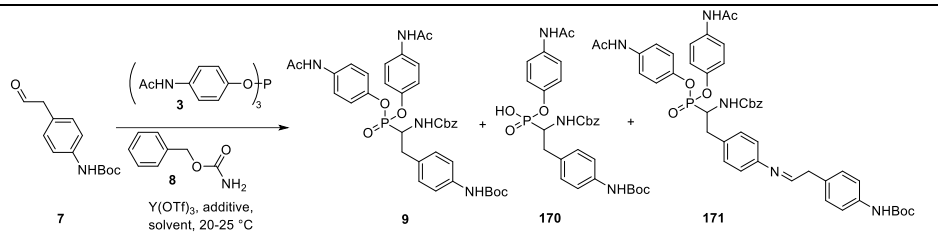

Entry[a]	Solvent	Additive (equiv.)	Conc. (M)	Product 9/IS (yield)[b]	HPLC area (%)		
					9	170	171
1	MeCN	-	0.07	1.26 (42 %)	71.9	17.6	10.5
2	MeCN/THF (1:1 v/v)	-	0.07	1.51 (44 %)	77.4	17.8	4.8
3	MeCN/THF (1:1 v/v)	-	0.17	1.55 (45 %)	72.3	23.3	4.4
4	MeCN/THF (1:1 v/v)	-	0.30	1.46	60.2	35.8	4.0
5	MeCN/THF (1:1 v/v)	Ac_2O (1.0)	0.17	1.62 (50 %)	74.3	18.1	7.6
6	MeCN/THF (1:1 v/v)	TFAA (1.0)	0.17	1.80 (52 %)	72.4	23.2	4.4
7	MeCN/THF (1:1 v/v)	TFAA (0.2)	0.17	1.69	58.5	39.1	2.4
8	MeCN/THF (1:1 v/v)	Succinic anhydride (1.0)	0.17	0.61	72.6	15.0	12.4
9	MeCN/THF (1:1 v/v)	Boc_2O (1.0)	0.17	0.91	70.4	16.7	12.9
10	MeCN/THF (1:1 v/v)	TFAA (1.0) + TMOF (1.0)	0.17	0.59	84.1	15.9	0.0
11	MeCN/THF (1:1 v/v)	TFAA (1.0) + 4Å MS	0.17	1.12	64.8	33.8	1.4

[a]0.2 mmol of aldehyde **7**, reaction time 4 h; [b]Isolated yield for reactions with scale 4.3 mmol.

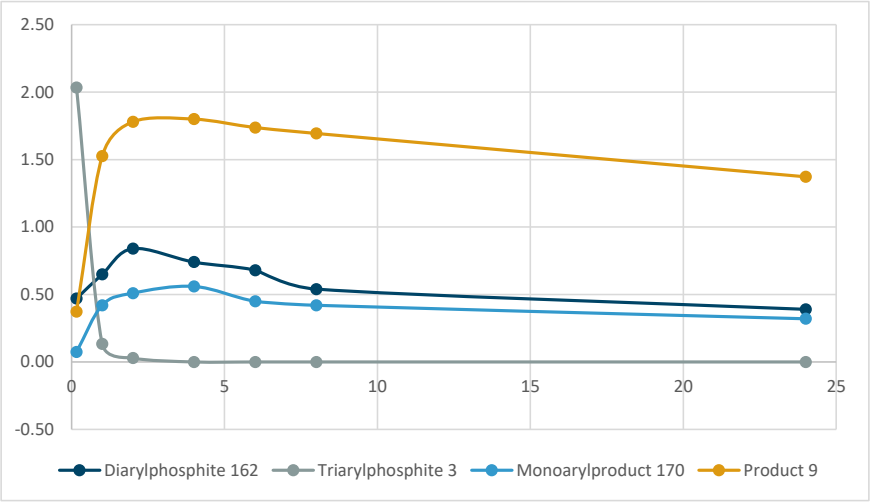

Figure 3.1. The kinetic profiling of UAMC-00050 depicts the course of the reaction. Points are calculated as the ratio between product **9** and IS. After 4 hours the peak of the product is reached, triarylphosphite is completely consumed after the first 2 hours. Conditions: 0.1 equiv. $Y(OTf)_3$ MeCN/THF 1:1, 0.17 M, 1.0 equiv. TFAA

The partial deprotection of the Boc group was observed during the reaction. We hypothesized that it led to polymerization and formation of colored impurities which proved to be challenging to separate. We decided to investigate the use of different protected aldehydes in the process. In the first case, the amino group of **4** was protected with Fmoc, and then the alcohol (**172**) was converted to an aldehyde **173** by oxidation with DMP. In the second case, our strategy was to oxidize 4-nitrophenethyl alcohol (**175**) to the corresponding aldehyde **176** with DMP. The nitroaldehyde **176** can be reacted with **3** and **8** to generate an appropriately nitro-substituted α-aminophosphonate **177** which then can be converted to **178** after the reduction of the nitro group (Scheme 3.6). In the case of the Fmoc-protected aldehyde, the Birum-Oleksyszyn reaction failed to provide the α-aminophosphonate **174** with a good purity profile of the final reaction mixture. While the 2-(4-nitrophenyl)acetaldehyde proved to be very sensitive and it rapidly decomposed when in contact with air, a Lewis acid, or a base like Na_2CO_3. We speculated that the impurities noted for the Birum-Oleksyszyn reaction with aldehyde **7** and the Fmoc-protected aldehyde **173** might arise from more complex side reactions than Boc deprotection. Thus, we decide to continue our optimization with Boc protecting group.

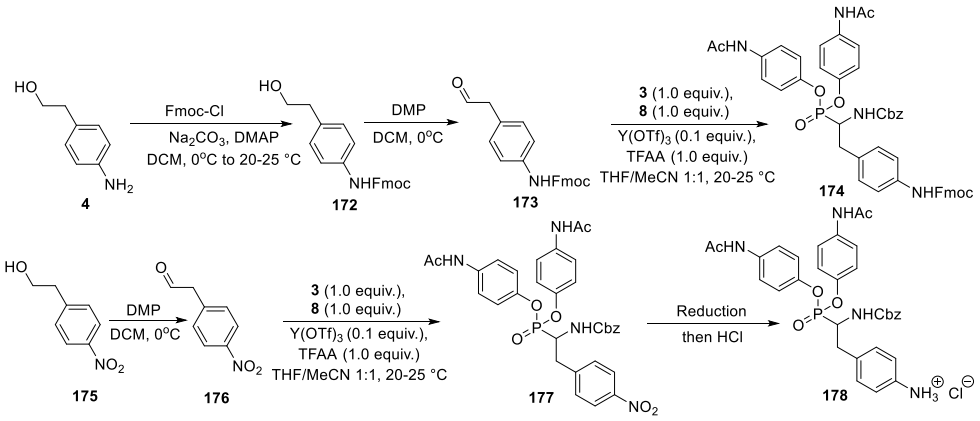

Scheme 3.6. Preparation of alternative aldehydes and planned reactions

3.1.4.4 Birum-Oleksyszyn reaction work-up and purification development

With optimized reaction conditions in hand, we focused on the work-up and purification process of the final material to avoid flash chromatography. At the end of the reaction, the HPLC chromatogram showed product **9** with a 23.2 % AN by HPLC, with paracetamol (**2**), diarylphosphite **162**, and aminal **168** as major impurities. The crude material was dissolved in a mixture of EtOAc/EtOH (4:1 v/v), capable of forming a homogeneous solution. The acidic by-products and side products (*e.g.* paracetamol (**2**), diarylphosphite **162**) were removed after washing the organic solution with 0.5 M aq. NaOH. The organic layer was separated from the aqueous solution, the solvent was removed and the crude material was mixed with celite. The solid mixture was placed on a silica pad and washed with EtOAc/Hexanes (2:1 v/v) (Solvent/**9** = 100 v/w) to remove the aminal **168** and other lipophilic impurities. The pad was then rinsed with EtOAc/EtOH (3:1 v/v) (Solvent/**9** = 100:1 v/w) to recover the product with purity 64.2 % AN by HPLC. Despite the basic wash, an 8.3 % HPLC area of paracetamol (**2**) was still present in the crude material. We used then antisolvent precipitation with a basic aqueous solution, in order to remove the remaining **2**. Crude **9** was dissolved in EtOH (Solvent/**9** = 10:1 v/w) and added dropwise in 10 volumes of an 0.5 % aq. $NaHCO_3$. The product was present in the collected precipitate with 74.1 % AN by HPLC. THF was also able to dissolve crude **9**, however, once the solution was added to the aqueous 0.5 % aq. $NaHCO_3$ the product precipitated as an oil. After the removal of THF, the solidified product **9** was collected with a purity of 71.7 % AN by HPLC. Under the same conditions, acetone proved to be a slightly better solvent for the purification of crude **9** than EtOH and THF. The product was obtained with a purity of 74.5 % AN by HPLC, but the precipitate was formed as very fine particles that clogged the filter making the isolation of the solid a long process. Changing the mode of addition (*i.e.* adding the bicarbonate solution to the crude solution in acetone) made a better filterable solid with a purity of 82.3 % AN by HPLC.

Our focus moved to the removal of the colored impurities, a series of products generated after the unwanted side reactions of the aldehyde **7**. We started to investigate charcoal sorbents as a standard treatment for the removal of colored impurities. Nine types of charcoal, four solvent systems and 2 different temperatures were tested (Table 3.8). In all experiments, the charcoal was loaded with a 1:1 mass ratio between the charcoal and the crude material. Acros NORIT™ A Supra in EtOAc failed to remove colored impurities from the crude material (Table 3.8, entry 1). We then moved our investigation to a series of charcoals manufactured by Cabot.[111] NORIT: CN1, CGP Super, A Supra EUR, ROX 0.8, and SX plux LC were tested in THF with a treatment time of 4 h (Table 3.8, entries 2 - 7), but none of them was able to completely remove the orange impurities. NORIT CN1 and CGP Super showed a slight change in the color of the solution after celite pad filtration. We decided to investigate if a longer time could help the discoloration. Unfortunately, all four experiments with NORIT: CN1, CGP SUPER, Darco, and GAC failed to provide any discoloration of the crude **9** solutions (Table 3.8, entries 8 - 11). Our focus was then moved to a different solvent system, THF was swapped to a mixture of EtOAc and EtOH (4:1 v/v). The crude material **9** was treated with NORIT C1 and NORIT CGP Super for 24 hours at room temperature. In both experiments (Table 3.8, entries 12 and 13) a slight discoloration of the solution was noted. NORIT Darco and NORIT GAC were tested with the mixture EtOAc/THF (1:1 v/v) (Table 3.8, entries 12 - 15), but unfortunately, none of them was able to remove the colorful impurities (Table 3.8, entries 14 and 15). A small color change was noted also when NORIT CGP was used with the mixture EtOAc/THF (1:1 v/v) (Table 3.8, entry 16). Lastly, we tested if treating the crude material **9** with the charcoal NORIT CGP in the mixture of EtOAc/THF (1:1 v/v) under reflux can help the removal of colored impurities. Again, after filtration through a celite pad, we noted no change in color of the crude **9** solutions. With this last result in hand, we decided to stop the charcoal screen and move to a slurry stirring method of purification for crude **9**.

The crude material was slurried and stirred in EtOAc (Solvent/**9** = 20:1 v/w) for 16 h at 20-25 °C, then the solid was collected by filtration obtaining an off-white product with purity 92 % AN by HPLC (Table 3.9, entry 1). When we refluxed 4 h after 16 h of stirring at 20-25 °C the product was isolated with the same purity (92 % AN by HPLC), but with a lower yield (86 %) (Table 3.9, entry 2). We were pleased to find that the purity was increased to 98 % AN by HPLC when acetone was added to EtOAc with a ratio EtOAc/acetone = 19:1 v/v, and the product was recovered with a yield of 88 % (Table 3.9, entry 3). Conditions in entry 3 were selected for further upscaling. At the 2.8 mmol scale, the product was obtained with a purity of 99 % AN by HPLC and yield 85 % (Table 3.9, entry 4). While at 22.1 mmol scales, product **9** was obtained with a purity of 98 % AN by HPLC and yield 86 % (Table 3.9, entry 5).

Table 3.8

Screening of conditions for the charcoal impurities removal

Entry[a]	Charcoal	Solvent	Time (h)	Result
1	Across NORIT™ A Supra	EtOAc	4	No change in color
2	CABOT NORIT CN1	THF	4	Small change in color
3	CABOT NORIT CGP SUPER	THF	4	Small change in color
4	CABOT NORIT A SUPRA EUR	THF	4	No change in color
5	CABOT NORIT ROX 0.8	THF	4	No change in color
6	CABOT NORIT C EXTRA USP	THF	4	No change in color
7	CABOT NORIT SX PLUS LC	THF	4	No change in color
8	CABOT NORIT CN1	THF	24	No change in color
9	CABOT NORIT CGP SUPER	THF	24	No change in color
10	CABOT NORIT Darco	THF	24	No change in color
11	CABOT NORIT GAC	THF	24	No change in color
12	CABOT NORIT CN1	EtOAc/EtOH (4:1 v/v)	24	Small change in color
13	CABOT NORIT CGP SUPER	EtOAc /EtOH (4:1 v/v)	24	Small change in color
14	CABOT NORIT Darco	EtOAc /THF (1:1 v/v)	24	No change in color
15	CABOT NORIT GAC	EtOAc /THF (1:1 v/v)	24	No change in color
16	CABOT NORIT CGP SUPER	EtOAc /THF (1:1 v/v)	24	Small change in color
17[b]	CABOT NORIT CGP SUPER	EtOAc /THF (1:1 v/v)	24	No change in color

[a]For all the experiment charcoal was added as 1:1 mass ratio for the crude product; [b]Reflux.

Table 3.9

Screening of conditions for the slurry purification of intermediate **9**

Entry[a]	Scale (mmol)	Solvent	Yield[b] (%)	Purity (%)
1	0.3	EtOAc	94	92
2[c]	0.3	EtOAc	86	92
3	0.3	EtOAc/acetone (19:1 v/v)	88	98
4	2.8	EtOAc/acetone (19:1 v/v)	85	99
5	22.1	EtOAc/acetone (19:1 v/v)	86	98

[a]Stirred at 20-25 °C for 16 h; [b]Isolated yield; [c]Stirred at 20-25 °C for 16 h and refluxed for 4 h.

With the optimized reaction conditions (*e.g.* catalyst, additive, solvent) and the optimized workup, the protocol for Birum-Oleksyszyn reaction was tested on a 43 mmol scale of aldehyde **7**. Product **9** was obtained with 44 % yield and with a purity of 98.2 % AN by HPLC.

3.1.5 *N*-Boc deprotection of intermediate 9

In the medicinal chemistry procedure, Boc protecting group was removed with TFA/DCM (1:1 v/v) at 20-25 °C within two hours. HCl-mediated *N*-Boc deprotection was investigated as a valuable and cheaper alternative that would have led directly to the HCl aniline salt **178**, which is necessary at the next step to obtain the HCl guanidine salt **1** (Scheme 3.7). Initially, we used 2.5 N HCl in ethanol, a solvent capable of dissolving **9**. The complete cleavage of the Boc group required 6 h. However, due to the long reaction time and the presence of water in the HCl ethanol solution, we noted the formation of monoarylphosphonate **179**. The similar problem was noted with the use of 5 - 6 N HCl in *i*PrOH. The hydrolysis of product **178** was curbed when 4 N HCl solution in dioxane was used. Both starting material **9** and aniline **178** were not completely soluble in dioxane, however, complete *N*-Boc deprotection was achieved after 3 h at 20-25 °C. The residual starting material **9** (0.54 % AN by HPLC) was completely removed after antisolvent precipitation. Purification of the crude salt **178** was performed by dissolving the crude material in EtOH 96 % (Solvent/**178** = 10:1 v/w), and adding it dropwise to 10 volumes of stirred EtOAc at 20-25 °C. Unfortunately, the product formed a series of clots made the recovery of the product challenging. Using absolute EtOH, instead of EtOH 96 %, prevented the formation of clots and the solid was obtained as off-white flakes with a purity of 96.9 % AN by HPLC (Table 3.10, entry 1). Other antisolvents, like *i*PrOAc, THF and MeCN, could not provide compound **178** with higher purity, respectively 90.0 %, 93.2 % and 94.7 % (Table 3.10, entries 2 - 4). The time between the beginning of the precipitation and the filtration of the solid was set at 0.5 hours. Increasing the contact time between the mother liquor and the precipitate led to a reduction of purity from 96.9 % to 95.8 % (Table 3.10, entry 5). Furthermore, higher temperatures (*i.e.* 65 °C or reflux) were not able to provide a material with higher purity (Table 3.10, entries 6 and 7). In the case of reflux, the product precipitated as a sticky solid, compromising the amount of material that was possible to recover after filtration. Conditions of *N*-Boc deprotection and work up in entry 1 were selected for the upscale. Compound **178** (14 mmol) was stirred for 3 h in 4 N HCl solution in dioxane. After the removal of the dioxane and the acid in vacuo, the crude material was dissolved in absolute EtOH and added dropwise to 10 volumes of stirred EtOAc at 20-25 °C. The solid was filtered after 30 minutes from the first drop of the alcoholic solution (Table 3.10, entry 8). After drying in vacuo compound **178** was obtained with a yield of 99 % and purity of 97.9 % AN by HPLC.

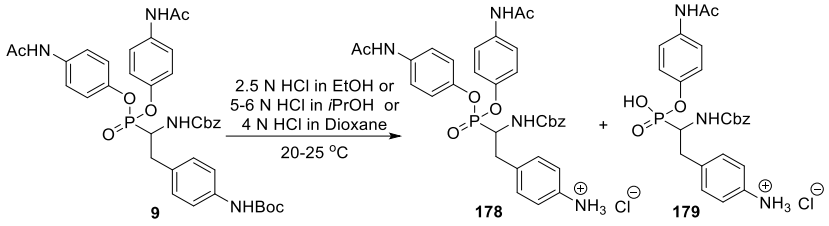

Scheme 3.7. HCl mediated *N*-Boc deprotection

Table 3.10

Screening of work-up conditions

Entry	Scale (mmol)	Antisolvent	Stirring treatment	Time (h)	Yield (%)	Purity (%)
1	0.7	EtOAc	20-25 °C	0.5	99	97
2	0.7	*i*PrOAc	20-25 °C	0.5	96	90
3	0.7	THF	20-25 °C	0.5	76	93
4	0.7	MeCN	20-25 °C	0.5	94	95
5	0.7	EtOAc	20-25 °C	24	99	96
6	0.7	EtOAc	65 °C for 1 h then 20-25 °C for 4 h	5	85	94
7	0.7	EtOAc	reflux for 1 h then 20-25 °C for 4 h	5	7	93
8	14.0	EtOAc	20-25 °C	0.5	99	98

3.1.6 Guanylation of intermediate 178

In the medicinal chemistry route, product **1** is prepared from TFA aniline salt **10** after insertion of the guanidyl group using *N*,*N*'-di-Boc-1*H*-pyrazole-1-carboxamidine (**11**), removal of the Boc groups with TFA in DCM, and salt exchange with DOWEX 1X8 Cl resin to convert TFA salt **13** to HCl salt **1**. The procedure has several limitations: a low overall yield from **10** to **13** (45 %), a long reaction time (5 days), the use of the expensive carboxamidine **11** and a low atom economy (78 %). We started to investigate a direct way to convert intermediate **178** to final product **1**, to reduce the number of steps, increase the overall yield and cut the cost of operation. Different literature reports describe the direct transformation of aromatic amine to guanidine (Table 3.11).

Table 3.11

Literature conditions for the direct guanylation of anilines

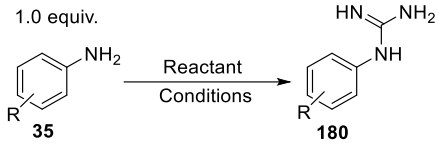

Entry	Reactant	Conditions	Reference
1	1.2 equiv. NH_2CN	0.1 equiv. $Sc(OTf)_3$, H_2O, 100 °C	Tsobokura *et al.*[112]
2	5.0 equiv. NH_2CN	Excess HNO_3, EtOH, reflux	Diab *et al.*[113]
3	1.0 equiv. 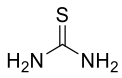	1.0 equiv. $CoCl_2$*$6H_2O$, 1.0 equiv. TEA, DMSO, r.t.	Kondraganti *et al.*[114]
4	1.0 equiv. 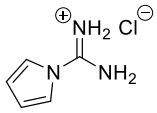	1.1 equiv. DIPEA, MeCN, r.t.	An *et al.*[115]
5	1.0 equiv. 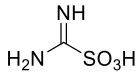	MeOH, r.t.	Kim *et al.*[116]
6	1.4 equiv. 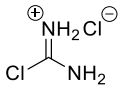	MeCN, 80 °C	Armitage *et al.*[117]
7	0.5 equiv. 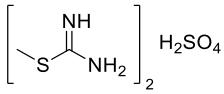	0.6 equiv. K_2CO_3, 90 - 100 °C	Goswami *et al.*[118]

As depicted in Table 3.11 there are several ways to convert directly aniline **35** to product **180**. We decided to focus on the conditions reported in entries 1 and 2, using cyanamide as a reactant, since they have the best atom economy. However, both cyanamide protocols were not directly applicable. Heating **178** in a protic solvent with the presence of a Brønsted or a Lewis acid led to major hydrolysis of the α-aminophosphonate. Nitric acid was initially avoided due to possible nitration on the paracetamol moiety.

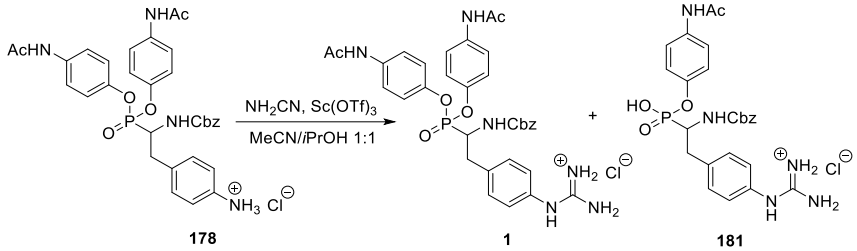

Scheme 3.8. Direct guanylation of **178** with cyanamide

The Tsobokura protocol with cyanamide (1.2 equiv.) and $Sc(OTf)_3$ (0.1 equiv.) catalyst was applied for the transformation of **178** to **1** with modified conditions. The reaction was run at 20-25 °C instead of 100 °C to avoid major hydrolysis of **178** and **1** (Scheme 3.8). As shown in Table 3.12, entry 1, water proved to be not a suitable solvent when the reaction was run at 20-25 °C, since, after 72 h only 8 % of starting material was converted into the product. Hence, a series of solvents were screened to improve the conversion of aniline **178** at 20-25 °C. *i*PrOH and acetone provided a poor conversion, respectively 12 % and 9 % (Table 3.12, entries 4 and 5), while MeCN, THF, and EtOH furnished a better conversion, respectively 19 %, 24 % and 30 % (Table 3.12, entries 2, 3, and 6). Having tested the pure solvents we started to test 1:1 v/v mixtures. The combination of the best mediums (EtOH and THF) provided a conversion of 35 % (Table 3.12, entry 7). Mixtures of MeCN with water, acetone and EtOH provided lower or similar results of acetonitrile alone, respectively 8 %, 17 % and 19 % (Table 3.12, entries 8, 10, and 11). While MeCN mixtures with THF and *i*PrOH provided a better conversion than acetonitrile alone, 36 % and 38 % respectively (Table 3.12, entries 9 and 13). The mixture of *i*PrOH/THF 1:1 v/v provided a conversion of 35 % (Table 3.12, entry 12). With our optimal medium composition in hand (MeCN/*i*PrOH 1:1 v/v) we moved our focus to the reaction's catalyst. Lewis acids like $Bi(OTf)_3$ and $Y(OTf)_3$ failed to provide any better conversion with (34 % and 25 % respectively) (Table 3.12, entries 15 and 16). Brønsted acids like HCl, HNO_3, and AcOH also could not provide any improvements compared to $Sc(OTf)_3$. In the case of nitric acid, the reaction yielded a complex mixture as a consequence of nitration of the paracetamol moiety, both starting material and guanidine counted as minor peaks in the HPLC chromatogram.

For the purification of crude **1** and removal of unreacted **178**, the solid was dissolved in absolute EtOH (Solvent/**1** = 10:1 v/w), just after the initial removal of volatiles. Then, 2.5 N HCl in EtOH (2.5 N HCl/**1** = 1:2 v/w) was added to convert any free base guanidine to salt and this ethanolic solution was added dropwise in 10 volumes of the selected antisolvent. The addition of *i*PrOAc, as an antisolvent, provided a solid which was easily filtered and washed with 5 volumes of *i*PrOAc (Table 3.13, entry 1). Other solvents (*i.e.* EtOAc, MeCN, THF, acetone and dioxane) failed to provide crude **1** with higher purity and yield (Table 3.13, entries 2 - 6).

Table 3.12

Optimization for the direct guanylation of **1**

Entry[a]	Catalyst (equiv.)	Solvent	Conversion (%)
1	$Sc(OTf)_3$ (0.1)	H_2O	4
2	$Sc(OTf)_3$ (0.1)	MeCN	19
3	$Sc(OTf)_3$ (0.1)	THF	24
4	$Sc(OTf)_3$ (0.1)	*i*PrOH	12
5	$Sc(OTf)_3$ (0.1)	Acetone	9
6	$Sc(OTf)_3$ (0.1)	EtOH	30
7	$Sc(OTf)_3$ (0.1)	EtOH/THF 1:1 v/v	35
8	$Sc(OTf)_3$ (0.1)	MeCN/H_2O 1:1 v/v	8
9	$Sc(OTf)_3$ (0.1)	MeCN/THF 1:1 v/v	36
10	$Sc(OTf)_3$ (0.1)	MeCN/Acetone 1:1 v/v	17
11	$Sc(OTf)_3$ (0.1)	MeCN/EtOH 1:1 v/v	19
12	$Sc(OTf)_3$ (0.1)	*i*PrOH/THF 1:1 v/v	35
13	$Sc(OTf)_3$ (0.1)	MeCN/*i*PrOH 1:1 v/v	38
14	$Bi(OTf)_3$ (0.1)	MeCN/*i*PrOH 1:1 v/v	34
15	$Y(OTf)_3$ (0.1)	MeCN/*i*PrOH 1:1 v/v	25
16	HCl (1.0)	MeCN/*i*PrOH 1:1 v/v	8
17	HNO_3 (1.0)	MeCN/*i*PrOH 1:1 v/v	40[b]
18	AcOH (1.0)	MeCN/*i*PrOH 1:1 v/v	11

[a]1.2 equiv. of NH_2CN, conc. 1.0 M, reaction time 72 h; [b]complex mixture.

Table 3.13

Screen of antisolvents for the work-up of **1**

Entry	Solvent	Yield (%)	Purity (%)
1	*i*PrOAc	85	89
2	MeCN	83	86
3	THF	63	88
4	Acetone	79	87
5	Dioxane	75	89
6	EtOAc	84	87

After the first stage of optimization, having selected the most promising catalyst ($Sc(OTf)_3$) and reaction solvent (MeCN/*i*PrOH 1:1 v/v) we worked to increase the efficiency of the reaction. We identified three factors to change in order to increase the yield and purity of the final material: concentration, reaction time and equivalents of cyanamide. A Design of Experiment (DoE) approach was selected to explore all three variables simultaneously and eventually identify any

interaction between the three factors. At first, we set the limits of the three variables: 0.1 - 2.0 M for the concentration, 1.2 - 10.0 for the cyanamide equivalents and 48 - 96 h for the reaction time. The DoE was performed with the support of the artificial intelligence (AI) web-based software xT SAAM.[119] The program uses stochastic optimization techniques to produce suggestions for the next experiments until an objective is satisfied and/or gathered data becomes modellable. The objective was to maximize the purity and yield of the final product as well as to create models for predicting purity and yield. In this study, 4 consecutive iterations of parallel experiments were carried out, totalling 22 experiments (Table 3.14). The results of purity and yield were collected and the software was used to create the final models. xT SAAM uses an automated mechanism to produce cross-validated linear regression with nonlinear features. From the response surface model (RSM) (Figure 3.2), it was clear that the best yield and purity were obtained when the concentration was set at 0.5 M and the NH_2CN equivalents and time were maximized.

With a concentration (0.5 M), equivalents of cyanamide (10.0) and reaction time (96 h), conversion rose to 95 %, and the final product was obtained on a small scale (0.08 mmol) with 86 % yield and 89 % AN by HPLC (Table 3.14, entry 19). After upscaling to a 0.77 mmol scale we noted a loss of conversion, yield, and purity. An increase of the equivalents of cyanamide to 15.0 was necessary to maintain a purity of **1** around 87 - 88 %.

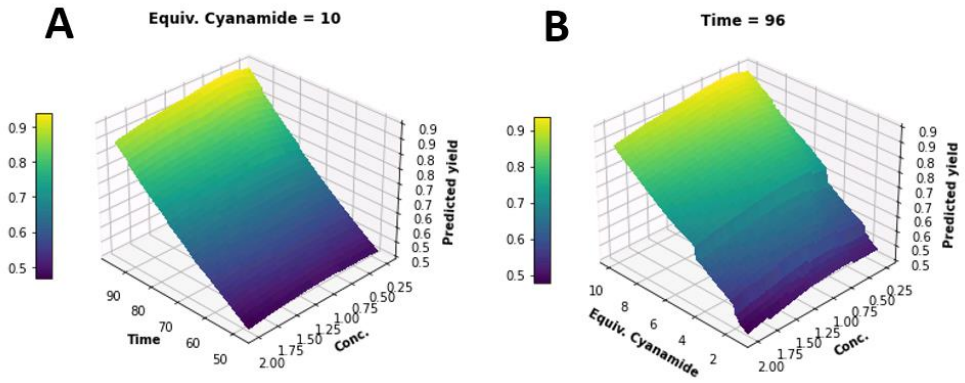

Figure 3.2. Predicted yield RSM for the cyanamide guanylation of **178** in iPrOH/MeCN (1:1 v/v), **A** when cyanamide equivalents are fixed at 10, **B** when time is fixed at 96 h. Yellow regions indicate the maximum predicted yield.

Table 3.14

DoE series of experiments for the optimization of the direct guanylation

Entry	Series	NH_2CN (equiv.)	Time (h)	Conc. (M)	Purity[a] (%)	Yield[b] (%)
1	1	1.9	86	1.7	46	42
2	1	4.7	86	0.7	76	65
3	1	2.4	52	0.7	32	29
4	1	1.5	95	0.7	42	25
5	1	1.6	89	0.5	27	20
6	1	3.4	68	0.6	20	37
7	2	4.6	94	0.4	73	70
8	2	4.7	92	0.5	84	81
9	2	2.2	88	1.0	62	60
10	2	1.4	86	1.6	40	38
11	2	7.5	86	0.5	87	84
12	2	10.0	86	0.4	89	85
13	3	7.0	86	0.5	81	73
14	3	10.0	86	0.5	87	81
15	3	8.0	89	0.3	76	72
16	3	7.0	96	0.5	84	78
17	4	10	96	0.5	89	86
18	4	9.5	90	0.4	89	86
19	4	8.3	94	0.4	87	84
20	4	7.9	86	0.5	84	75
21	4	6.9	87	0.5	86	84
22	4	5.8	93	0.6	87	83

[a]AN by HPLC; [b]Isolated yield.

With a second solvent screening we investigated 1:2 v/v mixtures (Table 3.15). The four best solvents from the first screen were selected and pooled in six different manners. The highest conversion was reached when the mixture MeCN/THF (1:2 v/v) was used as a medium, however, we decided to avoid any further investigation of this mixture due to the presence of clots in the flask and unsatisfactory mixing. The second best mixture *i.e.* THF/EtOH (2:1 v/v) was selected for further studies. The equivalents of cyanamide and the concentration were gradually increasing, this time using a one-variable-at-time instead of a DoE approach. The target conversion (> 95 %) was reached when the equivalents of cyanamide were raised to 10.0, after 96 h, using a concentration of 0.5 M (Table 3.15, entry 17). At higher concentrations (1.0 M) we reached a 96 % conversion of aniline **178** with 7.5 equivalents. Although it would be beneficial for the atom economy of the reaction to use 7.5 equivalents instead of 10.0 equivalents of cyanamide, the reaction mixture

became very viscous and the magnetic stirring was stopped after some time. To avoid any problems at a larger scale we preferred to use conditions entry 17. We were pleased to note that when the reaction in THF/EtOH (2:1 v/v) was up-scaled to 0.77 and 7.7 mmol, the conversion was maintained above 95 % without the necessity to increase the equivalents of cyanamide. The 7.7 mmol scales direct guanylation in THF/EtOH 2:1 v/v with 10 equivalents of NH_2CN, provided **1** with 91.0 % purity and 90.0 % yield. Among the impurities in the final material, we noted a small presence of monoarylguanidine (**181**) counting between 0.4 - 1.1 % AN by HPLC.

Table 3.15

Screening of 1:2 v/v solvent mixtures and optimization for the selected mixture

Entry	Reaction medium	NH_2CN (equiv.)	Time (h)	Conc. (M)	Conversion (%)
1	EtOH/THF 1:2 v/v	1.2	72	0.50	44
2	EtOH/THF 2:1 v/v	1.2	72	0.50	38
3[a]	MeCN/THF 1:2 v/v	1.2	72	0.50	54
4	MeCN/THF 2:1 v/v	1.2	72	0.50	42
5	MeCN/*i*PrOH 1:2 v/v	1.2	72	0.50	38
6	MeCN/*i*PrOH 2:1 v/v	1.2	72	0.50	36
7	EtOH/THF 1:2 v/v	2.0	72	0.20	50
8	EtOH/THF 1:2 v/v	2.0	72	0.50	64
9	EtOH/THF 1:2 v/v	5.0	72	0.20	66
10	EtOH/THF 1:2 v/v	5.0	72	0.35	74
11	EtOH/THF 1:2 v/v	5.0	72	0.50	86
12	EtOH/THF 1:2 v/v	7.5	72	0.20	74
13	EtOH/THF 1:2 v/v	7.5	72	0.50	89
14	EtOH/THF 1:2 v/v	7.5	96	0.50	94
15	EtOH/THF 1:2 v/v	10.0	72	0.20	76
16	EtOH/THF 1:2 v/v	10.0	72	0.50	90
17	EtOH/THF 1:2 v/v	10.0	96	0.50	96
18[a]	EtOH/THF 1:2 v/v	7.5	96	1.00	96
19[a]	EtOH/THF 1:2 v/v	10.0	96	1.00	97

[a]Formation of clots in the tube.

3.1.7 Purification of UAMC-00050

3.1.7.1 Crystallization

With our crude final material, we started to screen possible ways of purification in order to reach the target purity of 98 %. In our first attempt to crystallize the crude material, 17 solvents were screened (Table 3.16). Solvents were chosen among the most commonly used in chemical industry

to cover a variety of boiling temperatures and a range of polarity going from cyclohexane to water. Unfortunatelly, none of them were able to yield a filterable solid of pure **1**. Crude **1** was dissolved entirely in MeOH and EtOH and partially in *n*BuOH. In *i*PrOH and THF the product formed a series of clots at 20-25 °C, while deionized water was able to partially dissolve **1**. All other solvents could not dissolve the crude material at 20-25 °C. All the vials were warmed until the solvent's boiling point, and changes were noted in the case of acetone and MeCN, where a large part of the product formed a single clot. The only solvent capable of completely dissolving the crude product was warm water. The aqueous solution was left at 20-25 °C for 16 h, unfortunately, in the vial, it was formed a cloudy precipitate proved impossible to be filtered from the mother liquor. In the last experiments, crude **1** was completely dissolved in a mixture of EtOH/H_2O (1:1 v/v), and then deionized water was added dropwise (0.2 volumes). The flask was kept at 20-25 °C for 16 h and -20 °C for 24 h, unfortunately, at both temperatures, no precipitate was formed. Discouraged by these results we decided to move to different purification methods.

Table 3.16

Screen of solvents for the crystallization of crude **1**

Entry	**Solvent**	**Soluble at 20-25 °C**	**Soluble at reflux**	**Precipitate formation after cooling at 20-25 °C**
1	Cyclohexane	No	No	-[a]
2	2Me-THF	No	No	-
3	MIBK	No	No	-
4	*n*BuOH	Partially	Partially	No change[b]
5	Acetone	No	Clots	No change
6	*i*PrOAc	No	No	-
7	THF	Clots	Clots	No change
8	*i*PrOH	Clots	Clots	No change
9	MeOH	Yes	-	-
10	MeCN	No	Clots	No change
11	EtOH	Yes	-	-
12	EtOAc	No	No	-
13	DCM	No	No	-
14	MTBE	No	No	-
15	Toluene	No	No	-
16	Et_2O	No	No	-
17	H_2O	Partially	Yes	Cloudy precipitate

[a]"-" indicate that the precipitation after cooling at 20-25 °C was not take into consideration due to completely solubility of the material at 20-25 °C or completely insolubility of the material at reflux; [b]No change indicate that no modifications in the vial, containing the partially soluble or clots of material, were noted after cooling to 20-25 °C.

3.1.7.2 Antisolvent precipitation

We decided to test a series of antisolvent precipitations to see if it is possible to increase the purity. The crude material, with initial purity of 88 % AN by HPLC, was dissolved in absolute ethanol (absolute EtOH/**1** = 10:1 v/w) and slowly added dropwise to a stirred solution of 10 or 20 volumes of the selected antisolvent at 20-25 °C. In the case of organic solvents, results in Table 3.17, show that only precipitations in 10 volumes of *i*PrOAc and EtOAc (Table 3.17, entries 1 and 2) were able to slightly increase the purity of **1**. Other antisolvents like MeCN, THF, and acetone failed to increase the purity (Table 3.17, entries 3, 4, and 5). When the volumes of the EtOAc were increased from 10 to 20 (Table 3.17, entry 6), the product was obtained with a lower yield (79 %) and a lower purity (76 % AN by HPLC) compare to a similar experiment in EtOAc (Table 3.17, entry 2). The precipitation was then performed in a series of aqueous antisolvents, where the highly polar antisolvent could be able to remove all the impurities with higher polarity than the product (*i.e.* the monoaryl guanidine **150**). However, when the ethanol solution was added dropwise to water no precipitate was observed (Table 3.17, entry 7). Brine was then used instead of pure water. In this case, a precipitate was obtained, but with a lower purity (82 % AN by HPLC) than the crude material (Table 3.17, entry 8). As a last attempt, we used a solution of 0.5 % aq. NH_4HCO_3/Brine (1:1 v/v) in order to precipitate **1** as guanidine base and not as guanidinium hydrochloride. The precipitation failed to increase the purity and the 137 % yield is proof that the final compound is containing a considerable amount of NaCl and NH_4HCO_3 (Table 3.17, entry 9).

Table 3.17

Screen of antisolvents precipitations

Entry	Antisolvent	Antisolvent volumes	Yield (%)	Change of purity (%)
1	*i*PrOAc	10	92	88 → 89
2	EtOAc	10	90	88 → 91
3	MeCN	10	56	88 → 86
4	THF	10	87	88 → 85
5	Acetone	10	49	88 → 83
6	EtOAc	20	79	88 → 76
7	H_2O	10	0	N/A[a]
8	Brine	10 volumes	99	88 → 82
9	0.5% aq. NH_4HCO_3/Brine 1:1 v/v	20 volumes	137	88 → 87

[a]N/A the purity of the material after the antisolvent precipitation was not assessed due to completely solubility of the material in H_2O.

3.1.7.3 Reverse phase chromatography

After unsuccessful crystallization and antisolvent precipitations, we started to screen chromatographic methods to purify **1**. A normal phase purification on silica failed to provide a pure final material since a strong gradient (EtOAc/EtOH 3:1 v/v to pure EtOH) was required to move the product **1** along the silica sorbent and several impurities were coeluted with the product. Thus, reverse phase (RP) chromatography was selected as a method of purification. Columns with reverse phase C_{18} functionalized silica (RP-C_{18}) were selected as the stationary phase, while the gradient of 96 % EtOH in deionized water (DIW) was selected as the mobile phase. MeOH was inferior for elution, because instability of the product took place, and started to hydrolyze generating the monoaryl guanidinium side product **181**. In the first attempt of RP purification, the chromatogram showed a wide peak, and HPLC analysis of collected fractions showed co-elution of product **1** and amine **178**. Next, the acidic gradient EtOH 96 %/DIW (HCOOH 0.1%) was tested, however, no improvement was achieved compared to the previous separation. Then EtOH 96 % was substituted with MeCN. Unfortunately, the gradient MeCN/DIW was not able to elute all the products along the column. A significant amount of crude material was recovered from the column after being washed with 3 column volumes (CV) of EtOH 96 %. Hence, the polarity of the organic phase was increased by replacing the pure MeCN with a mixture of MeCN/EtOH 96 % (9:1 v/v), again as a gradient in DIW. The peak shape was improved compared to previous experiments and the product was completely eluted from the column. When *i*PrOH was used as a co-solvent in the gradient with (MeCN/*i*PrOH 9:1 v/v)/DIW the product was obtained with lower purity. Having selected (MeCN/EtOH 96 % 9:1 v/v)/DIW as the best combination for our separation, we started to investigate the optimal slope of the gradient change. After several experiments and optimization, we found that the best outcome was obtained when the gradient change was set as follows: 8 CV 0 % → 25 %, 4 CV isocratic 25 %, 4 CV 25 % → 100 % and 4 CV isocratic 100 % (Figure 3.3). Both peaks between 6 and 12 minutes correspond to the product. With this gradient, it was possible to remove all major impurities (*i.e.* monoaryl **181**, amine **178**). Using an RP-C_{18} column and a gradient of premixed MeCN/EtOH (9:1 v/v) in DIW we were able to purify crude **1** matching the desired purity of 98 %. The purification was tested on a 3.75 g scale obtaining **1** in two fractions, S1 with a purity of 98.1 % AN by HPLC and S2 with a purity of 99.4 % AN by HPLC. Combining the two fractions, pure **1** was recovered from crude **1** with a 79 % yield.

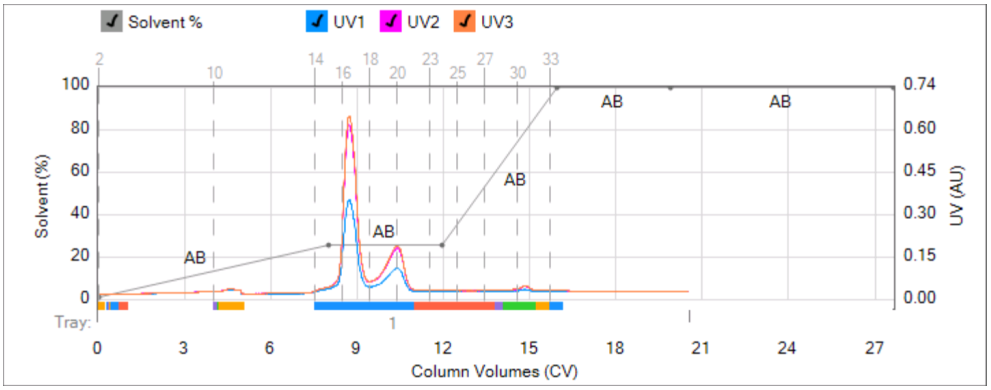

Figure 3.3. Chromatogram gradient (MeCN/EtOH 96 % 9:1 v/v)/DIW, 8 CV 0 % → 25 %, 4 CV isocratic 25 %, 4 CV 25 % → 100 % and 4 CV isocratic 100 %.

3.1.8 Process development route to UAMC-00050

In summary, an optimized process for the scalable preparation of the α-aminophosphonate UAMC-00050 has been developed. Key aldehyde **7** was prepared, according to the Anelli-Montanari protocol using bleach as the primary oxidant and TEMPO/KBr as the catalytic system. The yield was increased from 65 % to 71 % and the atom economy was improved from 33 % to 66 %. The Birum-Oleksyszyn reaction for the preparation of pivotal intermediate **9** was optimized. The combination of $Y(OTf)_3$ as the catalyst, TFAA as the additive and THF/MeCN (1:1 v/v) as the reaction medium increased the yield from 11 % to 44 %. Purification of **9** was achieved using alternative methods to flash chromatography (*e.g.* basic extraction, slurry purification, antisolvent precipitation). For the preparation of product **1**, an AI-based software (xT-SAAM), was used to improve the preparation of **1** using cyanamide as a reagent. The optimized reaction was used to replace the expensive *N*,*N*'-di-Boc-1*H*-pyrazole-1-carboxamidine cutting the cost for the preparation of UAMC-00050. The use of chlorinated solvents and flash chromatography purification of intermediates were removed from the process. Only the final material required flash chromatography purification in order to reach the target purity > 98 %. The new multi-gram process improved the overall yield of compound **1** from 3 % for the medicinal chemistry route to 22 %, the number of steps were reduced from 7 to 6, and in the last step the scale was increased from 0.77 mmol to 7.7 mmol. (Scheme 3.9).

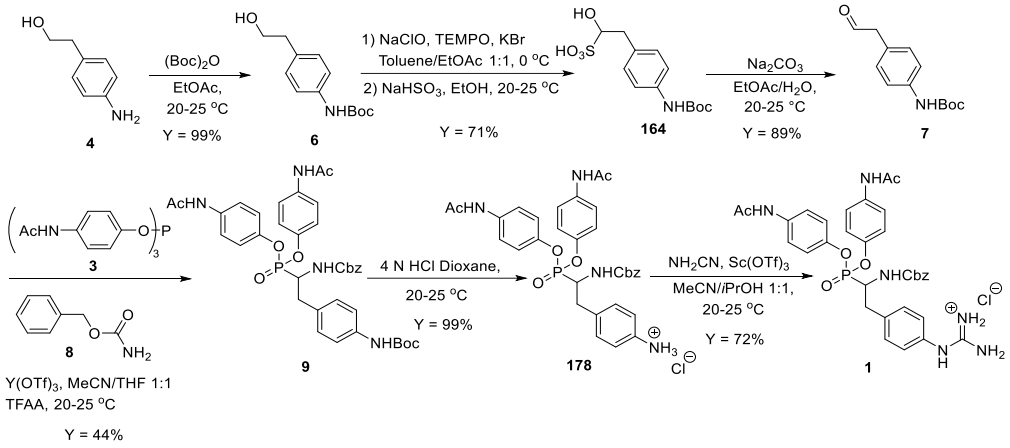

Scheme 3.9. Optimized synthetic route to UAMC-00050

3.1.9 Scope of $Y(OTf)_3$-catalyzed Birum-Oleksyszyn reaction

The efficiency of $Y(OTf)_3$, as a catalyst for the Birum-Oleksyszyn reaction, was investigated using various aldehydes **21**, carbamates **23**, and aryl phosphites **184** (Table 3.18). For the scope were selected both aromatic and aliphatic aldehydes to test how the type of aldehyde affects the yield. Aromatic aldehydes were selected with a variety of functional groups in *para* position in order to understand compatibility of yttrium triflate with the substrate and to be able to perform further reaction on the α-aminophosphonate (*e.g.* reduction, Suzuki-Miyaura coupling, esterification). The *tert*-butyl carbamate was selected to prove that such starting material is compatible with yttrium triflate. Aryl phosphite **3** was prepared according to the procedure for UAMC-00050. With the same protocol, phosphite **183**, was prepared from 4-methoxyphenol (**182**). The highest yields of products were obtained for activated phosphites, for example, tris(*p*-methoxyphenyl)phosphite and the tris(*p*-acetamidophenyl)phosphite (**3**), combined with benzyl carbamate (**8**) and an aromatic aldehyde (Table 3.18, entries 1 and 2). The EDG in phosphite facilitates the nucleophilic attack of the phosphorus atom on the imine. Aliphatic aldehydes represented by *tert*-butyl [4-(2-oxoethyl)phenyl]carbamate (**7**) and 2-phenylacetaldehyde afforded lower yields (38 - 48 %) of products (**9, 185c, and 185d**) (Table 3.18, entries 3, 4, and 5) compared to the yields (72 - 92 %) of products derived from benzaldehyde (**185a, 16, 185e,** and **185f**) (Table 3.18, entries 1, 6, 7, and 8). Among aromatic aldehydes, interesting results were obtained demonstrating how different halogen substituents in the *para*-position affect the yield of the respective product: 4-chlorobenzaldehyde (Table 3.18, entry 9) and 4-bromobenzaldehyde (Table 3.18, entry 10) provided higher yields of **185g** and **185h** (55 and 54 %, respectively) compared to 4-fluorobenzaldehyde (36 % of **185i**) (Table 3.18, entry 11) and 4-iodobenzaldehyde (25 % of

185k) (Table 3.18, entry 12). For product **185j** the poor yield might be caused by its diminished solubility of starting aldehyde in MeCN. Compared to the standard conditions of Birum-Oleksyszyn reaction (application of AcOH as a promotor), the selected Lewis acid catalyst allows performing the synthesis of α-aminophosphonates using acid-labile compounds, as demonstrated by the examples with *tert*-butyl carbamate (Table 3.18, entries 13 - 15) (**185k - 185m**) and Boc-protected amine (Table 3.18, entries 3 and 5) (**9** and **185d**). While yields of products **185k** and **185l** (43 and 41 %, respectively) were lower compared to those obtained for benzyl carbamate analogues (82 and 64 % for products **16** and **185n**) (Table 3.18, entries 6 and 16), for all α-aminophosphonates there were no elevated amounts of hydrolysis products. The lower conversion of starting materials might be explained by the higher steric hindrance of the *tert*-butyl group.[9] Similarly, tri(*o*-tolyl)phosphite provided lower yields of products **185o** and **185p** (34 and 26 %) (Table 3.18, entries 17 and 18) when compared to the analogous reaction with triphenyl phosphite (82 % and 55 % for products **16** and **185g**) (Table 3.18, entries 6 and 9) and tri(*p*-tolyl)phosphite (75 and 43 % for products **185e** and **185q**) (Table 3.18, entries 7 and 19). These differences in yields also might be attributed to the increased steric hindrance near the phosphorus atom, which obstructs the nucleophilic attack of phosphite toward imine. Arylaldehydes bearing a cyano group, when reacting with triphenyl phosphite or tri-*p*-tolyl phosphite, provided the corresponding product **185s** and **185t** with good yield (respectively, 63 and 67 %) (Table 3.18, entries 21 and 22). Good yields were obtained also with vanillin (75 % for product **185u**) (Table 3.18, entry 23) and with methyl 4-formylbenzoate (69 % for product **185v**) (Table 3.18, entry 24). In general, the developed catalytic conditions using $Y(OTf)_3$ are well-compatible with a variety of functional groups in both aldehyde and phosphite. When comparing products with benzaldehyde (**185a**, **185e**, and **185f**) (Table 3.18, entries 1, 7, and 8) and 4-chlorobenzaldehyde (**185b**, **185q**, and **185r**) (Table 3.18, entries 2, 19, and 20), the hydrolyzed side product was detected only in case of products **9**, **185b**, and **185f** testifying the lower stability of the paracetamol ester.

Table 3.18

Scope of Birum-Oleksyszyn reaction catalyzed by $Y(OTf)_3$ with isolated yield and reaction time

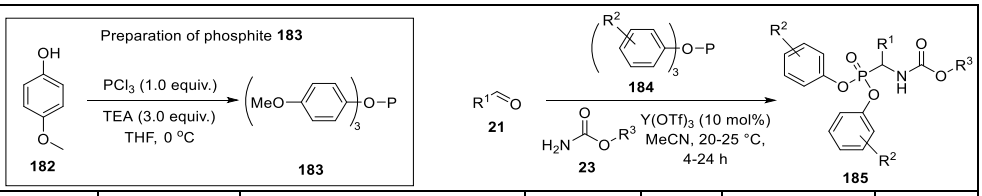

Entry	Product	Aldehyde (R^1CHO)	R^2	R^3	Reaction time (h)	Yield (%)
1	**185a**	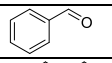	4-MeO	Bn	6	92
2	**185b**	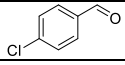	4-AcNH	Bn	4	87

3	**9**	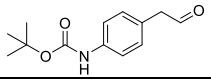	4-AcNH	Bn	4	42
4	**185c**	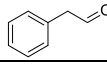	H	Bn	6	48
5	**185d**	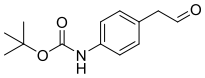	H	Bn	8	38
6	**16**		H	Bn	6	82
7	**185e**		4-Me	Bn	4	75
8	**185f**		4-AcNH	Bn	6	72
9	**185g**	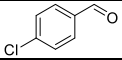	H	Bn	6	55
10	**185h**	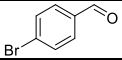	H	Bn	4	54
11	**185i**	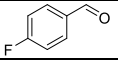	H	Bn	4	36
12	**185j**	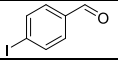	H	Bn	4	25
13	**185k**		H	*t*Bu	6	43
14	**185l**	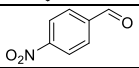	H	*t*Bu	4	41
15	**185m**	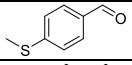	H	*t*Bu	24	17
16	**185n**	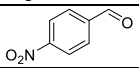	H	Bn	4	64
17	**185o**		2-Me	Bn	8	34
18	**185p**	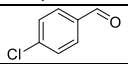	2-Me	Bn	8	26
19	**185q**	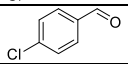	4-Me	Bn	8	43
20	**185r**	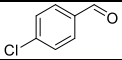	4-MeO	Bn	4	81
21	**185s**	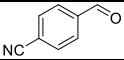	H	Bn	6	67
22	**185t**	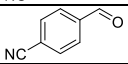	4-Me	Bn	6	63
23	**185u**	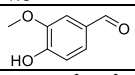	H	Bn	6	75
24	**185v**	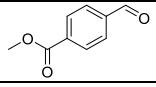	H	Bn	4	69

3.1.10 Yttrium-catalyzed Birum-Oleksyszyn reaction for the preparation of phosphonolactones

While testing the scope of the yttrium-catalyzed Birum-Oleksyszyn reaction, it was noted that when salicylaldehyde (**186**) was reacted with triphenyl phosphite (**26**) and benzyl carbamate (**8**), instead of the desired α-aminophosphonate **187**, a mixture of linear α-aminophosphonate **187** and phosphonolactone **188** was obtained. The ratio of the two products ranged from 75:25 (4 h) to 15:85 (24 h) (Table 3.19, entries 1 - 3) (Scheme 3.10). The cyclic product **188** was formed due to the internal reaction between the phosphonate diester and the salicylic hydroxy group. Derivatives of phosphonolactones possess a variety of interesting biological properties[120–122] and they had a role as flame retardant[123] and polymer building block.[124] Balam and coworkers prepared a series of γ-phosphonolactones through the Kabachnik-Fields reaction between 2-hydroxybenzaldehyes, heterocyclic amines, and diphenyl phosphite.[125] With the intention to use the Birum-Oleksyszyn reaction to prepare and isolate the phosphonolactone we started to screen conditions (*i.e.* concentration, phosphite structure, temperature) to increase the product ratio in favor of the phosphonolactone. Raising the concentration to 1.0 M did not result in any considerable change in the ratio of the two products (Table 3.19, entries 4 - 6). When using diphenyl phosphite (**49**) as phosphite we noted that the ratio at 4 h was much higher in favor of the linear α-aminophosphonate **187** rather than the phosphonolactone **188**, both at 0.5 M (90:10) and 1.0 M (93:7). Furthermore, complete decomposition of the two products was noted after 8 h at both concentrations (Table 3.19, entries 7 - 12). At 50 °C, the cyclization reaction was much faster. For the reaction with triphenyl phosphite (**26**) at 0.5 M, the ratio reached 17:83 after 4 h (Table 3.19, entry 13), raising to 9:91 after 8 h (Table 3.19, entry 14). Similar results were recorded at 1.0 M, where after 4 h the ratio was 19:81 (Table 3.19, entry 16), which increased in favor of product **188** to 13:87 after 8 h (Table 3.19, entry 17). For both concentrations, at 50 °C, both products were completely decomposed after 24 h (Table 3.19, entries 15 and 18). No products were detected using diphenyl phosphite at 50 °C after 4 h (Table 3.19, entries 19 and 20). Unfortunately, we could not use naphthalene as an internal standard due to overlapping with product **188**, hence, we could not establish when the maximum concentration of the product was reached. However, we decided to proceed with conditions in entry 13 (*i.e.* 50 °C, triphenyl phosphite and 0.5 M) for a multigram preparation of product **188**. Quench time was set at 4 h. The reaction was run at a 47 mmol scale, after 4 h the ratio of linear α-aminophosphonate **187** and phosphonolactone **188** was recorded as 32:68, which increased in favor of product **188** (27:73) after the removal of solvent. The residue proved to be a complex mixture of side products and byproducts, in which the target **188** constituted only 3.3 % AN by HPLC. Flash chromatography purification was used to separate the product from the complex mixture. However, after the separation, we could not find the product in any fraction, probably due to a decomposition of the product on silica. In conclusion, the preparation of phosphonolactones through a Birum-Oleksyszyn reaction is possible. Nevertheless, further optimizations are necessary

to increase the product concentration at the expense of all other side products. A screening of Lewis acids is required to find a suitable catalyst for this specific substrate.

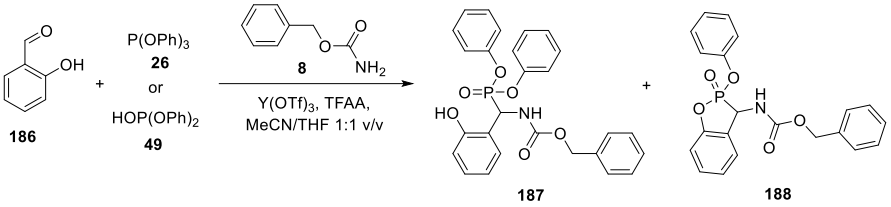

Scheme 3.10. Birum-Oleksyszyn reaction with salicylaldehyde (**186**) as starting material, yielding linear α-aminophosphonate **187** and a phosphonolactone **188**

Table 3.19
Screen of phosphite, temperature and concentration for the synthesis of product **187**

Entry	Phosphite	Temperature (°C)	Concentration (M)	Time (h)	Ratio 187/188
1	$P(OPh)_3$	20-25	0.5	4	75:25
2	$P(OPh)_3$	20-25	0.5	8	50:50
3	$P(OPh)_3$	20-25	0.5	24	15:85
4	$P(OPh)_3$	20-25	1.0	4	75:25
5	$P(OPh)_3$	20-25	1.0	8	49:51
6	$P(OPh)_3$	20-25	1.0	24	22:78
7	$(PhO)_2POH$	20-25	0.5	4	90:10
8	$(PhO)_2POH$	20-25	0.5	8	N/A
9	$(PhO)_2POH$	20-25	0.5	24	N/A
10	$(PhO)_2POH$	20-25	1.0	4	93:7
11	$(PhO)_2POH$	20-25	1.0	8	N/A
12	$(PhO)_2POH$	20-25	1.0	24	N/A
13	$P(OPh)_3$	50	0.5	4	17:83
14	$P(OPh)_3$	50	0.5	8	9:91
15	$P(OPh)_3$	50	0.5	24	N/A
16	$P(OPh)_3$	50	1.0	4	19:81
17	$P(OPh)_3$	50	1.0	8	13:87
18	$P(OPh)_3$	50	1.0	24	N/A
19	$(PhO)_2POH$	50	0.5	4	N/A
20	$(PhO)_2POH$	50	1.0	4	N/A

3.2 Activity-based probe and α-aminophosphonates selectivity

Activity-based protein profiling is a proteomics technique that uses activity-based probes (ABPs) to visualize and characterize enzyme activity within a complex proteome. These molecules are designed to react covalently with the active form of a target enzyme and allow their detection or isolation. Thus, ABPs give information about the activity level of an enzyme rather than its expression level.[126] The University of Antwerp is currently investigating the activity of ABPs **191** on uPA and other serine proteases. α-Aminophosphonates (**189**) are prepared with an alkyne group in the structure, then a biotin tag **190** is connected through the copper(I)-catalyzed cycloaddition between the azide and the alkyne moiety (Scheme 3.11).

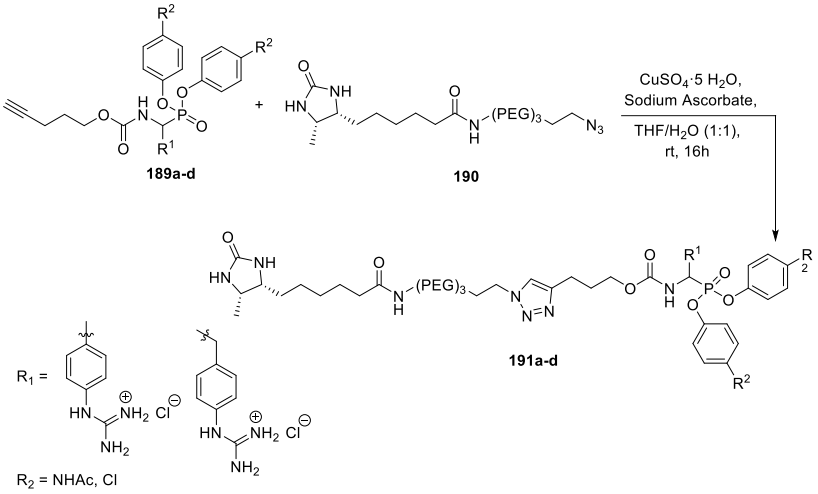

Scheme 3.11. Synthesis of ABPs starting from biotin-PEG-azide and the alkyne-substituted α-aminophosphonate

In Table 3.20 are reported IC_{50} values of four different alkyne-substituted α-aminophosphonates (**189a-d**) and four corresponding ABPs (**191a-d**) prepare after functionalization of **189a-d** with **190**. The *in vitro* experiments were performed by the Medicinal Chemistry Laboratories of the University of Antwerp. The data reports that the products containing a phosphonate ester with 4-chlorophenol showed a lower inhibition concentration on the uPA (Table 3.20, entries 4, 6, and 8). Interestingly, both the alkyne-substituted α-aminophosphonates and the ABPs with the benzaldehyde-derived R^1 moiety showed an $IC_{50} > 10$ μM on the thrombin (Table 3.20, entries 3, 4, 7, and 8). Inhibition of thrombin can be a problem due to the importance of the enzyme in the hemostasis, dysregulation of the thrombin activity can lead to either bleeding or thrombosis.[127]

Table 3.20

IC_{50} on selected enzymes of α-aminophosphonates **189a-d** and ABPs **191a-b**

Entry	Product	R^1	R^2	Thrombin	uPA
				IC_{50} (μM)[b]	
1	**189a**	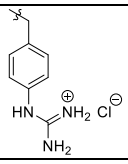	-NHAc	1.11 ± 0.05	0.005 ± 0.001
2	**189b**		-Cl	1.77 ± 0.05	0.005 ± 0.0003
3	**189c**	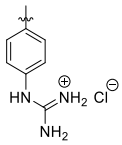	-NHAc	>10	1.52 ± 0.4
4	**189d**		-Cl	>10	0.22 ± 0.06
5	**191a**	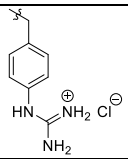	-NHAc	0.76 ± 0.02	0.01 ± 0.003
6	**191b**		-Cl	0.20 ± 0.02	0.006 ± 0.0001
7	**191c**	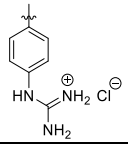	-NHAc	>10	5.19 ± 0.08
8	**191d**		-Cl	>10	0.16 ± 0.04

With the results from the ABPs screening in hand, the University of Antwerp suggested two compounds that might possess a better selectivity on uPA, therefore a better safety profile as a drug (Figure 3.4). UAMC-0004206 is an α-aminophosphonate derived from benzaldehyde, and similar to UAMC-00050, it also possesses a paracetamol phosphonate ester. The compound would serve as back-up for the lead compound UAMC-00050. While UAMC-0004207, also an α-amino-phosphonate derived from benzaldehyde, possesses a 4-chlorophenol phosphonate ester. This compound will be tested as proof of concept for the activity of α-amino-4-chloro-phenolphosphonates.

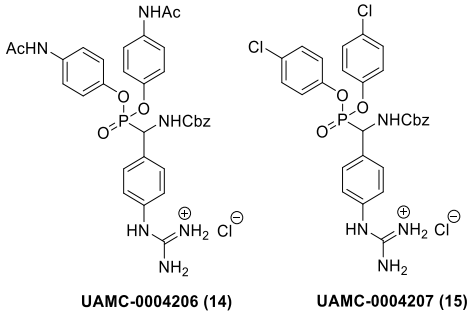

Figure 3.4. α-Aminophosphonates UAMC-0004206 and UAMC-0004207

3.3 Process optimization and preparation of UAMC-0004206

3.3.1 Route selection of UAMC-0004206

For the preparation of UAMC-0004206 (**14**), *tert*-butyl(4-formylphenyl)carbamate (**192**) was purchased and used as starting point for the synthesis of (**193**) (Scheme 3.12). The Birum-Oleksyszyn reaction conditions used for UAMC-00050 were adapted for compound **193**. *N*-Boc deprotection in compound **193** was performed with 4 N HCl in dioxane or TFA/DCM (1:1 v/v). For the synthesis of UAMC-0004206 (**14**), analogous to the medicinal chemistry synthesis of UAMC-00050, *N*,*N*′-di-Boc-1*H*-pyrazole-1-carboxamidine (**11**), was used to insert the guanidine moiety in the α-aminophosphonate. In this way, the resulting Boc-protected guanidine **196** was successfully purified by flash chromatography on silica to eliminate any impurities. The required purity (95 - 98 %) was easily achieved after one chromatographic purification. Next, the last *N*-Boc deprotection was performed with HCl to access directly the final compound or with TFA followed by a salt exchange with the resin DOWEX 1X8.

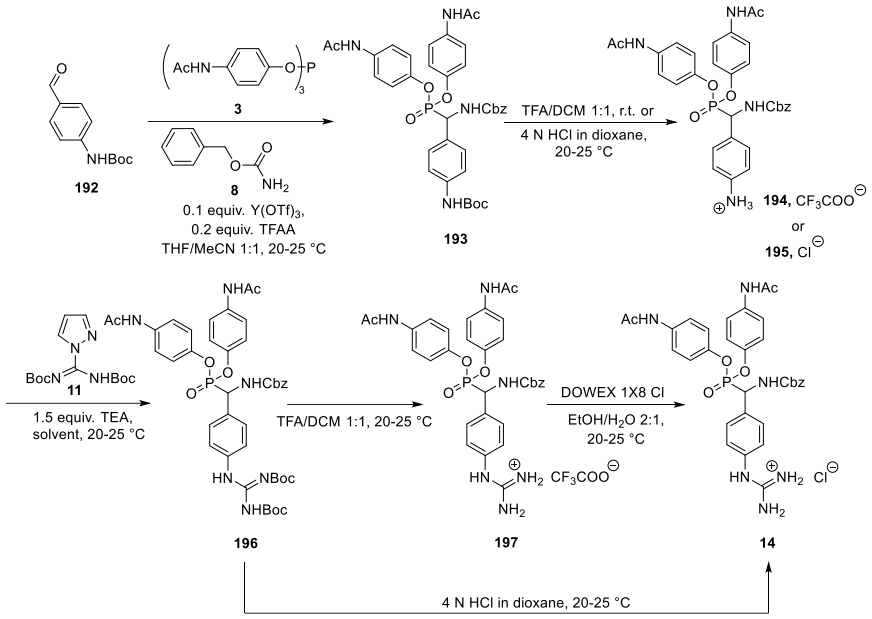

Scheme 3.12. Procedure for UAMC-0004206

3.3.2 Birum-Oleksyszyn synthesis of intermediate 160

The first step for the preparation of UAMC-0004206 (**14**) is the three-component Birum-Oleksyszyn reaction between *tert*-butyl(4-formylphenyl)carbamate (**192**), benzyl carbamate (**8**) and the triaryl-phosphite **3** (Table 3.21). With our knowledge derived from UAMC-00050 research, we decided to use 0.1 equivalents of yttrium triflate as a catalyst, a mixture of MeCN/THF (1:1 v/v) as reaction medium, and TFAA as an additive. A series of small-scale experiments (0.22 mmol) were run in order to find the optimum concentration, the right value of equivalents of TFAA and phosphite **3**, and the optimal quenching time of the reaction. The reaction outcome was calculated based on the ratio between chromatographic concentrations of product **160** and naphthalene as IS. With the same conditions optimized for UAMC-00050 (Table 3.21, entry 1). The highest ratio of product **193** and IS was obtained after 8 h (4.38). Reducing equivalents of TFAA from 1.0 to 0.2 did not negatively affect the reaction, and the ratio of **193** was slightly increased (4.45), maintaining its higher value at 8 h (Table 3.21, entry 2). The presence of TFAA proved to be fundamental for good conversion, since, without anhydride a 3.82 product **193**/IS ratio was reached after 24 h. Any excess of phosphite **3** (*i.e.* 1.5 equivalents), provided a lower product **193**/IS ratio (Table 3.21, entries 5 and 7) compare with entries 4 and 6. The concentration was raised from 0.17 M to 2.5 M, and the product **193**/IS ratio was increased to 1.50 M (5.50 at 4 h)

(Table 3.21, entry 8). Further increasing the concentration to 2.50 M caused a decrease in the product **193** ratio (4.63 at 6 h) (Table 3.21, entry 9). Contrary to UAMC-00050, the ratio between product **193** and monoaryl side product **198** was noted to decrease with the concentration increase (0.30 at 0.33 M, 0.22 at 1.00 M, 0.21 at 1.50 M, and 0.15 at 2.50 M) (Table 3.21, entries 4 - 9). The kinetic profiling of aldehyde **192**, side product (**198**), and product (**193**) for conditions of entry 8, are shown in Figure 3.5. It is possible to see the product increasing its ratio until reaching a peak at 4 h, then decreasing due to the decomposition of the product (**193**).

Table 3.21

Small-scale experiments (0.22 mmol of **192**) for the screening of concentration, equivalents of TFAA and phosphite, and quenching time in the Birum-Oleksyszyn reaction

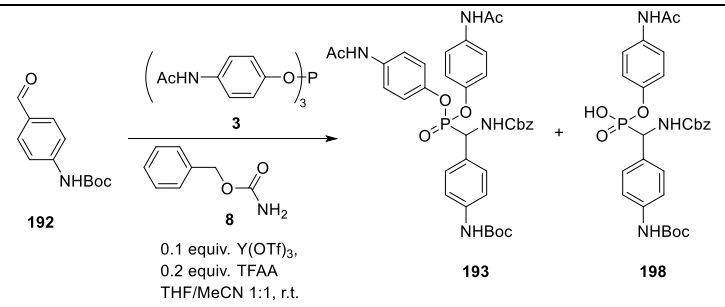

Entry	Phosphite 3 (equiv.)	TFAA (equiv.)	Conc. (M)	193/IS[a] (time)	Ratio 193/198
1	1.0	1.0	0.17	4.38 (8 h)	76:24
2	1.0	0.2	0.17	4.45 (8 h)	73:27
3	1.0	0.0	0.17	3.82 (24 h)	60:40
4	1.0	0.2	0.33	4.13 (24 h)	70:30
5	1.5	0.2	0.33	3.86 (8 h)	58:42
6	1.0	0.2	1.00	4.72 (8 h)	78:22
7	1.5	0.2	1.00	4.56 (8 h)	62:38
8	1.0	0.2	1.50	5.50 (4 h)	78:22
9	1.0	0.2	2.50	4.63 (6 h)	85:15

[a]highest value of **160**/IS recorded from 2 h to 24 h, reaction mixture analyzed every 2 h until 8 h.

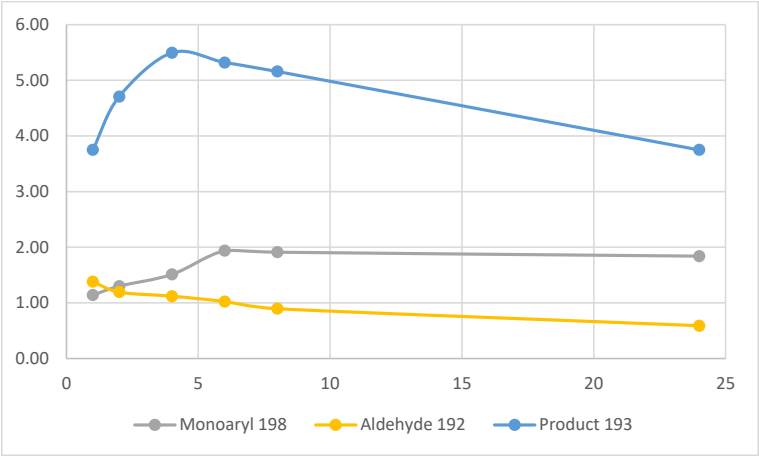

Figure 3.5. The kinetic profiling for intermediate **193** for the preparation of UAMC-0004206 depicts the course of the reaction. Points are calculated as the ratio between compound **193** and IS. After 4 hours the peak of the product is reached, triarylphosphite is completely consumed after the first 2 hours

From the screening, conditions in entries 2, 7, 8 and 9 (Table 3.21) were selected for larger scale experiments with isolated yields of product **193**. Four experiments were run at 2.2 mmol scale. Product **193** was isolated from the reaction mixture after flash chromatography. The standard conditions from UAMC-00050 provided **193** with a yield of 46 % and purity of 89 % AN by HPLC (Table 3.22, entry 1). At 1.00 M and with 1.5 equivalents of phosphite **3** α-aminophosphonate **193** was obtained with a yield of 59 % and purity of 84 % AN by HPLC (Table 3.22, entry 2). The best conditions from the small-scale screening (1.50 M and 4 h quench) provided the target product with 64 % yield and 84 % AN by HPLC (Table 3.22, entry 3), while the higher concentration of 2.5 M product **193** was obtained after purification with 55 % yield and purity 90 % AN by HPLC (Table 3.22, entry 4). The 2.2 mmol scale experiments confirmed the results of the first screening. Conditions in entry 4, (1.50 M, 1.0 equivalents of phosphite **3** and quench after 4 h) were selected for multigram preparation of **193**. Before moving to 4.4 and 11.0 mmol scale purification methods alternatives to flash chromatography were investigated. Unfortunately, since the product showed poor solubility in water-immiscible solvents (*i.e.* EtOAc, 2-Me-THF, MTBE, heptane, toluene) it was not possible to wash the crude material with a basic solution to remove all the paracetamol generated in the reaction. However, taking advantage of the poor solubility of the product in EtOAc, an alternative method of purification, based on a slurry stirring, was developed. The crude product was partially dissolved in 96 % EtOH (EtOH/aldehyde **192** = 40 v/w) and added dropwise to 2.5 volumes of stirred EtOAc at 0 °C. After 2 h of stirring at 0 °C, the product was collected by

filtration. This purification allowed us to reach a purity ranging from 87 to 94 % AN by HPLC directly from a crude reaction product with just one purification step (Table 3.22, entries 5 and 6).

Table 3.22

Batches with isolation of product **193**

Entry	Scale (mmol)	Phosphite 3 (equiv.)	Conc. (M)	Time (h)	Yield (%)	Purity (%)
1	2.2	1.0	0.17	8	46	89
2	2.2	1.5	1.00	4	59	84
3	2.2	1.0	1.50	4	64	84
4	2.2	1.0	2.50	4	55	90
5	4.4	1.0	1.50	4	55	94
6	11.0	1.0	1.50	4	63	87

3.3.3 *N*-Boc deprotection of intermediate 193

Initially, the Boc protecting group was removed using the same condition developed for the *N*-Boc deprotection of UAMC-00050 (Scheme 3.7). α-Aminophosphonate **193** was treated with 4 N HCl in dioxane for 3 h at 20-25 °C (Scheme 3.13), then the solvent was removed, the residue was dissolved in absolute EtOH and added dropwise in 10 volumes of stirred EtOAc at 0 °C. Unfortunately, no precipitate formed in EtOAc, therefore, volatiles were removed in vacuo, and the residue was dissolved again in absolute EtOH and added dropwise in 10 volumes of stirred MTBE at 0 °C. Precipitation of product **195** worked well and a well-formed solid was collected by filtration. The HCl salt of aniline **195** was obtained with good yields and purity among different batches. However, the monoaryl side product **200** was present in the final material with 3.8 % AN by HPLC. We hypothesized that the hydrolyzed product might form due to the presence of water in the 4 N HCl in dioxane. It was also noted, that in the next step, the guanylation with *N*,*N*′-di-Boc-1*H*-pyrazole-1-carboxamidine (**11**), the yields of the guanylated product **196** were higher when the TFA aniline salt was used instead of the HCl aniline salt. The TFA aniline salt (**194**) was prepared by treating the starting Boc-protected material **193** with TFA/DCM 1:1 v/v at 20-25 °C. After 45 minutes, volatiles was removed in vacuo, the crude product was dissolved in absolute EtOH, added dropwise in 10 volumes of stirred MTBE and solid **194** was collected by filtration. The TFA/DCM *N*-Boc deprotection proceeded smoothly in a short time, and almost no hydrolyzed product **199** was detected in the final material. Therefore we decided to use this protocol for larger scale preparation of TFA aniline salt **194**. The reaction was tested with 2.59 mmol of α-aminophosphonate **193**, aniline salt **194** was obtained with 99 % yield and purity 97 % AN by HPLC.

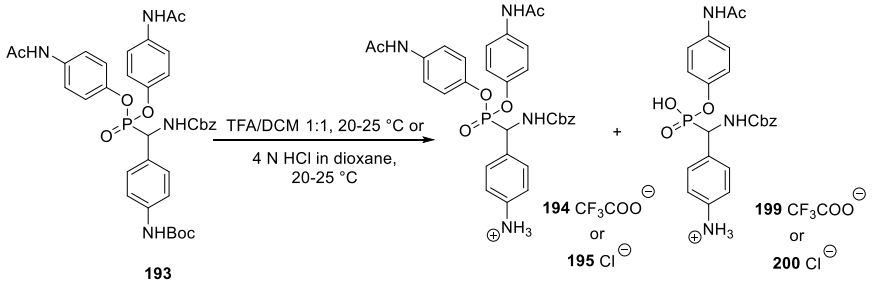

Scheme 3.13. *N*-Boc deprotection for UAMC-0004206 intermediate **193**

3.3.4 Guanylation of intermediate 194 and 195

In the original medicinal chemistry route, guanylation of aniline **194** was performed using *N*,*N*′-di-Boc-1*H*-pyrazole-1-carboxamidine (**11**) as reagents. This strategy, despite a poor atom economy and a high cost of the reagent, was preferred over the guanylation with cyanamide. The resulting Boc-protected product can be readily separated from most side products by chromatography on silica. Initially, 0.78 mmol of HCl salt of aniline **195** were treated with 1.2 equivalents of reagent **11** in *i*PrOH/MeCN (1:1 v/v) (Scheme 3.14). The reaction was quenched when the conversion of aniline **161** was higher than 90 % (Table 3.23, entry 1). Unfortunately, the conditions in entry 1 were not reproducible on the same scale and the yield of product **196** dropped to 54 % (Table 3.23, entry 2). Instead of HCl salt, TFA salt of aniline **194** was used as a starting material. After 96 h a conversion of **194** higher than 90 % was reached and the product was isolated with a yield of 74 % (Table 3.23, entry 3). After flash chromatography, it turned out that one impurity co-elutes with the product. Analysis of its mass spectrum allowed us to hypothesize that it might correspond to the structure of **201**, where one *tert*-butyl group in the product is exchanged with an *iso*-propyl group due to transesterification with *i*PrOH. The alcohol was then substituted with DCM and the mixture DCM/MeCN (1:1 v/v) was selected as the reaction medium. The new mixture allowed to slightly increase the yield, and the impurity **201** was not observed in the product anymore (Table 3.23, entry 4). Having concluded the first screen we focused on the work-up/purification methodology before moving to a larger scale reaction.

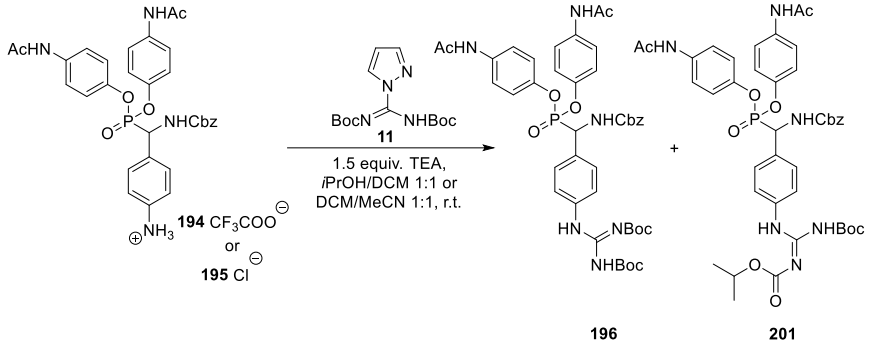

Scheme 3.14. Guanylation of aniline **194** or **195** with *N*,*N*′-di-Boc-1*H*-pyrazole-1-carboxamidine

Table 3.23

Optimization of the synthesis of product **196**

Entry	Scale (mmol)	Aniline	Solvent	Conc. (M)	Time (h)	Yield[a] (%)
1	0.78	**195**	*i*PrOH/MeCN 1:1 v/v	1.0	96	88
2	0.78	**195**	*i*PrOH/MeCN 1:1 v/v	1.0	96	54
3	0.70	**194**	*i*PrOH/MeCN 1:1 v/v	1.0	96	74
4	0.70	**194**	DCM/MeCN 1:1 v/v	1.0	96	75
5	2.68	**194**	DCM/MeCN 1:1 v/v	1.0	144	67
6	7.68	**194**	DCM/MeCN 1:1 v/v	1.0	120	43
7	10.20	**194**	DCM/MeCN 1:1 v/v	1.0	168	71

[a]Isolated yield.

As for UAMC-00050, to remove all unreacted aniline **194** and residual TEA, crude product **196** was dissolved in DCM and washed with 0.1 N aq. HCl. However, the dissolution of the product and separation of layers proved to be difficult, therefore we explored other alternatives to remove the unreacted aniline **194** and the TEA. Using the difference in polarity between the product and the reagents, *N*,*N*′-di-Boc-1*H*-pyrazole-1-carboxamidine (**11**) and triethylamine were removed after slurry purification in heptane/EtOAc (2:1 v/v). After filtration, product **196** was obtained with a purity of 85 % AN by HPLC, with 10 % AN by HPLC of aniline **194**. Product **196** was isolated from the starting aniline **194** by normal phase flash chromatography (gradient heptane/EtOAc). The first multigram synthesis of product **196** with 2.68 mmol of aniline **194**, was complicated by a much longer reaction time (144 h), which required reaching a conversion of starting material higher than 90 %. After slurry purification and flash chromatography, the product was isolated with a yield of 67 % (Table 3.23, entry 5). As the long reaction time did not lead to significant hydrolysis of the starting material or the product, we proceeded with further upscale without any modification to the reaction parameters (*e.g.* solvents, concentration). After running the reaction to 7.68 mmol,

the reaction suffered a slower conversion and the 90 % conversion threshold was crossed after 120 h. Unfortunately, some product was lost during the purification, which led to a moderate 43 % yield of product **196** (Table 3.23, entry 6). The last multigram synthesis was performed with 10.20 mmol of starting material, the 90 % conversion threshold was crossed after 168 h. Product **196** was isolated, after flash chromatography with 71 % yield and purity of 97 % AN by HPLC (Table 3.23, entry 7).

3.3.5 *N*-Boc deprotection of intermediate 196

The *N*-Boc deprotection was initially carried out with an excess of 4 N HCl in dioxane to obtain the desired chloride salt **14** required for the biological test. The complete conversion of the starting material **196** to product **14** required a long reaction time (20 h). Then the reaction mixture was concentrated, the residue dissolved in absolute EtOH and added dropwise to 10 volumes of stirred MTBE at 0 °C. HPLC assay of the final material showed the presence of the hydrolyzed monoaryl side product **203** which counted as 11 % AN by HPLC (Table 3.24, entry 1). As for the *N*-Boc deprotection of intermediate **193,** we speculated that this impurity might arise from the presence of water in the acid solution. Before switching to *N*-Boc deprotection with TFA, followed by a salt exchange, the anhydrous solution of 1 N HCl in Et_2O was tested. The complete conversion of **196** to guanidine **14** took 72 h and despite using a water-free reagent, the presence of the hydrolyzed product was noted again in the final material (Table 3.24, entry 2). Substitution of 4 N HCl in dioxane with TFA/DCM (1:1 v/v) avoided the formation of the hydrolyzed side product **202** and provided a complete conversion after 3 h with an 84 % yield of **197** at 0.11 mmol scale (Table 3.24, entry 3). Experiments on a larger scale were performed with the working condition in hand. At 0.51, 1.03, and 2.25 mmol scale, the desired product **197** was obtained with a yield of 99 % and with the side product **202** ranging from 0.5 to 1.0 % AN by HPLC in the final material (Table 3.24, entries 4 - 6).

Table 3.24

Optimization of the synthesis of product **197**

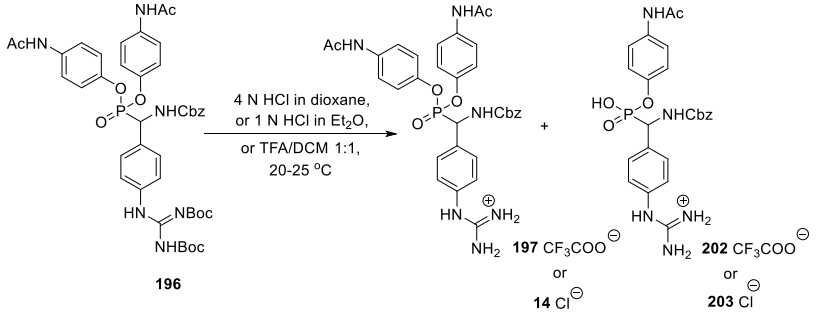

Entry	Scale (mmol)	Reagent	Time (h)	(197,14)/(202,203) ratio	Yield (%)
1	1.02	4 N HCl in dioxane	20	89.0:11.0	44
2	0.11	1 N HCl in Et_2O	72	94.4:5.6	78
3	0.11	TFA/DCM (1:1 v/v)	3	99.5:0.5	84
4	0.51	TFA/DCM (1:1 v/v)	3	99.1:0.9	99
5	1.03	TFA/DCM (1:1 v/v)	3	99.2:0.8	99
6	2.25	TFA/DCM (1:1 v/v)	3	99.0:1.0	99

3.3.6 Salt exchange of intermediate 197

The last step involved a salt exchange between trifluoroacetate and chloride (Scheme 3.15). The method used in the medicinal chemistry preparation of the UAMC-00050 was applied also for this substrate.[6] The TFA salt was dissolved in EtOH/H_2O (2:1 v/v) and stirred with DOWEX 1X8 Cl resin (Resin/Product **197** = 10:1 w/w) for 32 h. Then the mixture was filtered, and volatiles were removed in vacuo. The residue was dissolved in absolute EtOH and added dropwise to 10 volumes of stirred MTBE at 0 °C, the solid was collected by filtration and dried in vacuo to get an off-white product. The salt exchange was performed on eight different batches and the scale was kept below 2.0 mmol of TFA salt **197**. Overall, 5.79 g of final material **14** were collected from different batches with a purity higher than 95 % AN by HPLC, acceptable for *in vitro* tests (Table 3.25).

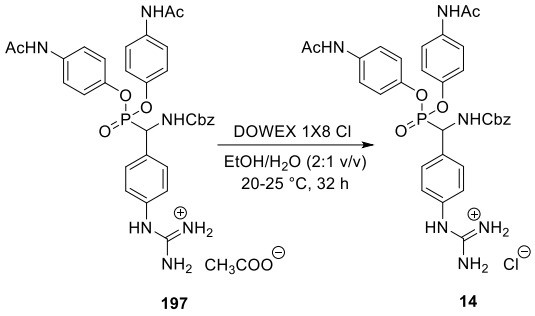

Scheme 3.15. Salt exchange with DOWEX 1X8 Cl in EtOH/H_2O (2:1 v/v)

Table 3.25

Batches of product **14** isolated after the salt exchange, progressive up-scale

Entry	Isolated product 14 (mmol)	Purity (%) AN by HPLC (254 nm)
1	0.1	95.5
2	0.5	97.7
3	1.0	95.1
4	1.1	98.4
5	2.0	97.7

3.4 Process development of UAMC-0004207

3.4.1 Route selection for UAMC-0004207

UAMC-0004207 possesses a similar structure to UAMC-0004206, where the only difference is located in the phosphonate ester. In this molecule, the paracetamol ester is substituted with a 4-chlorophenol ester. Due to the toxicity of the phenol, which is released once the molecule reacts with serine in the active site of the uPA enzyme, UAMC-0004207 was not planned to be used as back-up compound for UAMC-00050. This compound, instead, will be used to validate the inhibition mechanism of ABPs based on 4-chlorophenol phosphonate esters. We decided to use the used for preparing UAMC-0004206 (Scheme 3.16). Phosphite **205** was prepared from phenol **204** with the same procedure as for phosphite **3**. The Birum-Oleksyszyn reaction was run in MeCN/THF (1/1 v/v) mixture and promoted by 10 mol% of $Y(OTf)_3$. The optimal concentration, quench time and equivalents of TFAA were found after a conditions screening. As for UAMC-0004206 the guanidine moiety was inserted with *N*,*N*′-di-Boc-1*H*-pyrazole-1-carboxamidine, and the resulting Boc-protected compound **209** could be easily separated from the majority of impurities. Finally, for the *N*-Boc deprotection the same strategy for the previous α-

aminophosphonate: if suitable HCl could be used for deprotection and obtaining the desired salt **15** in one step, otherwise TFA would have been used for deprotection, followed by a salt exchange with DOWEX 1X8.

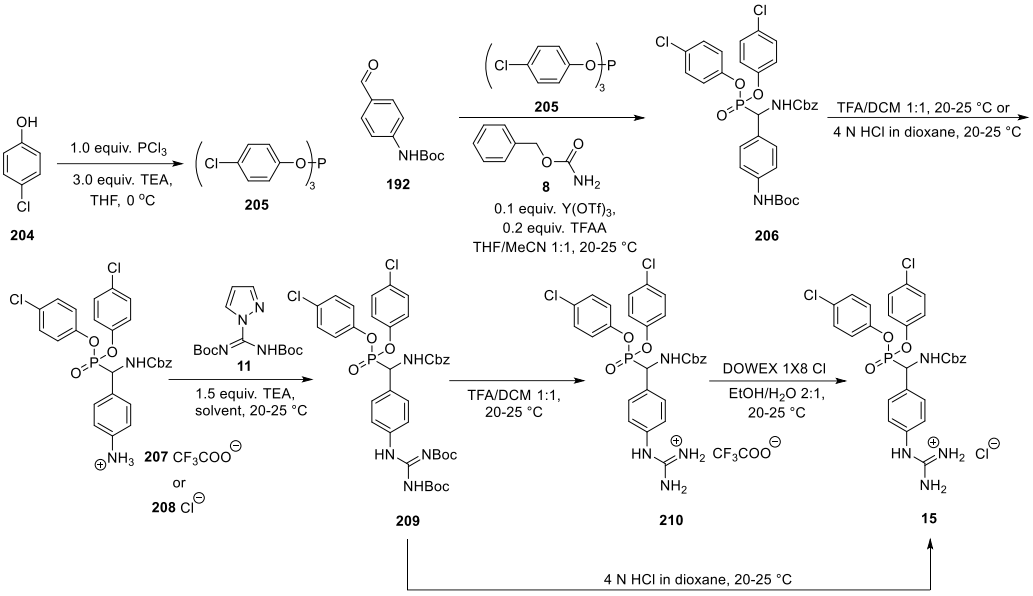

Scheme 3.16. Synthetic route for UAMC-0004207

3.4.2 Birum-Oleksyszyn reaction

As a starting point, we used the standard conditions for the Birum-Oleksyszyn reaction found during the process development of UAMC-00050. Aldehyde **192** (1.0 equiv.) was reacted with phosphite **205** (1.0 equiv.) and benzyl carbamate (**8**) (1.0 equiv.) in the presence of $Y(OTf)_3$ (0.1 equiv.) and TFAA (1.0 equiv.) using MeCN/THF (1:1 v/v) (0.17 M concentration) as a medium. The highest relative product concentration was reached after 8 h, with the ratio of product **206**/IS of 2.34 (Table 3.26, entry 1). When the same conditions were repeated with 0.2 equivalents of TFAA, the highest ratio of product **206**/IS (2.58) was reached after 24 h (Table 3.26, entry 2). Analogous to UAMC-0004206, in the next stage of optimization, the concentration and an excess of phosphite were varied to increase the ratio of product **206** further. At 0.33 M, the highest value of the ratio **206**/IS was increased to 2.93 (after 6 h) and at 1.00 M was increased to 3.33 (after 4 h) (Table 3.26, entries 3 and 4). Increasing the equivalents of phosphite **205** (1.5) allowed to increase in the ratio to 3.44, with the highest value reached after 4 h (Table 3.26, entry 5). As for UAMC-0004206, we noted a decrease in selectivity towards product **206** with an excess of phosphite **205**, at the same concentration with 1.0 equivalents of **205** the ratio product **206**/side product **211** was 91:9. In comparison, with 1.5 equivalents of **205,** the ratio decreased to 88:12 (Table 3.26, entries

4 and 5). With further increasing of concentration to 1.50 M, the product **206**/IS ratio increased to 4.24 (after 6 h) with 1.0 equivalents of **205** and 3.79 (after 2 h) with 1.5 equivalents of **205**. While at 2.50 M, the product **206**/IS ratio reached the value of 4.84 (after 2 h) with 1.0 equivalents of **205** (Table 3.26, entries 6 - 8).

Table 3.26

Screening of concentrations, equivalents of TFAA and phosphite **205** for the preparation of **206**

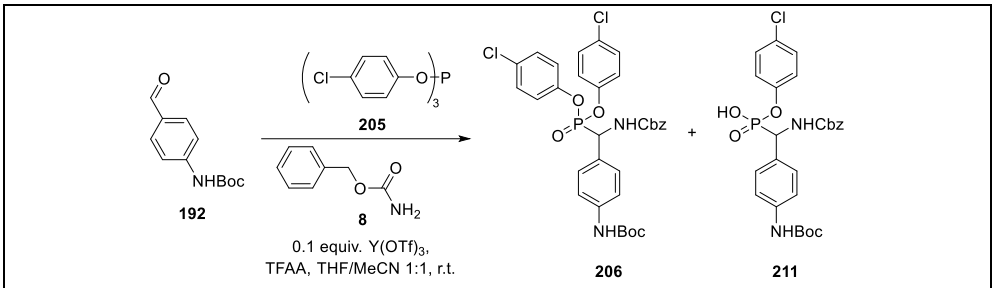

Entry	Phosphite 205 (equiv.)	TFAA (equiv.)	Conc. (M)	206/IS[a] (time)	206/211 ratio
1	1.0	1.0	0.17	2.34 (8 h)	92:8
2	1.0	0.2	0.17	2.58 (24 h)	89:11
3	1.0	0.2	0.33	2.93 (6 h)	88:12
4	1.0	0.2	1.00	3.33 (4 h)	91:9
5	1.5	0.2	1.00	3.44 (2 h)	88:12
6	1.0	0.2	1.50	4.24 (6 h)	97:3
7	1.5	0.2	1.50	3.79 (2 h)	92:8
8	1.0	0.2	2.50	4.84 (2 h)	96:4

With 4-chlorophenol α-aminophosphonate the selectivity, in general, was better towards the product than with paracetamol α-aminophosphonate (as in UAMC-00050 and UAMC-0004206). The ratio **206**/**211** was much lower than in the Birum-Oleksyszyn reaction for the preparation of UAMC-0004206 and as in the previous screening (Table 3.21) the ratio was noted to increase with the increase of concentration. The two best operation conditions from the small-scale screening (Table 3.26, entries 6 and 8) were selected for 2.3 mmol scale reaction, and the product was isolated after flash chromatography. At 1.5 M concentration, the reaction was quenched after 6 h and product **206** was isolated in 47 % yield and purity 91 % AN by HPLC (Table 3.27, entry 1). At 2.5 M the reaction was stopped after 2 h and product **206** was isolated with a 71 % yield and purity of 85 % (Table 3.27, entry 2). The higher yield obtained in entry 2 confirmed the observations from the first screen (Table 3.27). With 2.5 M concentration at 4.6 mmol scale of aldehyde **192** a similar 70 % yield was obtained (Table 3.27, entry 3), however, when the synthesis was performed at 11.5

and 13.3 mmol scale of **192**, the yield dropped respectively to 43 and 53 % (Table 3.27, entries 4 and 5). These poor results might be attributed to problems in the separation of the product from impurities.

Table 3.27

Batches of product **206** with isolated yield

Entry	Scale (mmol)	Conc. (M)	Time (h)	Yield (%)	Purity (%)
1	2.3	1.5	6	47	91
2	2.3	2.5	2	71	85
3	4.6	2.5	2	70	81
4	11.5	2.5	2	43	76
5	13.3	2.5	2	53	75

The kinetic profiling of aldehyde **192**, side product **211**, and product **206** for conditions of Table 3.26, entry 8, are depicted in Figure 3.6 (points are calculated as the ratio between the compound **206** and the internal standard). As for UAMC-0004206, it is possible to see the product increasing its ratio until reaching a peak at 2 h, then decreasing due to the decomposition of product **206**.

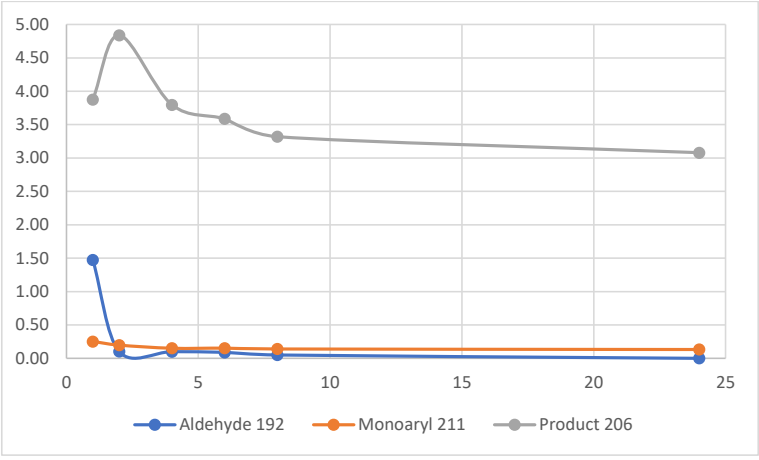

Figure 3.6. The kinetic profile for intermediate **206** for the preparation of UAMC-0004207 depicts the course of the reaction. Points are calculated as the ratio between compound **206** and IS. After 2 hours the peak of the product is reached.

3.4.3 *N*-Boc deprotection of intermediate 206

The *N*-Boc deprotection was initially performed under very similar conditions to the preparation of UAMC-00050 (Scheme 3.7). Intermediate **206** was treated with 4 N HCl in dioxane for 30 h at 20-25 °C (Scheme 3.17). Then, volatiles were removed in vacuo, the crude material dissolved in absolute EtOH and added dropwise to 10 volumes of stirred MTBE at 0 °C. The aniline **208** formed a yellow precipitate that was collected by filtration providing the product with 96 % yield and purity of 99 % AN by HPLC. The antisolvent precipitation was able to remove a large part of the impurities generated in the Birum-Oleksyszyn step. As for UAMC-0004206, the TFA aniline salt **207** proved to be superior to the HCl aniline salt **208** in the guanylation reaction with *N*,*N*′-di-Boc-1*H*-pyrazole-1-carboxamidine. For the preparation of TFA salt **207**, intermediate **206** was dissolved in TFA/DCM (1:1 v/v) and stirred at 20-25 °C for 3 h until complete conversion. The volatiles were removed in vacuo, and the crude material was dissolved in absolute EtOH and added dropwise in 10 volumes of stirred MTBE at 0 °C, unfortunately, no precipitate was formed. A small screening of antisolvents (*i.e.* Et_2O, heptane, cold MTBE) failed to provide suitable conditions for the precipitation of aniline TFA salt **207**. Accordingly, at the end of the reaction, the mixture was concentrated, and the crude oily TFA salt was used in the next step. However, later it was discovered that traces of TFA remained in the crude salt **207**, the acidic residual was connected with the poor yield of **209** after the upscale of guanylation reaction to 3.0 mmol. Crude aniline TFA salt **207** was then dissolved in EtOAc and washed with a solution of 0.5 % aq. NH_4HCO_3. The basic wash provided aniline free base **212** and allowed the complete removal of TFA, which improved the yield on the next step. The TFA/DCM protocol was upscaled to 3.4 mmol of intermediate **206** and aniline free base **212** was obtained with 97 % yield and purity of 75 % AN by HPLC.

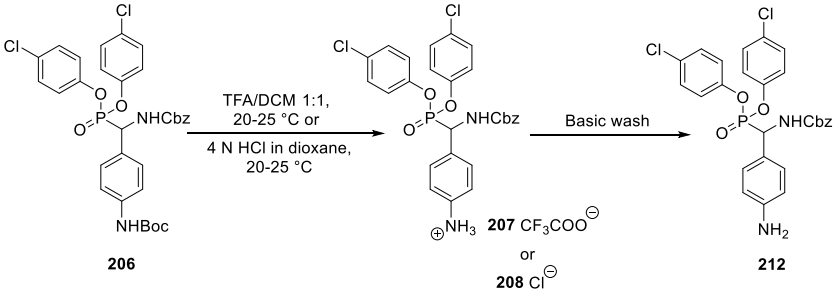

Scheme 3.17. *N*-Boc deprotection of intermediate **206**

3.4.4 Guanylation of intermediate 212

Research in preparation of UAMC-0004206 proved to be useful, hence the solvent mixture *i*PrOH/MeCN (1:1 v/v) was excluded to avoid transesterification of the *tert*-butyl group. Thus, screening for converting aniline HCl **208** to guanidine **209** was initiated from DCM/MeCN (1:1 v/v) in the presence of TEA (1.5 equiv.). Initially, the concentration was set at 2.0 M, and after 96 h the conversion achieved 89 % (Table 3.28, entry 1). However, at 2.0 M, a thick precipitate formed inside the flask after 30 minutes, the solid slowed down magnetic stirring, and some mixture remained on the flask's walls. The concentration was decreased to 1.0 M to allow a better stirring of the mixture, therefore ensuring a better mass transfer. The conversion was increased from 89 % to 92 % (Table 3.28, entry 2). On the other side, at 1.0 M concentration, the ratio between product **209** and side product **213** decreased from 82:18 (2.0 M) to 72:28. By analogy with the research on UAMC-0004206 (Table 3.23) TFA salt of aniline **207** as starting material was used instead HCl salt **208**. We were pleased to find that both the conversion (95 %) and the ratio **209**/**213** (98:2) were improved (Table 3.28, entry 3). As reported earlier, after the *N*-Boc deprotection, the HCl salt **208** was precipitated from EtOH/MTBE and isolated with a purity of 99 % AN by HPLC. Instead, the TFA salt **207** could not be purified with antisolvent precipitation. The advantages of working with a pure intermediate prompted us to carry out additional experiments with HCl salt **208** on a larger scale (0.6 mmol). Unfortunately, a lower conversion after 96 h was observed, dropping from 92 % to 69 % (Table 3.28, entry 4). Using 1.5 equivalents of DIPEA instead of TEA did not help to improve the conversion, which was further decreased to 60 %, on the other side, the ratio **209**/**213** was increased to 89:11 (Table 3.28, entry 5). Unsatisfied with the results of HCl aniline salt **208** we decided to proceed with the TFA aniline salt **207** as the starting material for this step. The guanylation was tested with 1.5 equivalents of TEA and DIPEA, for both experiments the conversion was almost complete, with 97 % and 98 %, respectively (Table 3.28, entries 6 and 7). The ratio **209**/**213** was also improved to 94:6 in the case of TEA and 99:1 in the case of DIPEA.

Table 3.28

Optimization of guanylation reaction

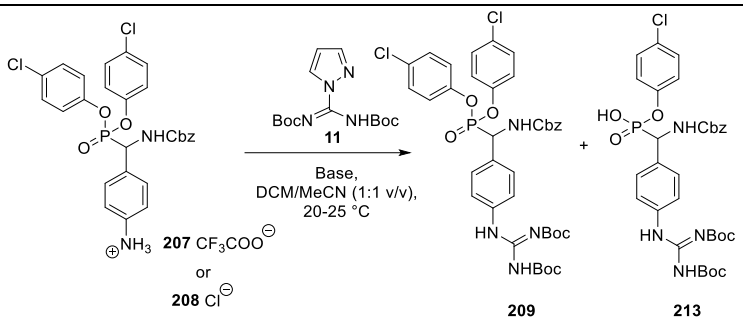

Entry[a]	Aniline	Scale (mmol)	Conc. (M)	Base (1.5 equiv.)	Conversion after 96 h (%)	Ratio 175/179
1	**208**	0.3	2.0	TEA	89	82:18
2	**208**	0.3	1.0	TEA	92	72:28
3	**207**	0.3	1.0	TEA	95	98:2
4	**208**	0.6	1.0	TEA	69	82:18
5	**208**	0.6	1.0	DIPEA	60	89:11
6	**207**	0.6	1.0	TEA	97	94:6
7	**207**	0.6	1.0	DIPEA	98	99:1

[a]*N*,*N*′-Di-Boc-1*H*-pyrazole-1-carboxamidine (1.2 equiv.), base (1.5 equiv.), DCM/MeCN (1:1 v/v), 20-25 °C.

Conditions in entry 7 were selected for further upscale. The TFA aniline salt **207** was treated with 1.2 equivalents of *N*,*N*′-di-Boc-1*H*-pyrazole-1-carboxamidine **11** in the presence of 1.5 equivalents of DIPEA in DCM/MeCN (1:1 v/v). After 96 h a conversion of 90 % was reached and after flash chromatography, the product was obtained in 37 % yield (Table 3.29, entry 1). In order to explain this low isolated yield we have speculated that part of the product might decompose during purification due to DIPEA present in the reaction mixture. The synthesis of **209** was repeated at 3.0 mmol scale, but unfortunately, the reaction proceeded slowly and 144 h were necessary to reach a conversion of 72 % (Table 3.29, entry 2). The volatiles were removed in vacuo, and then before the flash chromatography purifications, the crude material dissolved in EtOAc and washed with 0.5 % aqueous $KHSO_4$ to completely remove DIPEA. However, only 10 % of the product was isolated after flash chromatography. We speculated that the poor yield was due to residual trifluoroacetic acid left in the crude material after the *N*-Boc deprotection. Therefore a basic wash with 0.5 % aqueous NH_4HCO_3 was added as a treatment for the TFA aniline salt to generate free base **212**. With the new starting material **212** the equivalents of DIPEA, necessary to achieve a basic pH (8 - 10), were reduced to 0.8 and after 96 h a conversion of 83 % was reached (Table 3.29, entry 3). After work-up and purification, product **209** was isolated with a yield of 45

%. In a second batch, at 0.8 mmol scale, the equivalents of DIPEA were further reduced to 0.3 and a 91 % conversion was reached after 96 h, product **209** was isolated with a yield of 43 % (Table 3.29, entry 4). Satisfied with the new reaction and work-up conditions we increased the scale to 1.8 mmol where product **209** was isolated with 63 % yield and purity of 95 % AN by HPLC (Table 3.29, entry 5).

Table 3.29

Screening of work-up conditions for the guanylation of UAMC-0004207

Entry	Scale (mmol)	Treatment starting material	DIPEA (equiv.)	Conversion (%)	Work-Up	Yield (%)
1	2.1	None	1.5	90[a]	None	37
2	3.0	None	1.5	72[b]	Wash with 0.5 % aq. $KHSO_4$	10
3	0.8	Wash with 0.5 % aq. NH_4HCO_3	0.8	83[a]	Wash with 0.5 % aq. $KHSO_4$	45
4	0.8	Wash with 0.5 % aq. NH_4HCO_3	0.3	91[a]	Wash with 0.5 % aq. $KHSO_4$	43
5	1.9	Wash with 0.5 % aq. NH_4HCO_3	0.3	94[a]	Wash with 0.5 % aq. $KHSO_4$	63

[a]Conversion after 96 h; [b]conversion after 144 h.

3.4.5 *N*-Boc deprotection of guanidine 209

Based on our experience with the final *N*-Boc deprotection of UAMC-0004206, we started to test deprotection with TFA/DCM 1:1 v/v at 20-25 °C (Scheme 3.18), and the product was obtained after 2 h. However, it was impossible to find a suitable solvent for the precipitation of the product. The volatiles were removed by vacuo and product **210** was obtained with a purity of 94 % AN by HPLC, lower than the 95 % requirement (Table 3.30, entry 1). The deprotection was then performed, using 4 N HCl in dioxane, directly generating the hydrochloride salt **15**. Firstly, the reaction was run for 16 h, the volatiles were removed in vacuo, and the residue was dissolved in absolute EtOH and added dropwise to 10 volumes of stirred MTBE at 0 °C. The final product **15** was obtained by filtration as an off-white solid, with a purity of 90 % AN by HPLC, where the mono-Boc intermediate **214** represented the main impurity (Table 3.30, entry 2). The AN by HPLC of the final material did not change when product **15** was dissolved again in absolute EtOH and added dropwise in 10 volumes of stirred MTBE at 0 °C. The presence of impurity **214** indicated that a longer time was necessary for a complete deprotection. The final material was obtained with:

a purity of 95 % AN by HPLC when the reaction was run for 24 h (Table 3.30, entry 3), and a purity of 97 % AN by HPLC when the reaction was run for 30 h (Table 3.30, entry 4). With the optimized conditions in hand, we upscaled the reaction to 500 mg scale, and, among the five different batches, the hydrochloride salt UAMC-0004207 was obtained with yields between 73 % and 89 % and purities between 96 and 99 % AN by HPLC (Table 3.30, entry 5).

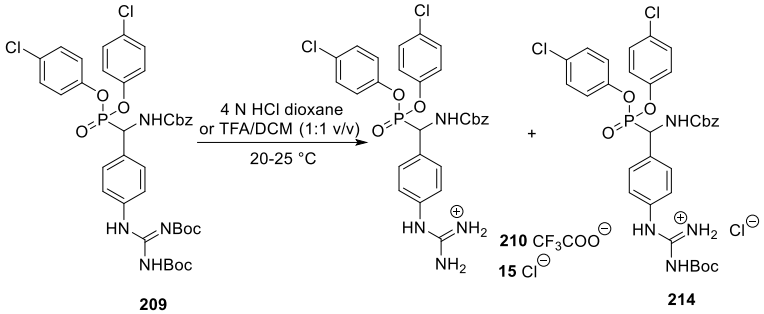

Scheme 3.18. *N*-Boc deprotection of intermediate **209**

Table 3.30

Batches of final deprotection for the preparation of UAMC-0004207

Entry	Scale (mmol)	Reagent	Time	Purity (%)[c]	Yield (%)
1[a]	0.1	TFA/DCM 1:1 v/v	2 h	94	54
2[b]	0.1	4 N HCl in Dioxane	16 h	90	65
3[b]	0.1	4 N HCl in Dioxane	24 h	95	64
4[b]	0.1	4 N HCl in Dioxane	30 h	97	61
5[b]	0.5	4 N HCl in Dioxane	30 h	96 - 99	73 - 89

[a]Final material obtained after removal of volatiles in vacuo. [b]Final material dissolved in abs. EtOH and precipitated in 10 volumes of MTBE at 0 °C then filtered; [c]AN by HPLC (254 nm).

3.5 Stereoselective preparation of UAMC-00050

3.5.1 Separation of enantiomers, screening of conditions and scale-up

Investigation into how stereochemistry can affect the activity of enzyme inhibitors is pivotal during drug development. UAMC-00050 consists of two enantiomers, but its binding activity on uPA was tested only for the racemic mixture. Data on the binding of each enantiomer is crucial for understanding interactions with the enzyme and developing more active molecules. Unfortunately, methods for the stereoselective preparation of α-aminophosphonates are very limited both in scope and in a degree of enantioselectivity. Accordingly, our primary target was the preparation of

individual enantiomers of UAMC-00050 by separating the racemic mixture and testing their binding with uPA. There are several commercially available chiral chromatographic columns for the separation of enantiomers. The size of the columns ranges from an analytical scale, where one can inject up to a few milligrams, to a simulated moving bed,[128] where kilograms of enantiomers can be isolated in a day. Since it was not known which substituents of α-aminophosphonate core will allow better chromatographic separation three aminophosphonates were selected: the final compound **1** and two intermediates **9** and **12**. For the screening of chromatographic conditions 10 different columns and 19 mobile phases were selected. As stationary phases we decide to work with three CHIRALPAK® columns (*i.e.* IA, IB, and IC) and two Lux Chiral Columns (*i.e.* LC1 and LC2). These columns are standardly used to develop methods for separation of enantiomers. As for the stationary phase were selected a series of standard mobile phases that are used to screen chiral methods for HPLC. Results for compound **9** are reported in Table 3.31 (all runs are 30 minutes). The best result was obtained with the column Lux Cellulose-1 (LC1, 4.6x250 mm) using 100 % MeCN + 0.1 % ethanolamine (Flow = 1 mL/min) as mobile phase. The method provided good separation of the two enantiomers and a good peak shape.

Table 3.31

Test of chiral columns and mobile phases for the chiral separation of racemic compound **9**

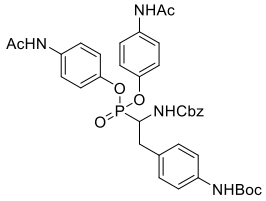

9

Mobile phase	**Columns**				
	IA	**IB**	**IC**	**LC1**	**LC2**
100 % MeOH F = 1 mL/min	IV	N/A	IV	III	N/A
100 % MeCN F = 1 mL/min	IV	IV	N/A	II	N/A
100 % MeCN + 0.1 % ethanolamine F = 1 mL/min	N/A	IV	II	**I**	II
100 % MeCN + 0.1 % diethanolamine F = 1 mL/min	N/A	N/A	II	N/A	N/A
100 % EtOH F = 0.5 mL/min	N/A	N/A	N/A	III	N/A
100 % *i*PrOH F = 0.3 mL/min	N/A	III	N/A	N/A	N/A
50 % MeCN in H_3PO_4 (0.1 % aq.) F = 1 mL/min	IV	N/A	N/A	N/A	N/A

50 % MeCN in H_2O F = 1 mL/min	N/A	IV	N/A	N/A	N/A
60 % MeCN in H_2O F = 1 mL/min	N/A	N/A	IV	N/A	N/A
60 % MeCN in H_3PO_4 (0.1 % aq.) F = 1 mL/min	N/A	N/A	IV	N/A	N/A

Tier list: I (good resolution and peak shape), II (moderate resolution and peak shape), III (bad resolution or k < 0.5), IV (no resolution), N/A conditions not tested.

A separation of the two enantiomers of product **1** would have been optimal since no more modifications were required for the isolated enantiomers. Unfortunately, none of the columns or mobile phases was able to provide a separation of the two enantiomers (Table 3.32) (all runs are 30 minutes).

Table 3.32

Test of chiral columns and mobile phases for the chiral separation of racemic compound **1**

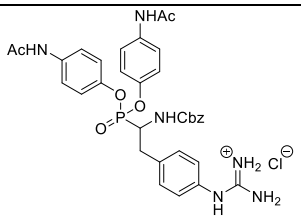

UAMC-00050 (**1**)

Mobile phase	**Columns**		
	IB	**IC**	**LC1**
100 % MeOH F = 1 mL/min	N/A	N/A	IV
100 % MeCN F = 1 mL/min	N/A	N/A	IV
100 % MeCN + 0.1 % ethanolamine F = 1 mL/min	IV	IV	IV
100 % MeCN + 0.1 % diethanolamine F = 1 mL/min	N/A	IV	N/A
100 % MeCN + 0.1 % TFA F = 1 mL/min	N/A	N/A	N/A
100 % MeCN + 0.05 % TFA + 0.05 % ethanolamine, F = 1 mL/min	N/A	N/A	IV
100 % MeCN + 0.05 % TFA + 0.1 % ethanolamine, F = 1 mL/min	N/A	N/A	IV
100 % MeCN + 0.01 % TFA + 0.1 % ethanolamine, F = 1 mL/min	N/A	N/A	IV
100 % EtOH F = 0.5 mL/min	N/A	N/A	IV

100 % EtOH + 0.1 % ethanolamine F = 0.5 mL/min	N/A	N/A	IV
100 % EtOH + 0.1 % TFA F = 0.5 mL/min	N/A	N/A	N/A
100 % *i*PrOH F = 0.3 mL/min	IV	N/A	N/A
50 % MeCN in H_2O F = 1 mL/min	N/A	N/A	N/A
60 % MeCN in H_2O F = 1 mL/min	N/A	IV	N/A
60 % MeCN in H_3PO_4 (0.1 % aq.) F = 1 mL/min	N/A	N/A	N/A
60 % MeCN in H_2O + 0.05 % TFA + 0.05 % ethanolamine, F = 1 mL/min	N/A	IV	N/A
10 % MeCN in H_2O + 0.1 % TFA + 0.1 % ethanolamine, F = 1 mL/min	N/A	IV	N/A

Tier list: I (good resolution and peak shape), II (moderate resolution and peak shape), III (bad resolution or k < 0.5), IV (no resolution), N/A conditions not tested.

Lastly, we tested intermediate **12**. In this case we selected one mobile phase (Heptane 50 %, DCM 40 %, *i*PrOH 10 %), 10 % of *i*PrOH was added to increase polarity of mobile phase, and we screen 6 different chiralpak® columns standardly used to initiate screen of conditions for enantiomers separation (*i.e.* IC, ID, IE, IF, IG, IH) (4.6x250 mm). The best separation of the two enantiomers was obtained with IG column (Table 3.33).

Table 3.33

Test of chiral columns and mobile phase for the chiral separation of racemic compound **12**

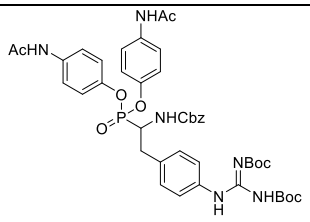

12

Mobile phase	**Columns**					
	IC	**ID**	**IE**	**IF**	**IG**	**IH**
Heptane 50 %, DCM 40 %, *i*PrOH 10 %. F = 1 mL/min	IV	IV	IV	IV	I	IV

Tier list: I (good resolution and peak shape), II (moderate resolution and peak shape), III (bad resolution or k < 0.5), IV (no resolution), N/A conditions not tested.

We selected racemic intermediate **12** for preparative separation since the compound is close to the final material. The conditions, isocratic eluents composed of heptane, DCM, *i*PrOH (50:40:10

v/v/v), with a chiralpak® IG column (4.6x250 mm) were used for the preparative chromatography. The racemic mixture of 12 (250 mg) was applied to the column as a solution in MeCN. The separation yielded approximately 50 mg of each enantiomer with a purity of 95 % AN by HPLC. (Figure 3.7) The pure enantiomers were then treated with TFA/DCM 1:1 v/v to cleave the Boc group, and the final product **1** was obtained with 99.7 % ee for the first enantiomer and 98.4 % ee for the second enantiomer.

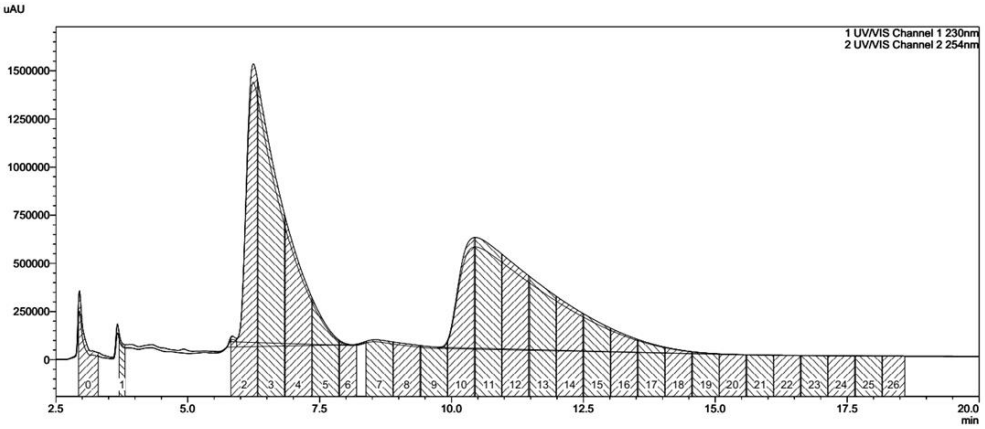

Figure 3.7. Chromatogram for the preparative separation of racemic compound **12**. Preparative HPLC, column CHIRALPAK IG (250x30 mm-5µm) eluent: isocratic heptane, DCM, *i*PrOH (50:40:10 v/v/v), flow 40 mL/min, detector channel 1: 230 nm, channel 2: 254 nm, fraction volume: 20 mL

3.5.2 Enantiomers 1 and 2 *in vitro* test on uPA enzyme

Two isolated enantiomers 1 and 2 were tested on the uPA enzyme. In Table 3.34 are reported values of IC_{50} for the racemic mixture of UAMC-00050 (**1**), enantiomer 1 and enantiomer 2. For the racemic mixture, the IC_{50} measured was 4.18 nM while for the two enantiomers was respectively 19.33 nM and 2.26 nM. Enantiomer 2 has a 10-fold higher affinity with the enzyme than enantiomer 1. However, the IC_{50} of enantiomer 2 is just twice as lower as the racemic mixture. This means that using UAMC-00050 as pure enantiomer 2 instead of the racemic mixture will not bring a big change in the therapeutic effect of the drug. Nevertheless, the two enantiomers need to be isolated, and their toxicity must be evaluated *in vivo* before proceeding to clinical experimentation with UAMC-00050.

Table 3.34

In vitro test of racemic and chiral UAMC-00050 **1** on uPA

Entry	UAMC-00050	IC_{50} (nM)
1	Racemic mixture	4.18
2	Enantiomer 1	19.33
3	Enantiomer 2	2.26

3.5.3 Catalysis of Birum-Oleksyszyn reaction with a chiral metal complex

Lewis acids complexed with chiral ligands were successfully used by Ohara *et al.*[41] and Zhou *et al.*[42] in the preparation of optically pure α-aminophosphonates. Inspired by their work we tested *L*-proline as a ligand in combination with four different Lewis acids (Table 3.35). First, the catalytic complex was prepared: selected metal triflate was dissolved in anhydrous MeCN and combined with *L*-proline. The amino acid/Lewis acid solution was stirred for 1 h, at the indicated temperature, and then aldehyde **7**, benzyl carbamate (**8**) and phosphite **3** were added to the solution. After the time required for the complete conversion of starting materials the product was isolated and analyzed by an HPLC equipped with a chiral column (LC-1), and mobile phase: isocratic MeCN (0.1 % ethanolamine) F = 1 mL/min. $Bi(OTf)_3$ was used in various amount: 0.10, 0.50, and 1.00 equivalents (Table 3.35, entries 1 - 4). The reaction proceeded faster and with a moderate yield with 0.50 and 1.00 equivalents, even at - 20 °C, but in all the cases no enantiomeric excess was obtained in the final product. $Cu(OTf)_2$ was used with 0.10 and 1.00 equivalents, lower yields of **9** were obtained with $Cu(OTf)_2$ compared with $Bi(OTf)_3$ and also in this case 0 % ee was obtained in both experiments (Table 3.35, entries 5 and 6). $Y(OTf)_3$ and $Sc(OTf)_3$ were used with 0.20 equivalents loading, both a 20 °C and 0 °C (Table 3.35, entries 7 - 10). From these four experiments, it was clear, that the reaction significantly slowed down at 0 °C: after 48 h, the reaction with $Y(OTf)_3$ achieved a 3 % yield, and a 5 % yield with $Sc(OTf)_3$. In any case, at 20 °C and 0 °C no enantiomeric excess was obtained with the *L*-proline/Lewis acid complex. Next, we moved our focus to the testing of diastereoselective synthesis of α-aminophosphonate.

Table 3.35

Screening of *L*-proline/Lewis acid complexes for the enantioselective synthesis of product **9**

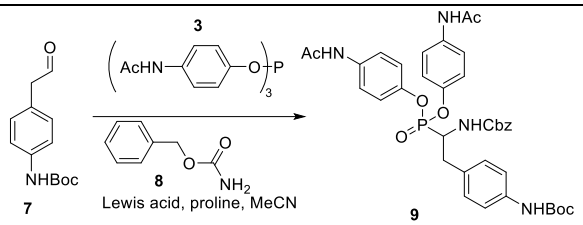

Entry	Scale (mg)	Lewis acid (equiv.)	Proline (equiv.)	Time (h)	Temp. (°C)	Solvent	Yield (%)	ee (%)
1	100	$Bi(OTf)_3$ (0.1)	0.15	72	20	MeCN	14	0
2	100	$Bi(OTf)_3$ (0.5)	0.75	1	20	MeCN	32	0
3	100	$Bi(OTf)_3$ (0.5)	0.75	6	- 20	MeCN	21	0
4	100	$Bi(OTf)_3$ (1.0)	1.50	5	20	MeCN	28	0
5	100	$Cu(OTf)_2$ (0.1)	0.15	24	20	MeCN	5	0
6	100	$Cu(OTf)_2$ (1.0)	1.50	24	20	MeCN	13	0
7	200	$Y(OTf)_3$ (0.2)	0.30	24	20	MeCN	22	0
8	200	$Y(OTf)_3$ (0.2)	0.30	44	0	MeCN	3	0
9	200	$Sc(OTf)_3$ (0.2)	0.30	24	20	MeCN	15	0
10	200	$Sc(OTf)_3$ (0.2)	0.30	44	0	MeCN	5	0

3.5.4 Diastereoselective synthesis of α-aminophosphonates

3.5.4.1 Synthesis of α-aminophosphonates with a chiral amine

Considering the difficulties in the enantioselective synthesis of UAMC-00050 with metal catalysis an alternative approach was investigated: the diastereoselective synthesis. For this research, a model α-aminophosphonate was selected, where an amino component was (*S*)-(-)-1-phenylethylamine instead of an achiral carbamate. Our goal was to assess if any stereoinduction can be achieved from this chiral amine during the formation of aminophosphonate asymmetric center. Simple triphenyl phosphite (**26**) was used as a model for triaryl phosphite **3**. During the investigation of chiral catalyst for the enantioselective synthesis of α-aminophosphonates (See section 3.5.3) we had to spend a considerable amount of time on the purification of aminophosphonate to reach the required purity (> 90 %) for the chiral HPLC analysis. On the other hand, stereoselective synthesis provides a significant advantage in separating stereoisomers, their analysis, and their assignment. The first run of the model reaction (Scheme 3.19) provided dr of 76:24, which is in accordance with previous uses of the (*S*)-(-)-1-phenylethylamine.[67,68] We were especially pleased to find, that the diastereoisomeric ratio of phosphonate **215** could be directly

assessed without tedious purifications using a simple HPLC assay, where peaks of two diastereomers had a good shape and were well-resolved.

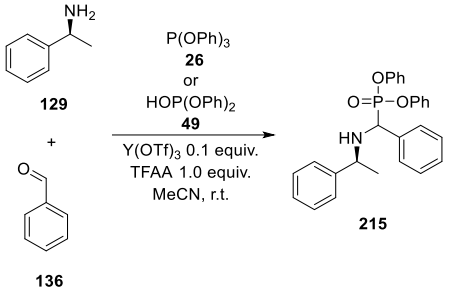

Scheme 3.19. Diastereoselective reaction with **129**, **136**, and **26** or **49** catalyzed by $Y(OTf)_3$

Inspired by the reaction outcome we started investigating whether there was a way to increase dr without changing the aldehyde or the amine as was done by Tibhe *et al.*[67,68] First, screened conditions included reactions without catalyst and/or the additive and its effect on yield and dr As shown in Table 3.36, the reaction proceeded even without the catalyst, reaching a product **181**/IS ratio of 0.44 with triphenyl phosphite after 24 h (Table 3.36, entry 2) 0.34 with diphenyl phosphite after 24 h (Table 3.36, entry 6). On the other hand with 0.1 equivalents of $Y(OTf)_3$ only traces of the product were obtained when using triphenyl phosphite (Table 3.36, entries 9 and 10), but a higher **215**/IS ratio (0.79) was reached with diphenyl phosphite after 4 h. (Table 3.36, entry 13) The effect of the additive TFAA (1.0 equiv.) was also tested. Its use in the absence of the catalyst provided an improved **215**/IS ratio (0.52 after 24 h) for $P(OPh)_3$ (Table 3.36, entries 3 and 4) while in the case of $HOP(OPh)_2$ it reduced the ratio to **215**/IS 0.24 and 0.25 (Table 3.36, entry 7 and 8). While in the presence of the catalyst, TFAA anhydride helped increase the ratio of product in experiments with $P(OPh)_3$ and $HOP(OPh)_2$, the highest value (0.86) was reached with $HOP(OPh)_2$ at 4 h. It is worth mentioning that in almost all the experiments a decrease of dr after 24 h was noted, and in the absence of a catalyst the addition of TFAA provided lower diastereoselectivity. With these results in hand, we decided to use the reaction between aldehyde **136**, amine **129** and diphenyl phosphite **49** in anhydrous MeCN (1.0 M) at 20-25 °C with 0.1 equivalents of $Y(OTf)_3$ as standard conditions to test how changing reaction parameters can affect the **215**/IS ratio and the dr. Conditions from Table 3, entry 15 were selected, despite the slightly lower dr after 4 h, because of the higher **215**/IS ratio.

Table 3.36

Tests of various phosphites, catalyst presence, and TFAA presence, for a diastereoselective Birum-Oleksyszyn reaction

Entry[a]	Phosphite	Additive (1.0 equiv.)	Catalyst (0.1 equiv)	Time (h)	215/IS	dr
1	$P(OPh)_3$	None	None	4	0.13	80:20
2	$P(OPh)_3$	None	None	24	0.44	79:21
3	$P(OPh)_3$	TFAA	None	4	0.26	73:27
4	$P(OPh)_3$	TFAA	None	24	0.52	69:31
5	$HOP(OPh)_2$	None	None	4	0.3	76:24
6	$HOP(OPh)_2$	None	None	24	0.34	73:27
7	$HOP(OPh)_2$	TFAA	None	4	0.24	75:25
8	$HOP(OPh)_2$	TFAA	None	24	0.25	69:31
9	$P(OPh)_3$	None	$Y(OTf)_3$	4	N/A	N/A
10	$P(OPh)_3$	None	$Y(OTf)_3$	24	0.03	80:20
11	$P(OPh)_3$	TFAA	$Y(OTf)_3$	4	0.22	76:24
12	$P(OPh)_3$	TFAA	$Y(OTf)_3$	24	0.71	73:27
13	$HOP(OPh)_2$	None	$Y(OTf)_3$	4	0.79	73:27
14	$HOP(OPh)_2$	None	$Y(OTf)_3$	24	0.67	68:32
15	$HOP(OPh)_2$	TFAA	$Y(OTf)_3$	4	0.86	73:27
16	$HOP(OPh)_2$	TFAA	$Y(OTf)_3$	24	0.78	69:31

[a]MeCN (1.0 M), reaction at 20-25 °C.

To understand the effect of solvents on diastereoselectivity we screened 15 different reaction mediums. Regarding the **215**/IS ratio only MeCN/THF (1:1 v/v mixture), EtOAc and β-pinene managed to perform better than standard conditions (aldehyde **136**, amine **129** and diphenyl phosphite **49** in anhydrous MeCN (1.0 M) at 20-25 °C with 0.1 equivalents of $Y(OTf)_3$) (Table 3.36, entry 15) with **215**/IS ratio respectively 0.87, 0.88 and 1.04 after 4 h (Table 3.37, entries 3, 5, and 27). All other solvents provided comparable or lower **215**/IS ratio, in the case of MeOH and DMSO the product was obtained only in trace levels (0.04 and 0.09 after 4 h) (Table 3.37, entries 11 and 15). Regarding the diastereoselectivity reaction, several solvents provide changes in the diastereoselectivity of the reaction. THF, EtOAc, H_2O, *i*PrOAc, MIBK and 2-Me-THF (Table 3.37, entries 1, 5, 7, 19, 21, and 23) provided mild variations of the dr with values from 75:25 when the reaction was carried in water to 79:21 when the reaction was carried in *i*PrOAc. Solvents like toluene, DCM, and cyclohexane (Table 3.37, entries 9, 13, and 25) were able to provide a dr comparable to or bigger than 80:20 in particular, toluene was the solvent that provided the higher diastereoselective ratio with 82:18 when used with $HOP(OPh)_2$. Having noted that several solvents were able to increase the dr we tested one chiral solvent, β-Pinene. As reported by Nagata *et al*.,

chiral solvents can be helpful for asymmetric reactions.[129] β-Pinene provided a good dr after 4 h, despite being lower than the toluene value, but the dr dropped to 65:35 after 24 h, probably due to the decomposition of the major diastereoisomer (Table 3.37, entries 27 and 28). Using $P(OPh)_3$ **26** instead of $HOP(OPh)_2$ **49**, in toluene improved dr to 83:17, but the **215**/IS ratio was decreased from 0.68 to 0.26 after 4 h (Table 3.37, entry 29).

Table 3.37

Screening of various solvents for a diastereoselective Birum-Oleksyszyn reaction

Entry [a]	**Phosphite**	**Solvent**	**Time (h)**	**215/IS**	**dr**
1	$HOP(OPh)_2$	THF	4	0.71	76:24
2	$HOP(OPh)_2$	THF	24	0.75	68:32
3	$HOP(OPh)_2$	THF/MeCN 1:1	4	0.87	73:27
4	$HOP(OPh)_2$	THF/MeCN 1:1	24	0.77	69:31
5	$HOP(OPh)_2$	EtOAc	4	0.88	78:22
6	$HOP(OPh)_2$	EtOAc	24	0.82	75:25
7	$HOP(OPh)_2$	H_2O	4	0.71	75:25
8	$HOP(OPh)_2$	H_2O	24	0.71	75:25
9	$HOP(OPh)_2$	Toluene	4	0.68	82:18
10	$HOP(OPh)_2$	Toluene	24	0.70	81:19
11	$HOP(OPh)_2$	MeOH	4	0.04	85:15
12	$HOP(OPh)_2$	MeOH	24	0.03	76:24
13	$HOP(OPh)_2$	DCM	4	0.59	80:20
14	$HOP(OPh)_2$	DCM	24	0.59	79:21
15	$HOP(OPh)_2$	DMSO	4	0.09	66:34
16	$HOP(OPh)_2$	DMSO	24	0.13	71:29
17	$HOP(OPh)_2$	Acetone	4	0.44	72:28
18	$HOP(OPh)_2$	Acetone	24	0.45	68:32
19	$HOP(OPh)_2$	*i*PrOAc	4	0.67	79:21
20	$HOP(OPh)_2$	*i*PrOAc	24	0.76	74:26
21	$HOP(OPh)_2$	MIBK	4	0.62	77:23
22	$HOP(OPh)_2$	MIBK	24	0.65	72:28
23	$HOP(OPh)_2$	2-Me-THF	4	0.52	78:22
24	$HOP(OPh)_2$	2-Me-THF	24	0.54	70:30
25	$HOP(OPh)_2$	Cyclohexane	4	0.32	80:20
26	$HOP(OPh)_2$	Cyclohexane	24	0.39	78:22
27	$HOP(OPh)_2$	β-pinene	4	1.04	80:20
28	$HOP(OPh)_2$	β-pinene	24	0.93	65:35

Entry [a]	Phosphite	Solvent	Time (h)	215/IS	dr
29	$P(OPh)_3$	Toluene	4	0.26	83:17
30	$P(OPh)_3$	Toluene	24	0.53	81:19

[a]0.1 equiv. of $Y(OTf)_3$ as a catalyst, 1.0 equiv. of TFAA as an additive reaction run at 20-25 °C, concentration 1.0 M.

Inspired by the work of Nakamura *et al.* we decided to investigate the effect of Cinchona alkaloids additives on the reaction.[54] Quinine was selected as a chiral additive and added to the reaction in various amounts: from 0.05 to 1.0 equivalents (Table 3.38, entries 1 - 8). Initially, 1.0 equivalents of quinine were added to the reaction without the catalyst (Table 3.38, entries 1 and 2), albeit a good dr (83:17 after 4 h) was achieved, the product was obtained with a very low **215**/IS ratio, even after 24 h (0.07). In the presence of the catalyst, the reaction proceeded well, with 0.05 or 0.1 equivalents of additive (Table 3.38, entries 3 - 6), while a lower **215**/IS ratio (0.42 after 4 h) was achieved with 1.0 equivalents of quinine (Table 3.38, entry 7 and 8). Except for entries 1 and 2, no improvement of diastereoselectivity was registered with quinine as an additive.

Table 3.38

Quinine as a chiral additive for a diastereoselective Birum-Oleksyszyn reaction

Entry[a]	Additive (equiv.)	Catalyst (0.1 equiv)	Time (h)	215/IS	dr
1	Quinine (1.0)	None	4	0.05	83:17
2	Quinine (1.0)	None	24	0.07	78:22
3	Quinine (0.05)	$Y(OTf)_3$	4	1.00	73:27
4	Quinine (0.05)	$Y(OTf)_3$	24	0.93	69:31
5	Quinine (0.1)	$Y(OTf)_3$	4	0.97	73:27
6	Quinine (0.1)	$Y(OTf)_3$	24	0.91	69:31
7	Quinine (1.0)	$Y(OTf)_3$	4	0.42	75:25
8	Quinine (1.0)	$Y(OTf)_3$	24	0.37	71:29

[a]1.0 equiv. of $HOP(OPh)_2$ **49**, 1.0 equiv. of TFAA as an additive, MeCN (1.0 M), reaction at 20-25 °C

Five Lewis acids and one Brønsted acid (0.1 equiv.) were tested to see their effect on the reaction outcome (Table 3.39). $Bi(OTf)_3$, $TiCl_4$ and AcOH provided inferior results to the standard conditions (Table 3.39, entry 1) with dr after 4 h of 73:27, 72:28, and 70:30, respectively (Table 3.39, entries 2, 6, and 10). In the case of $TiCl_4$, a significant decrease of dr (59:41) was noted after 24 h. Camphorsulfonic acid did not provide any significant change in dr after 4 h (77:23) compared to standard conditions (Table 3.39, entry 8). $Sc(OTf)_3$, provided much lower diastereoselectivity than the standard conditions, with a dr of 66:34 after 4 h, decreasing to 55:45 after 24 h (Table 3.39, entries 4 and 5). A decrease of **215**/IS ratio and dr for all tested catalysts was observed after

4 h. Only AcOH provided a stable diastereomeric ratio over the reaction time and increased **215**/IS ratio after 24 h (Table 3.39, entry 11).

Table 3.39

Screening of catalysts for a diastereoselective Birum-Oleksyszyn reaction

Entry[a]	**Catalyst (0.1 equiv)**	**Time (h)**	**215/IS**	**dr**
1	$Y(OTf)_3$	4	0.86	73:27
2	$Bi(OTf)_3$	4	1.00	73:27
3	$Bi(OTf)_3$	24	0.91	72:28
4	$Sc(OTf)_3$	4	0.86	66:34
5	$Sc(OTf)_3$	24	0.64	55:45
6	$TiCl_4$	4	0.47	72:28
7	$TiCl_4$	24	0.31	59:41
8	CSA	4	0.37	77:23
9	CSA	24	0.25	73:27
10	AcOH	4	0.98	70:30
11	AcOH	24	1.08	70:30

[a]1.0 equiv. of $HOP(OPh)_2$ **49**, 1.0 equiv. of TFAA as an additive, MeCN (1.0 M), reaction at 20-25 °C.

Next, reaction temperature and concentration were screened. For the temperature, three different values were selected: 50 °C, 0 °C and - 78 °C (Table 3.40, entries 1 - 8). Interesting results were obtained when the reaction was carried at 50 °C, after 4 h we registered a racemic mixture of product **215** (48:52), but after 24 h product, **215** was obtained with dr (29:71), with complete inversion of the diastereomeric ratio (Table 3.40, entries 1 and 2). At 0 °C no change in dr was observed with a lower **215**/IS ratio than under the standard conditions. The reaction was left to warm up to room temperature for 8 h, providing 74:26 dr after 24 h at 20-25 °C (Table 3.40, entries 3 and 4). The reaction was also tested at - 78 °C. Acetonitrile was unsuitable for such a temperature since it froze; toluene was then used due to a lower melting point. In both cases, the reaction did not proceed at - 78 °C, both experiments were left to warm up at 20-25 °C after 8 h. With toluene, the diastereoselectivity of the reaction was comparable with previous experiments in that solvent (Table 3.40, entries 5 and 6). As for concentration, four different values were tested, from 0.1 M to neat. An increase of **215**/IS ratio after 24 h was noted with the increase of the concentration, going from 0.08 at 0.1 M to 0.94 in neat conditions (Table 3.40, entries 8, 10, 13, and 15). Regarding the dr no significant improvements were observed for all conditions.

Table 3.40

Screening of temperatures and concentrations for a diastereoselective Birum-Oleksyszyn reaction

Entry[a]	Solvent (M)	Time (h)	Temp. (°C)	215/IS	dr
1	MeCN (1.0)	4	50	0.84	48:52
2	MeCN (1.0)	24	50	0.74	29:71
3	MeCN (1.0)	4	0	0.44	76:24
4	MeCN (1.0)	24	20-25	0.40	74:26
5	Toluene (1.0)	4	- 78	N/A	N/A
6	Toluene (1.0)	24	20-25	0.41	81:19
7	MeCN (0.1)	4	20-25	0.05	77:23
8	MeCN (0.1)	24	20-25	0.08	66:34
9	MeCN (0.5)	4	20-25	0.57	72:28
10	MeCN (0.5)	24	20-25	0.50	68:32
11	MeCN (2.0)	4	20-25	0.86	73:27
12	MeCN (2.0)	24	20-25	0.89	71:29
13	Neat	4	20-25	0.8	76:24
14	Neat	24	20-25	0.94	74:26

[a]1.0 equiv. of $HOP(OPh)_2$ **49**, 0.1 equiv. of $Y(OTf)_3$ as a catalyst, 1.0 equiv. of TFAA as an additive, reaction at 20-25 °C.

As reported by Park *et al.*,[130] and Song *et al.*,[131] water can positively affect the outcome of asymmetric reactions. We decided to add 1.0 and 10.0 equivalents of deionized water to our reaction mixture (Table 3.41, entries 1 - 4). In both experiments, the increase in dr was negligible. We noted a decrease in the **215**/IS ratio, both with 1.0 or 10.0 equivalents of water, probably explained by the hydrolysis of phenyl phosphonic esters. Interestingly, the reaction run in water as a solvent (Table 3.37, entries 7 and 8) proceeded better (**215**/IS 0.71 after 4 h) compared to those where water (10.0 equiv.) was an additive to MeCN (Table 3.41, entries 3 and 4).

Table 3.41

Screening of water as an additive for a diastereoselective Birum-Oleksyszyn reaction

Entry[a]	Water (equiv.)	Time (h)	215/IS	dr
1	1.0	4	0.76	74:26
2	1.0	24	0.73	72:28
3	10.0	4	0.30	74:26
4	10.0	24	0.21	72:28

[a]1.0 equiv. of $HOP(OPh)_2$ **49**, 0.1 equiv. of $Y(OTf)_3$ as a catalyst, 1.0 equiv. of TFAA as an additive, reaction in MeCN (1.0 M) at 20-25 °C.

L-Proline/Lewis acid chiral catalytic complexes have been already used for asymmetric synthesis.[132,133] We decided to test if *L*-proline/$Y(OTf)_3$ complex might affect the model reaction. To do so, the yttrium-proline complex was generated in three different ways. With method A, 0.1 equivalents of $Y(OTf)_3$ were stirred in MeCN with 0.15 equivalents of proline, and then to the solution, 1.0 equivalents each of aldehyde **136**, amine **129**, phosphite **49** and TFAA were added. With method B, 0.15 equivalents of proline were added as an additive to the reaction between 1.0 equivalents of aldehyde **136**, amine **129**, phosphite **49**, 0.1 equivalents of $Y(OTf)_3$ and 1.0 equivalents of TFAA. With method C, 0.15 equivalents of proline, dissolved in MeCN, were deprotonated with 0.15 equivalent of $NaHCO_3$, then 0.1 equivalents of $Y(OTf)_3$ were added and the solution was stirred for 1 h at 20-25 °C then as in method A, 1.0 equivalents of aldehyde **136**, amine **129**, phosphite **49** and TFAA were added. As depicted in Table 3.42, no substantial improvements of dr were observed. In all experiments (Table 3.42, entries 1 - 6) decrease of **215**/IS ratio was noted compared to standard conditions, which was correlated to decreased activity of the catalyst due to the formation of the complex with *L*-proline.

Table 3.42

Screening of *L*-proline/yttrium (III) complexes for a diastereoselective Birum-Oleksyszyn reaction

Entry[a]	***L*-Proline/yttrium complex formation**	**Time (h)**	**215/IS**	**dr**
1	Method A	4	0.72	75:25
2	Method A	24	0.65	73:27
3	Method B	4	0.65	74:26
4	Method B	24	0.58	72:28
5	Method C	4	0.61	74:26
6	Method C	24	0.55	71:29

[a]1.0 equiv. of $HOP(OPh)_2$ **49**, 0.1 equiv. of $Y(OTf)_3$ as a catalyst, 1.0 equiv. of TFAA as an additive, MeCN (1.0 M) reaction at 20-25 °C.

From the collected data we can conclude, that the highest dr was reached with toluene as a solvent and TFAA was omitted from the reaction. Product **215** was obtained with IS ratio of: 0.48 after 4 h and 0.42 after 24 h, while dr was registered as 84:16 after 4 h and 81:19 after 24 h (Table 3.43, entries 1 and 2). When the same conditions were repeated in the absence of the catalyst, the IS ratio was much lower: 0.08 after 4 h and 0.16 after 24 h but the dr was kept at the value of 84:16 even after 24 h (Table 3.43, entries 3 and 4).

Table 3.43

Screening of conditions with toluene as a solvent for a diastereoselective Birum-Oleksyszyn reaction

Entry[a]	Catalyst	Time (h)	215/IS	dr
1	$Y(OTf)_3$	4	0.48	84:16
2	$Y(OTf)_3$	24	0.42	81:19
3	No	4	0.08	85:15
4	No	24	0.16	84:16

[a]1.0 equiv. of $HOP(OPh)_2$ **49**, toluene (1.0 M), reaction at 20-25 °C, no TFAA.

To summarize, 48 different reaction conditions were tested for a diastereoselective synthesis of α-aminophosphonate **215** from benzaldehyde (**136**), diphenyl phosphite (**49**) and (*S*)-(-)-1-phenylethylamine (**129**). The only parameter that had a considerable positive effect on the dr of the reaction was the selection of solvent: in particular, toluene was able to increase the dr from 76:24 to 82:18 (Table 3.37, entry 9). All the other variables showed little or no effect on the diastereoselectivity. On the other side, a lower dr was noted when the reaction was carried with $Sc(OTf)_3$ as a Lewis acid (Table 3.39, entry 5) and an inverted dr was registered after 24 h at 50 °C (Table 3.40, entry 2). With all results obtained from the model reaction, the next question was whether it can be adapted to Birum-Oleksyszyn reaction, which includes a carbamate as a coupling partner. In particular, if a chiral center, required for the stereoselective synthesis, can be incorporated in a carbamate moiety and what will be its effect on the diastereoselective outcome of the reaction.

3.5.4.2 Use of chiral carbamates for a diastereoselective synthesis of α-aminophosphonates

There are seminal works, where chiral carbamates have been employed for the diastereoselective synthesis of α-aminophosphonates: Oshikawa *et al.*[73] and Chung *et al.*[74] Both authors used carbamates generated from menthol and camphor derivatives. Obtained α-aminophosphonates were then hydrolyzed to yield α-aminophosphonic acids and analyzed for optical yield ranging from 3.3 to 42.2 %. Inspired by these works we decided to prepare a series of chiral carbamates **23** and couple them with benzaldehyde (**136**) and $P(OPh)_3$ **26** or $HOP(OPh)_2$ **49** using 0.1 equivalents of $Y(OTf)_3$ as catalyst, 1.0 equivalents of TFAA as an additive in anhydrous MeCN at 20-25 °C In the case of a good stereoinduction and high dr we could separate diastereomers of **216**, cleave the carbamate under acidic conditions and functionalize the amine **217** with benzyl chloroformate (**218**) to yield the desired enantioenriched α-aminophosphonate (**16**) (Scheme 3.20).

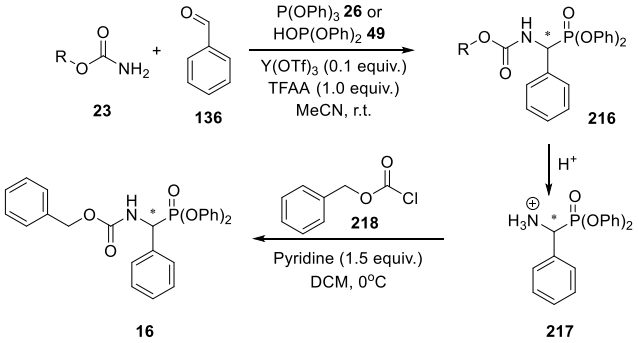

Scheme 3.20. Synthetic pathway for the enantioselective synthesis of α-aminophosphonate using chiral carbamate as a chiral auxiliary

Five different chiral alcohols (**219**) were selected for conversion to the corresponding carbamate (**221**) by a reaction with 2.2.2-trichloroacetyl isocyanate to generate intermediate **220** and then potassium carbonate (Scheme 3.21). The set of alcohols includes: bulky quinine (**102b**) and hydroquinidine (**222**); (*S*)-1-phenylethanol (**223**) to compare results with (*S*)-(-)-1-phenylethyl-amine (**129**); (*R*)-1-(3,5-bistrifluoromethylphenhyl)ethanol (**224**) was selected to understand if the two CF_3 groups in *meta* positions can have any effect on the dr; borneol (**225**) was selected as a camphor analogue to match the carbamate used by Oshikawa and Chung.

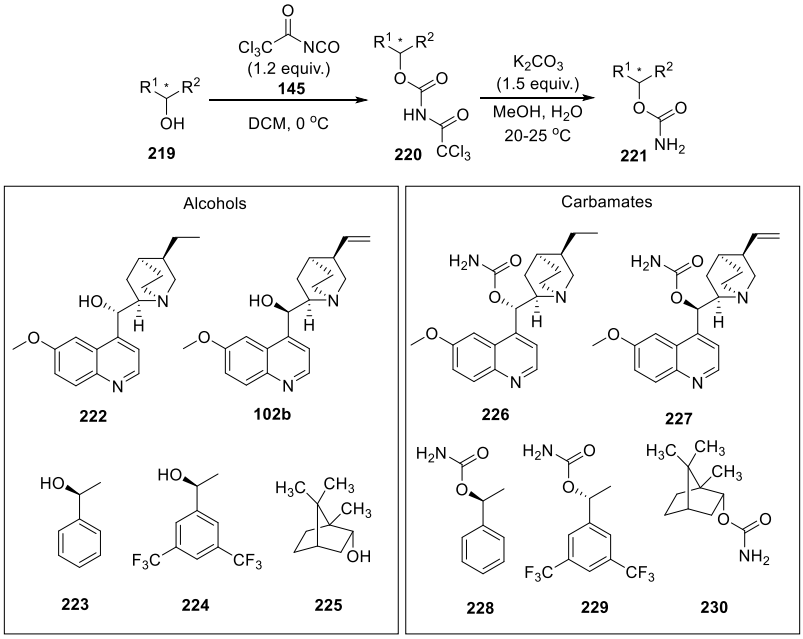

Scheme 3.21. Preparation of carbamate from alcohol

DFT calculation (at ZORA-M062X/def2-TZVP level of theory) was used to generate the 3D structure of (*S*)-(-)-1-phenylethylamine and five prepared carbamates. As depicted in Figure 3.8, in the case of the amine, the distance between the chiral carbon and the NH_2 is 0.147 nm that as shown in the previous series of experiments, which can lead to an average diastereoisomeric ratio of 75:25. In the case of the carbamates the *C-N* distance goes from 0.355 nm to 0.358 nm, almost 2.5 times longer than the amine *C-N* bond. With the next series of experiments, our goal was to determine if the longer *C-N* bond would affect the diastereoselectivity of the reaction.

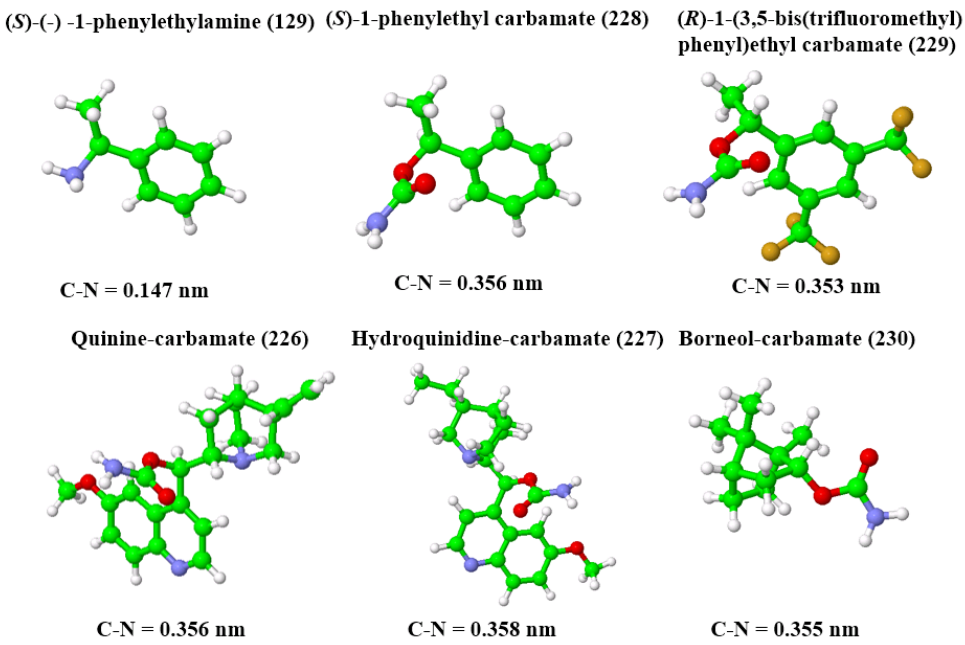

Figure 3.8. 3D structures of with (*S*)-(-)-1-phenylethylamine and prepared carbamates **192**, **193**, **194**, **195** and **196**; structures were generated with a DFT calculation ZORA-M062X/def2-TZVP and used to calculate the chiral carbon – NH_2 distance (C-N).

Borneol carbamate **230** was dissolved in MeCN, the solution was left in a partially open vial for 60 days at 20-25 °C. At the end of which, a conglomerate of crystals was formed at the bottom of the vial. One single crystal was isolated and analyzed with single-crystal X-Ray diffraction (SC-XRD). Compound **230** crystallizes in the monoclinic crystal system with I2 space group, where each unit cells contain 8 molecules of **230**. In the crystal lattice were noted 2 symmetrically independent molecules. The two molecules formed an asymmetric unit where two molecules of **230** were paired together with a hydrogen bond between the amino group and the oxygen in the carbamate (Figure 3.9). The distance between the chiral carbon and the amino group was different for the two **230** moieties: 0.357 nm and 0.354 nm. With a difference between the structure generated in DFT of respectively: 0.002 and - 0.001 nm.

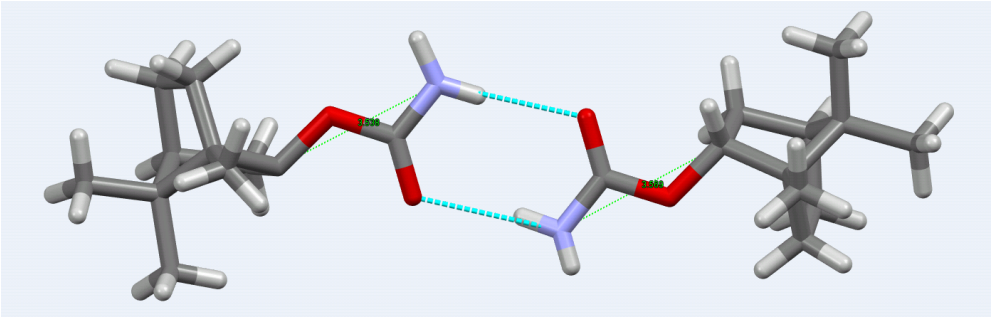

Figure 3.9. Dimer formed between the two independent structure of compound **230**. The C-N distance is different for the two structure. 0.354 nm on the left and 0.357 on the right.

The first carbamates to be tested were bulky Cinchona alkaloids (hydroquinidine and quinine) (Table 3.44). In the reaction of hydroquinidine carbamate **226** with benzaldehyde (**136**) and $HOP(OPh)_2$ **49** catalyzed by 0.1 equivalents of $Y(OTf)_3$ (Table 3.44, entry 1) no product was detected after 24 h and the carbamate was left unreacted in the reaction mixture. We speculated that quinuclidine moiety might coordinate with the metal catalyst, thus inhibiting the reaction. In order to neutralize any excess electron density in the side chain of this carbamate reaction was repeated with 1.0 equivalents of the additive: TFAA or HCl (Table 3.44, entries 2 - 5). With $P(OPh)_3$ and $HOP(OPh)_2$, the additive did not change the course of the reaction, after 24 h carbamate was left unreacted in the reaction mixture as before. One last attempt was carried out using a less bulky trimethyl phosphite, but also, in this case, Cinchona carbamate was left unreacted after 24 h (Table 3.44, entry 6). Despite a poor outcome of hydroquinidine carbamate **226**, a set of experiments was carried out with the quinine carbamate **227**. In the reaction of **227** with benzaldehyde and diphenyl phosphite in the presence of 0.1 equivalents of $Y(OTf)_3$ and 1.0 equivalents of TFAA (Table 3.44, entry 7), the carbamate **227** was left unreacted and no product was detected after 24 h. In order to neutralize any interactions between the Lewis acid catalyst and the carbamate a large excess of $Y(OTf)_3$ (3.0 equiv.) was used. However, also, in this case, the carbamate was left unreacted even after 96 h (Table 3.44, entries 8 - 11).

Table 3.44

Hydroquinidine and quinine carbamates screening

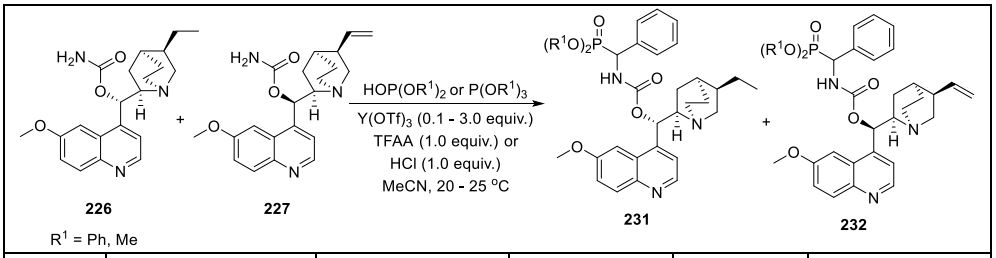

Entry[a]	Carbamate	Phosphite	Additive (1.0 equiv.)	$Y(OTf)_3$ equiv.	(231 or 232)/IS ratio
1	Hydroquinidine	$HOP(OPh)_2$	None	0.1	N/A
2	Hydroquinidine	$P(OPh)_3$	TFAA	0.1	N/A
3	Hydroquinidine	$P(OPh)_3$	HCl	0.1	N/A
4	Hydroquinidine	$HOP(OPh)_2$	TFAA	0.1	N/A
5	Hydroquinidine	$HOP(OPh)_2$	HCl	0.1	N/A
6	Hydroquinidine	$P(OMe)_3$	TFAA	0.1	N/A
7	Quinine	$HOP(OPh)_2$	TFAA	0.1	N/A
8	Quinine	$HOP(OPh)_2$	TFAA	3.0	N/A
9	Quinine	$HOP(OPh)_2$	TFAA	3.0	N/A
10	Quinine	$P(OPh)_3$	TFAA	3.0	N/A
11[b]	Quinine	$P(OPh)_3$	TFAA	3.0	N/A

[a]Reaction at 20-25 °C for 24 h; [b]Reaction at 20-25 °C for 96 h.

The next set of experiments employed less bulky carbamates. Initially (*R*)-1-(3,5-bis(trifluoromethyl)phenyl)ethyl carbamate (**229**) was reacted with $HOP(OPh)_2$ **49** and benzaldehyde (**136**) in the presence of 0.1 equivalents of $Y(OTf)_3$ and 1.0 equivalents of TFAA (Table 3.45). Product **234** was obtained with a **234**/IS ratio of 0.30 after 4 h and 0.33 after 24 h, and with dr of 57:43 both times (Table 3.45, entries 1 and 2). The more bulky triphenyl phosphite (**26**) was used as a reactant in order to increase diastereoselectivity: it improved to 69:31 after 4 h and 60:40 after 24 h, with an increase of **234**/IS ratio, respectively 0.67 after 4 h and 0.51 after 24 h (Table 3.45, entries 3 and 4). The reaction between carbamate **229**, benzaldehyde (**136**) and $P(OPh)_3$ (**26**) was repeated on a 1.35 mmol scale. It was quenched after 4 h and the product was isolated: both the HPLC and the ^{1}H NMR assay confirmed a dr value of 75:25 (Figure 3.10 A). Next, we tested (*S*)-1-phenylethyl carbamate (**228**), to compare results with (*S*)-(-)-1-phenylethylamine (**129**) and see if the increased distance from the chiral to the reaction center (0.209 nm) might have an effect on the dr. (*S*)-1-phenylethyl carbamate (**228**) was reacted with benzaldehyde (**136**) in the presence of 0.1 equivalents of $Y(OTf)_3$, 1.0 equivalents of TFAA, and 1.0 equivalents of $HOP(OPh)_2$ **49** or $P(OPh)_3$

26 (Table 3.45, entries 5 - 8). On the opposite of (*R*)-1-(3,5-bis(trifluoromethyl)phenyl)ethyl carbamate (**229**), in the case of (*S*)-1-phenylethyl carbamate (**228**), the **233**/IS ratio was 3 times higher when $HOP(OPh)_2$ **49** was used instead of $P(OPh)_3$ **26**. Unfortunately, we could not measure diastereomeric ratio with an HPLC due to a complete overlapping of the two product peaks. Therefore ^1H NMR assay was used instead (Figure 3.10 B). The product was collected from the reaction with diphenyl phosphite, and after purification the dr was calculated to be 51:49, which indicated a much less effective stereoinduction for the chiral auxiliary with a longer *C-N* distance.

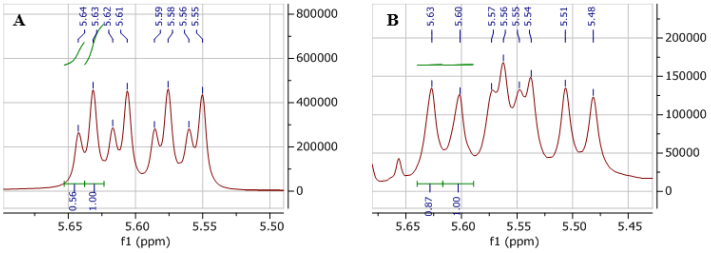

Figure 3.10. ^1H NMR spectrum (fragment) of α-aminophosphonate products obtained from: A) (*R*)-1-(3,5-bis(trifluoromethyl)phenyl)ethyl carbamate, solvent: DMSO-d_6, dr determined with the ratio between peaks at 5.64 ppm and 5.63 ppm; B) (*S*)-1-phenylethyl carbamate, solvent $CDCl_3$, dr determined with the ratio between peaks at 5.63 ppm and 5.60 ppm

Finally, the reaction of borneol carbamate **230**, was investigated, using the same conditions of the two previous carbamates: reaction with benzaldehyde (**136**), triphenyl phosphite (**26**) or diphenylphosphite (**49**), in the presence of 0.1 equivalents of $Y(OTf)_3$ and 1.0 equivalents of TFAA (Table 3.45, entries 9 - 12). The **235**/IS ratio was comparable when using $P(OPh)_3$ **26** or $HOP(OPh)_2$ **49** while, as for (*S*)-1-phenylethyl carbamate derived α-aminophosphonate **233**, also for the borneol carbamate derived α-aminophosphonate **235**, HPLC assay showed one clear peak. Assessment of dr for the reaction product was possible only with ^1H NMR assay. Figure 3.11 A shows a peak of the CH proton of the newly formed chiral center. The peak has a ddd multiplicity typical of 1:1 diastereoisomers mixtures. However after purification of the crude mixture by flash chromatography, the peak of the same proton has a dd multiplicity, and after a ^{31}P decoupling, it turned into a doublet (Figure 3.11, B and C). The ^1H NMR assay lead us to think that after the purification we isolated a single diastereoisomer of product **235**.

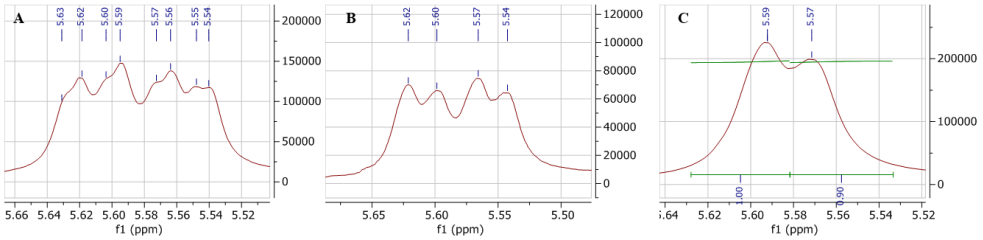

Figure 3.11. CH proton of the α-aminophosphonate **235**: solvent $CDCl_3$, A) crude mixture after reaction, B) isolated product, C) isolated product ^{31}P-decoupled, from the presence of a dd in the isolated product a 100:0 dr was assigned to product **235**.

Table 3.45

Diastereoselective Birum-Oleksyszyn reaction with chiral carbamates, conditions screening

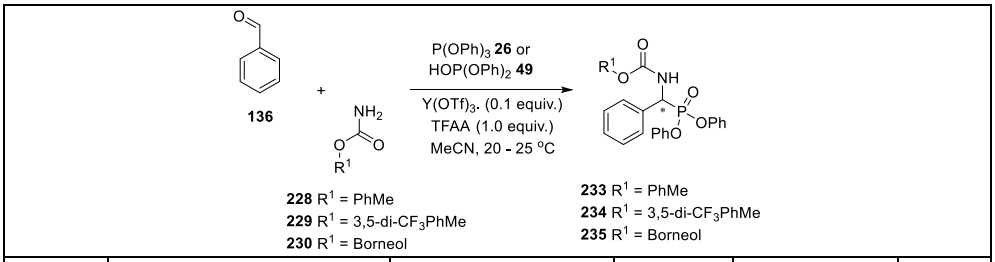

Entry[a]	Carbamate (R^1OCONH_2)	Phosphite	Time (h)	Product/ IS	dr
1	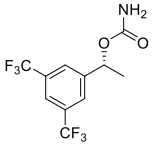	$HOP(OPh)_2$	4	0.30	57:43[b]
2			24	0.33	57:43[b]
3		$P(OPh)_3$	4	0.67	69:31[b]
4			24	0.51	60:40[b]
5	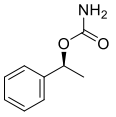	$HOP(OPh)_2$	4	0.37	51:49[c]
6			24	0.24	51:49[c]
7		$P(OPh)_3$	4	0.12	51:49[c]
8			24	0.10	51:49[c]
9	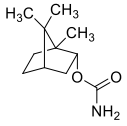	$HOP(OPh)_2$	4	0.43	100:0[c]
10			24	0.30	100:0[c]
11		$P(OPh)_3$	4	0.40	100:0[c]
12			24	0.39	100:0[c]

[a]0.1 equiv. of $Y(OTf)_3$ and 1.0 equiv. of TFAA in anhydrous MeCN; [b]dr measured with HPLC assay; [c]dr measured with ^1H NMR assay after purification of the product by flash chromatography.

In order to confirm our data registered from the HPLC and the ^{1}H NMR assay we planned to remove the carbamate moiety from α-aminophosphonates **200** and **201**, the corresponding amine would have been converted to Cbz-protected α-aminophosphonates **16** after functionalization with benzyl chloroformate (**145**) (Scheme 3.22). The resulting product **16** has been analyzed with a chiral column (chiralpak® IC 3) with mobile phase: isocratic MeCN/H_2O 1:1 v/v (Flow = 1 mL/min) in order to confirm the presence of eventual diastereoselectivity of the reaction.

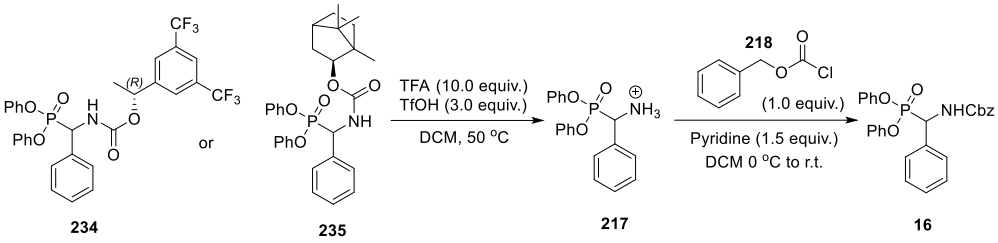

Scheme 3.22. Removal of carbamate with TFA/TfOH and functionalization of the amine with benzyl chloroformate

The carbamate moiety was removed from the α-aminophosphonate **234** and **235** after treatment with 10.0 equivalents of trifluoroacetic acid, and 3.0 equivalents of triflic acid in anhydrous DCM at 50 °C. The amine **217** was not isolated and used as crude in the next step. The Cbz group was inserted reacting amine **217** with benzyl chloroformate (**218**) in the presence of 1.5 equivalents of pyridine in DCM at 0 °C to yield **16**, which was then isolated and analyzed with chiral HPLC (Scheme 3.22). In the case of α-aminophosphonate **235** derived from the borneol carbamate, the chiral column chromatogram showed two peaks with almost the same area (51:49), indicating a racemic mixture (Figure 3.12).

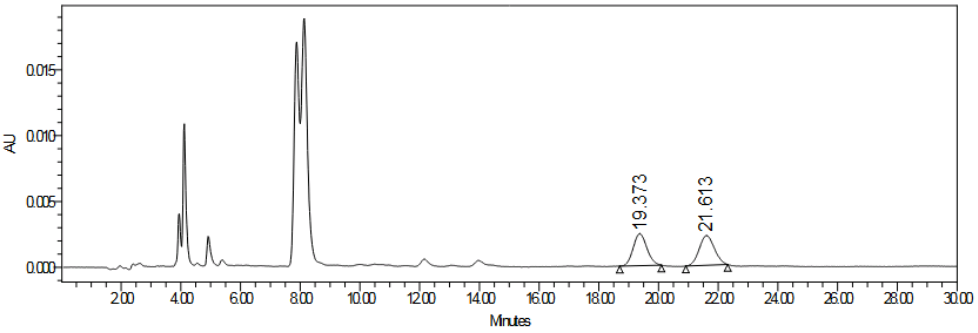

Figure 3.12. Chromatogram of α-aminophosphonate **16**, generated from borneol-substituted α-aminophosphonate **235**; method: chiralpakIC3, isocratic MeCN (50 %) and H_2O (50 %), flow 1 mL/min, 254 nm.

On the other hand, when α-aminophosphonate **234** was converted to a Cbz-protected α-aminophosphonate **16**, the chiral column chromatogram showed two peaks with different areas (64:36), indicating an enantiomeric excess of 28 % (Figure 3.13). The er of final product **16** was lower than the dr recorded for α-aminophosphonate **234**, probably due to slight racemization during the removal of carbamate and functionalization with benzyl chloroformate.

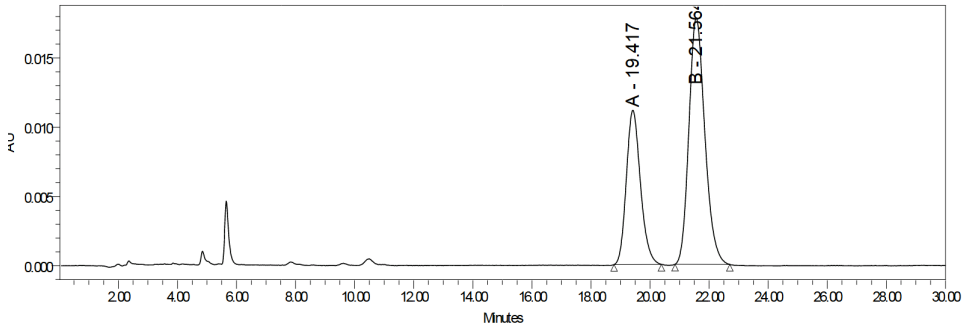

Figure 3.13. Chiral column chromatogram of α-aminophosphonate **16** prepared from α-aminophosphonate **234**; method: chiralpakIC3, isocratic MeCN (50 %) and H_2O (50 %), flow 1 mL/min, 254 nm.

In summary, the enantioselective synthesis of UAMC-00050 intermediate with chiral proline/metal complexes as catalysts failed to provide any ee in the α-aminophosphonate **9**. The diastereoselective synthesis of an α-aminophosphonate from a chiral carbamate also provided poor results except for (*R*)-1-(3,5-bis(trifluoromethyl)phenyl)ethyl carbamate (**229**). This carbamate allowed the preparation of α-aminophosphonate **234** with a 75:25 dr which was then converted to α-aminophosphonate **16** with 64:36 er (probably due to some erosion of the chirality at α-aminophosphonate carbon). Achieved stereoselectivity is too low for any preparative purposes and makes it premature to transfer the reaction from the model compounds to reagents required for the preparation of UAMC-00050 **1** and its analogues. Furthermore, the product must be able to survive the harsh conditions of the carbamate cleavage. However, the present results are an important step in the field of the diastereoselective synthesis of α-aminophosphonates from chiral carbamate, which lacked discoveries for the last 26 years. With the actual knowledge, the best way to provide multigram quantities of the two enantiomers is the separation of the racemic mixture of the product (**16**) with a preparative chiral HPLC.

4 EXPERIMENTAL PART

4.1 General information

Unless otherwise specified, all commercially available reagents were used as received. ^{1}H, ^{13}C, and ^{31}P NMR spectra were obtained on a 400 MHz Bruker Avance 400 spectrometer at ambient temperatures of 400, 101 and 162 MHz, respectively. Chemical shifts (δ) are reported in parts per million (ppm) relative to residual DMSO peak (s, δ 2.50 for ^{1}H and t, δ 39.53 for ^{13}C, respectively), for ^{31}P NMR it was calibrated with the use of an external standard (H_3PO_4). ^{13}C NMR spectra were recorded without ^{31}P and ^{19}F decoupling. Multiplicities are given as s (singlet), d (doublet), t (triplet), q (quartet), and m (multiplet). Complex splittings are described by a combination of these abbreviations, *e.g.* dd (doublet of doublets). Reaction conversion was estimated by LC-MS on Waters Acquity UPLC H-class instrument, column Waters Acquity UPLC BEH-C18, 2.1 × 50 mm, 1.7 µm, eluent 5 - 95 % MeCN in 0.1 % aq. HCOOH; flow rate: 0.8 mL/min; detection Waters PDA Detector (200-300 nm). HPLC chromatogram were recorded with Waters Alliance instrument equipped with 2695 separations module, consisting of quaternary pump, degasser, autosampler and column heater. Waters 2489 dual wavelength absorbance detector was used for detection of analytes or Shimadzu Prominence-I LC-2030C; columns: Prevail™ organic acid or Apollo C18-13, 4.6 × 150 mm; eluent gradient 25 - 95 % or 40 - 95 % MeCN in 0.1 % aq. H_3PO_4: flow rate: 1.0 mL/min, temperature: 40 °C, UV detector: 254 nm. HRMS spectra were acquired on an electrospray ionization mass spectrometer with a TOF analyzer, using the following parameters: positive ionization mode, drying gas 10 mL/min and 325 °C, ionization 100 V. Diffraction data was collected on an XtaLAB Synergy-S Dualflex diffractometer (Rigaku Oxford Diffraction) equipped with a HyPix6000 detector and microfocus sealed X-ray tube with CuKα radiation (λ = 1.54184 Å). Structure was solved by direct methods with ShelXT program using intrinsic phasing and refined by full-matrix least-squares techniques on F2 with SHELXL package. Graphics of the crystal structures were drawn using Mercury software.

4.2 Compounds synthesized for the preparation of UAMC-00050

Tris(4-acetamidophenyl) phosphite (3)

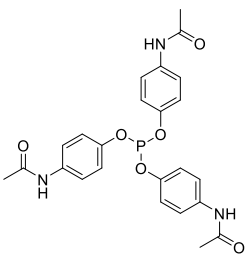

In an oven-dried 500 mL flask equipped with a magnetic stirrer and a dropping funnel, were added 4-acetamidophenol (**2**) (10.00 g, 0.066 mol. 3.0 equiv.; water content < 0.030 %), previously dried in vacuum for 24 h, anhydrous THF (100 mL) (water content < 0.005 %) and anhydrous triethylamine (9.20 mL, 0.066 mol. 3.0 equiv.; water content <0.04 %). The flask was cooled in an ice bath for 10 minutes, then phosphorous trichloride (1.92 mL, 0.022 mol., 1.0 equiv.) was added dropwise. The mixture was stirred for 1 h at 0 °C, then insolubles were filtered off and the filter cake was washed with anhydrous THF (50 mL; water content < 0.005 %).

The filtrate was collected in a 500 mL flask and volatiles were stripped off in vacuo (5 mbar). Once the solid was formed in the flask was kept in vacuo (5 mbar) for 6 h. Yield of **3**: 10.38 g (98 %) as a white foamy solid. Purity 94.0 % area normalized (AN) by HPLC. ^{1}H NMR (400 MHz, DMSO-d_6) δ: 9.99 (s, 3H), 7.58 (d, J = 9.0 Hz, 6H), 7.09 (d, J = 9.0 Hz, 6H), 2.03 (s, 9H). ^{13}C NMR (101 MHz, DMSO-d_6) δ: 168.58, 146.50 (d, $^{2}J_{C,P}$ = 3.5 Hz), 136.44, 121.19 (d, $^{3}J_{C,P}$ = 6.4 Hz), 120.91, 25.34. ^{31}P NMR (162 MHz, DMSO-d_6) δ: 129.32. HRMS (ESI+) m/z calc'd for $C_{24}H_{24}N_3O_6P$ $[M+H]^+$:482.1481, found 482.1492.

***tert*-Butyl (4-(2-hydroxyethyl)phenyl)carbamate (5)**

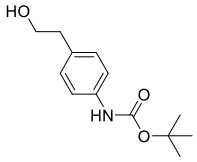

In a 500 mL flask equipped with a magnetic stirrer, were added 4-aminophenetyl alcohol (**4**) (10.0 g, 0.073 mol, 1.0 equiv.), EtOAc (200 mL) and di-*tert*-butyldicarbonate (17.50 g, 0.08 mol, 1.1 equiv.). The mixture was stirred for 16 h at 20-25 °C *(Caution: increase of pressure in the flask)*, then the solvent was removed in vacuo to give an off-white product. To the flask containing the crude material was added 26 mL of MeCN/MTBE 1:1 v/v, and the mixture was warmed up until complete dissolution of the solid. The solution was left cool down at 20-25 °C for 1 h; then, 10 mg of pure compound **5** was added as a seed. The mixture was left at 20-25 °C for 4 h when precipitated formed. Crystalline product was collected by filtration and filter cake washed with heptane (85 mL). The crystalline **5** was dried under vacuo (5 mbar) for 16 h. Yield of **5**: 17.13 g (98 %) as a white solid. Purity 99.6 % AN by HPLC. ^{1}H NMR (400 MHz, DMSO-d_6) δ: 9.19 (s, 1H), 7.34 (d, J = 8.5 Hz, 2H), 7.08 (d, J = 8.5 Hz, 2H), 4.58 (t, J = 5.3 Hz, 1H), 3.55 (q, J = 7.2 Hz, 2H), 2.64 (t, J = 7.2 Hz, 2H,), 1.46 (s, 9H). ^{13}C NMR (101 MHz, DMSO-d_6) δ: 153.29, 137.88, 133.49, 129.40, 118.59, 79.23, 62.84, 38.88, 28.61. HRMS (ESI+) m/z calc'd for $C_{13}H_{19}NO_3Na$ $[M+Na]^+$:260.1263, found 260.1267.

Sodium 2-(4-((*tert*-butoxycarbonyl)amino)phenyl)-1-hydroxyethane-1-sulfonate (164)

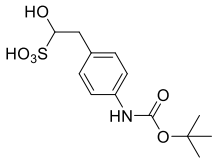

In a 500 mL flask equipped with a magnetic stirrer and a dropping funnel, were added in this sequence: intermediate **6** (17.15 g, 0.072 mol, 1.0 equiv.), dissolved in EtOAc (90.0 mL), TEMPO (0.114 g, $7.3*10^{-4}$ mol, 0.01 equiv.) dissolved in toluene (90.0 mL), and KBr (0.869 g, $7.3*10^{-3}$ mol, 0.1 equiv.) dissolved in saturated aq. $NaHCO_3$ (67.0 mL). The mixture was vigorously stirred for 10 minutes in an ice bath, then aq. solution of NaClO 11 - 15 % (67.0 mL) was added dropwise in 5 minutes. The reaction was vigorously stirred for 10 minutes, then it was quenched with 10 % aq. sodium thiosulfate (250.0 mL), the product was extracted from the reaction mixture with EtOAc (3 × 200 mL), combined organic layers were then washed with brine (500 mL) and dried over Na_2SO_4. Volatiles were removed in vacuo. The crude aldehyde was dissolved in ethanol (340.0 mL) in a 500 mL flask equipped with a magnetic stirrer and a dropping funnel, then a solution of sodium bisulfite (11.71 g, 0.113 mol, 1.5 equiv.) in deionized water (20 mL), was added dropwise in 5 minutes. The mixture was stirred for 18 h at 20-25°C and then 1 h at 0 °C to effect a

complete precipitation. The solid was collected by filtration, washed with cold ethanol (300 mL), and dried in vacuo for 18 h. Yield of **164**: 20.75 g (85 %) as a white solid. Purity 99.0 % AN by HPLC. ^{1}H NMR (400 MHz, DMSO-d_6) δ: 7.30 (d, J = 2.7 Hz, 4H), 4.61 (dd, J = 10.6, 2.7 Hz, 1H), 4.32 (dd, J = 14.4, 2.7 Hz, 1H), 2.88 (dd, J = 14.4, 10.6 Hz, 1H), 1.50 (s, 9H). ^{13}C NMR (101 MHz, DMSO-d_6) δ: 153.34, 134.15, 130.32, 127.68, 117.93, 82.43, 79.59, 34.45, 25.39. HRMS (ESI$^-$) m/z calc'd for $C_{13}H_{18}NO_6S$ $[M]^-$: 316.0861, found 316.0855.

***tert*-Butyl (4-(2-oxoethyl)phenyl)carbamate (7)**

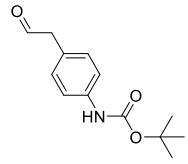

In a 500 mL flask equipped with a magnetic stirrer, were added adduct **164** (19.68 g, 0.085 mol. 1.0 equiv.) dissolved in deionized water (260 mL), sodium carbonate (17.20 g, 0.162 mol, 2.2 equiv.) and EtOAc (300 mL), the mixture was stirred for 3 h at 20-25 °C. Then layers were separated in a 1.0 L separation funnel. Aq. layer was extracted with EtOAc (3 × 250 mL), combined organic layers were washed with brine (400 mL) and dried on Na_2SO_4 (250 g). The solvent was removed in vacuo. Yield of **7**: 13.04 g (91 %) as a pale yellow solid. Purity 99.0 % AN by HPLC. ^{1}H NMR (400 MHz, DMSO-d_6) δ: 9.63 (t, J = 4.0 Hz, 1H), 9.32 (s, 1H), 7.44 (d, J = 8.5 Hz, 2H), 7.11 (d, J = 8.5 Hz, 2H), 3.65 (d, J = 2.0 Hz, 2H), 1.47 (s, 9H). ^{13}C NMR (101 MHz, DMSO-d_6) δ: 200.52, 152.80, 138.44, 129.91, 126.04, 118.39, 78.99, 48.95, 28.13. HRMS (ESI+) m/z calc'd for $C_{13}H_{17}NO_3Na$ $[M+Na]^+$: 258.1106, found 258.1115.

***tert*-Butyl (4-(2-(((benzyloxy)carbonyl)amino)2(bis(4acetamidophenoxy)phosphoryl)ethyl)-phenyl) carbamate (9).**

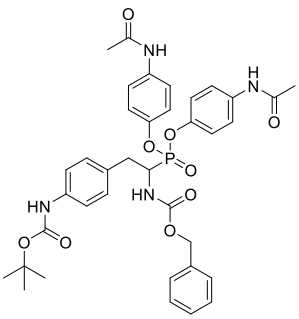

In a 500 mL flask equipped with a magnetic stirrer, under argon, were added: *tert*-butyl (4-(2-oxoethyl)phenyl)carbamate (**7**) (10.0 g, 0.043 mol, 1.0 equiv.), $Y(OTf)_3$ (2.30 g, 4.3 mmol, 0.1 equiv.) dissolved in anhydrous MeCN (130.0 mL; water content <0.001 %), benzyl carbamate (**8**) (6.50 g, 0.043 mol, 1.0 equiv.), tris(4-acetamidophenyl)phosphite (**3**) (23.00 g, 0.043 mol, 1.0 equiv.), anhydrous THF (130.0 mL; water content < 0.005 %) and TFAA (5.98 mL, 0.043 mol, 1.0 equiv.). The mixture was stirred for 4 h at 20-25 °C. The solvent was removed in vacuo and the residue was dissolved in a mixture of EtOAc/EtOH 4:1 v/v (500 mL). The organic solution was washed with 0.5 M aq. NaOH (4 × 500 mL) and brine (500 mL). The organic layers were dried on Na_2SO_4 (300 g) and the solvent was removed in vacuo. A silica pad with 200 g of silica gel was packed in a 500 mL glass filter. The residue was dissolved in EtOAc/EtOH 3:1 v/v (100 mL), celite (20 g) was added to the solution, and the solvent was removed in vacuo. The crude material pre-dispersed on celite was placed on top of the silica pad and washed with EtOAc/heptane 2:1 v/v (2000 mL) to collect fraction 1, which was discarded. The collection flask was changed and the silica pad was washed with EtOAc/EtOH 3:1 v/v (1000 mL) to collect fraction

2, the solvent was removed in vacuo from fraction 2 to give a yellow foamy solid. The crude product was dissolved in acetone (100 mL) and a solution of 0.5 % aq. $NaHCO_3$ (200 mL) was added dropwise. The solid was collected by filtration, washed with MTBE (100 mL) and dried in vacuo overnight. The dry solid was slurried in EtOAc/acetone 19:1 v/v (300 mL), stirred for 24 h, collected by filtration, washed with EtOAc (100 mL) and dried in vacuo overnight. Yield of **9**: 13.55 g (44 %) as a white solid. Purity 98.2 % AN by HPLC. ^{1}H NMR (400 MHz, DMSO-d_6) δ: 10.01 (s, 2H), 9.32 (s, 1H), 8.12 (d, J = 9.5 Hz, 1H), 7.58 (m, 4H), 7.40 (d, J = 8.5 Hz, 2H,), 7.30 (m, 3H), 7.18 (m, 8H), 4.98 (dd, J = 31.0, 13.5 Hz, 2H), 4.43 (q, J = 12.1 Hz, 1H), 3.18 (d, J = 12.3 Hz, 1H), 2.92 (m, 1H), 2.04 (s, 6H), 1.49 (s, 9H). ^{13}C NMR: (101 MHz, DMSO-d_6) δ: 168.68, 156.37 (d, $^3J_{C,P}$ = 4.7 Hz), 153.25, 145.73 (d, $^2J_{C,P}$ = 9.8 Hz), 145.45 (d, $^2J_{C,P}$ = 9.6 Hz), 138.59, 137.60 (d, $^3J_{C,P}$ = 11.3 Hz), 130.99, 130.81, 129.82, 128.70, 128.01, 127.57, 121.28 (d, $^3J_{C,P}$ = 3.4 Hz), 121.01 (d, $^3J_{C,P}$ = 3.7 Hz), 120.61 (d, $^3J_{C,P}$ = 6.5 Hz), 118.34, 79.39, 65.86, 50.48 (d, $^1J_{C,P}$ = 156.8 Hz), 34.05 (d, $^2J_{C,P}$ = 4.0 Hz), 28.61, 24.37. ^{31}P NMR (162 MHz, DMSO-d_6) δ: 18.35. HRMS (ESI+): m/z calc'd for $C_{37}H_{41}N_4O_9PNa$ $[M+Na]^+$: 739.2509, found 739.2519.

4-(2-(((Benzyloxy)carbonyl)amino)-2-(bis(4-acetamidophenoxy)phosphoryl)ethyl)benzenaminium chloride (178).

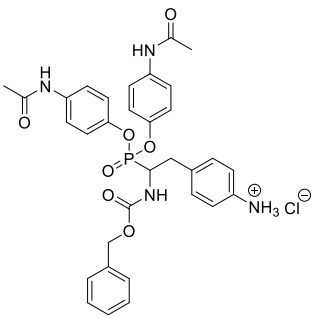

In a 500 mL flask equipped with a magnetic stirrer were added in this sequence: Boc-protected compound **9** (10.00 g, 0.014 mol) and 4 N HCl in dioxane (150 mL), the solution was stirred for 3 h at 20-25 °C *(Caution: increase of pressure in the flask).* The solvent was removed in vacuo, the residue was dissolved in absolute EtOH (100 mL; Water content < 0.005 %) and the solution was added dropwise to stirred EtOAc (1000 mL). The mixture was stirred for 30 minutes at 20-25 °C, the precipitate was collected by filtration, washed with EtOAc (100 mL) and dried in vacuo overnight. Yield of **178**: 9.05 g (99 %) as an off-white powder. Purity 97.9 % AN by HPLC. ^{1}H NMR (400 MHz, DMSO-d_6) δ: 10.09 (d, J = 2.7 Hz, 2H), 9.76 (s, 2H), 8.17 (d, J = 9.5 Hz, 1H), 7.65 (m, 4H), 7.35 (m, 5H), 7.21 (t, J = 6.7 Hz, 5H), 7.09 (m, 4H), 4.96 (dd, J = 31.0, 13.5 Hz, 2H), 4.45 (m, 1H), 3.25 (m, 1H), 2.99 (m, 1H), 2.03 (s, 6H). ^{13}C NMR (101 MHz, DMSO-d_6) δ: 168.70, 156.31 (d, $^3J_{C,P}$ = 4.6 Hz), 145.66 (d, $^2J_{C,P}$ = 9.8 Hz), 145.38 (d, $^2J_{C,P}$ = 9.8 Hz), 137.27, 137.05 (d, $^3J_{C,P}$ = 10.5 Hz), 130.80, 128.80, 128.23, 127.82, 122.25, 121.23 (d, $^3J_{C,P}$ = 3.6 Hz), 120.96 (d, $^3J_{C,P}$ = 3.8 Hz), 120.61 (d, $^3J_{C,P}$ = 7.8 Hz), 66.05, 50.28 (d, $^1J_{C,P}$ = 157.4 Hz), 34.11 (d, $^2J_{C,P}$ = 5.0 Hz), 31.16, 24.36. ^{31}P NMR (162 MHz, DMSO-d_6) δ: 18.00. HRMS (ESI+) m/z calc'd for $C_{32}H_{34}N_4O_7P$ $[M+H]^+$: 617.2165, found 617.2175.

1-(4-(2-(((Benzyloxy)carbonyl)amino)-2-(bis(4-acetamidophenoxy)phosphoryl)ethyl)phenyl) guanidinium chloride (1).

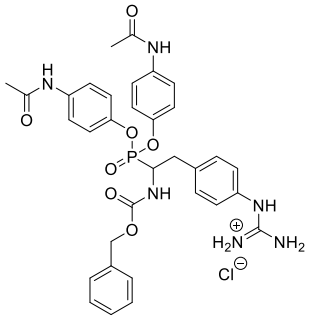

In an oven-dried 50 mL flask equipped with a magnetic stirrer, were added compound **178** (5.00 g, 7.7 mmol, 1.0 equiv), $Sc(OTf)_3$ (377 mg, 0.77 mmol, 0.1 equiv) dissolved in anhydrous THF/absolute EtOH 2:1 v/v (15.4 mL; water content < 0.005 %) and NH_2CN (3.23 g, 77.0 mmol, 10.0 equiv.). The solution was stirred for 96 h at 20-25 °C then the solvent was removed in vacuo, the crude product was dissolved in absolute EtOH (50 mL), added dropwise to stirred *i*PrOAc (500 mL) at 20-25 °C and slurried for 1 h. The solid was collected by filtration, washed with *i*PrOAc (250 mL) and dried in vacuo for 16 h. The crude material was dissolved in 500 mL of deionized water/EtOH (10:1 v/v) and loaded on a 300 g YMC-DispoPack AT RP-C_{18} reverse phase column. The column was eluted with (MeCN/EtOH 9:1 v/v) in deionized water, gradient 0 - 100 %. The target fractions were collected, the selected tubes were divided in two flasks S1 and S2, then the solvent was removed with freeze-drying to get product **1**. Yield: 3.85 g (72 %). Purity fraction 1 (S1) 98.1 % AN by HPLC and fraction 2 (S2) 99.4 % AN by HPLC. ^{1}H NMR (400 MHz, DMSO-d_6) δ: 10.04 (d, J = 2.7 Hz, 2H), 9.94 (s, 1H), 8.18 (d, J = 9.5 Hz, 1H), 7.58 (m, 4H), 7.50 (s, 3H), 7.37 (d, J = 8.5 Hz, 2H), 7.30 (m, 3H), 7.20 (m, 2H), 7.10 (m, 6H), 4.95 (dd, J = 31.0, 13.5 Hz, 2H), 4.45 (q, J = 12.5 Hz, 1H), 3.22 (m, 1H), 3.00 (m, 1H), 2.02 (s, 6H). ^{13}C NMR (101 MHz, DMSO-d_6) δ: 168.71, 156.38, 156.30 (d, $^3J_{C,P}$ = 4.1 Hz), 145.65 (d, $^3J_{C,P}$ = 9.7 Hz), 145.40 (d, $^3J_{C,P}$ = 9.7 Hz), 137.27, 137.06 (d, $^3J_{C,P}$ = 10.4 Hz), 135.82, 135.64, 134.32, 130.82, 128.76, 128.26, 127.90, 124.43, 121.22 (d, $^3J_{C,P}$ = 3.6 Hz), 120.95 (d, $^3J_{C,P}$ = 3.7 Hz), 120.62 (d, $^3J_{C,P}$ = 7.7 Hz), 66.08, 50.14 (d, $^3J_{C,P}$ = 157.2 Hz), 34.00 (d, $^3J_{C,P}$ = 4.1 Hz), 24.36. ^{31}P NMR (162 MHz, DMSO-d_6) δ: 17.39. HRMS (ESI+) m/z calc'd for $C_{33}H_{37}N_6O_7P$ $[M+H]^+$: 659.2383, found 659.2398.

(9*H*-Fluoren-9-yl)methyl(4-(2-hydroxyethyl)phenyl) carbamate (172)

In a 50 mL flask equipped with a magnetic stirrer, were added 4-aminophenethyl alcohol (**4**) (1.00 g, 7.3 mmol, 1.0 equiv.), Na_2CO_3 (5.15 g, 18.0 mmol, 2.5 equiv.) and DMAP (50 mg, 0.73 mmol, 0.1 equiv.), DCM (10 mL) and deionized water (5 mL). The mixture was cooled at 0 °C then Fmoc-Cl (2.85 g, 11 mmol, 1.5 equiv.) dissolved in anhydrous DCM (2 mL) was added dropwise via syringe. The mixture was stirred at 0 °C for 0.5 h at 20-25 °C for 2 h. Then at the solution was added 0.5 M aq. $NaHCO_3$ (200 mL) and the product was extracted with DCM (3 × 100 mL). The combined organic layers were dried on Na_2SO_4. The solvent was removed in vacuo and the crude material was purified by flash

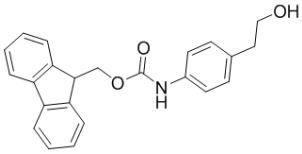

chromatography on silica (eluent heptane/EtOAc 20 - 100 %). Yield of **206**: 1.99 g (76 %) as an off-white solid. Purity 97.9 % AN by HPLC. ^{1}H NMR (400 MHz, DMSO-d_6) δ: 9.59 (s, 1H), 7.91 (d, *J* = 7.5 Hz, 2H), 7.75 (d, *J* = 7.5 Hz, 2H), 7.43 (t, *J* = 8.5 Hz, 3H), 7.35 (td, *J* = 7.5, 0.8 Hz, 3H), 7.10 (d, *J* = 8.5 Hz, 2H), 4.59 (t, *J* = 5.2 Hz, 1H), 4.46 (d, *J* = 6.7 Hz, 2H), 4.30 (t, *J* = 6.7 Hz, 1H), 3.56 (q, *J* = 7.1 Hz, 2H), 2.64 (t, *J* = 7.1 Hz, 2H). ^{13}C NMR (101 MHz, DMSO-d_6) δ: 153.91, 144.28, 141.28, 137.37, 134.02, 129.54, 128.15, 127.59, 125.61, 120.66, 118.78, 65.95, 62.77, 47.12, 38.87. HRMS (ESI+) m/z calc'd for $C_{23}H_{21}NO_3Na$ 382.1419, found 382.1438.

(9*H*-Fluoren-9-yl)methyl (4-(2-oxoethyl)phenyl)carbamate (173)

In an oven-dried 50 mL flask equipped with a magnetic stirrer, were added alcohol **172** (1.00 g, 2.78 mmol, 1.0 equiv.) and anhydrous DCM (20 mL). The solution was cooled to 0 °C and DMP

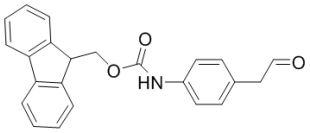

(1.42 g, 3.34 mmol, 1.2 equiv.) was added portionwise. The mixture was stirred for 4 h at 0 °C then it was quenched with saturated aq. $NaHCO_3$/10 % aq. $Na_2S_2O_3$ (1:1 v/v) (50 mL) and the product extracted with EtOAc (3 × 50 mL). The combined organic layers were dried over Na_2SO_4. Volatiles were removed in vacuo and the crude was purified by flash chromatography on silica (eluent heptane/EtOAc 20 - 100 %). Yield of **173**: 0.32 g (32 %). Purity 95.6 % AN by HPLC. ^{1}H NMR (400 MHz, DMSO-d_6) δ: 9.70 (s, 1H), 9.64 (t, *J* = 2.0 Hz, 1H), 7.91 (d, *J* = 7.5 Hz, 2H), 7.75 (d, *J* = 7.5 Hz, 2H), 7.43 (t, *J* = 7.5 Hz, 4H), 7.35 (t, *J* = 7.5 Hz, 2H), 7.13 (d, *J* = 8.5 Hz, 2H), 4.49 (d, *J* = 6.7 Hz, 2H), 4.31 (t, *J* = 6.7 Hz, 1H), 3.68 (d, *J* = 2.0 Hz, 2H). ^{13}C NMR (101 MHz, DMSO-d_6) δ: 201.02, 153.90, 144.26, 141.29, 138.38, 130.50, 128.16, 127.60, 127.08, 125.60, 120.66, 119.04, 66.02, 49.38, 47.12. HRMS (ESI+) m/z calc'd for $C_{23}H_{19}NO_3Na$ 380.1263, found 380.1284.

2-(4-Nitrophenyl)acetaldehyde (210)

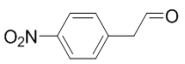

In an oven-dried 100 mL flask equipped with a magnetic stirrer, were added 2-(4-nitrophenyl)ethan-1-ol **209** (1.00 g, 5.98 mmol, 1.0 equiv.) and anhydrous DCM (43 mL). The solution was cooled at 0 °C then the DMP (3.04 g, 7.18 mmol, 1.2 equiv.) was added portionwise. The reaction was stirred at 0 °C for 3 h and 20-25 °C for 16 h. The mixture was quenched with 10 % aq. $Na_2S_2O_3$ (50 mL) and the product extracted with DCM (3 × 100 mL). The combined organic layers were washed with saturated aq. $NaHCO_3$ (100 mL) and brine (100 mL). The organic phase was dried over Na_2SO_4 and volatiles were removed in vacuo at room temperature (*no heating*). Yield of **210**: 0.86 g (87 %) as a yellow solid. Purity 74.3 % AN by HPLC. ^{1}H NMR: (400 MHz, DMSO-d_6) δ: 9.81 (t, *J* = 1.5 Hz, 1H), 8.22 (d, *J* = 8.9 Hz, 2H), 7.39 (d, *J* = 8.9 Hz, 2H), 3.87 (d, *J* = 1.8 Hz, 2H). ^{13}C NMR: (101 MHz, DMSO-d_6) δ: 197.18, 139.33, 136.16, 133.21, 131.35, 130.60, 129.35, 124.04, 50.06.

Dibenzyl (2-(4-((*tert*-butoxycarbonyl)amino)phenyl)ethane-1,1-diyl)dicarbamate (168)

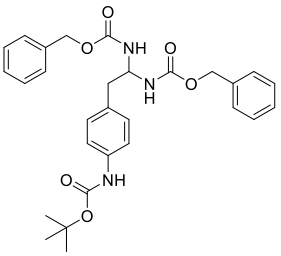

In a 25 mL flask were added aldehyde **7** (0.20 g, 0.85 mmol, 1.0 equiv.) benzyl carbamate (**8**) (0.26 g, 1.7 mmol, 2.0 equiv.), $Y(OTf)_3$ (0.05 g, 0.085 mmol, 0.1 equiv.) anhydrous MeCN (2.5 mL). The solution was stirred at 20-25 °C for 4 h. The precipitate was collected by filtration, washed with 2 mL of MeCN, and dried in vacuo for 16 h. Yield of **168**: 0.10 g (23 %). Purity 100 % AN by HPLC. ^{1}H NMR (400 MHz, DMSO-d_6) δ: 9.28 (s, 1H), 7.71 (s, 2H), 7.35 (t, J = 7.5 Hz, 6H), 7.30 (t, J = 7.5 Hz, 6H), 7.12 (d, J = 7.5 Hz, 2H), 5.16 (s, 1H), 5.00 (m, 4H), 2.83 (d, J = 6.8 Hz, 2H), 1.49 (s, 9H). ^{13}C NMR (101 MHz, DMSO-d_6) δ: 155.41, 153.27, 138.31, 137.56, 131.41, 129.94, 128.76, 128.15, 128.06, 118.32, 79.33, 65.55, 61.70, 28.62. HRMS (ESI+) m/z calc'd for $C_{29}H_{33}N_3O_6Na$ $[M+Na]^+$: 542.2267, found 542.2267.

4.3 Compounds prepared for the scope Birum-Oleksyszyn reaction

Tris(4-methoxyphenyl) phosphite (183)

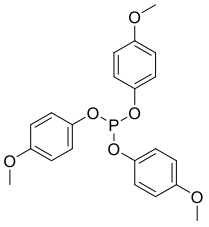

In an oven-dried 250 mL flask equipped with a magnetic stirrer, were added 4-methoxyphenol (**182**) (5.00 g, 0.04 mol, 3.0 equiv.), previously dried in vacuum for 24 h, anhydrous THF (50 mL) and anhydrous TEA (5.58 mL, 0.04 mol, 3.0 equiv.), the solution was cooled to 0 °C and after 10 minutes was added dropwise phosphorous trichloride (1.17 mL, 0.013 mol, 1.0 equiv.) via syringe. The mixture was stirred at 0 °C for 1 h, then was the solid was removed by filtration, washed on filter with anhydrous THF (25 mL). Collected, filtrate was concentrated in vacuo (5 mbar). Once solid was formed in the flask was kept in a vacuo (5 mbar) for 6 h. Yield of **183**: 3.59 g (69 %) as an off-white solid. Purity 75 % AN by HPLC. ^{1}H NMR (400 MHz, DMSO-d_6) δ: 7.22 (dd, J = 9.1, 1.1 Hz, 6H), 6.98 (d, J = 9.1 Hz, 6H), 3.73 (s, 9H). ^{13}C NMR (101 MHz, DMSO-d_6) δ: 156.87, 143.58 (d, $^{2}J_{C,P}$ = 7.5 Hz), 120.91 (d, $^{3}J_{C,P}$ = 4.6 Hz), 114.94, 55.37. ^{31}P NMR (162 MHz, DMSO-d_6) δ: 129.49. HRMS (ESI+): m/z calc'd for $C_{21}H_{22}O_6P$ $[M+H]^+$:400.1076, found 400.1084.

General procedure A: synthesis of α-aminophosphonates 185a-185v

In a 100 mL flask equipped with a magnetic stirrer, were added: aldehyde (1.0 equiv.) $Y(OTf)_3$ (0.1 equiv.), carbamate (1.0 equiv.) phosphite (1.0 equiv.) and anhydrous MeCN. The solution was stirred at 20-25 °C for the indicated time. Volatiles were removed in vacuo.

Purification method A: the crude product was suspended in MeCN (20 mL per 3 g of crude), the mixture was warmed up until the complete dissolution of the solid. Then the solution was kept 20-25 °C for 20 h until complete precipitation of the product. The solid was collected by filtration and washed with MeCN (20 mL per 3 g of crude) then dried in vacuo (5 mbar) for 16 h.

Purification method B: the crude product was purified by flash chromatography on silica (gradient heptane/EtOAc 10 - 100 %). The selected tubes were collected and volatiles were removed by vacuo.

Benzyl ((diphenoxyphosphoryl)(phenyl)methyl)carbamate (16)

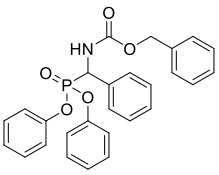

According to general procedure A: benzaldehyde (1.00 mL, 9.4 mmol, 1.0 equiv.), $Y(OTf)_3$ (504 mg, 0.94 mmol, 0.1 equiv.), benzyl carbamate (1.42 g, 9.4 mmol, 1.0 equiv.), triphenyl phosphite (2.47 mL, 9.4 mmol, 1.0 equiv.), and anhydrous MeCN (28 mL). Purification method A. Yield of **16** 3.64 g (82 %) as a white solid. Purity 99 % AN by HPLC. ^{1}H NMR (400 MHz, DMSO-d_6) δ: 8.95 (d, J = 10.3 Hz, 1H), 7.66 (d, J = 8.0 Hz, 2H), 7.35 (m, 12H), 7.19 (m, 2H), 7.07 (d, J = 8.0 Hz, 2H), 6.97 (d, J = 8.0 Hz, 2H), 5.64 (dd, J = 23.1, 12.5 Hz, 1H), 5.12 (dd, J = 36.0, 12.5 Hz, 2H). ^{13}C NMR (101 MHz, DMSO-d_6) δ: 156.50 (d, $^3J_{C,P}$ = 8.5 Hz), 150.57 (d, $^2J_{C,P}$ = 10.0 Hz), 150.28 (d, $^2J_{C,P}$ = 9.7 Hz), 137.12, 134.83, 130.29 (d, $^3J_{C,P}$ = 4.5 Hz), 129.02 (d, $^3J_{C,P}$ = 5.9 Hz), 128.91 (d, $^4J_{C,P}$ = 1.5 Hz), 128.83, 128.72 (d, $^4J_{C,P}$ = 2.5 Hz), 128.41, 125.74 (d, $^2J_{C,P}$ = 9.1 Hz), 120.83, 120.76 (d, $^3J_{C,P}$ = 4.3 Hz), 66.67, 53.39 (d, $^1J_{C,P}$ = 157.2 Hz). ^{31}P NMR (162 MHz, DMSO-d_6) δ: 15.28. HRMS (ESI+) m/z calc'd for $C_{27}H_{23}N_2O_7P$ [M+H]+: 474.1470, found 474.1476.

Benzyl ((bis(4-methoxyphenoxy)phosphoryl)(phenyl)methyl)carbamate (185a)

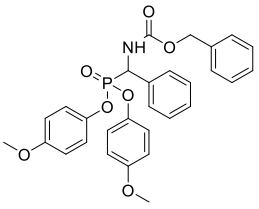

According to general procedure A: benzaldehyde (1.00 mL, 9.4 mmol, 1.0 equiv.), $Y(OTf)_3$ (504 mg, 0.94 mmol, 0.1 equiv.), benzyl carbamate (1.42 g, 9.4 mmol, 1.0 equiv.), tris(4-methoxyphenyl) phosphite (3.76 g, 9.4 mmol, 1.0 equiv.), and MeCN (28 mL). Stirred for 6 h. Purification method A. Yield of **185a**: 3.49 g (92 %). Purity 100 % AN by HPLC. ^{1}H NMR (400 MHz, DMSO-d_6) δ: 8.87 (d, J = 10.1 Hz, 1H), 7.61 (d, J = 7.5 Hz, 2H), 7.37 (m, 8H), 6.95 (d, J = 7.5 Hz, 2H), 6.86 (m, 6H), 5.53 (dd, J = 22.3, 10.1 Hz, 1H), 5.10 (dd, J = 38.0, 12.5 Hz, 2H), 3.69 (s, 6H). ^{13}C NMR (101 MHz, DMSO-d_6) δ: 156.84 (d, $^3J_{C,P}$ = 6.1 Hz), 156.48 (d, $^2J_{C,P}$ = 8.6 Hz), 144.01 (d, $^2J_{C,P}$ = 10.1 Hz), 143.68 (d, $^2J_{C,P}$ = 9.8 Hz), 137.14, 135.02, 128.97 (d, $^3J_{C,P}$ = 5.9 Hz), 128.87 (d, $^4J_{C,P}$ = 1.7 Hz),

128.83, 128.64 (d, $^{4}J_{C,P}$ = 2.7 Hz), 128.43, 121.69 (d, $^{3}J_{C,P}$ = 3.7 Hz), 121.62 (d, $^{3}J_{C,P}$ = 3.9 Hz), 115.11 (d, $^{3}J_{C,P}$ = 5.1 Hz), 66.64, 55.90, 53.16 (d, $^{1}J_{C,P}$ = 156.8 Hz). ^{31}P NMR (162 MHz, DMSO-d_6) δ: 14.78. HRMS (ESI+) m/z calc'd for $C_{29}H_{28}NO_7P$ $[M+H]^+$:534.1682, found 534.1689.

Benzyl ((bis(4-acetamidophenoxy)phosphoryl)(4-chlorophenyl)methyl)carbamate (185b)

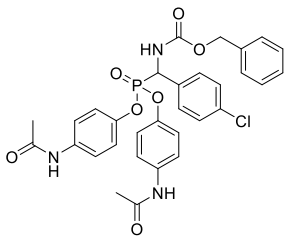

According to general procedure A: 4-chlorobenzaldehyde (1.00 g, 7.1 mmol, 1.0 equiv.), Y(OTf)$_3$ (381 mg, 0.71 mmol, 0.1 equiv.), benzyl carbamate (1.07 g, 7.1 mmol, 1.0 equiv.), tris(4-acetamidophenyl) phosphite (3.42 g, 7.1 mmol, 1.0 equiv.), and MeCN (21 mL). Stirred for 4 h. Method of purification A. Yield of **185b**: 4.00 g (87 %) as an off-white solid. Purity 94 % AN by HPLC. ^{1}H NMR (400 MHz, DMSO-d_6) δ: 9.98 (s, 2H), 8.89 (d, *J* = 10.1 Hz, 1H), 7.63 (dd, *J* = 8.5, 1.8 Hz, 2H), 7.48 (m, 6H), 7.33 (m, 5H), 6.96 (d, *J* = 8.5 Hz, 2H), 6.90 (d, *J* = 8.5 Hz, 2H), 5.58 (dd, *J* = 22.3, 10.1 Hz, 1H), 5.08 (dd, *J* = 33.4, 12.5 Hz, 2H), 2.01 (s, 6H). ^{13}C NMR (101 MHz, DMSO-d_6) δ: 168.66, 156.39 (d, $^{3}J_{C,P}$ = 8.8 Hz), 145.60 (d, $^{2}J_{C,P}$ = 10.1 Hz), 145.29 (d, $^{2}J_{C,P}$ = 9.7 Hz), 137.02 (d, $^{3}J_{C,P}$ = 3.7 Hz), 137.00, 134.08, 133.47 (d, $^{3}J_{C,P}$ = 3.5 Hz), 130.79 (d, $^{3}J_{C,P}$ = 5.7 Hz), 128.92, 128.82, 128.45, 128.41, 120.93 (d, $^{3}J_{C,P}$ = 3.7 Hz), 120.84 (d, $^{3}J_{C,P}$ = 4.0 Hz), 120.55 (d, $^{3}J_{C,P}$ = 4.4 Hz), 66.73, 52.56 (d, $^{1}J_{C,P}$ = 157.4 Hz), 24.36. ^{31}P NMR (162 MHz, DMSO-d_6) δ: 14.93. HRMS (ESI+) m/z calc'd for $C_{31}H_{29}ClN_3O_7P$ $[M+H]^+$: 622.1510, found 622.1526.

Benzyl (1-(diphenoxyphosphoryl)-2-phenylethyl)carbamate (185c)

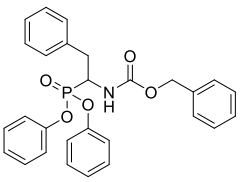

According to general procedure A: 2-phenylacetaldehyde (1.00 mL, 8.3 mmol, 1.0 equiv.), Y(OTf)$_3$ (445 mg, 0.83 mmol, 0.1 equiv.), benzyl carbamate (1.25 g, 8.3 mmol, 1.0 equiv.), triphenyl phosphite (2.18 mL, 8.3 mmol, 1.0 equiv.), and MeCN (25 mL). Stirred for 6 h. Method of purification B. Yield of **185c**: 1.94 g (48 %) as a white solid. Purity 99 % AN by HPLC. ^{1}H NMR (400 MHz, DMSO-d_6) δ: 8.20 (d, *J* = 9.5 Hz, 1H), 7.39 (m, 4H), 7.24 (m, 15H), 4.97 (dd, *J* = 16.2, 12.9 Hz, 2H), 4.55 (m, 1H), 3.29 (dt, *J* = 8.0, 3.3 Hz, 1H), 3.02 (m, 1H). ^{13}C NMR (101 MHz, DMSO-d_6) δ: 155.89 (d, $^{3}J_{C,P}$ = 4.7 Hz), 150.12 (d, $^{2}J_{C,P}$ = 9.8 Hz), 149.85 (d, $^{2}J_{C,P}$ = 9.7 Hz), 149.81, 137.11, 136.94, 136.91, 129.88 (d, $^{3}J_{C,P}$ = 7.1 Hz), 129.13, 128.26, 127.66, 127.24, 126.62, 125.30 (d, $^{2}J_{C,P}$ = 14.6 Hz), 120.64 (d, $^{3}J_{C,P}$ = 3.9 Hz), 120.40 (d, $^{3}J_{C,P}$ = 4.0 Hz), 65.46, 49.98 (d, $^{1}J_{C,P}$ = 158.1 Hz), 34.15 (d, $^{2}J_{C,P}$ = 4.8 Hz). ^{31}P NMR (162 MHz, DMSO-d_6) δ: 18.06. HRMS (ESI+) m/z calc'd for $C_{27}H_{23}N_2O_7P$ $[M+H]^+$: 488.1627, found 488.1639.

Benzyl(2-(4-((*tert*-butoxycarbonyl)amino)phenyl)-1-(diphenoxyphosphoryl)ethyl)carbamate (185d)

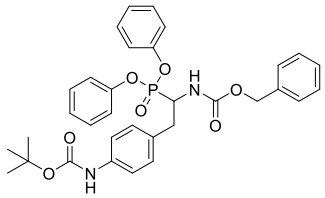

According to general procedure A: *tert*-butyl (4-(2-oxoethyl) phenyl)carbamate (1.00 g, 4.3 mmol, 1.0 equiv.), $Y(OTf)_3$ (231 mg, 0.43 mmol, 0.1 equiv.), benzyl carbamate (1.00 g, 4.3 mmol, 1.0 equiv.), triphenyl phosphite (1.11 mL, 4.3 mmol, 1.0 equiv.), and MeCN (13 mL). Stirred for 8 h. Purification method B. Yield of **185d**: 0.98 g (38 %) as a pale yellow solid. Purity 78 % AN by HPLC. ^{1}H NMR (400 MHz, DMSO-d_6) δ: 9.32 (s, 1H), 8.15 (d, J = 9.5 Hz, 1H), 7.39 (m, 6H), 7.21 (m, 13H), 4.97 (dd, J = 33.4, 12.5 Hz, 2H), 4.46 (m, 1H), 3.20 (m, 1H), 2.92 (m, 1H), 1.49 (s, 9H). ^{13}C NMR (101 MHz, DMSO-d_6) δ: 156.38 (d, $^{3}J_{C,P}$ = 4.8 Hz), 153.25, 150.59 (d, $^{2}J_{C,P}$ = 9.7 Hz), 150.32 (d, $^{2}J_{C,P}$ = 9.7 Hz), 138.60, 137.44, 130.94, 130.77, 130.34 (d, $^{3}J_{C,P}$ = 6.8 Hz), 129.82, 128.71, 128.01, 127.58, 125.76 (d, $^{3}J_{C,P}$ = 14.6 Hz), 121.13 (d, $^{3}J_{C,P}$ = 3.8 Hz), 120.88 (d, $^{3}J_{C,P}$ = 4.0 Hz), 118.34, 79.39, 65.84, 50.63 (d, $^{1}J_{C,P}$ = 157.1 Hz), 33.98 (d, $^{2}J_{C,P}$ = 4.9 Hz), 28.62. ^{31}P NMR (162 MHz, DMSO-d_6) δ: 18.11 HRMS (ESI+) m/z calc'd for $C_{27}H_{23}N_2O_7P$ $[M+Na]^+$: 625.2101, found 625.2080.

Benzyl ((bis(*p*-tolyloxy)phosphoryl)(phenyl)methyl)carbamate (185e)

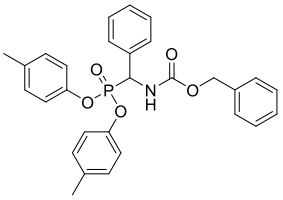

According to general procedure A: benzaldehyde (1.00 mL, 9.4 mmol, 1.0 equiv.), $Y(OTf)_3$ (504 mg, 0.94 mmol, 0.1 equiv.), benzyl carbamate (1.42 g, 9.4 mmol, 1.0 equiv.), tri-*p*-tolyl phosphite (2.94 mL, 9.4 mmol, 1.0 equiv.), and MeCN (28 mL). Purification method A. Yield of **185e**: 3.31 g (75 %) Purity 93 % AN by HPLC. ^{1}H NMR (400 MHz, DMSO-d_6) δ: 8.87 (d, J = 10.1 Hz, 1H), 7.61 (m, 2H), 7.36 (m, 8H), 7.12 (m, 4H), 6.92 (d, J = 8.5 Hz, 2H), 6.82 (d, J = 8.5 Hz, 2H), 5.54 (dd, J = 22.3, 10.1 Hz, 1H), 5.10 (dd, J = 33.4, 12.5 Hz, 2H), 2.25 (s, 6H). ^{13}C NMR (101 MHz, DMSO) δ: 156.45 (d, $^{3}J_{C,P}$ = 8.8 Hz), 148.40 (d, $^{2}J_{C,P}$ = 9.9 Hz), 148.10 (d, $^{2}J_{C,P}$ = 9.7 Hz), 137.13, 134.92 (d, $^{3}J_{C,P}$ = 7.4 Hz), 134.77, 130.53 (d, $^{3}J_{C,P}$ = 5.1 Hz), 128.97 (d, $^{3}J_{C,P}$ = 5.9 Hz), 128.87 (d, $^{4}J_{C,P}$ = 1.9 Hz), 128.82, 128.65 (d, $^{4}J_{C,P}$ = 2.7 Hz), 128.40, 120.51, 120.44 (d, $^{3}J_{C,P}$ = 4.3 Hz), 66.62, 53.26 (d, $^{1}J_{C,P}$ = 157.0 Hz), 20.70. ^{31}P NMR (162 MHz, DMSO-d_6) δ: 14.79. HRMS (ESI+) m/z calc'd for $C_{27}H_{23}N_2O_7P$ $[M+H]^+$: 502.1783, found 502.1801.

Benzyl ((bis(4-acetamidophenoxy)phosphoryl)(phenyl)methyl)carbamate (185f)

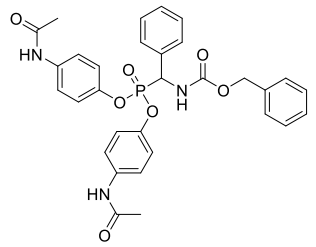

According to general procedure A: benzaldehyde (1.00 mL, 9.4 mmol, 1.0 equiv.), $Y(OTf)_3$ (504 mg, 0.94 mmol, 0.1 equiv.), benzyl carbamate (1.42 g, 9.4 mmol, 1.0 equiv.), tris(4-acetamidophenyl) phosphite (4.52 g, 9.4 mmol, 1.0 equiv.), and MeCN (28 mL). Stirred for 6 h. Purification method B. Yield of **185f**: 4.11 g (72 %). Purity 97 % AN by HPLC. ^{1}H NMR (400 MHz, DMSO-d_6) δ: 9.98 (s, 2H), 8.89 (d, J = 10.1 Hz, 1H), 7.62 (d, J = 8.5 Hz, 2H), 7.51 (t, J = 8.5 Hz, 4H), 7.37 (m, 8H), 6.97 (d, J = 8.5 Hz, 2H), 6.88 (d, J = 8.5 Hz, 2H), 5.55 (dd, J = 22.3, 10.1 Hz, 1H), 5.10 (dd, J = 33.4, 12.5 Hz, 2H), 2.02 (d, J = 2.5 Hz, 6H). ^{13}C NMR (101 MHz, DMSO-d_6) δ: 168.20, 156.00 (d, $^{3}J_{C,P}$ = 8.7 Hz), 145.23 (d, $^{2}J_{C,P}$ = 10.0 Hz), 144.93 (d, $^{2}J_{C,P}$ = 9.7 Hz), 136.65, 136.52 (d, $^{3}J_{C,P}$ = 5.7 Hz), 134.47, 128.53 (d, $^{3}J_{C,P}$ = 5.9 Hz), 128.44 (d, $^{4}J_{C,P}$ = 1.4 Hz), 128.36, 128.21 (d, $^{4}J_{C,P}$ = 1.7 Hz), 127.94, 120.49 (d, $^{3}J_{C,P}$ = 3.7 Hz), 120.42 (d, $^{3}J_{C,P}$ = 4.0 Hz), 120.07 (d, $^{3}J_{C,P}$ = 2.1 Hz), 66.21, 52.76 (d, $^{1}J_{C,P}$ = 156.9 Hz), 23.90. ^{31}P NMR (162 MHz, DMSO-d_6) δ: 15.53. HRMS (ESI+) m/z calc'd for $C_{31}H_{30}N_3O_7P$ $[M+H]^+$:588.1900, found 588.1909.

Benzyl ((4-chlorophenyl)(diphenoxyphosphoryl)methyl)carbamate (185g)

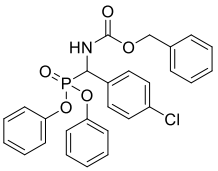

According to general procedure A: 4-chlorobenzaldehyde (1.00 g, 7.1 mmol, 1.0 equiv.), $Y(OTf)_3$ (381 mg, 0.71 mmol, 0.1 equiv.), benzyl carbamate (1.07 g, 7.1 mmol, 1.0 equiv.), triphenyl phosphite (1.86 mL, 7.1 mmol, 1.0 equiv.), and MeCN (21 mL). Stirred for 6 h. Method of purification A. Yield of **185g**: 2.09 g (55 %) as an off-white solid. Purity 95 % AN by HPLC. ^{1}H NMR (400 MHz, DMSO-d_6) δ: 8.94 (d, J = 10.1 Hz, 1H), 7.67 (d, J = 8.5 Hz, 2H), 7.48 (d, J = 8.5 Hz, 2H), 7.34 (t, J = 8.5 Hz, 9H), 7.20 (t, J = 8.5 Hz, 2H), 7.05 (d, J = 8.5 Hz, 2H), 7.00 (d, J = 8.5 Hz, 2H), 5.65 (dd, J = 22.3, 10.1 Hz, 1H), 5.10 (dd, J = 33.4, 12.5 Hz, 2H). ^{13}C NMR (101 MHz, DMSO-d_6) δ: 156.42 (d, $^{3}J_{C,P}$ = 8.7 Hz), 150.48 (d, $^{2}J_{C,P}$ = 10.0 Hz), 150.19 (d, $^{2}J_{C,P}$ = 9.7 Hz), 137.05, 133.95, 133.51 (d, $^{3}J_{C,P}$ = 3.6 Hz), 130.81 (d, $^{3}J_{C,P}$ = 5.8 Hz), 130.33 (d, $^{3}J_{C,P}$ = 6.5 Hz), 128.92 (d, $^{4}J_{C,P}$ = 1.9 Hz), 128.84, 128.43, 125.81 (d, $^{2}J_{C,P}$ = 9.9 Hz), 120.78 (d, $^{3}J_{C,P}$ = 3.9 Hz), 120.70 (d, $^{3}J_{C,P}$ = 4.2 Hz), 66.72, 52.70 (d, $^{1}J_{C,P}$ = 157.9 Hz). ^{31}P NMR (162 MHz, DMSO-d_6) δ: 14.18. HRMS (ESI+) m/z calc'd for $C_{27}H_{23}ClNO_5P$ $[M+H]^+$: 508.1081, found 508.1096.

Benzyl ((4-bromophenyl)(diphenoxyphosphoryl)methyl)carbamate (185h)

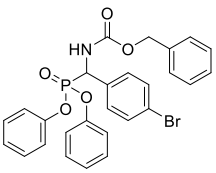

According to general procedure A: 4-bromobenzaldehyde (1.00 g, 5.4 mmol, 1.0 equiv.), $Y(OTf)_3$ (289 mg, 0.54 mmol, 0.1 equiv.), benzyl carbamate (0.82 g, 5.4 mmol, 1.0 equiv.), triphenyl phosphite (1.42 mL, 5.4 mmol, 1.0 equiv.), and MeCN (40 mL). Stirred for 4 h. Method of purification B. Yield of **185h**: 1.61 g (54 %) as an off-white solid. Purity 100 % AN by HPLC. ^{1}H NMR (400 MHz, DMSO-d_6) δ: 8.96 (d, J = 10.1 Hz, 1H), 7.62 (s, 4H), 7.35 (m, 9H), 7.20 (t, J = 8.5 Hz, 2H), 7.07 (d, J = 8.5 Hz, 2H), 7.03 (d, J = 8.5 Hz, 2H), 5.66 (dd, J = 22.3, 10.1 Hz, 1H), 5.12 (dd, J = 33.4, 12.5 Hz, 2H). ^{13}C NMR (101 MHz, DMSO-d_6) δ: 155.97 (d, $^3J_{C,P}$ = 8.4 Hz), 150.02 (d, $^2J_{C,P}$ = 10.0 Hz), 149.73 (d, $^2J_{C,P}$ = 9.6 Hz), 136.59, 133.93, 131.38 (d, $^4J_{C,P}$ = 1.8 Hz), 130.65 (d, $^3J_{C,P}$ = 5.9 Hz), 129.86 (d, $^3J_{C,P}$ = 6.5 Hz), 128.37, 127.96, 125.34 (d, $^2J_{C,P}$ = 10.1 Hz), 121.69, 121.65, 120.32 (d, $^3J_{C,P}$ = 4.0 Hz), 120.25 (d, $^3J_{C,P}$ = 4.2 Hz), 66.26, 52.32 (d, $^1J_{C,P}$ = 157.6 Hz). ^{31}P NMR (162 MHz, DMSO-d_6) δ: 13.70. HRMS (ESI+) m/z calc'd for $C_{27}H_{23}N_2O_7P$ $[M+H]^+$:552.0575, found 552.0582.

Benzyl ((diphenoxyphosphoryl)(4-fluorophenyl)methyl)carbamate (185i)

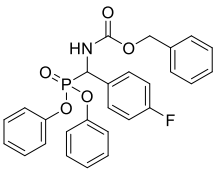

According to general procedure A: 4-fluorobenzaldehyde (1.00 g, 8.1 mmol, 1.0 equiv.), $Y(OTf)_3$ (434 mg, 0.81 mmol, 0.1 equiv.), benzyl carbamate (1.00 g, 8.1 mmol, 1.0 equiv.), triphenyl phosphite (1.73 mL, 8.1 mmol, 1.0 equiv.), and MeCN (40 mL). Stirred for 4 h. Method of purification A. Yield of **185i**: 1.43 g (36 %) as an off-white solid. Purity 100 % AN by HPLC. ^{1}H NMR (400 MHz, DMSO-d_6) δ: 8.92 (d, J = 10.1 Hz, 1H), 7.70 (m, 2H), 7.34 (m, 9H), 7.24 (t, J = 8.5 Hz, 2H), 7.19 (t, J = 8.5 Hz, 2H), 7.06 (d, J = 8.5 Hz, 2H), 6.98 (d, J = 8.5 Hz, 2H) 5.65 (dd, J = 22.3, 10.1 Hz), 5.10 (dd, J = 33.4, 12.5 Hz). ^{13}C NMR (101 MHz, DMSO-d_6) δ: 161.94 (d, $^1J_{C,F}$ = 243.2 Hz), 155.91 (d, $^3J_{C,P}$ = 8.6 Hz), 150.02 (d, $^2J_{C,P}$ = 10.0 Hz), 149.74 (d, $^2J_{C,P}$ = 9.7 Hz), 136.58, 130.72, 130.64, 130.58, 129.81 (d, $^3J_{C,P}$ = 5.0 Hz), 128.33, 127.94, 125.27 (d, $^2J_{C,P}$ = 8.6 Hz), 120.29, 120.22 (d, $^3J_{C,P}$ = 4.4 Hz), 115.29 (dd, $^2J_{C,F}$ = 21.6 Hz, $^4J_{C,P}$ = 1.7 Hz), 66.20, 52.12 (d, $^1J_{C,P}$ = 158.2 Hz). ^{31}P NMR (162 MHz, DMSO-d_6) δ: 14.50. HRMS (ESI+) m/z calc'd for $C_{27}H_{23}FNO_5P$ $[M+H]^+$: 492.1298, found 492.1377.

Benzyl ((diphenoxyphosphoryl)(4-iodophenyl)methyl)carbamate (185j)

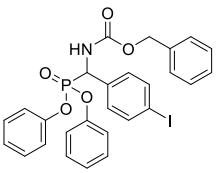

According to general procedure A: 4-iodobenzaldehyde (1.00 g, 4.3 mmol, 1.0 equiv.), $Y(OTf)_3$ (231 mg, 0.43 mmol, 0.1 equiv.), benzyl carbamate (0.65 g, 4.3 mmol, 1.0 equiv.), triphenyl phosphite (1.13 mL, 4.3 mmol, 1.0 equiv.), and MeCN (40 mL). Stirred for 4 h. Method of purification A. Yield of **185j**: 0.71 g (25 %) as a white solid. Purity 91 % AN by HPLC. ^{1}H NMR (400 MHz, DMSO-d_6) δ: 8.86 (d, J = 10.1 Hz, 1H), 7.70 (d, J = 8.5 Hz, 2H), 7.38 (d, J = 8.5 Hz, 2H), 7.26 (m, 9H), 7.12 (t, J = 8.5 Hz, 2H), 6.99 (d, J = 8.5 Hz, 2H), 6.94 (d, J = 8.5 Hz, 2H), 5.53 (dd, J = 22.3, 10.1 Hz, 1H), 5.03 (dd, J = 33.4, 12.5 Hz, 2H).

^{13}C NMR (101 MHz, DMSO-d_6) δ: 155.96 (d, $^{3}J_{C,P}$ = 8.6 Hz), 150.01 (d, $^{2}J_{C,P}$ = 10.0 Hz), 149.72 (d, $^{2}J_{C,P}$ = 9.6 Hz), 137.22, 136.59, 134.29, 130.68 (d, $^{3}J_{C,P}$ = 5.8 Hz), 129.85 (d, $^{3}J_{C,P}$ = 6.7 Hz), 128.36, 127.94, 125.33 (d, $^{2}J_{C,P}$ = 10.6 Hz), 120.33 (d, $^{3}J_{C,P}$ = 4.0 Hz), 120.24 (d, $^{3}J_{C,P}$ = 4.1 Hz), 94.73, 66.25, 52.45 (d, $^{1}J_{C,P}$ = 157.4 Hz). ^{31}P NMR (162 MHz, DMSO-d_6) δ: 13.54. HRMS (ESI+) m/z calc'd for $C_{27}H_{23}INO_5P$ $[M+H]^+$: 600.0437, found 600.0446.

***tert*-Butyl ((diphenoxyphosphoryl)(phenyl)methyl)carbamate (185k)**

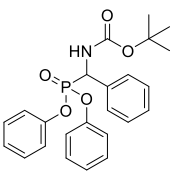

According to general procedure A: benzaldehyde (1.00 g, 9.4 mmol, 1.0 equiv.), Y(OTf)$_3$ (504 mg, 0.94 mmol, 0.1 equiv.), *tert*-butyl carbamate (1.43 g, 9.4 mmol, 1.0 equiv.), triphenyl phosphite (2.47 mL, 9.4 mmol, 1.0 equiv.), and MeCN (28 mL). Stirred for 6 h. Method of purification B. Yield of **185k**: 1.78 g (43 %) as a white solid. Purity 99 % AN by HPLC. ^{1}H NMR (400 MHz, DMSO-d_6) δ: 8.48 (d, J = 10.1 Hz, 1H), 7.63 (d, J = 8.5 Hz, 2H), 7.36 (m, 7H), 7.19 (t, J = 8.5 Hz, 2H), 7.09 (d, J = 8.5 Hz, 2H), 7.00 (d, J = 8.5 Hz, 2H), 5.56 (dd, J = 22.3, 10.3 Hz, 1H), 1.40 (s, 9H). ^{13}C NMR (101 MHz, DMSO-d_6) δ: 155.14 (d, $^{3}J_{C,P}$ = 8.2 Hz), 150.20 (d, $^{2}J_{C,P}$ = 10.0 Hz), 149.86 (d, $^{2}J_{C,P}$ = 9.6 Hz), 134.60, 129.79 (d, $^{3}J_{C,P}$ = 7.5 Hz), 128.60 (d, $^{3}J_{C,P}$ = 6.0 Hz), 128.37 (d, $^{4}J_{C,P}$ = 1.9 Hz), 128.12 (d, $^{4}J_{C,P}$ = 2.8 Hz), 125.20 (d, $^{2}J_{C,P}$ = 11.8 Hz), 120.32 (d, $^{3}J_{C,P}$ = 4.2 Hz), 120.25 (d, $^{3}J_{C,P}$ = 4.2 Hz), 79.11, 52.34 (d, $^{1}J_{C,P}$ = 156.5 Hz), 28.11. ^{31}P NMR (162 MHz, DMSO-d_6) δ: 15.16. HRMS (ESI+) m/z calc'd for $C_{27}H_{23}N_2O_7P$ $[M+H]^+$: 462.1468, found 462.1446.

***tert*-Butyl ((diphenoxyphosphoryl)(4-nitrophenyl)methyl)carbamate (185l)**

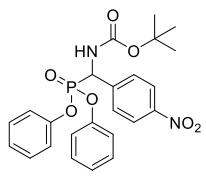

According to general procedure A: 4-nitrobenzaldehyde (1.00 g, 6.6 mmol, 1.0 equiv.), Y(OTf)$_3$ (354 mg, 0.94 mmol, 0.1 equiv.), *tert*-butyl carbamate (0.78 g, 6.6 mmol, 1.0 equiv.), triphenyl phosphite (1.73 mL, 6.6 mmol, 1.0 equiv.), and MeCN (20 mL). Stirred for 4 h. Method of purification B. Yield of **185l**: 1.31 g (41 %) as a pale yellow solid. Purity 87 % AN by HPLC. ^{1}H NMR (400 MHz, DMSO-d_6) δ: 8.67 (d, J = 10.1 Hz, 1H), 8.26 (d, J = 8.5 Hz, 2H), 7.93 (m, 2H), 7.35 (t, J = 8.5 Hz, 4H), 7.19 (m, 2H), 7.08 (m, 4H), 5.78 (dd, J = 22.3, 10.01Hz, 1H), 1.39 (s, 9H). ^{13}C NMR (101 MHz, DMSO-d_6) δ: 156.23, 155.11 (d, $^{3}J_{C,P}$ = 7.9 Hz), 150.03 (d, $^{2}J_{C,P}$ = 9.8 Hz), 149.71 (d, $^{2}J_{C,P}$ = 9.5 Hz), 147.28 (d, $^{3}J_{C,P}$ = 3.5 Hz), 142.37, 129.89 (d, $^{2}J_{C,P}$ = 10.1 Hz), 129.76 (d, $^{3}J_{C,P}$ = 5.5 Hz), 125.40 (d, $^{2}J_{C,P}$ = 12.9 Hz), 123.49 (d, $^{4}J_{C,P}$ = 1.9 Hz), 120.31 (d, $^{3}J_{C,P}$ = 4.0 Hz), 120.23 (d, $^{3}J_{C,P}$ = 4.2 Hz), 79.47, 77.02, 52.08 (d, $^{1}J_{C,P}$ = 155.8 Hz), 28.06. ^{31}P NMR (162 MHz, DMSO-d_6) δ: 13.60 HRMS (ESI+) m/z calc'd for $C_{27}H_{23}N_2O_7P$ [M+Na]+: 507.1311, found 507.1297.

***tert*-Butyl ((diphenoxyphosphoryl)(4-(methylthio)phenyl)methyl)carbamate (185m)**

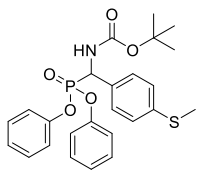

According to general procedure A: 4-(methylthio)benzaldehyde (1.00 g, 6.6 mmol, 1.0 equiv.), $Y(OTf)_3$ (354 mg, 0.94 mmol, 0.1 equiv.), *tert*-butyl carbamate (0.78 g, 6.6 mmol, 1.0 equiv.), triphenyl phosphite (1.73 mL, 6.6 mmol, 1.0 equiv.), and MeCN (20 mL). Stirred for 24 h. Method of purification B. Stirred for 24 h. Yield of **185m**: 0.54 g (17 %) as an off-white solid. Purity 72 % AN by HPLC. ^{1}H NMR (400 MHz, DMSO-d_6) δ: 8.44 (d, J = 10.1 Hz, 1H), 7.57 (dd, J = 8.5, 1.9 Hz, 2H), 7.37 (td, J = 8.5, 2.2 Hz, 4H), 7.28 (d, J = 8.5 Hz, 2H), 7.20 (t, J = 8.5 Hz, 2H), 7.10 (d, J = 8.5 Hz, 2H), 7.04 (d, J = 8.5 Hz, 2H), 5.50 (dd, J = 22.3, 10.1 Hz, 1H), 2.48 (s, 3H), 1.40 (s, 9H). ^{13}C NMR (101 MHz, DMSO-d_6) δ: 155.11 (d, $^3J_{C,P}$ = 8.6 Hz), 150.20 (d, $^2J_{C,P}$ = 10.0 Hz), 149.86 (d, $^2J_{C,P}$ = 9.6 Hz), 138.33 (d, $^3J_{C,P}$ = 3.3 Hz), 131.06, 129.82 (d, $^3J_{C,P}$ = 8.8 Hz), 129.11 (d, $^3J_{C,P}$ = 6.0 Hz), 125.72, 125.70, 125.22 (d, $^2J_{C,P}$ = 13.3 Hz), 120.35 (d, $^3J_{C,P}$ = 4.0 Hz), 120.25 (d, $^3J_{C,P}$ = 4.2 Hz), 79.14, 51.88 (d, $^1J_{C,P}$ = 157.4 Hz), 28.11, 14.58. ^{31}P NMR (162 MHz, DMSO-d_6) δ: 15.49 HRMS (ESI+) m/z calc'd for $C_{27}H_{23}N_2O_7P$ [M+Na]+: 508.1333, found 508.1323.

Benzyl ((diphenoxyphosphoryl)(4-nitrophenyl)methyl)carbamate (185n)

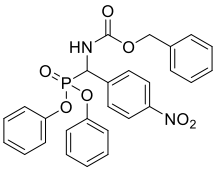

According to general procedure A: 4-nitrobenzaldehyde (1.00 g, 6.6 mmol, 1.0 equiv.), $Y(OTf)_3$ (354 mg, 0.66 mmol, 0.1 equiv.), benzyl carbamate (1.00 g, 6.6 mmol, 1.0 equiv.), triphenyl phosphite (1.73 mL, 6.6 mmol, 1.0 equiv.), and MeCN (20 mL). Stirred for 4 h. Purification method A. Yield of **185n**: 2.19 g (64 %) as a pale yellow solid. Purity 100 % AN by HPLC. ^{1}H NMR (400 MHz, DMSO-d_6) δ: 9.11 (d, J = 10.1 Hz, 1H), 8.28 (d, J = 8.5 Hz, 2H), 7.96 (d, J = 8.5 Hz, 2H), 7.36 (m, 9H), 7.20 (t, J = 8.5 Hz, 2H), 7.05 (m, 4H), 5.88 (dd, J = 22.3, 10.1 Hz, 1H), 5.12 (dd, J = 33.4, 12.5 Hz, 2H). ^{13}C NMR (101 MHz, DMSO-d_6) δ: 155.99 (d, $^3J_{C,P}$ = 8.7 Hz), 149.92 (d, $^2J_{C,P}$ = 9.9 Hz), 149.64 (d, $^2J_{C,P}$ = 9.6 Hz), 147.34 (d, $^3J_{C,P}$ = 3.4 Hz), 142.10, 136.52, 129.91 (d, $^3J_{C,P}$ = 7.8 Hz), 129.72 (d, $^3J_{C,P}$ = 5.5 Hz), 128.39, 128.00, 125.45 (d, $^2J_{C,P}$ = 10.5 Hz), 123.55 (d, $^4J_{C,P}$ = 2.0 Hz), 120.33 (d, $^3J_{C,P}$ = 4.0 Hz), 120.24 (d, $^3J_{C,P}$ = 4.2 Hz), 66.38, 52.57 (d, $^1J_{C,P}$ = 155.9 Hz). ^{31}P NMR (162 MHz, DMSO-d_6) δ: 12.90. HRMS (ESI+) m/z calc'd for $C_{27}H_{23}N_2O_7P$ $[M+H]^+$: 519.1321, found 519.1325.

Benzyl ((bis(*o*-tolyloxy)phosphoryl)(phenyl)methyl)carbamate (185o)

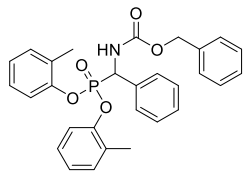

According to general procedure A: benzaldehyde (0.80 mL, 7.5 mmol, 1.0 equiv.), $Y(OTf)_3$ (402 mg, 7.5 mmol, 0.1 equiv.), benzyl carbamate (1.13 g, 7.5 mmol, 1.0 equiv.), tri-*o*-tolyl phosphite (2.33 mL, 7.5 mmol, 1.0 equiv.), and MeCN (22 mL). Purification method B. Yield **185o**: 1.28 g (34 %). Purity 100 % AN by HPLC. ^{1}H NMR (400 MHz, DMSO-d_6) δ: 8.92 (d, J = 10.1 Hz, 1H), 7.63 (d, J = 8.5 Hz, 2H), 7.36 (m, 8H), 7.18 (m, 2H), 7.05 (m, 6H), 5.64 (dd, J = 22.3 10.1 Hz, 1H), 5.06 (dd, J = 33.4, 12.5 Hz, 1H), 1.98

(d, J = 22.2 Hz, 6H). ^{13}C NMR (101 MHz, DMSO-d_6) δ: 156.03 (d, $^3J_{C,P}$ = 9.1 Hz), 148.72 (d, $^2J_{C,P}$ = 8.4 Hz), 148.63 (d, $^2J_{C,P}$ = 8.0 Hz), 136.61, 134.57, 131.35 (d, $^3J_{C,P}$ = 3.8 Hz), 129.01, 128.96, 128.91, 128.61 (d, $^3J_{C,P}$ = 5.8 Hz), 128.39, 128.34, 128.25, 127.93, 127.86, 126.94 (d, $^2J_{C,P}$ = 11.0 Hz), 125.06 (d, $^3J_{C,P}$ = 3.8 Hz), 119.92 (d, $^4J_{C,P}$ = 1.8 Hz), 119.69 (d, $^4J_{C,P}$ = 1.2 Hz), 66.16, 53.09 (d, $^1J_{C,P}$ = 158.0 Hz), 15.68. ^{31}P NMR (162 MHz, DMSO-d_6) δ: 15.28. HRMS (ESI+) m/z calc'd for $C_{27}H_{23}N_2O_7P$ $[M+H]^+$: 502.1795, found 502.1783.

Benzyl ((bis(*o*-tolyloxy)phosphoryl)(4-chlorophenyl)methyl)carbamate (185p)

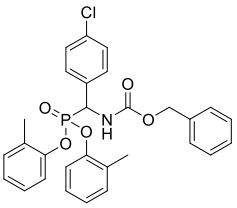

According to general procedure A: 4-chlorobenzaldehyde (1.00 g, 7.1 mmol, 1.0 equiv.), Y(OTf)$_3$ (381 mg, 0.71 mmol, 0.1 equiv.), benzyl carbamate (1.07 g, 7.1 mmol, 1.0 equiv.), tri-*o*-tolyl phosphite (2.19 mL, 7.1 mmol, 1.0 equiv.), and MeCN (21 mL). Stirred for 8 h. Method of purification B. Yield of **185p**: 0.99 g (26 %). Purity 100 % AN by HPLC. ^{1}H NMR (400 MHz, DMSO-d_6) δ: 8.95 (d, J = 10.1 Hz, 1H), 7.68 (dd, J = 8.5, 2.0 Hz, 2H), 7.49 (d, J = 8.5 Hz, 2H), 7.34 (m, 5H), 7.22 (d, J = 8.5 Hz, 2H), 7.08 (m, 6H), 5.70 (dd, J = 22.3, 10.1 Hz, 1H), 5.08 (dd, J = 33.4, 12.5 Hz, 2H), 2.00 (d, J = 14.9 Hz, 6H). ^{13}C NMR (101 MHz, DMSO-d_6) δ: 156.44 (d, $^3J_{C,P}$ = 8.9 Hz), 149.11 (d, $^2J_{C,P}$ = 5.1 Hz), 149.01 (d, $^2J_{C,P}$ = 4.9 Hz), 137.01, 134.18, 133.52 (d, $^3J_{C,P}$ = 3.6 Hz), 131.85 (d, $^3J_{C,P}$ = 4.4 Hz), 130.89 (d, $^3J_{C,P}$ = 5.8 Hz), 129.45 (d, $^3J_{C,P}$ = 5.3 Hz), 129.37 (d, $^3J_{C,P}$ = 5.4 Hz), 128.87 (d, $^3J_{C,P}$ = 1.8 Hz), 128.81, 128.42, 128.34, 127.44 (d, $^2J_{C,P}$ = 11.4 Hz), 125.62, 120.41 (d, $^4J_{C,P}$ = 2.3 Hz), 120.16 (d, $^4J_{C,P}$ = 1.7 Hz), 66.69, 52.91 (d, $^1J_{C,P}$ = 158.1 Hz), 16.09. ^{31}P NMR (162 MHz, DMSO-d_6) δ: 14.22. HRMS (ESI+) m/z calc'd for $C_{29}H_{27}ClNO_5P$ $[M+H]^+$: 536.1394, found 536.1395.

Benzyl ((bis(*p*-tolyloxy)phosphoryl)(4-chlorophenyl)methyl)carbamate (185q)

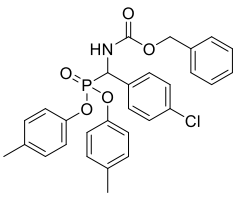

According to general procedure A: 4-chlorobenzaldehyde (1.00 g, 7.1 mmol, 1.0 equiv.), Y(OTf)$_3$ (381 mg, 0.71 mmol, 0.1 equiv.), benzyl carbamate (1.07 g, 7.1 mmol, 1.0 equiv.), tri-*p*-tolyl phosphite (2.22 mL, 7.1 mmol, 1.0 equiv.), and MeCN (21 mL). Stirred for 8 h. Method of purification A. Yield of **185q**: 1.62 g (43 %). Purity 100 % AN by HPLC. ^{1}H NMR (400 MHz, DMSO-d_6) δ: 8.90 (d, J = 10.1 Hz, 1H), 7.65 (d, J = 8.5 Hz, 2H), 7.47 (d, J = 8.5 Hz, 2H), 7.36 (m, 6H), 7.12 (d, J = 8.5 Hz, 4H), 6.93 (d, J = 8.5 Hz, 2H), 6.87 (d, J = 8.5 Hz, 2H), 5.59 (dd, J = 22.3, 10.1 Hz, 1H), 5.09 (dd, J = 33.4, 12.5 Hz, 2H), 2.25 (s, 6H). ^{13}C NMR (101 MHz, DMSO-d_6) δ: 155.94 (d, $^3J_{C,P}$ = 8.8 Hz), 147.88 (d, $^2J_{C,P}$ = 9.8 Hz), 147.58 (d, $^2J_{C,P}$ = 9.7 Hz), 136.60, 134.45 (d, $^2J_{C,P}$ = 12.2 Hz), 133.63, 132.99 (d, $^3J_{C,P}$ = 3.5 Hz), 130.32 (d, $^3J_{C,P}$ = 5.6 Hz), 130.10 (d, $^3J_{C,P}$ = 6.7 Hz), 128.42 (d, $^4J_{C,P}$ = 1.4 Hz), 128.36, 127.95, 120.02, 119.94 (d, $^3J_{C,P}$ = 4.2 Hz), 66.23, 52.16 (d, $^1J_{C,P}$ = 157.2 Hz), 20.24. ^{31}P NMR (162 MHz, DMSO-d_6) δ: 13.54. HRMS (ESI+) m/z calc'd for $C_{29}H_{27}ClNO_5P$ $[M+H]^+$: 536.1394, found 536.1395.

Benzyl ((bis(4-methoxyphenoxy)phosphoryl)(4-chlorophenyl)methyl)carbamate (185r)

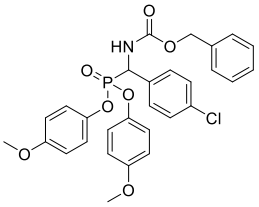

According to general procedure A: 4-chlorobenzaldehyde (0.50 g, 3.6 mmol, 1.0 equiv.), $Y(OTf)_3$ (193 mg, 0.36 mmol, 0.1 equiv.), benzyl carbamate (0.54 g, 3.6 mmol, 1.0 equiv.), tris(4-methoxyphenyl) phosphite (1.44 g, 3.6 mmol, 1.0 equiv.), and MeCN (11 mL). Stirred for 4 h. Method of purification B. Yield of **185r**: 1.65 g (81 %) of a white solid. ^{1}H NMR (400 MHz, DMSO-d_6) δ: 8.89 (d, J = 10.1 Hz, 1H), 7.64 (dd, J = 8.5, 1.8 Hz, 2H), 7.46 (d, J = 8.5 Hz, 2H), 7.35 (m, 5H), 6.95 (dd, J = 8.5, 0.9 Hz, 2H), 6.87 (m, 6H), 5.58 (dd, J = 22.3, 10.1 Hz, 1H), 5.10 (dd, J = 33.4, 12.5 Hz, 2H), 3.70 (s, 6H). ^{13}C NMR (101 MHz, DMSO-d_6) δ: 156.42 (d, $^3J_{C,P}$ = 7.3 Hz), 155.96 (d, $^2J_{C,P}$ = 8.6 Hz), 143.48 (d, $^2J_{C,P}$ = 10.0 Hz), 143.14 (d, $^3J_{C,P}$ = 9.7 Hz), 136.61, 133.69, 132.97 (d, $^3J_{C,P}$ = 3.5 Hz), 130.30 (d, $^3J_{C,P}$ = 5.9 Hz), 128.42 (d, $^4J_{C,P}$ = 1.8 Hz), 128.37, 127.99, 121.21 (d, $^3J_{C,P}$ = 3.7 Hz), 121.13 (d, $^3J_{C,P}$ = 3.9 Hz), 114.68 (d, $^2J_{C,P}$ = 7.1 Hz), 66.24, 55.45, 52.05 (d, $^1J_{C,P}$ = 157.3 Hz). ^{31}P NMR (162 MHz, DMSO-d_6) δ: 14.16. HRMS (ESI+) m/z calc'd for $C_{29}H_{27}ClNO_7P$ $[M+H]^+$: 568.1292, found 568.1302.

Benzyl ((4-cyanophenyl)(diphenoxyphosphoryl)methyl)carbamate (185s)

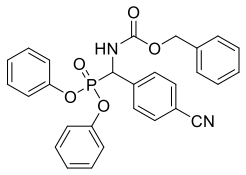

According to general procedure A: 4-cianobenzaldehyde (1.00 g, 7.6 mmol, 1.0 equiv.), $Y(OTf)_3$ (407 mg, 0.76 mmol, 0.1 equiv.), benzyl carbamate (1.15 g, 7.6 mmol, 1.0 equiv.), triphenyl phosphite (2.00 mL, 7.6 mmol, 1.0 equiv.), and MeCN (22 mL). Stirred for 6 h. Purification method B. Yield of **185s**: 2.54 g (67 %) as a white solid. Purity 93 % AN by HPLC. ^{1}H NMR (400 MHz, DMSO-d_6) δ: 9.07 (d, J = 12.0 Hz, 1H), 7.90 (m, 4H), 7.35 (m, 9H), 7.21 (t, J = 8.5 Hz, 2H), 7.05 (m, 4H), 5.83 (dd, J = 22.3, 10.1 Hz, 1H), 5.13 (dd, J = 33.4, 12.5 Hz, 2H). ^{13}C NMR (101 MHz, DMSO-d_6) δ: 155.98 (d, $^3J_{C,P}$ = 8.6 Hz), 149.96 (d, $^2J_{C,P}$ = 9.9 Hz), 149.68 (d, $^2J_{C,P}$ = 9.6 Hz), 140.07, 136.53, 132.38 (d, $^4J_{C,P}$ = 2.0 Hz), 129.89 (d, $^3J_{C,P}$ = 7.3 Hz), 129.40 (d, $^3J_{C,P}$ = 6.0 Hz), 128.38, 128.00, 125.43 (d, $^2J_{C,P}$ = 9.9 Hz), 120.30 (d, $^3J_{C,P}$ = 4.0 Hz), 120.23 (d, $^3J_{C,P}$ = 4.2 Hz), 118.59, 118.57, 115.23, 111.10 (d, $^3J_{C,P}$ = 3.2 Hz), 66.37, 52.74 (d, $^1J_{C,P}$ = 156.1 Hz). ^{31}P NMR (162 MHz, DMSO-d_6) δ: 13.45 HRMS (ESI+) m/z calc'd for $C_{27}H_{23}N_2O_7P$ $[M+H]^+$: 499.1428, found 499.1423.

Benzyl ((bis(*p*-tolyloxy)phosphoryl)(4-cyanophenyl)methyl)carbamate (185t)

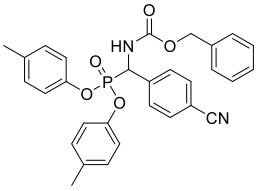

According to general procedure A: 4-cianobenzaldehyde (1.00 g, 7.6 mmol, 1.0 equiv.), $Y(OTf)_3$ (407 mg, 0.76 mmol, 0.1 equiv.), benzyl carbamate (1.15 g, 7.6 mmol, 1.0 equiv.), tri-*p*-tolyl phosphite (2.37 mL, 7.6 mmol, 1.0 equiv.), and MeCN (22 mL). Stirred for 6 h. Purification method B. Yield of **185t**: 2.71 g (63 %) as a white solid. ^{1}H NMR (400 MHz, DMSO-d_6) δ: 9.00 (d, J = 10.1 Hz, 1H), 7.87 (m, 4H), 7.35 (m, 5H), 7.13 (m, 4H), 6.91 (m, 4H), 5.74 (dd, J = 22.3, 10.1 Hz, 1H), 5.10 (dd, J = 33.4,

12.5 Hz, 2H), 2.24 (s, 6H). ^{13}C NMR (101 MHz, DMSO-d_6) δ: 155.95 (d, $^{3}J_{C,P}$ = 8.7 Hz), 147.81 (d, $^{2}J_{C,P}$ = 9.8 Hz), 147.52 (d, $^{2}J_{C,P}$ = 9.6 Hz), 140.21, 136.54, 134.55 (d, $^{3}J_{C,P}$ = 11.7 Hz), 132.35 (d, $^{4}J_{C,P}$ = 1.8 Hz), 130.14 (d, $^{3}J_{C,P}$ = 7.7 Hz), 129.36 (d, $^{3}J_{C,P}$ = 5.5 Hz), 128.38, 127.99, 119.98 (d, $^{3}J_{C,P}$ = 4.1 Hz), 119.92 (d, $^{3}J_{C,P}$ = 4.2 Hz), 118.59, 115.01, 111.04, 111.01, 66.33, 52.66 (d, $^{3}J_{C,P}$ = 155.8 Hz), 20.23. ^{31}P NMR (162 MHz, DMSO-d_6) δ: 13.46. HRMS (ESI+) m/z calc'd for $C_{27}H_{23}N_2O_7P$ $[M+H]^+$: 527.1742, found 527.1736.

Benzyl ((diphenoxyphosphoryl)(4-hydroxy-3-methoxyphenyl)methyl)carbamate (185u)

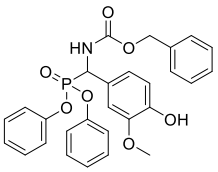

According to general procedure A: vanillin (1.00 g, 6.6 mmol, 1.0 equiv.), $Y(OTf)_3$ (354 mg, 0.66 mmol, 0.1 equiv.), benzyl carbamate (1.00 g, 6.6 mmol, 1.0 equiv.), triphenyl phosphite (1.72 mL, 6.6 mmol, 1.0 equiv.), and MeCN (20 mL). Stirred for 6 h. Purification method B. Yield of **185u**: 2.57 g (75 %) as a white solid. Purity 98 % AN by HPLC. ^{1}H NMR (400 MHz, DMSO-d_6) δ: 9.11 (s, 1H), 8.76 (d, J = 10.1 Hz, 1H), 7.34 (m, 9H), 7.24 (m, 1H), 7.19 (m, 2H), 7.07 (d, J = 8.5 Hz, 2H), 6.76 (d, J = 8.5 Hz, 1H), 5.47 (dd, J = 22.3, 10.1 Hz, 1H), 5.10 (dd, J = 33.4, 12.5 Hz, 2H), 3.73 (s, 3H). ^{13}C NMR (101 MHz, DMSO-d_6) δ: 155.90 (d, $^{3}J_{C,P}$ = 8.1 Hz), 150.24 (d, $^{2}J_{C,P}$ = 10.1 Hz), 149.95 (d, $^{2}J_{C,P}$ = 9.8 Hz), 147.46 (d, $^{4}J_{C,P}$ = 2.0 Hz), 146.63 (d, $^{4}J_{C,P}$ = 2.8 Hz), 136.71, 129.80 (d, $^{3}J_{C,P}$ = 4.2 Hz), 128.37, 127.96, 125.17 (d, $^{2}J_{C,P}$ = 9.0 Hz), 124.66, 121.42 (d, $^{3}J_{C,P}$ = 7.1 Hz), 120.33 (d, $^{3}J_{C,P}$ = 4.0 Hz), 120.25 (d, $^{3}J_{C,P}$ = 4.1 Hz), 115.20, 112.86 (d, $^{3}J_{C,P}$ = 5.6 Hz), 66.13, 55.70, 52.65 (d, $^{1}J_{C,P}$ = 159.2 Hz). ^{31}P NMR (162 MHz, DMSO-d_6) δ: 15.18. HRMS (ESI+) m/z calc'd for $C_{27}H_{23}N_2O_7P$ $[M+H]^+$: 520.1528, found 520.1525.

Methyl 4-((((benzyloxy)carbonyl)amino)(diphenoxyphosphoryl)methyl)benzoate (185v)

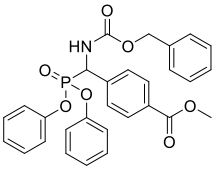

According to general procedure A: methyl 4-formylbenzoate (1.00 g, 6.1 mmol, 1.0 equiv.), $Y(OTf)_3$ (327 mg, 0.61 mmol, 0.1 equiv.), benzyl carbamate (0.92 g, 6.1 mmol, 1.0 equiv.), triphenyl phosphite (1.60 mL, 6.1 mmol, 1.0 equiv.), and MeCN (20 mL). Stirred for 4 h. Method of purification B. Yield of **185v**: 2.60 g (69 %) as a white solid. Purity 86 % AN by HPLC. ^{1}H NMR (400 MHz, DMSO-d_6) δ: 9.03 (d, J = 10.1 Hz, 1H), 7.97 (d, J = 8.5 Hz, 2H), 7.79 (d, J = 8.5 Hz, 2H), 7.32 (m, 9H), 7.17 (t, J = 8.5 Hz, 2H), 7.02 (dd, J = 21.5, 8.5 Hz, 4H), 5.73 (dd, J = 22.3, 10.1 Hz, 1H), 5.09 (dd, J = 33.4, 12.5 Hz, 2H), 3.84 (s, 3H). ^{13}C NMR (101 MHz, DMSO-d_6) δ: 165.88, 156.02 (d, $^{3}J_{C,P}$ = 8.4 Hz), 150.00 (d, $^{2}J_{C,P}$ = 9.9 Hz), 149.70 (d, $^{2}J_{C,P}$ = 9.7 Hz), 139.77, 136.58, 129.88 (d, $^{3}J_{C,P}$ = 7.2 Hz), 129.44 (d, $^{4}J_{C,P}$ = 2.9 Hz), 129.23 (d, $^{4}J_{C,P}$ = 1.7 Hz), 128.81 (d, $^{3}J_{C,P}$ = 5.6 Hz), 128.38, 127.97, 125.38 (d, $^{2}J_{C,P}$ = 10.3 Hz), 120.32 (d, $^{3}J_{C,P}$ = 4.0 Hz), 120.25 (d, $^{3}J_{C,P}$ = 4.2 Hz), 66.31, 52.78 (d, $^{1}J_{C,P}$ = 156.1 Hz), 52.23. ^{31}P NMR (162 MHz, DMSO-d_6) δ: 13.50. HRMS (ESI+) m/z calc'd for $C_{29}H_{26}NO_7P$ $[M+H]^+$: 532.1525, found 532.1506.

4.4 Compounds synthesized for the preparation of UAMC-0004206

Benzyl ((bis(4-acetamidophenoxy)phosphoryl)(4-((*tert*-butoxycarbonyl)amino)phenyl)-methyl) carbamate (193)

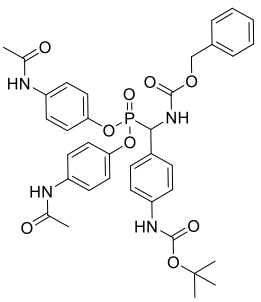

In an oven-dried 100 mL flask equipped with a magnetic stirrer bar were added: aldehyde **192** (5.00 g, 0.023 mol, 1.0 equiv.), $Y(OTf)_3$ (1.23 g, 2.3 mmol, 0.1 equiv.), anhydrous MeCN (17 mL), benzyl carbamate (**8**) (3.48 g, 0.023 mol, 1.0 equiv.), phosphite **3** (11.07 g, 0.023 mol, 1.0 equiv.) and anhydrous THF (17 mL). The solution was stirred for 4 h. Volatiles were removed in vacuo, the residue was dissolved in 96 % EtOH (200 mL) and the solution was added dropwise to stirred EtOAc (500 mL) and stirred for 2 h at 0 °C. The solid was collected by filtration, dried in the vacuum (5 mbar) for 16 h. Yield of **193**: 11.70 g (63 %) as a pale yellow solid. Purity 87 % AN by HPLC. ^{1}H NMR (400 MHz, DMSO-d_6) δ: 9.97 (s, 2H), 9.41 (s, 1H), 8.78 (d, J = 10.1 Hz, 1H), 7.49 (m, 8H), 7.33 (m, 5H), 6.98 (d, J = 9.1 Hz, 2H), 6.90 (d, J = 9.1 Hz, 2H), 5.45 (dd, J = 22.3, 10.1 Hz, 1H), 5.08 (dd, J = 33.4, 12.5 Hz, 2H), 2.02 (d, J = 2.5 Hz, 6H), 1.47 (s, 9H). ^{13}C NMR (101 MHz, DMSO-d_6) δ: 168.19, 155.94, 152.73, 145.28, 144.95, 139.51, 136.67, 136.48, 128.91, 128.36, 127.92, 127.72, 120.53, 120.42, 120.07, 117.92, 79.18, 66.16, 52.15, 28.11, 23.90. ^{31}P NMR (162 MHz, DMSO-d_6) δ: 15.23 HRMS (ESI+) m/z calc'd for $C_{36}H_{39}N_4O_9PNa$ $[M+Na]^+$: 725.2336, found 725.2352

4-((((Benzyloxy)carbonyl)amino)(bis(4-acetamidophenoxy)phosphoryl)methyl)benzenaminium trifluoroacetate (194)

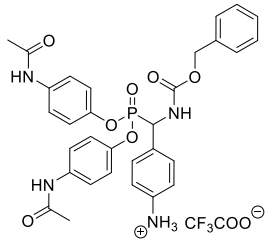

In a 250 mL flask equipped with a magnetic stirrer, were added the Boc-protected intermediate **193** (6.60 g, 8.2 mmol, 1.0 equiv.) and DCM (33 mL) and TFA (33 mL). The mixture was stirred for 45 minutes at 20-25 °C. Volatiles removed in vacuo, and the residue was dissolved in absolute EtOH (66 mL). The solution was added dropwise to stirred MTBE (660 mL) at 0 °C and stirred at 0 °C for 2 h. The solid was collected by filtration, washed with MTBE (330 mL) and dried in vacuo (5 mbar) for 16 h. Yield of **194**: 6.01 g (99 %) as a yellow solid. Purity 97 % AN by HPLC. ^{1}H NMR (400 MHz, DMSO-d_6) δ: 10.13 (s, 2H), 8.94 (d, J = 10.1 Hz, 1H), 7.74 (d, J = 9.1 Hz, 2H), 7.56 (m, 4H), 7.37 (m, 6H), 6.98 (d, J = 9.1 Hz, 2H), 6.91 (d, J = 9.1 Hz, 2H), 5.61 (dd, J = 22.3, 10.1 Hz, 1H), 5.10 (dd, J = 33.4, 12.5 Hz, 2H), 2.04 (d, J = 2.5 Hz, 6H). ^{13}C NMR (101 MHz, DMSO-d_6) δ: 168.73, 158.79, 156.43, 145.58, 145.27, 137.10, 137.04, 134.75, 132.70, 130.23,

128.84, 128.43, 123.60, 120.94, 120.85, 120.60, 66.76, 52.76, 24.35. ^{31}P NMR (162 MHz, DMSO-d_6) δ: 14.69. HRMS (ESI+) m/z calc'd for $C_{31}H_{31}N_4O_7PNa$ $[M+Na]^+$: 625.1828, found 625.1841.

Benzyl (*E*)-((bis(4-acetamidophenoxy)phosphoryl)(4-(*N*,*N*'-bis(*tert*-butyloxycarbonyl)guanidino)phenyl)methyl)carbamate (196)

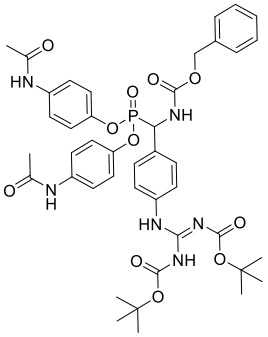

In an oven-dried 50 mL flask equipped with a magnetic stirrer, were added: aniline **194** (7.31 g, 10.2 mmol, 1.0 equiv.), *N*,*N*'- bis(*tert*-butyloxycarbonyl-1-guanyl-pyrazole (**11**) (3.79 g, 12.2 mmol, 1.2 equiv.), anhydrous DCM/anhydrous MeCN (1:1 v/v) (10.2 mL), and TEA (2.13 mL, 15.3 mmol, 1.5 equiv.). The solution was stirred at 20-25 °C for 168 hours, then volatiles were removed in vacuo. The crude material was slurried in heptane/EtOAc 2:1 v/v (150 mL) and stirred for 2 h at 20-25 °C, the solid was collected by filtration, washed with a mixture heptane/EtOAc 2:1 v/v (75 mL) and dried in vacuum (5 mbar) for 16 h. The product was purified by flash chromatography on silica (eluent DCM/MeOH 20 - 100 %). The selected tubes were collected and volatiles were removed by vacuo. Yield of **196**: 6.31 g (71 %) as a white solid. Purity 97 % AN by HPLC. ^{1}H NMR (400 MHz, DMSO-d_6) δ: 11.41 (s, 1H), 10.03 (s, 1H), 9.96 (s, 2H), 8.84 (d, *J* = 10.1 Hz, 1H), 7.58 (s, 4H), 7.51 (m, 4H), 7.35 (m, 5H), 6.98 (d, *J* = 9.1 Hz, 2H), 6.91 (d, *J* = 9.1 Hz, 2H), 5.54 (dd, *J* = 22.3, 10.1 Hz, 1H), 5.10 (dd, *J* = 33.4, 12.5 Hz, 2H), 2.02 (d, *J* = 2.5 Hz, 6H), 1.51 (s, 9H), 1.40 (s, 9H). ^{13}C NMR (101 MHz, DMSO-d_6) δ: 168.65, 163.08, 156.44, 153.23, 152.54, 145.70, 145.37, 137.10, 136.98, 131.27, 129.25, 128.83, 128.44, 123.10, 121.03, 120.91, 120.57, 83.86, 79.37, 66.70, 28.24, 24.36. ^{31}P NMR (162 MHz, DMSO-d_6) δ: 14.93. HRMS (ESI+) m/z calc'd for $C_{42}H_{50}N_6O_{11}P$ $[M+H]^+$: 845.3290, found 845.3275.

Amino((4-((((benzyloxy)carbonyl)amino)(bis(4-acetamidophenoxy)phosphoryl)methyl)-phenyl) amino)methaniminium trifluoroacetate (197)

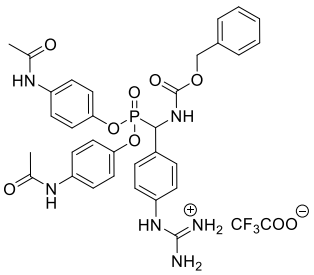

In a 50 mL flask equipped with a magnetic stirrer, were added the intermediate **196** (1.94 g, 2.3 mmol, 1.0 equiv.) and DCM (9 mL) and TFA (9 mL). The solution was stirred for at 20-25 °C for 3 h. Volatiles were removed in vacuo and the residue was dissolved in absolute EtOH (18 mL). The solution was added dropwise to stirred MTBE (180 mL) at 0 °C and stirred 1 h at 0 °C. The solid was collected by filtration and dried in vacuo (5 mbar) for 16 h. Yield of **197**: 1.77 g (97 %) as an off-white solid. Purity 96 % AN by HPLC. ^{1}H NMR (400 MHz, DMSO-d_6) δ: 10.08 (s, 1H), 10.02 (s, 1H), 8.93 (d, *J* = 10.1 Hz, 2H), 7.69 (m, 5H), 7.54 (d, *J* = 9.1 Hz, 4H), 7.43 (d, *J* = 9.1 Hz, 4H), 7.36 (m, 5H), 7.28 (d, *J* = 9.1 Hz, 2H), 7.00 (d, *J* = 9.1 Hz, 2H), 6.96 (d, *J* = 9.1 Hz, 2H), 5.58 (dd, *J* = 22.3, 10.1 Hz, 1H), 5.09 (dd, *J* = 33.4, 12.5 Hz, 2H), 2.03 (d, *J* = 2.5 Hz, 6H). ^{13}C NMR (101 MHz, DMSO-d_6) δ: 168.29,

159.27, 156.01, 155.81, 145.27, 144.92, 136.66, 136.63, 136.57, 135.58, 132.45, 129.84, 128.42, 128.06, 123.99, 120.61, 120.47, 120.18, 66.30, 52.25, 23.91. ^{31}P NMR (162 MHz, DMSO-d_6) δ: 14.65 HRMS (ESI+) m/z calc'd for $C_{32}H_{34}N_6O_7P$ $[M+H]^+$: 645.2258, found 645.2227.

Amino((4-((((benzyloxy)carbonyl)amino)(bis(4-acetamidophenoxy)phosphoryl)methyl)-phenyl)amino)methaniminium chloride (14)

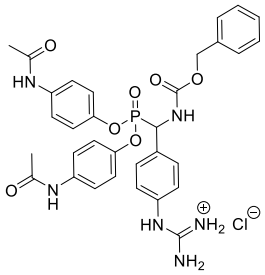

In a 250 mL flask equipped with a magnetic stirrer, were added: trifluoroacetate salt (2.25 g, 2.9 mmol, 1.0 equiv.) EtOH/H_2O 2:1 v/v (68 mL) and DOWEX 1X8 Cl (22.5 g), the mixture was stirred at 20-25 °C for 32 h. The resin was filtered off and volatiles were removed in vacuo. The residue was dissolved in absolute EtOH (22.5 mL) and added dropwise to stirred MTBE (225 mL) at 20-25 °C. The mixture was stirred for 1 h and the solid was collected by filtration. The solid was dried in vacuo (5 mbar) for 16 h. Yield of **14**: 1.38 g (71 %) as an off-white solid. Purity 97.7 % AN by HPLC. ^{1}H NMR (400 MHz, DMSO-d_6) δ: 10.09 (s, 2H), 10.03 (s, 1H), 8.92 (d, J = 10.1 Hz, 1H), 7.67 (dd, J = 9.1, 1.7 Hz, 2H), 7.55 (m, 8H), 7.34 (m, 5H), 7.26 (d, J = 9.1 Hz, 2H), 6.99 (d, J = 9.1 Hz, 2H), 6.94 (d, J = 9.1 Hz, 2H), 5.57 (dd, J = 22.3, 10.1 Hz, 1H), 5.08 (dd, J = 33.4, 12.5 Hz, 2H), 2.03 (d, J = 2.5 Hz, 6H). ^{13}C NMR (101 MHz, DMSO-d_6) δ: 168.72, 156.32, 145.65, 145.33, 137.10, 137.06, 137.02, 135.83, 132.91, 130.26, 128.86, 128.49, 124.37, 121.01, 120.87, 120.59, 66.72, 52.76, 24.36. ^{31}P NMR (162 MHz, DMSO-d_6) δ: 14.63 HRMS (ESI+) m/z calc'd for $C_{32}H_{34}N_6O_7P$ $[M+H]^+$: 645.2258, found 645.2227.

4.5 Compounds synthesized for the preparation of UAMC-0004207

Tris(4-chlorophenyl)phosphite (205)

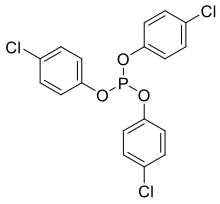

In an oven-dried 250 mL Schlenk flask equipped with a magnetic stirrer, under argon, were added: 4-chlorophenol (**204**) (10.00 g, 0.078 mol, 3.0 equiv.) and anhydrous THF (100 mL). The solution was cooled to 0 °C in an ice bath, then TEA (10.87 mL, 0.078 mol, 3.0 equiv.) was added followed by PCl_3 (2.26 mL, 0.026 mol, 1.0 equiv.) added dropwise over 10 minutes. The mixture was stirred at 0 °C for 1 h. The solid was filtered off and the filter cake was washed with anhydrous THF (50 mL). Volatiles were removed in vacuo at room temperature (*no heating*). Once the solid was formed it was further kept under vacuo (5 mbar) for 6 h. Yield of **205**: 10.47 g (80 %) of a white solid. Purity 82 % AN by HPLC. ^{1}H NMR (400 MHz, DMSO-d_6) δ: 7.50 (m, 6H), 7.33 (m, 6H). ^{13}C NMR (101 MHz, DMSO-d_6) δ: 148.41, 130.30, 130.15, 121.78. ^{31}P NMR (162 MHz, DMSO-d_6) δ: -17.67 HRMS (ESI+) m/z calc'd for $C_{18}H_{13}Cl_3O_3P$ $[M+H]^+$:412.9668, found 412.9658.

Benzyl ((bis(4-chlorophenoxy)phosphoryl)(4-((tert butoxycarbonyl)amino)phenyl)-methyl) carbamate (206)

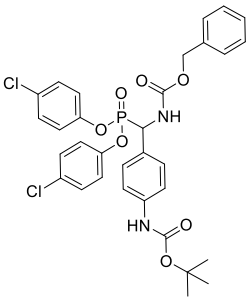

In a dry 50 mL flask equipped with a magnetic stirrer, were added: aldehyde **192** (2.94 g, 13.3 mmol, 1.0 equiv.), $Y(OTf)_3$ (713 mg, 1.33 mmol, 0.1 equiv.), anhydrous MeCN (2.7 mL), benzyl carbamate (**8**) (2.01 g, 13.3 mmol, 1.0 equiv.), phosphite **205** (2.11 g, 13.3 mmol, 1.0 equiv.), and anhydrous THF (2.7 mL). The solution was stirred at 20-25 °C for 2 h, then volatiles were removed in vacuo. The residue was purified by flash chromatography on silica (eluent heptane/EtOAc 10 - 100 %). The selected tubes were collected and volatiles were removed by vacuo. Yield of **206**: 6.18 g (53 %) as a pale yellow solid. Purity 75 % AN by HPLC. ^{1}H NMR (400 MHz, DMSO-d_6) δ: 9.41 (s, 1H), 8.83 (d, J = 10.1 Hz, 1H), 7.47 (m, 4H), 7.37 (m, 8H), 7.11 (d, J = 8.9 Hz, 2H), 7.02 (d, J = 8.9 Hz, 2H), 5.54 (dd, J = 22.3, 10.1 Hz, 1H), 5.08 (dd, J = 33.4, 12.5 Hz, 2H) 1.47 (s, 9H). ^{13}C NMR (101 MHz, DMSO-d_6) δ: 156.79, 156.36, 153.18, 149.38, 149.02, 140.14, 137.06, 130.23, 129.88, 129.59, 129.37, 128.83, 128.48, 127.58, 79.66, 66.72, 52.65, 28.57. ^{31}P NMR (162 MHz, DMSO-d_6) δ: 15.40. HRMS (ESI+) m/z calc'd for $C_{32}H_{31}Cl_2N_2O_7PNa$ $[M+Na]^+$:679.1147, found 679.1144.

4-((((Benzyloxy)carbonyl)amino)(bis(4-chlorophenoxy)phosphoryl)methyl)benzenaminium trifluoroacetate (212)

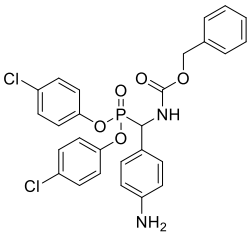

In a 50 mL flask equipped with a magnetic stirrer, were added: Boc-protected intermediate **206** (2.24 g, 3.4 mmol, 1.0 equiv.), DCM (11 mL) and TFA (11 mL). The mixture was stirred at 20-25 °C for 3 h then volatiles were removed in vacuo. The residue was dissolved in EtOAc (50 mL) and washed with 0.1% aq. NH_4HCO_3 (3 x 50 mL) and brine (50 mL) then dried on Na_2SO_4. Volatiles were removed by vacuo and the product was dried in vacuo (5 mbar) for 16 h. Yield of **212**: 2.60 g (99 %) as an orange solid. Purity 87 % AN by HPLC. ^{1}H NMR (400 MHz, DMSO-d_6) δ: 8.97 (d, J = 10.1 Hz, 1H), 7.72 (dd, J = 8.9, 1.9 Hz, 2H), 7.38 (m, 11H), 7.11 (d, J = 8.9 Hz, 2H), 7.02 (d, J = 8.9 Hz, 2H), 5.70 (dd, J = 22.3, 10.1 Hz, 1H), 5.09 (dd, J = 33.4, 12.5 Hz, 2H). ^{13}C NMR (101 MHz, DMSO-d_6) δ: 156.40, 149.24, 148.90, 136.98, 133.70, 133.54, 130.29, 130.20, 130.00, 128.86, 128.51, 123.29, 122.62, 122.48, 66.83, 52.80. ^{31}P NMR (162 MHz, DMSO-d_6) δ: 14.85. HRMS (ESI+) m/z calc'd for $C_{27}H_{23}Cl_2N_2O_5PNa$ $[M+Na]^+$:579.0619, found 579.0624.

Benzyl (*E*)-((bis(4-chlorophenoxy)phosphoryl)(4-(*N*,*N*'-bis(*tert*-butyloxycarbonyl)guanidino)phenyl)methyl)carbamate (209)

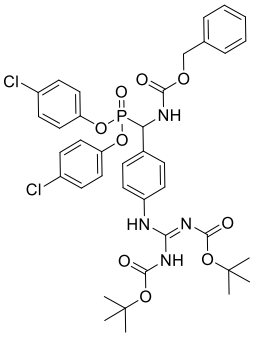

In 50 mL flask equipped with a magnetic stirrer, were added: free base **212** (1.28 g, 1.9 mmol, 1.0 equiv.), *N*,*N*'-bis(*tert*-butyloxycarbonyl-1-guanyl-pyrazole (**11**) (714 mg, 2.3 mmol, 1.2 equiv.), DCM/MeCN (1:1 v/v) (1.9 mL), and DIPEA (496 µL, 2.85 mmol, 1.5 equiv.). The mixture was stirred at 20-25 °C for 96 hours then volatiles were removed in vacuo. The crude was dissolved in EtOAc (50 mL) and washed with 0.1 % aq. $KHSO_4$ (3 x 50 mL) and brine (50 mL) then dried on Na_2SO_4. Volatiles were removed in vacuo and the crude material was purified by flash chromatography on silica (eluent heptane/EtOAc 20 - 100 %). The selected tubes were collected and volatiles were removed by vacuo. Yield of **209**: 1.01 g (63 %) as a white solid. Purity 95 % AN by HPLC. ^{1}H NMR (400 MHz, DMSO-d_6) δ: 11.42 (s, 1H), 10.03 (s, 1H), 8.89 (d, J = 10.1 Hz, 1H), 7.58 (m, 4H), 7.38 (m, 9H), 7.11 (d, J = 8.9 Hz, 2H), 7.01 (d, J = 8.9 Hz, 2H), 5.63 (dd, J = 22.3, 10.1 Hz, 1H), 5.10 (dd, J = 33.4, 12.5 Hz, 2H), 1.51 (s, 9H), 1.40 (s, 9H). ^{13}C NMR (101 MHz, DMSO-d_6) δ: 163.09, 156.79, 156.39, 153.33, 152.53, 149.30, 148.97, 137.26, 137.02, 130.73, 130.26, 129.92, 129.59, 129.29, 128.84, 128.52, 128.48, 123.33, 122.65, 122.51, 117.39, 83.86, 79.37, 66.78, 52.82, 28.21. ^{31}P NMR (162 MHz, DMSO-d_6) δ: 15.16. HRMS (ESI+) m/z calc'd for $C_{38}H_{42}Cl_2N_4O_9P$ $[M+H]^+$:799.2066, found 799.2090.

Amino ((4-((((benzyloxy)carbonyl)amino)(bis(4-chlorophenoxy)phosphoryl)methyl)phenyl) amino)methaniminium chloride (15)

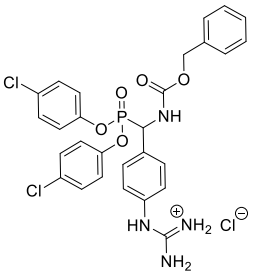

In a 25 mL flask equipped with a magnetic stirrer were added: intermediate **209** (400 mg, 0.5 mmol) and 4 N HCl in dioxane (4 mL). The mixture was stirred at 20-25 °C for 30 h. Volatiles were removed in vacuo, the residue was dissolved in absolute EtOH (5 mL), added dropwise in MTBE (200 mL) at 0 °C, and stirred for 1 h at 0 °C. The solid was recovered by filtration and dried in vacuum (5 mbar) for 16 h. Yield of **15**: 275 mg (88 %) as an off-white solid. Purity 96 % AN by HPLC. ^{1}H NMR (400 MHz, DMSO-d_6) δ: 10.06 (s, 1H), 8.96 (d, J = 10.1 Hz, 1H), 7.68 (dd, J = 8.9, 1.6 Hz, 2H), 7.57 (s, 3H), 7.41 (m, 4H), 7.35 (m, 5H), 7.25 (d, J = 8.9 Hz, 2H), 7.12 (d, J = 8.9 Hz, 2H), 7.06 (d, J = 8.9 Hz, 2H), 5.67 (dd, J = 22.3, 10.1 Hz 1H), 5.08 (dd, J = 33.4, 12.5 Hz, 2H). ^{13}C NMR (101 MHz, DMSO-d_6) δ 156.43, 156.31, 149.31, 148.93, 136.98, 136.02, 135.99, 132.34, 130.30, 129.97, 128.87, 128.58, 124.42, 122.67, 122.49, 66.80, 52.77. ^{31}P NMR (162 MHz, DMSO-d_6) δ: 14.85. HRMS (ESI+) m/z calc'd for $C_{28}H_{26}Cl_2N_4O_5P$ $[M+H]^+$:599.1018, found 599.1042.

4.6 Compounds prepared for the stereoselective synthesis of α-aminophosphonates

General procedure B: synthesis of carbamates

In an oven-dried 25 mL flask equipped with a magnetic stirrer and a dropping funnel were added: an indicated alcohol (1.0 equiv.) and anhydrous DCM (5 mL). The solution was cooled at 0 °C then 2.2.2-trichloroacetylisocyanate (**145**) (1.2 equiv.). was added dropwise. The solution was stirred for 2 h at 0 °C. Volatiles were removed in vacuo then the crude was dissolved in a mixture of MeOH (5 mL) and water (0.7 mL). Then K_2CO_3 (1.5 equiv.) was added and the mixture was stirred at 20-25 °C for 16 h. Volatiles were removed in vacuo and water (7 mL) was added to the crude. The aqueous layer was extracted with EtOAc (3 × 25 mL). The combined organic layers were washed with brine (50 mL) and dried over Na_2SO_4. Volatiles were removed in vacuo, crude product was purified by flash chromatography on silica (eluent DCM/MeOH 10 - 100%). The selected tubes were collected and volatiles were removed by vacuo.

(*S*)-((1*S*,2*R*,4*S*,5*R*)-5-Ethylquinuclidin-2-yl)(6-methoxyquinolin-4-yl)methyl carbamate (226)

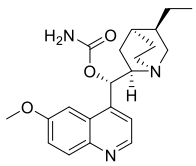

According to general procedure B: hydroquinidine (**222**) (500 mg, 1.5 mmol, 1.0 equiv.), anhydrous DCM (5 mL). 2.2.2-trichloroacetylisocyanate (**145**) (214 uL, 1.8 mmol, 1.2 equiv.). K_2CO_3 (138 mg, 2.3 mmol, 1.5 equiv.). Yield of **226**: 328 mg (58 %) of an off-white solid. Purity 99 % AN by HPLC. ^{1}H NMR (400 MHz, DMSO-d_6) δ: 8.72 (d, *J* = 4.4 Hz, 1H), 7.95 (d, *J* = 9.2 Hz, 1H), 7.51 (d, *J* = 2.7 Hz, 1H), 7.42 (m, 2H), 6.72 (d, *J* = 85.5 Hz, 2H), 6.22 (d, *J* = 8.6 Hz, 1H), 3.93 (s, 3H), 3.21 (q, *J* = 8.6 Hz, 1H), 2.72 (m, 2H), 2.58 (m, 3H), 1.67 (m, 3H), 1.44 (m, 8H), 0.88 (t, *J* = 7.3 Hz, 3H). ^{13}C NMR (101 MHz, DMSO-d_6) δ: 157.52, 156.61, 147.95, 145.88, 144.45, 131.67, 127.58, 121.72, 119.47, 102.76, 72.51, 59.57, 55.85, 50.40, 49.45, 37.42, 27.37, 26.12, 25.45, 24.15, 12.42. HRMS (ESI+): m/z calc'd for $C_{21}H_{28}N_3O_3$ $[M+H]^+$: 370.2131, found 370.2145.

(*R*)-(6-methoxyquinolin-4-yl)((1S,2R,4S,5R)-5-vinylquinuclidin-2-yl)methyl carbamate (227)

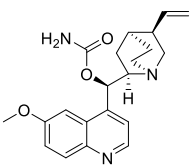

According to general procedure B: quinine (**102b**) (500 mg, 1.5 mmol, 1.0 equiv.), anhydrous DCM (5 mL). 2.2.2-trichloroacetylisocyanate (**145**) (220 uL, 1.9 mmol, 1.2 equiv.). K_2CO_3 (139 mg, 2.3 mmol, 1.5 equiv.). Yield of **227**: 256 mg (52 %) as a white solid. Purity 86 % AN by HPLC. ^{1}H NMR (400 MHz, DMSO-d_6) δ: 8.71 (d, *J* = 4.4 Hz, 1H), 7.95 (d, *J* = 9.2 Hz, 1H), 7.52 (d, *J* = 2.7 Hz, 1H), 7.43 (m, 3H), 6.72 (d, *J* = 105.1 Hz, 2H), 6.18 (d, *J* = 8.6 Hz, 1H), 5.89 (m, 1H), 5.00 (m, 2H), 3.91 (s, 3H), 3.27 (m, 1H), 3.06 (m, 1H), 2.86 (m, 1H), 2.46 (s, 1H), 2.22 (s, 1H), 1.77 (m, 4H), 1.48 (m, 2H). ^{13}C NMR (101 MHz, DMSO-d_6) δ: 157.58, 156.51, 147.97,

145.64, 144.47, 142.79, 131.70, 127.43, 121.73, 119.55, 114.71, 102.74, 59.49, 55.99, 42.15, 27.60, 24.85. HRMS (ESI+): m/z calc'd for $C_{21}H_{26}N_3O_3$ $[M+H]^+$: 368.1974, found 368.1987.

(*R*)-1-(3,5-bis(trifluoromethyl)phenyl)ethyl carbamate (229)

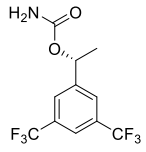

According to general procedure B: (*R*)-1-[3,5-bis(trifluoromethyl)phenyl]ethanol (**224**) (1.00 g, 3.9 mmol, 1.0 equiv.), anhydrous DCM (8 mL). 2.2.2-trichloroacetylisocyanate (**145**) (554 uL, 4.7 mmol, 1.2 equiv.). K_2CO_3 (349 mg, 2.3 mmol, 1.5 equiv.). No purification needed. Yield of **229**: 1.08 g (92 %) as a white solid. Purity 99 % AN by HPLC. ^{1}H NMR (400 MHz, $CDCl_3$) δ: 7.80 (s, 1H), 7.79 (s, 2H), 5.87 (q, *J* = 6.7 Hz, 1H), 4.84 (s, 2H), 1.58 (d, *J* = 6.7 Hz, 3H). ^{13}C NMR (101 MHz, $CDCl_3$) δ: 155.63, 144.67, 131.88 (q, *J* = 33.3 Hz), 126.12, 123.19 (q, *J* = 271.3 Hz) 121.80, 77.34, 71.70, 30.92, 22.47. HRMS (ESI+): m/z calc'd for $C_{11}H_9NO_2Na$ $[M+Na]^+$:324.0435, found 324.1501.

(*S*)-1-phenylethyl carbamate (228)

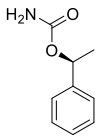

According to general procedure B: (*S*)-(-)-1-phenylethanol (**223**) (1.00 g, 8.2 mmol, 1.0 equiv.), anhydrous DCM (8 mL). 2.2.2-trichloroacetylisocyanate (**145**) (1.17 mL, 9.8 mmol, 1.2 equiv.). K_2CO_3 (737 mg, 12.0 mmol, 1.5 equiv.). No purification needed. Yield of **228**: 1.32 g (44 %) as a white solid. Purity 82 % AN by HPLC. ^{1}H NMR (400 MHz, $CDCl_3$) δ: 7.26 (d, *J* = 4.9 Hz, 4H), 7.20 (m, 1H), 5.70 (q, *J* = 6.7 Hz, 1H), 4.87 (s, 2H), 1.46 (d, *J* = 6.7 Hz, 3H). ^{13}C NMR: (101 MHz, $CDCl_3$) δ: 156.63, 141.91, 128.51, 127.84, 125.98, 73.05, 22.33. HRMS (ESI+): m/z calc'd for $C_9H_{11}NO_2Na$ $[M+Na]^+$:188.0687, found 188.1283.

(1*S*,2*R*,4*S*)-1,7,7-trimethylbicyclo[2.2.1]heptan-2-yl carbamate (230)

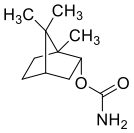

According to general procedure B: borneol (**225**) (1.00 g, 6.5 mmol, 1.0 equiv.), anhydrous DCM (6 mL). 2.2.2-trichloroacetylisocyanate (**145**) (0.93 mL, 7.8 mmol, 1.2 equiv.). K_2CO_3 (583 mg, 9.7 mmol, 1.5 equiv.). No purification needed. Yield of **230**: 1.22 g (91 %) as an off-white solid. Purity 95 % AN by HPLC. Single crystal preparation: compound **230** (350 mg) was dissolved in the minimum amount of MeCN (0.6 mL) and left in vial cover by a septum with three needles in it. After 60 days a conglomerate of crystals formed at the bottom of the vial. One crystal was recovered from the conglomerate and analyzed with SC-XRD. ^{1}H NMR (400 MHz, $CDCl_3$) δ: 4.81 (m, 3H), 2.33 (m, 1H), 1.88 (m, 1H), 1.73 (m, 1H), 1.65 (t, *J* = 4.6 Hz, 1H), 1.24 (m, 2H), 1.03 (dd, *J* = 13.7, 3.5 Hz, 1H), 0.89 (s, 3H), 0.86 (s, 3H), 0.84 (s, 3H). ^{13}C NMR (101 MHz, $CDCl_3$) δ: 157.63, 80.45, 48.75, 47.63, 44.88, 36.64, 28.20, 26.98, 19.74, 18.85, 13.47.

Diphenyl (phenyl(((*S*)-1-phenylethyl)amino)methyl)phosphonate (215)

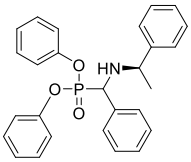

In an oven-dried 25 mL flask were added: benzaldehyde (**136)** (1.00 g, 1.0 equiv, 9.42 mmol), $Y(OTf)_3$ (505 mg, 0.1 equiv., 0.94 mmol), anhydrous MeCN (9.42 mL), (*S*)-(-)-1-phenylethylamine (**129**) (1.20 mL, 1.0 equiv., 9.4 mmol) and diphenyl phosphite (**49**) (1.84 mL, 1.0 equiv., 9.42 mmol). The mixture was stirred at 20-25 °C for 4 h, then volatiles were removed in vacuo and the product was purified by flash chromatography on silica (eluent heptane/EtOAc 20 - 100 %). The selected tubes were collected and volatiles were removed by vacuo. Yield of **215**: 2.71 g (65 %) as a viscous oil. Purity 70 % AN by HPLC. ^{1}H NMR (400 MHz, DMSO-d_6) δ: 7.49 (m, 2H), 7.40 (m, 5H), 7.32 (m, 2H), 7.25 (m, 5H), 7.15 (m, 4H), 6.77 (m, 2H), 4.18 (d, *J* = 23.4 Hz, 1H), 3.71 (m, 1H), 1.38 (d, *J* = 6.7 Hz, 3H). ^{13}C NMR (101 MHz, DMSO-d_6) δ: 158.89, 158.52, 157.80, 150.65, 150.31, 130.32, 130.16, 129.83, 129.58, 129.09, 129.03, 128.94, 127.99, 127.55, 125.63, 125.08, 121.03, 120.91, 120.56, 119.25, 115.69, 58.63, 56.02, 24.11. ^{31}P NMR (162 MHz, DMSO-d_6) δ: 17.34. HRMS (ESI+): m/z calc'd for $C_{27}H_{27}NO_3P$ $[M+H]^+$:444.1729, found 444.1716.

(*R*)-1-(3,5-bis(trifluoromethyl)phenyl)ethyl((diphenoxyphosphoryl)(phenyl)methyl)-carbamate (234)

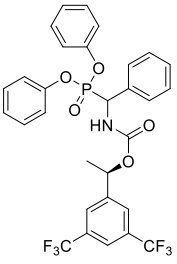

In a 25 mL flask equipped with a magnetic stirrer were added: benzaldehyde (**136**) (137 µL, 1.35 mmol, 1.0 equiv.), $Y(OTf)_3$ (73 mg, 0.14 mmol, 0.1 equiv.), anhydrous MeCN (1.35 mL), (*R*)-1-(3,5-bis(trifluoromethyl)phenyl)ethyl carbamate (**229**) (407 mg, 1.35 mmol, 1.0 equiv.), triphenyl phosphite (**26**) (356 µL, 1.35 mmol, 1.0 equiv.) and TFAA (188 µL, 1.35 mmol, 1.0 equiv.). The mixture was stirred at 20-25 °C for 4 h, then volatiles were removed in vacuo and the product was purified by flash chromatography on silica (eluent heptane/EtOAc 25 - 100 %). The selected tubes were collected and the volatiles were removed by vacuo. Yield of **234**: 402 mg (70 %) as a white solid. Purity 69 % AN by HPLC. ^{1}H NMR (400 MHz, DMSO-d_6) δ: 9.07 (m, 1H), 8.11 (d, *J* = 7.4 Hz, 2H), 8.01 (s, 1H), 7.62 (m, 2H), 7.34 (m, 5H), 7.22 (m, 3H), 7.10 (m, 2H), 6.97 (t, *J* = 6.7 Hz, 2H), 6.80 (d, *J* = 6.7 Hz, 1H), 5.94 (m, 1H), 5.54 (m, 1H), 1.52 (d, *J* = 6.7 Hz, 3H). ^{13}C NMR (101 MHz, DMSO-d_6) δ: 155.58, 150.32, 146.33, 134.66, 130.85 (q, *J* = 33.5 Hz), 130.36, 130.08, 129.03, 128.96, 128.84, 128.72, 126.93, 125.83, 125.65, 123.73 (q, *J* = 271.0 Hz) 71.78, 53.13, 23.04. ^{31}P NMR (162 MHz, DMSO-d_6) δ: 14.65. HRMS (ESI+): m/z calc'd for $C_{30}H_{25}F_6NO_5P$ $[M+H]^+$:624.1375, found 624.1379.

(*S*)-1-Phenylethyl ((diphenoxyphosphoryl)(phenyl)methyl)carbamate (233)

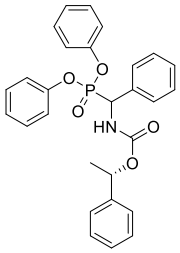

In a 25 mL flask equipped with a magnetic stirrer were added: benzaldehyde (**136**) (48 µL, 0.47 mmol, 1.0 equiv.), $Y(OTf)_3$ (25 mg, 0.05 mmol, 0.1 equiv.), anhydrous MeCN (0.47 mL), (*S*)-1-phenylethyl carbamate (**228**) (78 mg, 0.47 mmol, 1.0 equiv.), triphenyl phosphite (**26**) (123 µL, 0.47 mmol, 1.0 equiv.) and TFAA (65 µL, 0.47 mmol, 1.0 equiv.). The mixture was stirred at 20-25 °C for 4 h, then volatiles were removed in vacuo and the product was purified by flash chromatography on silica (eluent heptane/EtOAc 20 - 100 %). The selected tubes were collected and the volatiles were removed by vacuo. Yield of **233**: 154 mg (16 %) as an off-white solid. Purity 66 % AN by HPLC. ^{1}H NMR (400 MHz, $CDCl_3$) δ: 7.50 (m, 2H), 7.33 (m, 9H), 7.15 (m, 6H), 6.96 (d, *J* = 8.7 Hz, 1H), 6.85 (d, *J* = 8.7 Hz, 1H), 6.79 (m, 1H), 5.95 (ddd, *J* = 14.3, 10.0, 4.2 Hz, 1H), 5.79 (q, *J* = 6.7 Hz, 1H), 5.55 (ddd, *J* = 26.6, 21.9/10.1 Hz, 1H), 1.52 (m, 3H). ^{13}C NMR (101 MHz, $CDCl_3$) δ: 150.07, 141.42, 134.20, 129.80, 129.68, 128.87, 128.67, 128.51, 128.23, 127.94, 126.02, 125.39, 120.48, 120.37, 115.36, 74.00, 22.38. ^{31}P NMR (162 MHz, DMSO-d_6) δ: 14.01. HRMS (ESI+): m/z calc'd for $C_{28}H_{26}NO_5PNa$ $[M+Na]^+$: 510.1446, found 510.1453.

(2*S*)-1,7,7-Trimethylbicyclo[2.2.1]heptan-2-yl ((diphenoxyphosphoryl)(phenyl)methyl)-carbamate (235)

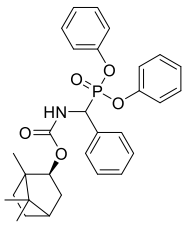

In a 25 mL flask equipped with a magnetic stirrer were added: benzaldehyde (**136**) (258 µL, 2.54 mmol, 1.0 equiv.), $Y(OTf)_3$ (136 mg, 0.25 mmol, 0.1 equiv.), anhydrous MeCN (2.54 mL), (1S,2R,4S)-1,7,7-trimethylbicyclo-[2.2.1]heptan-2-yl carbamate (**230**) (500 mg, 2.54 mmol, 1.0 equiv.), triphenyl phosphite (**26**) (502 µL, 2.54 mmol, 1.0 equiv.) and TFAA (353 µL, 2.54 mmol, 1.0 equiv.). The mixture was stirred at 20-25 °C for 4 h, then volatiles were removed in vacuo and the product was purified by flash chromatography on silica (eluent heptane/EtOAc 20 - 100 %). The selected tubes were collected and the volatiles were removed by vacuo. Yield of **235**: 593 mg (45 %) as a white solid. Purity 52 % AN by HPLC. ^{1}H NMR (400 MHz, $CDCl_3$) δ: 7.36 (m, 6H), 7.17 (m, 7H), 6.85 (m, 2H), 6.01 (s, 1H), 6.04 (s, 1H), 5.62 (dd, *J* = 22.0, 9.0 Hz, 1H), 4.83 (dd, *J* = 22.3, 10.1 Hz, 1H), 2.31 (m, 1H), 1.88 (m, 1H), 1.72 (m, 1H), 1.64 (m, 1H), 1.26 (m, 1H), 0.98 (dd, *J* = 13.7, 3.5 Hz, 1H), 0.87 (m, 9H). ^{13}C NMR (101 MHz, $CDCl_3$) δ: 156.33, 150.06, 134.30, 129.90, 129.78, 129.55, 129.02, 128.77, 128.41, 125.61, 125.51, 120.62, 120.44, 120.15, 81.62, 52.78, 49.01, 48.83, 47.95, 47.90, 44.89, 36.75, 28.07, 27.09, 21.16, 19.81, 18.91, 13.64, 13.54. ^{31}P NMR (162 MHz, DMSO-d_6) δ: 14,30 HRMS (ESI+): m/z calc'd for $C_{30}H_{34}NO_5PNa$ $[M+Na]^+$: 542.2072, found 542.2074.

5 CONCLUSIONS

1. The overall yield for the preparation of UAMC-00050 was increased from 3 % for the medicinal chemistry route to 22 % for the process chemistry route. Major efforts were applied for the preparation of aldehyde **7**, phosphonate **9**, and for the preparation and purification of product **1**. DMP oxidation for the synthesis of aldehyde **7** was substituted with a green and cheap NaClO/TEMPO/KBr oxidation. The key reaction (Birum-Oleksyszyn) was extensively studied for the construction of UAMC-00050. The screening of the catalyst relieved $Y(OTf)_3$ as the most efficient catalyst for the construction of UAMC-00050. Further optimization of the reaction conditions, using the catalyst in combination with TFAA as an additive and THF/MeCN (1:1 v/v) as solvent enabled to increase in the yield of the **9** from 11 % to 44 %. Guanidine **1** was prepared from aniline **178** in a single step. Cyanamide was selected as the reactant and smart DoE was applied to optimize the guanylation reaction. The newly developed protocol allowed us to cut costs for the preparation of UAMC-00050. In all intermediate steps, for the synthesis of **6**, **7**, and **9** flash chromatography was removed and intermediates were purified using alternative methods suitable for a larger scale like crystallization, slurry or antisolvent precipitation. Only flash chromatography was required for the final product in order to reach the target purity > 98 %. The improved route was executed on a multi-gram scale and is suitable for preclinical batch preparation of UAMC-00050.

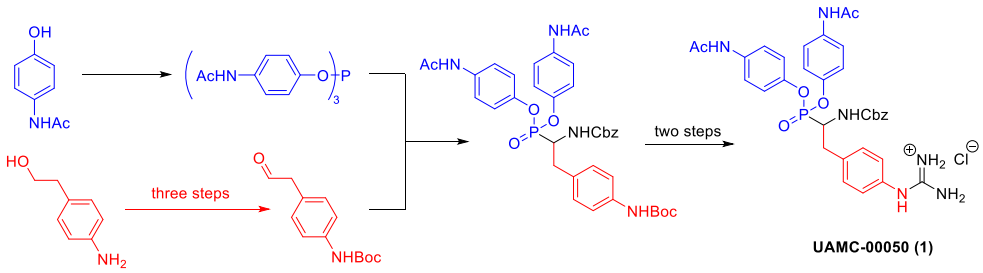

2. A five-step scheme was developed for the preparation of 5.79 g of UAMC-0004206. The target compound was obtained from aldehyde **192** with an overall yield of 30 %. In the Birum-Oleksyszyn step, the concentration was found to be an important parameter for the reaction outcome. For the guanylation step with *N*,*N*'-di-Boc-1*H*-pyrazole-1-carboxamidine (**11**), the use of the *i*PrOH in combination with MeCN was assumed to be the source of impurity in the final material. Using DCM instead of *i*PrOH allowed us to isolate a pure material.

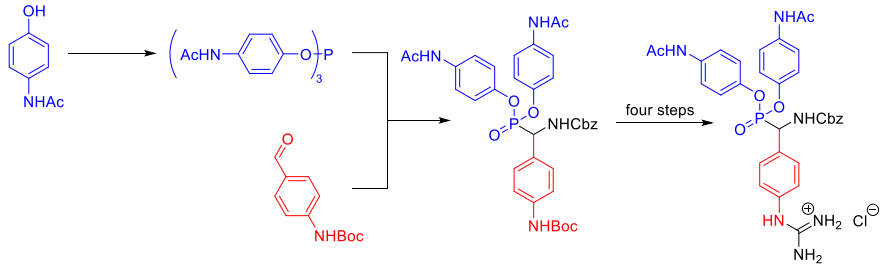

UAMC-0004206 (14)

3. A four-step scheme was developed for the preparation of 1.9 g of UAMC-0004207. The final compound was obtained from aldehyde **192** with an overall yield of 26 %. Similar to UAMC-0004206, in the Birum-Oleksyszyn reaction, the concentration was found to be an important parameter for the reaction outcome. The additional development effort was necessary due to residual TFA in the aniline which had a negative impact on the guanylation reaction with *N*,*N*'-di-Boc-1*H*-pyrazole-1-carboxamidine (**11**). A basic wash with 0.5 % aq. NH_4HCO_3 of the starting material and an acid wash of the crude product with 0.5 % aq. $KHSO_4$ before the chromatographic purification allowed to increase in the yield of the protected guanidine.

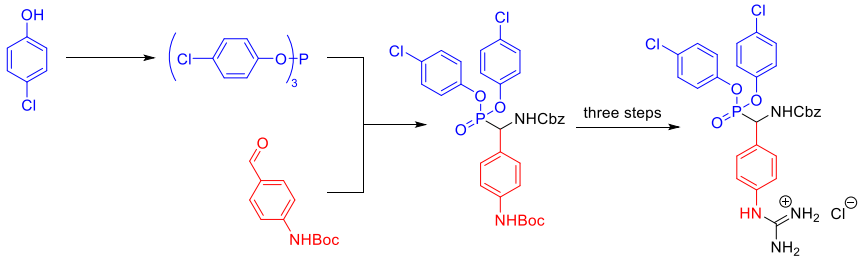

UAMC-0004207 (15)

4. The two enantiomers of UAMC-00050 were isolated and tested *in vitro*. The enzymatic test highlighted a 10-fold difference between the two stereoisomers, in which enantiomer 1 has a better affinity with uPA than enantiomer 2. The IC50 of enantiomer 1 resulted to be only twice lower than the racemic mixture. A stereoselective synthetic preparation of UAMC-00050 was investigated to provide material for toxicological studies in a later stage of the drug development.

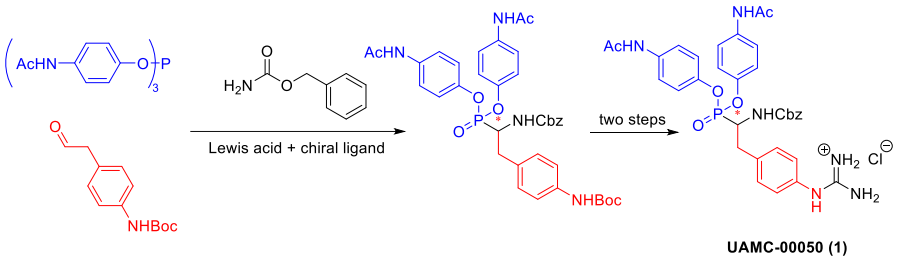

5. The chiral carbamate derivative of α-aminophosphonate was prepared, in a diastereomeric ratio 75:25, using (*R*)-1-(3,5-bis(trifluoromethyl)phenyl)ethyl carbamate as a chiral auxiliary for Birum-Oleksyszyn reaction. The mixture of diastereoisomers was then converted to the desired Cbz-protected α-aminophosphonate after acid cleavage of chiral auxiliary and functionalization of the amino group with benzyl chloroformate. The conversion resulted in a mixture of enantiomer with 64:36 er. Despite modest enantioselectivity, the method is an important addition to the development of the stereoselective Birum-Oleksyszyn reaction which was neglected for more than two decades.

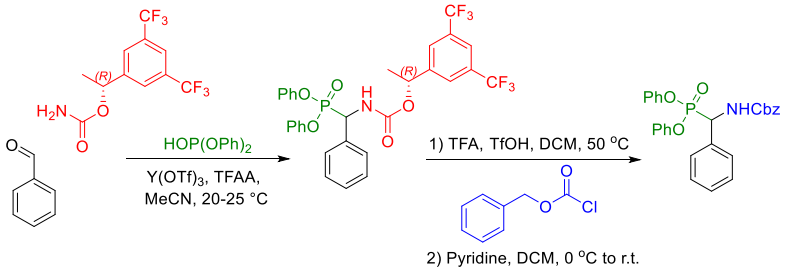

6 REFERENCES

(1) Craig, J. P.; Nichols, K. K.; Akpek, E. K.; Caffery, B.; Dua, H. S.; Joo, C.-K.; Liu, Z.; Nelson, J. D.; Nichols, J. J.; Tsubota, K.; Stapleton, F. TFOS DEWS II Definition and Classification Report. *Ocul. Surf.* **2017**, *15* (3), 276–283. https://doi.org/10.1016/j.jtos.2017.05.008.

(2) Stapleton, F.; Alves, M.; Bunya, V. Y.; Jalbert, I.; Lekhanont, K.; Malet, F.; Na, K.-S.; Schaumberg, D.; Uchino, M.; Vehof, J.; Viso, E.; Vitale, S.; Jones, L. TFOS DEWS II Epidemiology Report. *Ocul. Surf.* **2017**, *15* (3), 334–365. https://doi.org/10.1016/j.jtos.2017.05.003.

(3) Stevenson, W.; Chauhan, S. K.; Dana, R. Dry Eye Disease: An Immune-Mediated Ocular Surface Disorder. *Arch. Ophthalmol.* **2012**, *130* (1), 90–100. https://doi.org/10.1001/archophthalmol.2011.364.

(4) Paulsen, A. J.; Cruickshanks, K. J.; Fischer, M. E.; Huang, G.-H.; Klein, B. E. K.; Klein, R.; Dalton, D. S. Dry Eye in the Beaver Dam Offspring Study: Prevalence, Risk Factors, and Health-Related Quality of Life. *Am. J. Ophthalmol.* **2014**, *157* (4), 799–806. https://doi.org/10.1016/j.ajo.2013.12.023.

(5) Joossens, J.; Ali, O. M.; El-Sayed, I.; Surpateanu, G.; Van der Veken, P.; Lambeir, A.-M.; Setyono-Han, B.; Foekens, J. A.; Schneider, A.; Schmalix, W.; Haemers, A.; Augustyns, K. Small, Potent, and Selective Diaryl Phosphonate Inhibitors for Urokinase-Type Plasminogen Activator with In Vivo Antimetastatic Properties. *J. Med. Chem.* **2007**, *50* (26), 6638–6646. https://doi.org/10.1021/jm700962j.

(6) Joossen, C.; Baán, A.; Moreno-Cinos, C.; Joossens, J.; Cools, N.; Lanckacker, E.; Moons, L.; Lemmens, K.; Lambeir, A.-M.; Fransen, E.; Delputte, P.; Caljon, G.; Van Der Veken, P.; Maes, L.; De Meester, I.; Kiekens, F.; Augustyns, K.; Cos, P. A Novel Serine Protease Inhibitor as Potential Treatment for Dry Eye Syndrome and Ocular Inflammation. *Sci. Rep.* **2020**, *10* (1), 17268. https://doi.org/10.1038/s41598-020-74159-w.

(7) Oleksyszyn, J.; Subotkowska, L.; Mastalerz, P. Diphenyl 1-Aminoalkanephosphonates. *Synthesis* **1979**, *1979* (12), 985–986. https://doi.org/10.1055/s-1979-28903.

(8) Birum, G. H. Urylenediphosphonates. General Method for the Synthesis of .Alpha.-Ureidophosphonates and Related Structures. *J. Org. Chem.* **1974**, *39* (2), 209–213. https://doi.org/10.1021/jo00916a019.

(9) Veken, P. V. der; Sayed, I. E.; Joossens, J.; Stevens, C. V.; Augustyns, K.; Haemers, A. Lewis Acid Catalyzed Synthesis of N-Protected Diphenyl 1-Aminoalkyl-phosphonates. *Synthesis* **2005**, *2005* (4), 634–638. https://doi.org/10.1055/s-2004-837307.

(10) Moss, S. E.; Klein, R.; Klein, B. E. K. Long-Term Incidence of Dry Eye in an Older Population. *Optom. Vis. Sci.* **2008**, *85* (8), 668–674. https://doi.org/10.1097/OPX.0b013e318181a947.

(11) Dallaston, M. A.; Bettencourt, C. J.; Chow, S.; Gebhardt, J.; Spangler, J.; Johnston, M. R.; Wall, C.; Brusnahan, J. S.; Williams, C. M. Ranking Oxidant Sensitiveness: A Guide for Synthetic Utility. *Chem. – Eur. J.* **2019**, *25* (41), 9614–9618. https://doi.org/10.1002/chem.201902036.

(12) Varga, P. R.; Keglevich, G. Synthesis of α-Aminophosphonates and Related Derivatives; The Last Decade of the Kabachnik–Fields Reaction. *Molecules* **2021**, *26* (9), 2511. https://doi.org/10.3390/molecules26092511.

(13) Shastri, R. A. Review on the Synthesis of α-Aminophosphonate Derivatives. *Chem. Sci. Trans.* **2019**, *8* (3). https://doi.org/10.7598/cst2019.1585.
(14) Sravya, G.; Balakrishna, A.; Zyryanov, G. V.; Mohan, G.; Reddy, C. S.; Bakthavatchala Reddy, N. Synthesis of α-Aminophosphonates by the Kabachnik-Fields Reaction. *Phosphorus Sulfur Silicon Relat. Elem.* **2021**, *196* (4), 353–381. https://doi.org/10.1080/10426507.2020.1854258.
(15) Macarie, L.; Simulescu, V.; Ilia, G. Ultrasonic Irradiation Used in Synthesis of Aminophosphonates. *Monatshefte Für Chem. - Chem. Mon.* **2019**, *150* (2), 163–171. https://doi.org/10.1007/s00706-018-2327-3.
(16) Bhattacharya, A. K.; Thyagarajan, G. Michaelis-Arbuzov Rearrangement. *Chem. Rev.* **1981**, *81* (4), 415–430. https://doi.org/10.1021/cr00044a004.
(17) Galkina, I. V.; Khayarov, K. R.; Davletshin, R. R.; Gaynullin, A. Z.; Gerasimov, A. V.; Shulaeva, M. P.; Pozdeev, O. K.; Egorova, S. N.; Usupova, L. M.; Galkin, V. I. The Pudovik Reaction: The Synthesis of Bioactive α-Aminophosphonates with Long Alkyl Chains. *Phosphorus Sulfur Silicon Relat. Elem.* **2019**, *194* (4–6), 463–466. https://doi.org/10.1080/10426507.2018.1539848.
(18) Fields, E. K. The Synthesis of Esters of Substituted Amino Phosphonic Acids. *J. Am. Chem. Soc.* **1952**, *74* (6), 1528–1531. https://doi.org/10.1021/ja01126a054.
(19) Agbowuro, A. A.; Hwang, J.; Peel, E.; Mazraani, R.; Springwald, A.; Marsh, J. W.; McCaughey, L.; Gamble, A. B.; Huston, W. M.; Tyndall, J. D. A. Structure-Activity Analysis of Peptidic Chlamydia HtrA Inhibitors. *Bioorg. Med. Chem.* **2019**, *27* (18), 4185–4199. https://doi.org/10.1016/j.bmc.2019.07.049.
(20) Xu, F.; Luo, Y.; Wu, J.; Shen, Q.; Chen, H. Facile One-Pot Synthesis of α-Amino Phosphonates Using Lanthanide Chloride as Catalyst. *Heteroat. Chem.* **2006**, *17* (5), 389–392. https://doi.org/10.1002/hc.20219.
(21) Bhagat, S.; Chakraborti, A. K. An Extremely Efficient Three-Component Reaction of Aldehydes/Ketones, Amines, and Phosphites (Kabachnik−Fields Reaction) for the Synthesis of α-Aminophosphonates Catalyzed by Magnesium Perchlorate. *J. Org. Chem.* **2007**, *72* (4), 1263–1270. https://doi.org/10.1021/jo062140i.
(22) Bhagat, S.; Chakraborti, A. K. Zirconium(IV) Compounds As Efficient Catalysts for Synthesis of α-Aminophosphonates. *J. Org. Chem.* **2008**, *73* (15), 6029–6032. https://doi.org/10.1021/jo8009006.
(23) Li, X.-C.; Gong, S.-S.; Zeng, D.-Y.; You, Y.-H.; Sun, Q. Highly Efficient Synthesis of α-Aminophosphonates Catalyzed by Hafnium(IV) Chloride. *Tetrahedron Lett.* **2016**, *57* (16), 1782–1785. https://doi.org/10.1016/j.tetlet.2016.03.033.
(24) Yuan, C.; Qi, Y. Studies on Organophosphorus Compounds; Part XX. A Facile Synthesis of α-Amino-Substituted Benzylphosphonic and -Phosphinic Acids by Use of Thiophosphoramide. *Synthesis* **1986**, *1986* (10), 821–825. https://doi.org/10.1055/s-1986-31790.
(25) Abdel-Megeed, M. F.; El-Hiti, G. A.; Badr, B. E.; Azaam, M. M. Synthesis of a Series of Diphenyl (Arylamino)(Pyridin-3-Yl)Methylphosphonates as Potential Antimicrobial Agents. *Phosphorus Sulfur Silicon Relat. Elem.* **2013**, *188* (7), 879–885. https://doi.org/10.1080/10426507.2012.717141.
(26) Awad, M. K.; Abdel-Aal, M. F.; Atlam, F. M.; Hekal, H. A. Molecular Docking, Molecular Modeling, Vibrational and Biological Studies of Some New Heterocyclic α-Aminophosphonates. *Spectrochim. Acta. A. Mol. Biomol. Spectrosc.* **2019**, *206*, 78–88. https://doi.org/10.1016/j.saa.2018.07.083.

(27) Arigala, U. R. S.; Matcha, C.; Yoon, K. R. Zn(OAc)2•2H2O-catalyzed Synthesis of A-aminophosphonates under Neat Reaction. *Heteroat. Chem.* **2012**, *23* (2), 160–165. https://doi.org/10.1002/hc.20765.
(28) Gabriela Vogt, A.; Perin, G.; Luchese, C.; da Silva, P. C.; Antunes Wilhelm, E.; Santos Silva, M. Organylselanyl α-Amino Phosphonates: Synthesis, NMR Spectroscopic Study, and Antioxidant and Antinociceptive Activities. *Eur. J. Org. Chem.* **2018**, *2018* (5), 627–639. https://doi.org/10.1002/ejoc.201701565.
(29) Dmitriev, M. E.; Rossinets, E. A.; Ragulin, V. V. Amidoalkylation of Hydrophosphoryl Compounds. *Russ. J. Gen. Chem.* **2011**, *81* (6), 1092–1104. https://doi.org/10.1134/S1070363211060041.
(30) Dmitriev, M. E.; Ragulin, V. V. Arbuzov-Type Reaction of Acylphosphonites and N-Alkoxycarbonylimine Cations Generated in Situ with Trifluoroacetic Anhydride. *Tetrahedron Lett.* **2012**, *53* (13), 1634–1636. https://doi.org/10.1016/j.tetlet.2012.01.094.
(31) Kahan, F. M.; Kahan, J. S.; Cassidy, P. J.; Kropp, H. The Mechanism of Action of Fosfomycin (Phosphonomycin). *Ann. N. Y. Acad. Sci.* **1974**, *235* (1), 364–386. https://doi.org/10.1111/j.1749-6632.1974.tb43277.x.
(32) Maruyama, H. B.; Arisawa, M.; Sawada, T. Alafosfalin, a New Inhibitor of Cell Wall Biosynthesis: In Vitro Activity against Urinary Isolates in Japan and Potentiation with Beta-Lactams. *Antimicrob. Agents Chemother.* **1979**. https://doi.org/10.1128/AAC.16.4.444.
(33) Xu, W.; Zhang, S.; Yang, S.; Jin, L.-H.; Bhadury, P. S.; Hu, D.-Y.; Zhang, Y. Asymmetric Synthesis of α-Aminophosphonates Using the Inexpensive Chiral Catalyst 1,1'-Binaphthol Phosphate. *Molecules* **2010**, *15* (8), 5782–5796. https://doi.org/10.3390/molecules15085782.
(34) Brooks, W. H.; Guida, W. C.; Daniel, K. G. The Significance of Chirality in Drug Design and Development. *Curr. Top. Med. Chem.* **2011**, *11* (7), 760–770.
(35) Merino, P.; Marqués-López, E.; Herrera, R. P. Catalytic Enantioselective Hydrophosphonylation of Aldehydes and Imines. *Adv. Synth. Catal.* **2008**, *350* (9), 1195–1208. https://doi.org/10.1002/adsc.200800131.
(36) Ordóñez, M.; Viveros-Ceballos, J. L.; Cativiela, C.; Sayago, F. J. An Update on the Stereoselective Synthesis of α-Aminophosphonic Acids and Derivatives. *Tetrahedron* **2015**, *71* (12), 1745–1784. https://doi.org/10.1016/j.tet.2015.01.029.
(37) Mikołajczyk, M.; Łyżwa, P. Recent Progress in Asymmetric Synthesis of Aminophosphonic Acids Mediated by Chiral Sulfinyl Auxiliary. *Pure Appl. Chem.* **2017**, *89* (3), 357–365. https://doi.org/10.1515/pac-2016-1023.
(38) Banerjee, I.; Panda, T. K. Recent Advances in the Carbon–Phosphorus (C–P) Bond Formation from Unsaturated Compounds by s- and p-Block Metals. *Org. Biomol. Chem.* **2021**, *19* (30), 6571–6587. https://doi.org/10.1039/D1OB01019K.
(39) Gbubele, J. D.; Olszewski, T. K. Asymmetric Synthesis of Organophosphorus Compounds Using H–P Reagents Derived from Chiral Alcohols. *Org. Biomol. Chem.* **2021**, *19* (13), 2823–2846. https://doi.org/10.1039/D1OB00124H.
(40) Nazish, M.; Jakhar, A.; Khan, N. H.; Verma, S.; Kureshy, R. I.; Abdi, S. H. R.; Bajaj, H. C. Enantioselective Hydrophosphonylation of N- Benzyl Imines, Isatin Derived Ketimines and Isatins Catalyzed by in-Situ Generated Ti(IV) Macrocyclic Salen Complexes. *Appl. Catal. Gen.* **2016**, *515*, 116–125. https://doi.org/10.1016/j.apcata.2015.12.037.
(41) Ohara, M.; Nakamura, S.; Shibata, N. Direct Enantioselective Three-Component Kabachnik–Fields Reaction Catalyzed by Chiral Bis(Imidazoline)-Zinc(II) Catalysts. *Adv. Synth. Catal.* **2011**, *353* (18), 3285–3289. https://doi.org/10.1002/adsc.201100482.

(42) Zhou, X.; Shang, D.; Zhang, Q.; Lin, L.; Liu, X.; Feng, X. Enantioselective Three-Component Kabachnik−Fields Reaction Catalyzed by Chiral Scandium(III)−N,N′-Dioxide Complexes. *Org. Lett.* **2009**, *11* (6), 1401–1404. https://doi.org/10.1021/ol9000813.
(43) Abell, J. P.; Yamamoto, H. Catalytic Enantioselective Pudovik Reaction of Aldehydes and Aldimines with Tethered Bis(8-Quinolinato) (TBOx) Aluminum Complex. *J. Am. Chem. Soc.* **2008**, *130* (32), 10521–10523. https://doi.org/10.1021/ja803859p.
(44) Saito, B.; Katsuki, T. Synthesis of an Optically Active C1-Symmetric Al(Salalen) Complex and Its Application to the Catalytic Hydrophosphonylation of Aldehydes. *Angew. Chem.* **2005**, *117* (29), 4676–4678. https://doi.org/10.1002/ange.200501008.
(45) Saito, B.; Egami, H.; Katsuki, T. Synthesis of an Optically Active Al(Salalen) Complex and Its Application to Catalytic Hydrophosphonylation of Aldehydes and Aldimines. *J. Am. Chem. Soc.* **2007**, *129* (7), 1978–1986. https://doi.org/10.1021/ja0651005.
(46) Sasai, H.; Arai, S.; Tahara, Y.; Shibasaki, M. Catalytic Asymmetric Synthesis of .Alpha.-Amino Phosphonates Using Lanthanoid-Potassium-BINOL Complexes. *J. Org. Chem.* **1995**, *60* (21), 6656–6657. https://doi.org/10.1021/jo00126a003.
(47) Gröger, H.; Saida, Y.; Arai, S.; Martens, J.; Sasai, H.; Shibasaki, M. First Catalytic Asymmetric Hydrophosphonylation of Cyclic Imines: Highly Efficient Enantioselective Approach to a 4-Thiazolidinylphosphonate via Chiral Titanium and Lanthanoid Catalysts. *Tetrahedron Lett.* **1996**, *37* (52), 9291–9292. https://doi.org/10.1016/S0040-4039(97)82944-9.
(48) Schlemminger, I.; Saida, Y.; Gröger, H.; Maison, W.; Durot, N.; Sasai, H.; Shibasaki, M.; Martens, J. Concept of Improved Rigidity: How to Make Enantioselective Hydrophosphonylation of Cyclic Imines Catalyzed by Chiral Heterobimetallic Lanthanoid Complexes Almost Perfect. *J. Org. Chem.* **2000**, *65* (16), 4818–4825. https://doi.org/10.1021/jo991882r.
(49) Lim, H.; Datilus, V.; Teriak, R.; Chohan, P.; Kaur, P. Manganese-Proline Derived New Catalyst System for the Enantioselective Synthesis of α-Hydroxyphosphonates and α-Aminophosphonates. *Tetrahedron Lett.* **2017**, *58* (15), 1480–1483. https://doi.org/10.1016/j.tetlet.2017.02.088.
(50) Akiyama, T.; Morita, H.; Bachu, P.; Mori, K.; Yamanaka, M.; Hirata, T. Chiral Brønsted Acid-Catalyzed Hydrophosphonylation of Imines—DFT Study on the Effect of Substituents of Phosphoric Acid. *Tetrahedron* **2009**, *65* (26), 4950–4956. https://doi.org/10.1016/j.tet.2009.03.023.
(51) Gutierrez, E. G.; Moorhead, E. J.; Smith, E. H.; Lin, V.; Ackerman, L. K. G.; Knezevic, C. E.; Sun, V.; Grant, S.; Wenzel, A. G. Electron-Withdrawing, Biphenyl-2,2′-Diol-Based Compounds for Asymmetric Catalysis. *Eur. J. Org. Chem.* **2010**, *2010* (16), 3027–3031. https://doi.org/10.1002/ejoc.201000070.
(52) Cheng, X.; Goddard, R.; Buth, G.; List, B. Direct Catalytic Asymmetric Three-Component Kabachnik–Fields Reaction. *Angew. Chem. Int. Ed.* **2008**, *47* (27), 5079–5081. https://doi.org/10.1002/anie.200801173.
(53) Hoffmann, S.; Seayad, A. M.; List, B. A Powerful Brønsted Acid Catalyst for the Organocatalytic Asymmetric Transfer Hydrogenation of Imines. *Angew. Chem. Int. Ed.* **2005**, *44* (45), 7424–7427. https://doi.org/10.1002/anie.200503062.
(54) Nakamura, S.; Nakashima, H.; Yamamura, A.; Shibata, N.; Toru, T. Organocatalytic Enantioselective Hydrophosphonylation of Sulfonylimines Having a Heteroarenesulfonyl Group as a Novel Stereocontroller. *Adv. Synth. Catal.* **2008**, *350* (9), 1209–1212. https://doi.org/10.1002/adsc.200800134.

(55) Nakamura, S.; Hayashi, M.; Hiramatsu, Y.; Shibata, N.; Funahashi, Y.; Toru, T. Catalytic Enantioselective Hydrophosphonylation of Ketimines Using Cinchona Alkaloids. *J. Am. Chem. Soc.* **2009**, *131* (51), 18240–18241. https://doi.org/10.1021/ja908940e.
(56) Fini, F.; Sgarzani, V.; Pettersen, D.; Herrera, R. P.; Bernardi, L.; Ricci, A. Phase-Transfer-Catalyzed Asymmetric Aza-Henry Reaction Using N-Carbamoyl Imines Generated In Situ from α-Amido Sulfones. *Angew. Chem. Int. Ed.* **2005**, *44* (48), 7975–7978. https://doi.org/10.1002/anie.200502646.
(57) Pettersen, D.; Marcolini, M.; Bernardi, L.; Fini, F.; Herrera, R. P.; Sgarzani, V.; Ricci, A. Direct Access to Enantiomerically Enriched α-Amino Phosphonic Acid Derivatives by Organocatalytic Asymmetric Hydrophosphonylation of Imines. *J. Org. Chem.* **2006**, *71* (16), 6269–6272. https://doi.org/10.1021/jo060708h.
(58) Li, W.; Wang, Y.; Xu, D. Asymmetric Synthesis of α-Amino Phosphonates by Using Cinchona Alkaloid-Based Chiral Phase Transfer Catalyst: Asymmetric Synthesis of α-Amino Phosphonates by Using Cinchona Alkaloid-Based Chiral Phase Transfer Catalyst. *Eur. J. Org. Chem.* **2018**, *2018* (39), 5422–5426. https://doi.org/10.1002/ejoc.201801013.
(59) Joly, G. D.; Jacobsen, E. N. Thiourea-Catalyzed Enantioselective Hydrophosphonylation of Imines: Practical Access to Enantiomerically Enriched α-Amino Phosphonic Acids. *J. Am. Chem. Soc.* **2004**, *126* (13), 4102–4103. https://doi.org/10.1021/ja0494398.
(60) Kumar, A.; Sharma, V.; Kaur, J.; Kumar, V.; Mahajan, S.; Kumar, N.; Chimni, S. S. Cinchona-Derived Thiourea Catalyzed Hydrophosphonylation of Ketimines—an Enantioselective Synthesis of α-Amino Phosphonates. *Tetrahedron* **2014**, *39* (70), 7044–7049. https://doi.org/10.1016/j.tet.2014.06.013.
(61) Chen, D.-H.; Sun, W.-T.; Zhu, C.-J.; Lu, G.-S.; Wu, D.-P.; Wang, A.-E.; Huang, P.-Q. Enantioselective Reductive Cyanation and Phosphonylation of Secondary Amides by Iridium and Chiral Thiourea Sequential Catalysis. *Angew. Chem. Int. Ed.* **2021**, *60* (16), 8827–8831. https://doi.org/10.1002/anie.202015898.
(62) Thorat, P. B.; Goswami, S. V.; Magar, R. L.; Patil, B. R.; Bhusare, S. R. An Efficient Organocatalysis: A One-Pot Highly Enantioselective Synthesis of α-Aminophosphonates. *Eur. J. Org. Chem.* **2013**, *2013* (24), 5509–5516. https://doi.org/10.1002/ejoc.201300494.
(63) Chen, Q.; Li, J.; Yuan, C. Sulfinimine-Mediated Asymmetric Synthesis of Acyclic and Cyclic α-Aminophosphonates. *Synthesis* **2008**, *2008* (18), 2986–2990. https://doi.org/10.1055/s-2008-1067247.
(64) Li, P.; Jiang, M.; Liu, J.-T. Asymmetric Pudovik Reaction of Chiral Fluoroalkyl α,β-Unsaturated Ketimines and Diphenyl Phosphite. *Chin J Chem* **2014**, *32*, 1003–1006. https://doi.org/doi.org/10.1002/cjoc.201400419.
(65) Kaur, P.; Wever, W.; Rajale, T.; Li, G. Asymmetric Hydrophosphylation of Chiral N-Phosphonyl Imines Provides an Efficient Approach to Chiral α-Amino Phosphonates: Asymmetric Hydrophosphylation of Chiral N-Phosphonyl Imines. *Chem. Biol. Drug Des.* **2010**, *76* (4), 314–319. https://doi.org/10.1111/j.1747-0285.2010.01013.x.
(66) Boratyński, P. J.; Skarżewski, J.; Sidorowicz, Ł. Stereochemistry of Hydrophosphonylation of 9-Aminoquinine Schiff Bases. *Arkivoc* **2012**, *2012* (4), 204–215. https://doi.org/10.3998/ark.5550190.0013.415.
(67) Tibhe, G. D.; Lagunas-Rivera, S.; Vargas-Díaz, E.; García-Barradas, O.; Ordoñez, M. Uncatalyzed One-Pot Diastereoselective Synthesis of α-Amino Phosphonates Under Solvent-Free Conditions. *Eur. J. Org. Chem.* **2010**, *2010* (34), 6573–6581. https://doi.org/10.1002/ejoc.201001096.

(68) Tibhe, G. D.; Reyes-González, M. A.; Cativiela, C.; Ordóñez, M. Microwave-Assisted High Diastereoselective Synthesis of α-Aminophosphonates under Solvent and Catalyst Free-Conditions. *J. Mex. Chem. Soc.* **2012**, *56* (2), 183–187.
(69) Ando, K.; Egami, T. Facile Synthesis of A-amino Phosphonates in Water by Kabachnik–Fields Reaction Using Magnesium Dodecyl Sulfate. *Heteroat. Chem.* **2011**, *22* (3/4), 358–362. https://doi.org/10.1002/hc.20689.
(70) Fan, W.; Queneau, Y.; Popowycz, F. The Synthesis of HMF-Based α-Amino Phosphonates via One-Pot Kabachnik–Fields Reaction. *RSC Adv.* **2018**, *8* (55), 31496–31501. https://doi.org/10.1039/C8RA05983G.
(71) Bedolla-Medrano, M.; Hernández-Fernández, E.; Ordóñez, M. Phenylphosphonic Acid as Efficient and Recyclable Catalyst in the Synthesis of α-Aminophosphonates under Solvent-Free Conditions. *Synlett* **2014**, *25* (8), 1145–1149. https://doi.org/10.1055/s-0033-1341069.
(72) Todorov, P. T.; Wesselinova, D. W.; Pavlov, N. D.; Martinez, J.; Calmes, M.; Naydenova, E. D. Cytotoxic Activity of New Racemic and Optically Active N-Phosphonoalkyl Bicyclic β-Amino Acids against Human Malignant Cell Lines. *Amino Acids* **2012**, *43* (4), 1445–1450. https://doi.org/10.1007/s00726-012-1217-y.
(73) Oshikawa, T.; Yamashita, M. Preparation of Optically Active 1-Aminoalkylphosphonic Acids from Chiral Carbamates and Chiral Ureas. *Bull. Chem. Soc. Jpn.* **1989**, *62* (10), 3177–3181. https://doi.org/10.1246/bcsj.62.3177.
(74) Chung, S.-K.; Kang, D.-H. Asymmetric Synthesis of α-Aminophosphonates via Diastereoselective Addition of Phosphite to Chiral Imine Derivatives. *Tetrahedron Asymmetry* **1996**, *7* (1), 21–24. https://doi.org/10.1016/0957-4166(95)00411-4.
(75) Ahluwalia, V. K.; Kidwai, M. Basic Principles of Green Chemistry. In *New Trends in Green Chemistry*; Ahluwalia, V. K., Kidwai, M., Eds.; Springer Netherlands: Dordrecht, 2004; pp 5–14. https://doi.org/10.1007/978-1-4020-3175-5_3.
(76) Y. Wada N. Foster T. Yoshida. *Safety of Reactive Chemicals and Pyrotechnics, Volume 5 - 1st Edition*, 1st ed.; Elsevier: Amsterdam, 1995.
(77) Parmeggiani, C.; Cardona, F. Transition Metal Based Catalysts in the Aerobic Oxidation of Alcohols. *Green Chem.* **2012**, *14* (3), 547–564. https://doi.org/10.1039/C2GC16344F.
(78) Wertz, S.; Studer, A. Nitroxide-Catalyzed Transition-Metal-Free Aerobic Oxidation Processes. *Green Chem.* **2013**, *15* (11), 3116–3134. https://doi.org/10.1039/C3GC41459K.
(79) Heravi, M.; Ghalavand, N.; Hashemi, E. Hydrogen Peroxide as a Green Oxidant for the Selective Catalytic Oxidation of Benzylic and Heterocyclic Alcohols in Different Media: An Overview. *Chemistry* **2020**, *2*, 101–178. https://doi.org/10.3390/chemistry2010010.
(80) Assal, M. E.; Kuniyil, M.; Shaik, M. R.; Khan, M.; Al-Warthan, A.; Siddiqui, M. R. H.; Adil, S. F. Synthesis, Characterization, and Relative Study on the Catalytic Activity of Zinc Oxide Nanoparticles Doped $MnCO_3$, MnO_2, and Mn_2O_3 Nanocomposites for Aerial Oxidation of Alcohols. *J. Chem.* **2017**, *2017*, 1–17. https://doi.org/10.1155/2017/2937108.
(81) Kim, S. S.; Jung, H. C. An Efficient Aerobic Oxidation of Alcohols to Aldehydes and Ketones with TEMPO/Ceric Ammonium Nitrate as Catalysts. *Synthesis* **2003**, *2003* (14), 2135–2137. https://doi.org/10.1055/s-2003-41065.
(82) Hoover, J. M.; Stahl, S. S. Highly Practical Copper(I)/TEMPO Catalyst System for Chemoselective Aerobic Oxidation of Primary Alcohols. *J. Am. Chem. Soc.* **2011**, *133* (42), 16901–16910. https://doi.org/10.1021/ja206230h.
(83) Hoover, J. M.; Steves, J. E.; Stahl, S. S. Copper(I)/TEMPO-Catalyzed Aerobic Oxidation of Primary Alcohols to Aldehydes with Ambient Air. *Nat. Protoc.* **2012**, *7* (6), 1161–1166. https://doi.org/10.1038/nprot.2012.057.

(84) Steves, J. E.; Stahl, S. S. Copper(I)/ABNO-Catalyzed Aerobic Alcohol Oxidation: Alleviating Steric and Electronic Constraints of Cu/TEMPO Catalyst Systems. *J. Am. Chem. Soc.* **2013**, *135* (42), 15742–15745. https://doi.org/10.1021/ja409241h.
(85) Esguerra, K. V. N.; Fall, Y.; Lumb, J.-P. A Biomimetic Catalytic Aerobic Functionalization of Phenols. *Angew. Chem. Int. Ed.* **2014**, *53* (23), 5877–5881. https://doi.org/10.1002/anie.201311103.
(86) Kumpulainen, E. T. T.; Koskinen, A. M. P. Catalytic Activity Dependency on Catalyst Components in Aerobic Copper–TEMPO Oxidation. *Chem. – Eur. J.* **2009**, *15* (41), 10901–10911. https://doi.org/10.1002/chem.200901245.
(87) Wu, X.-F. A General and Efficient Zinc-Catalyzed Oxidation of Benzyl Alcohols to Aldehydes and Esters. *Chem. – Eur. J.* **2012**, *18* (29), 8912–8915. https://doi.org/10.1002/chem.201201105.
(88) Syiemlieh, I. Water Soluble New Bimetallic Catalyst [CuZn(Bz)3(Bpy)2]PF6 in Hydrogen Peroxide Mediated Oxidation of Alcohols to Aldehydes/Ketones and C-N Functional Groups. *J. Organomet. Chem.* **2018**, *878*, 48–59. https://doi.org/doi.org/10.1016/j.jorganchem.2018.10.001.
(89) Wagh, R. B.; Nagarkar, J. M. An Efficient and Sustainable Protocol for Oxidation of Alcohols to Carbonyl Compounds. *Tetrahedron Lett.* **2018**, *59* (37), 3443–3447. https://doi.org/10.1016/j.tetlet.2018.08.011.
(90) Hashemian, S.; Sedrpoushan, A.; Eshbala, F. H. Co-Zeolite Imidazolate Frameworks (ZIF-9@Zeolite) as Heterogen Catalyst for Alcohols Oxidation. *Catal. Lett.* **2017**, *147* (1), 196–203. https://doi.org/10.1007/s10562-016-1855-x.
(91) Lei, Z.; Wang, R. Oxidation of Alcohols Using H2O2 as Oxidant Catalyzed by AlCl3. *Catal. Commun.* **2008**, *9* (5), 740–742. https://doi.org/10.1016/j.catcom.2007.08.012.
(92) Moriyama, K.; Takemura, M.; Togo, H. Selective Oxidation of Alcohols with Alkali Metal Bromides as Bromide Catalysts: Experimental Study of the Reaction Mechanism. *J. Org. Chem.* **2014**, *79* (13), 6094–6104. https://doi.org/10.1021/jo5008064.
(93) Mirafzal, G. A.; Lozeva, A. M. Phase Transfer Catalyzed Oxidation of Alcohols with Sodium Hypochlorite. *Tetrahedron Lett.* **1998**, *39* (40), 7263–7266. https://doi.org/10.1016/S0040-4039(98)01584-6.
(94) Hampton, P. D.; Whealon, M. D.; Roberts, L. M.; Yaeger, A. A.; Boydson, R. Continuous Organic Synthesis in a Spinning Tube-in-Tube Reactor: TEMPO-Catalyzed Oxidation of Alcohols by Hypochlorite. *Org. Process Res. Dev.* **2008**, *12* (5), 946–949. https://doi.org/10.1021/op800051t.
(95) Dong, Z.; Gao, P.; Xiao, Y. Efficient Selective Oxidation of Alcohols to Aldehydes Catalyzed by a Morpholinone Nitroxide. *Synth. Commun.* **2019**, *49* (23), 3380–3388. https://doi.org/10.1080/00397911.2019.1666284.
(96) Wang, Y.; Song, X.; Shao, S.; Zhong, H.; Lin, F. An Efficient, Soluble, and Recyclable Multiwalled Carbon Nanotubes-Supported TEMPO for Oxidation of Alcohols. *RSC Adv.* **2012**, *2* (20), 7693–7698. https://doi.org/10.1039/C2RA21206D.
(97) Hinzmann, A.; Stricker, M.; Busch, J.; Glinski, S.; Oike, K.; Gröger, H. Selective TEMPO-Oxidation of Alcohols to Aldehydes in Alternative Organic Solvents. *Eur. J. Org. Chem.* **2020**, *2020* (16), 2399–2408. https://doi.org/10.1002/ejoc.201901365.
(98) Pulido, D.; Casadó-Anguera, V.; Pérez-Benito, L.; Moreno, E.; Cordomí, A.; López, L.; Cortés, A.; Ferré, S.; Pardo, L.; Casadó, V.; Royo, M. Design of a True Bivalent Ligand with Picomolar Binding Affinity for a G Protein-Coupled Receptor Homodimer. *J. Med. Chem.* **2018**, *61* (20), 9335–9346. https://doi.org/10.1021/acs.jmedchem.8b01249.

(99) Hédou, D.; Deau, E.; Harari, M.; Sanselme, M.; Fruit, C.; Besson, T. Rational Multistep Synthesis of a Novel Polyfunctionalized Benzo[d]Thiazole and Its Thiazolo[5,4-b]Pyridine Analogue. *Tetrahedron* **2014**, *70* (35), 5541–5549. https://doi.org/10.1016/j.tet.2014.06.103.
(100) Ciriminna, R.; Pagliaro, M. Industrial Oxidations with Organocatalyst TEMPO and Its Derivatives. *Org. Process Res. Dev.* **2010**, *14* (1), 245–251. https://doi.org/10.1021/op900059x.
(101) Zhuang, H.; Li, H.; Zhang, S.; Yin, Y.; Han, F.; Sun, C.; Miao, C. TEMPO and Its Derivatives Mediated Reactions under Transition-Metal-Free Conditions. *Chin. Chem. Lett.* **2020**, *31* (1), 39–48. https://doi.org/10.1016/j.cclet.2019.06.027.
(102) Lucio Anelli, P.; Biffi, C.; Montanari, F.; Quici, S. Fast and Selective Oxidation of Primary Alcohols to Aldehydes or to Carboxylic Acids and of Secondary Alcohols to Ketones Mediated by Oxoammonium Salts under Two-Phase Conditions. *J. Org. Chem.* **1987**, *52* (12), 2559–2562. https://doi.org/10.1021/jo00388a038.
(103) Furigay, M. H.; Boucher, M. M.; Mizgier, N. A.; Brindle, C. S. Separation of Aldehydes and Reactive Ketones from Mixtures Using a Bisulfite Extraction Protocol. *J. Vis. Exp. JoVE* **2018**, No. 134. https://doi.org/10.3791/57639.
(104) Hu, Q.; Jayasinghe-Arachchige, V. M.; Zuchniarz, J.; Prabhakar, R. Effects of the Metal Ion on the Mechanism of Phosphodiester Hydrolysis Catalyzed by Metal-Cyclen Complexes. *Front. Chem.* **2019**, *7*. https://doi.org/10.3389/fchem.2019.00195.
(105) Torres, R. A.; Himo, F.; Bruice, T. C.; Noodleman, L.; Lovell, T. Theoretical Examination of Mg2+-Mediated Hydrolysis of a Phosphodiester Linkage as Proposed for the Hammerhead Ribozyme. *J. Am. Chem. Soc.* **2003**, *125* (32), 9861–9867. https://doi.org/10.1021/ja021451h.
(106) Veeranjaneyulu, B.; Das, B. Improved Facile Synthesis of α-Amino Phosphonates by the Reaction of α-Amido Sulfones with Dialkyl Trimethyl Silyl Phosphites Catalyzed by Fe(III) Chloride. *Synth. Commun.* **2017**, *47* (5), 449–456. https://doi.org/10.1080/00397911.2016.1270323.
(107) Ramirez, F.; Bhatia, S. B.; Smith, C. P. Reaction of Trialkyl Phosphites with Aromatic Aldehydes: Carboncarbon Condensations from the Reaction Ofp-Nitrobenzaldehyde and Ofo-Nitrobenzaldehyde with Trialkyl Phosphites—New Routes to Glycol Phosphates. *Tetrahedron* **1967**, *23* (5), 2067–2080. https://doi.org/10.1016/0040-4020(67)80040-1.
(108) Sekine, M.; Yamamoto, I.; Hashizume, A.; Hata, T. Silyl Phosphites v. the Reactions of Tris(Trimethylsilyl) Phosphite with Carbonyl Compounds. *Chem. Lett.* **1977**, *6* (5), 485–488. https://doi.org/10.1246/cl.1977.485.
(109) Dmitriev, M. E.; Ragulin, V. V. New Opinions on the Amidoalkylation of Hydrophosphorylic Compounds. *Tetrahedron Lett.* **2010**, *51* (19), 2613–2616. https://doi.org/10.1016/j.tetlet.2010.03.020.
(110) Vinyukov, A. V.; Dmitriev, M. E.; Ragulin, V. V. One-Pot Synthesis of N-Cbz-α-Aminophosphonic Acids. *Phosphorus Sulfur Silicon Relat. Elem.* **2017**, *192* (4), 437–441. https://doi.org/10.1080/10426507.2016.1248289.
(111) *Home*. Cabot Corporation. https://www.cabotcorp.com/ (accessed 2022-03-28).
(112) Tsubokura, K.; Iwata, T. Direct Guanylation of Amino Groups by Cyanamide in Water: Catalytic Generation and Activation of Unsubstituted Carbodiimide by Scandium(III) Triflate. *Synlett* **2014**, *25*, 1302–1306.
(113) Diab, S.; Teo, T.; Kumarasiri, M.; Li, P.; Yu, M.; Lam, F.; Basnet, S. K. C.; Sykes, M. J.; Albrecht, H.; Milne, R.; Wang, S. Discovery of 5-(2-(Phenylamino)Pyrimidin-4-Yl)Thiazol-2(3H)-One Derivatives as Potent Mnk2 Inhibitors: Synthesis, SAR Analysis and Biological Evaluation. *ChemMedChem* **2014**, *9* (5), 962–972. https://doi.org/10.1002/cmdc.201300552.

(114) Kondraganti, L.; Manabolu, S. babu; Dittakavi, R. Synthesis of Benzimidazoles via Domino Intra and Intermolecular C-N Cross-Coupling Reaction. *ChemistrySelect* **2018**, *3* (42), 11744–11748. https://doi.org/10.1002/slct.201802754.
(115) An, T.; Kang, B.; Kang, S.; Pac, J.; Youk, J.; Lin, D.; Lee, Y. Guanidine Cyclic Diimides and Their Polymers. *Chem. Commun.* **2019**, *55* (69), 10222–10225. https://doi.org/10.1039/C9CC04522H.
(116) Kim, K.; Lin, Y.-T.; Mosher, H. S. Monosubstituted Guanidines from Primary Amines and Aminoiminomethanesulfonic Acid. *Tetrahedron Lett.* **1988**, *29* (26), 3183–3186. https://doi.org/10.1016/0040-4039(88)85116-5.
(117) Armitage, I.; Fu, M.; Hicks, F.; Kattuboina, A.; Li, J. S. N.; McCarron, A.; Zhu, L. The Use of Chloroformamidine Hydrochloride as a Reagent for the Synthesis of Guanidines from Electron Deficient Aromatic Amines. *J. Heterocycl. Chem.* **2017**, *54* (1), 728–734. https://doi.org/10.1002/jhet.2567.
(118) Goswami, S.; Hazra, A.; Jana, S. One-Pot Two-Step Solvent-Free Rapid and Clean Synthesis of 2-(Substituted Amino)Pyrimidines by Microwave Irradiation. *Bull. Chem. Soc. Jpn.* **2009**. https://doi.org/10.1246/bcsj.82.1175.
(119) *XT SAAM | Exponential Technologies Ltd.* https://www.x-t.ai/xt-saam/ (accessed 2022-01-11).
(120) Parsons, D. E.; Lee, S. H.; Sun, Y. J.; Velez, G.; Bassuk, A. G.; Smith, M.; Mahajan, V. B. Peptidomimetics Therapeutics for Retinal Disease. *Biomolecules* **2021**, *11* (3), 339. https://doi.org/10.3390/biom11030339.
(121) Uchiyama, A.; Mukai, M.; Fujiwara, Y.; Kobayashi, S.; Kawai, N.; Murofushi, H.; Inoue, M.; Enoki, S.; Tanaka, Y.; Niki, T.; Kobayashi, T.; Tigyi, G.; Murakami-Murofushi, K. Inhibition of Transcellular Tumor Cell Migration and Metastasis by Novel Carba-Derivatives of Cyclic Phosphatidic Acid. *Biochim. Biophys. Acta BBA - Mol. Cell Biol. Lipids* **2007**, *1771* (1), 103–112. https://doi.org/10.1016/j.bbalip.2006.10.001.
(122) Point, V.; Malla, R. K.; Diomande, S.; Martin, B. P.; Delorme, V.; Carriere, F.; Canaan, S.; Rath, N. P.; Spilling, C. D.; Cavalier, J. Synthesis and Kinetic Evaluation of Cyclophostin and Cyclipostins Phosphonate Analogs As Selective and Potent Inhibitors of Microbial Lipases. *J. Med. Chem.* **2012**, *55* (22), 10204–10219. https://doi.org/10.1021/jm301216x.
(123) Salmeia, K. A.; Gaan, S. An Overview of Some Recent Advances in DOPO-Derivatives: Chemistry and Flame Retardant Applications. *Polym. Degrad. Stab.* **2015**, *113*, 119–134. https://doi.org/10.1016/j.polymdegradstab.2014.12.014.
(124) Bauer, K. N.; Liu, L.; Andrienko, D.; Wagner, M.; Macdonald, E. K.; Shaver, M. P.; Wurm, F. R. Polymerizing Phostones: A Fast Way to In-Chain Poly(Phosphonate)s with Adjustable Hydrophilicity. *Macromolecules* **2018**, *51* (4), 1272–1279. https://doi.org/10.1021/acs.macromol.7b02473.
(125) Balam, S. K.; Soora Harinath, J.; Krishnammagari, S. K.; Gajjala, R. R.; Polireddy, K.; Baki, V. B.; Gu, W.; Valasani, K. R.; Avula, V. K. R.; Vallela, S.; Zyryanov, G. V.; Pasupuleti, V. R.; Cirandur, S. R. Synthesis and Anti-Pancreatic Cancer Activity Studies of Novel 3-Amino-2-Hydroxybenzofused 2-Phospha-γ-Lactones. *ACS Omega* **2021**, *6* (17), 11375–11388. https://doi.org/10.1021/acsomega.1c00360.
(126) Fang, H.; Peng, B.; Ong, S. Y.; Wu, Q.; Li, L.; Yao, S. Q. Recent Advances in Activity-Based Probes (ABPs) and Affinity-Based Probes (AfBPs) for Profiling of Enzymes. *Chem. Sci.* **2021**, *12* (24), 8288–8310. https://doi.org/10.1039/D1SC01359A.

(127) Crawley, J. T. B.; Zanardelli, S.; Chion, C. K. N. K.; Lane, D. A. The Central Role of Thrombin in Hemostasis. *J. Thromb. Haemost.* **2007**, *5* (s1), 95–101. https://doi.org/10.1111/j.1538-7836.2007.02500.x.
(128) Juza, M.; Mazzotti, M.; Morbidelli, M. Simulated Moving-Bed Chromatography and Its Application to Chirotechnology. *Trends Biotechnol.* **2000**, *18* (3), 108–118. https://doi.org/10.1016/S0167-7799(99)01419-5.
(129) Nagata, Y.; Takeda, R.; Suginome, M. Asymmetric Catalysis in Chiral Solvents: Chirality Transfer with Amplification of Homochirality through a Helical Macromolecular Scaffold. *ACS Cent. Sci.* **2019**, *5* (7), 1235–1240. https://doi.org/10.1021/acscentsci.9b00330.
(130) Park, S. J.; Hwang, I.-S.; Chang, Y. J.; Song, C. E. Bio-Inspired Water-Driven Catalytic Enantioselective Protonation. *J. Am. Chem. Soc.* **2021**, *143* (6), 2552–2557. https://doi.org/10.1021/jacs.0c11815.
(131) Song, C. E.; Park, S. J.; Hwang, I.-S.; Jung, M. J.; Shim, S. Y.; Bae, H. Y.; Jung, J. Y. Hydrophobic Chirality Amplification in Confined Water Cages. *Nat. Commun.* **2019**, *10* (1), 851. https://doi.org/10.1038/s41467-019-08792-z.
(132) Mahajan, N.; Koul, S.; Razdan, T. K. Bismuth Triflate-L(−)-Proline Catalyzed Synthesis of Chiral 2,5-Diaryl-2,3-Dihydropyrano[2,3-b]Quinolin-4-Ones. *J. Heterocycl. Chem.* **2011**, *48* (6), 1302–1307. https://doi.org/10.1002/jhet.762.
(133) Aplander, K.; Ding, R.; Krasavin, M.; Lindström, U. M.; Wennerberg, J. Asymmetric Lewis Acid Catalysis in Water: α-Amino Acids as Effective Ligands in Aqueous Biphasic Catalytic Michael Additions. *Eur. J. Org. Chem.* **2009**, *2009* (6), 810–821. https://doi.org/10.1002/ejoc.200800922.

AKNOWLEDGMENTS

The last four years were not exactly a stroll down the river, hence a special thanks to:

My supervisors Dr. Chem. Kirill Shubin for teaching me how to be a process chemist and for supervising the doctoral work.

Prof. Dr. Chem Aigars Jirgensons for supervising the doctoral work and reviewing the last dissemination work.

Paz for the incredible work as project manager in the IT-DED^3 network.

Marco and Alice for reviewing the thesis, for the computational calculations and for the constant moral support, because in life there are moments in which: "*non posso ne scendere ne salire, ne scendere ne salire*".

My family, for their love and their constant support.

Sabīne, for her kindness and her constant smile, which made this path less hard.

This project has received funding from the European Union's Horizon 2020 research and innovation program under the Marie Skłodowska-Curie Initial Training Network (ITN) "ITDED3" (H2020-MSCA-ITN-2017) grant agreement no. 765608.

7 Appendix I

Tris(4-acetamidophenyl) phosphite (3)

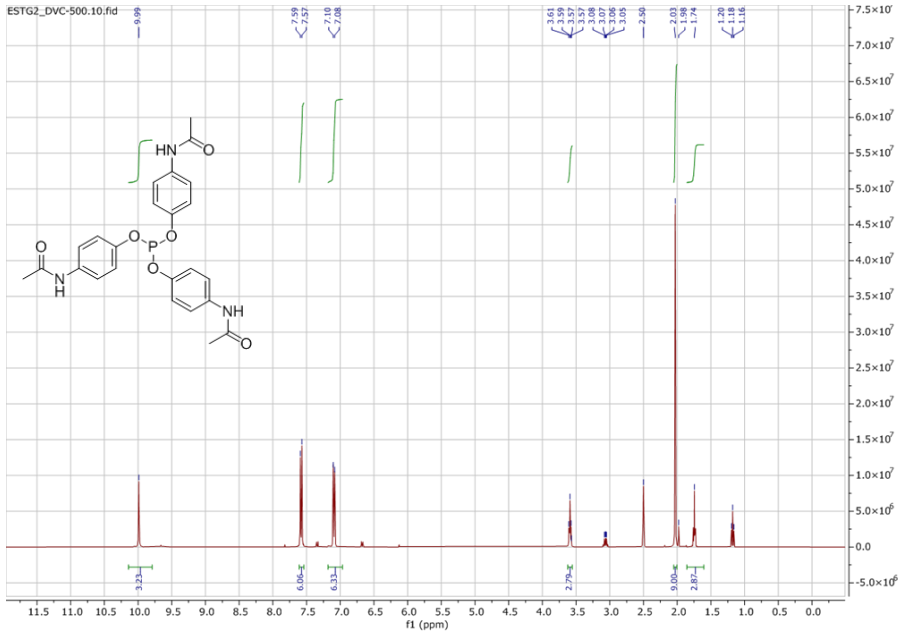

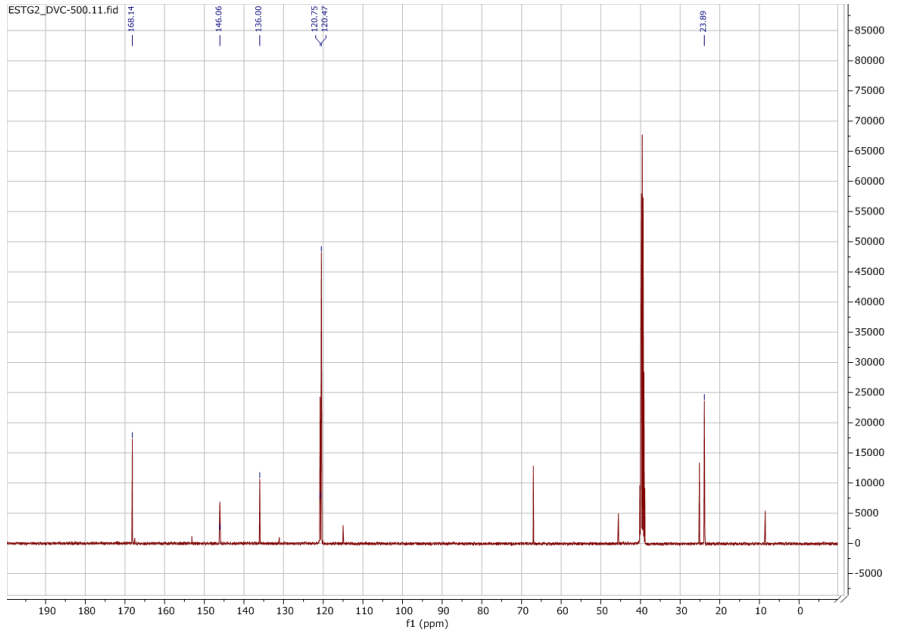

tert-Butyl (4-(2-hydroxyethyl)phenyl)carbamate (5)

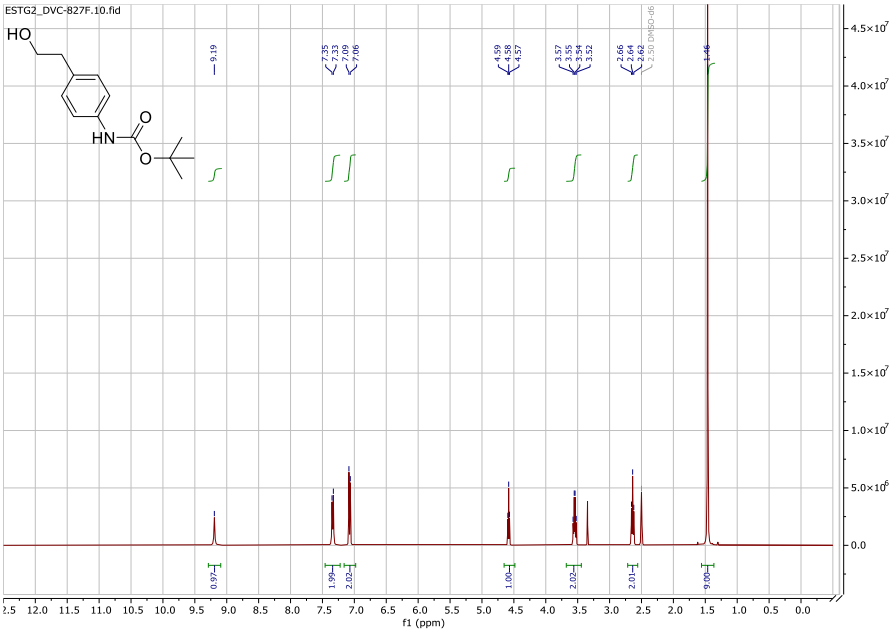

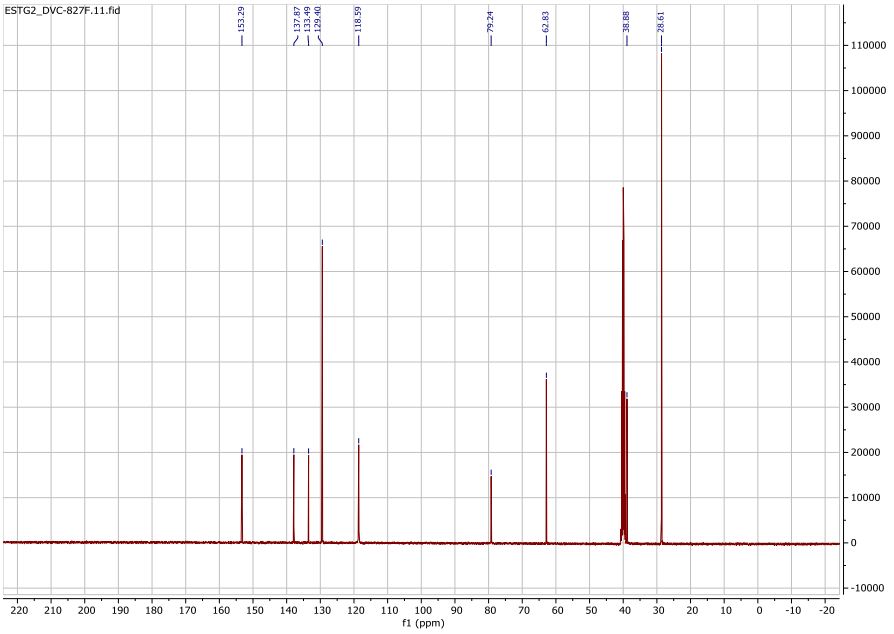

Sodium 2-(4-((tert-butoxycarbonyl)amino)phenyl)-1-hydroxyethane-1-sulfonate (164)

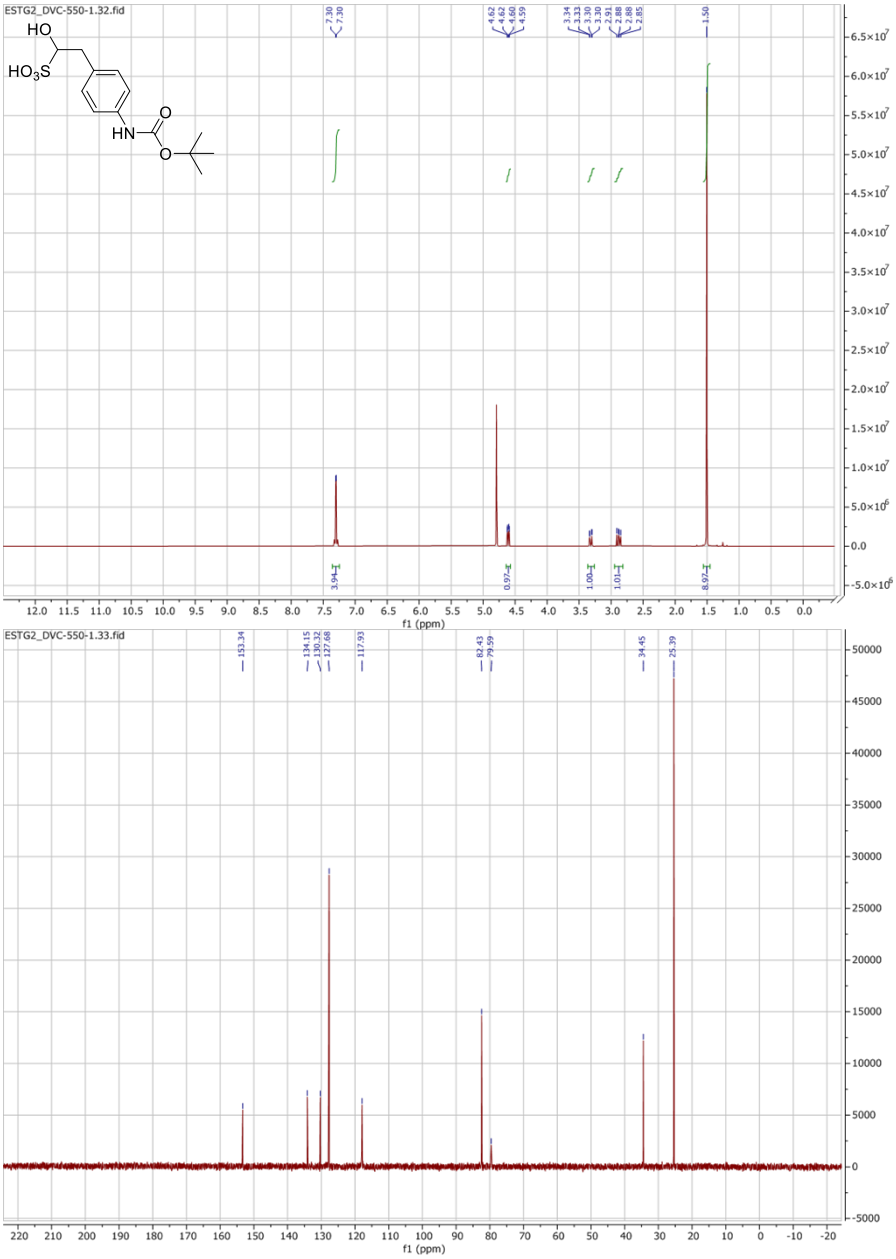

***tert*-Butyl (4-(2-oxoethyl)phenyl)carbamate (7)**

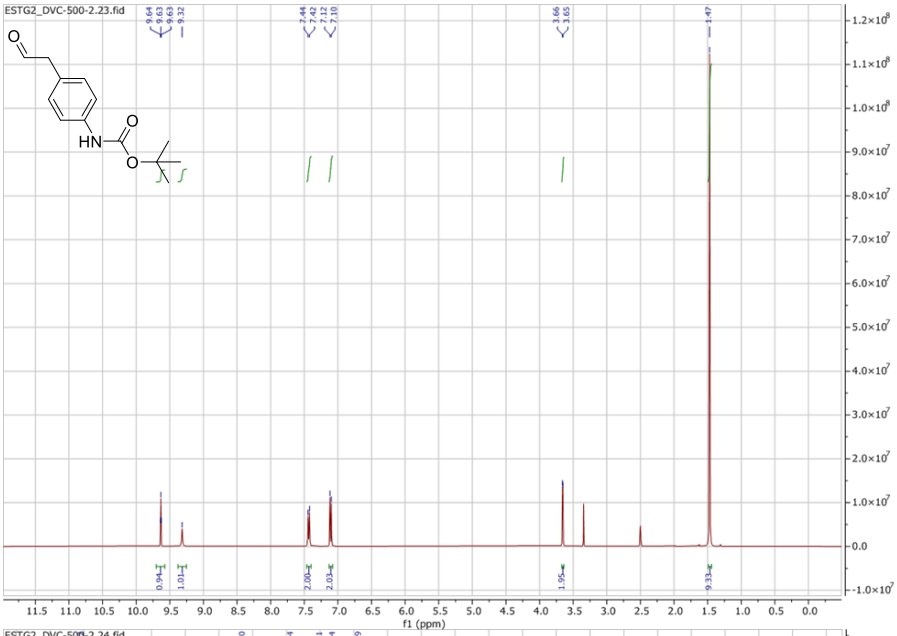

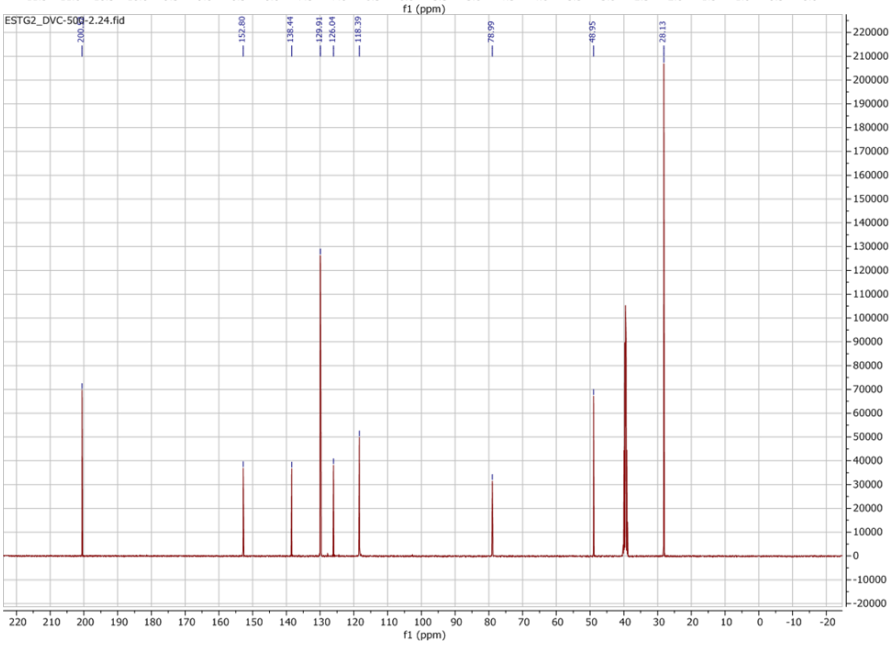

***tert*-Butyl(4-(2-(((benzyloxy)carbonyl)amino)2(bis(4acetamidophenoxy)phosphoryl)ethyl)-phenyl) carbamate (9).**

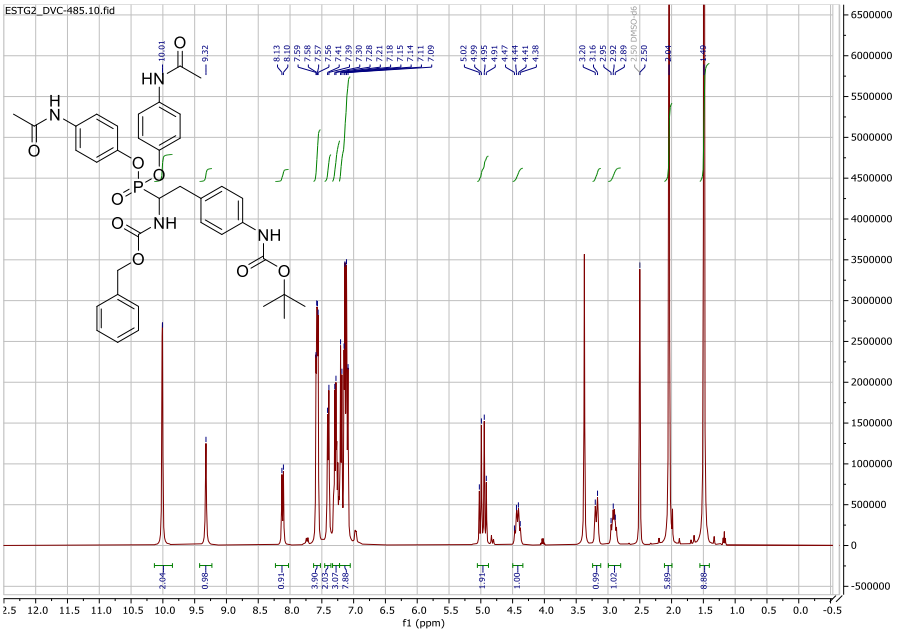

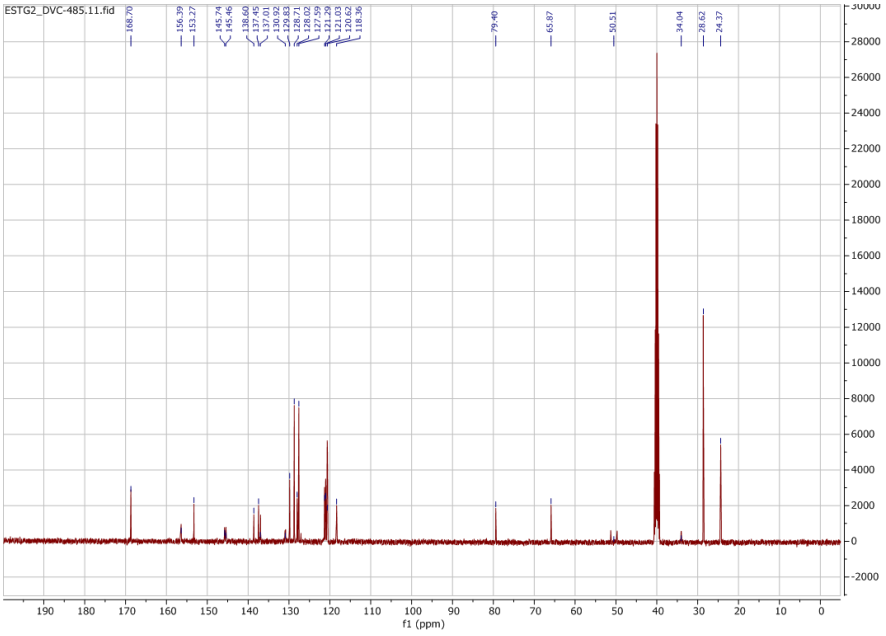

4-(2-(((benzyloxy)carbonyl)amino)-2-(bis(4-acetamidophenoxy)phosphoryl)ethyl)benzenaminium chloride (178).

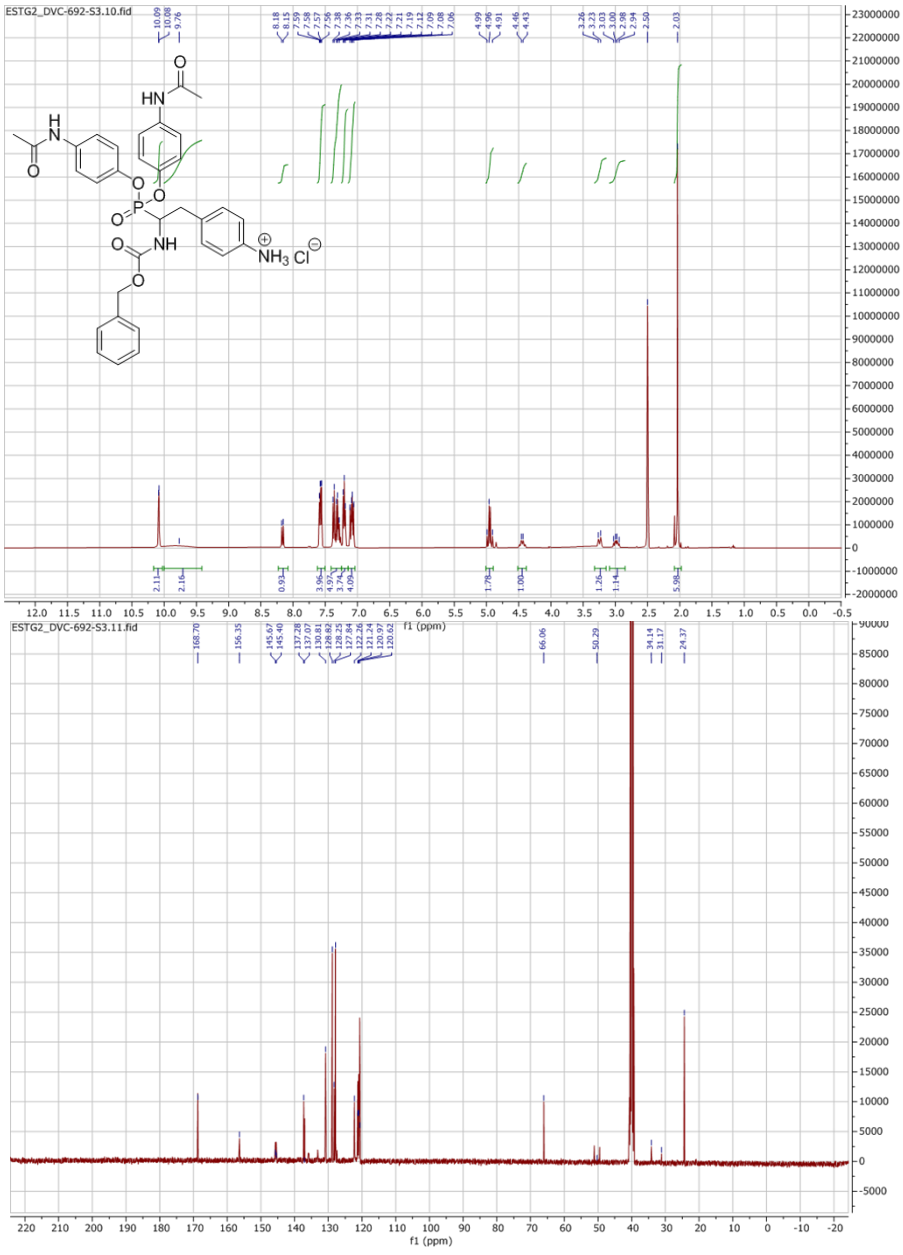

1-(4-(2-(((benzyloxy)carbonyl)amino)-2-(bis(4-acetamidophenoxy)phosphoryl)ethyl)phenyl) guanidinium chloride (1).

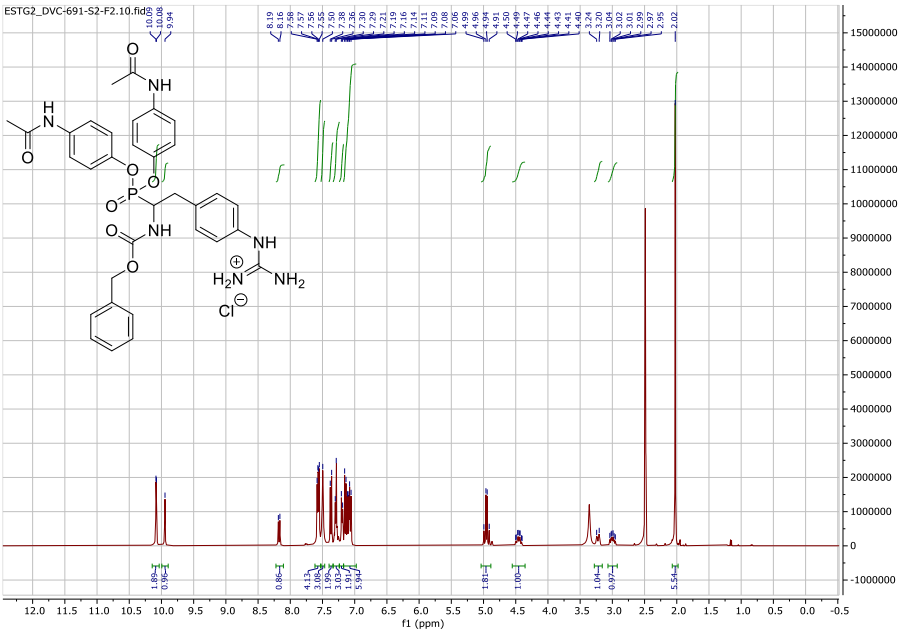

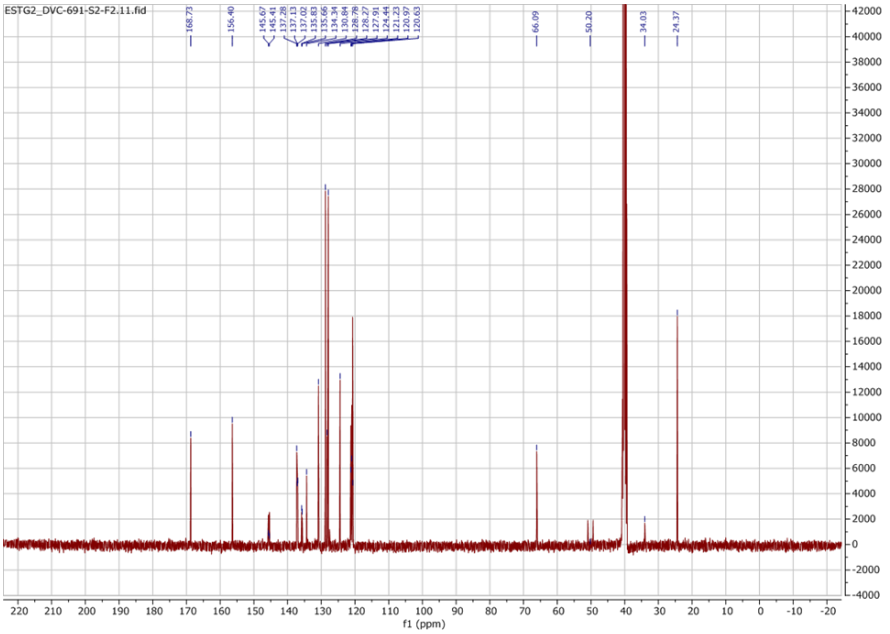

(9*H*-fluoren-9-yl)methyl (4-(2-hydroxyethyl)phenyl)carbamate (172)

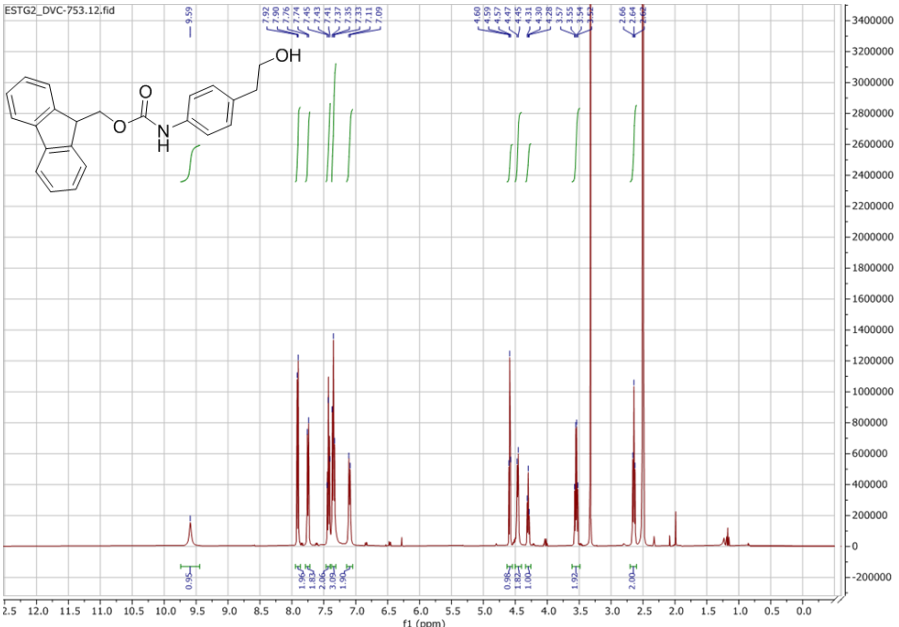

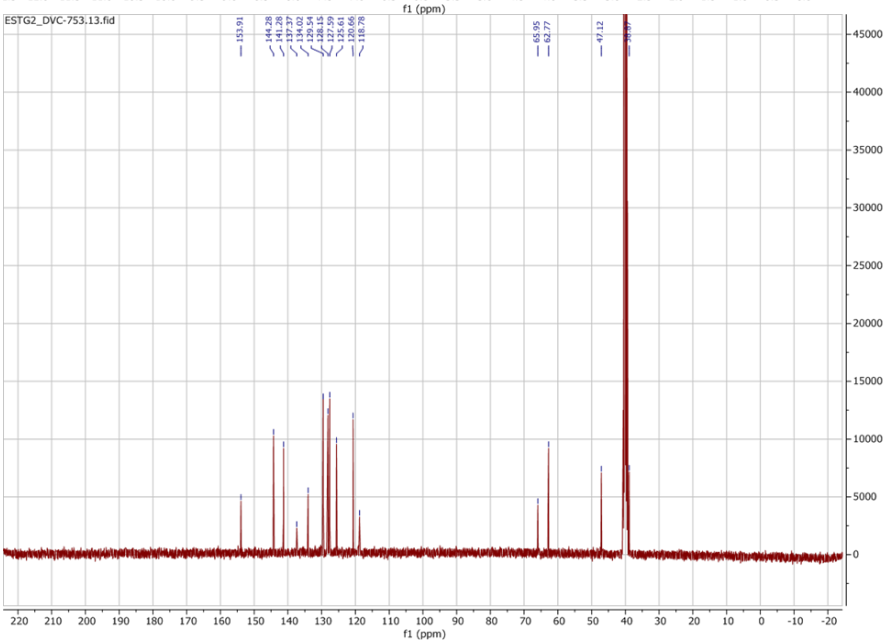

(9*H*-fluoren-9-yl)methyl (4-(2-oxoethyl)phenyl)carbamate (173)

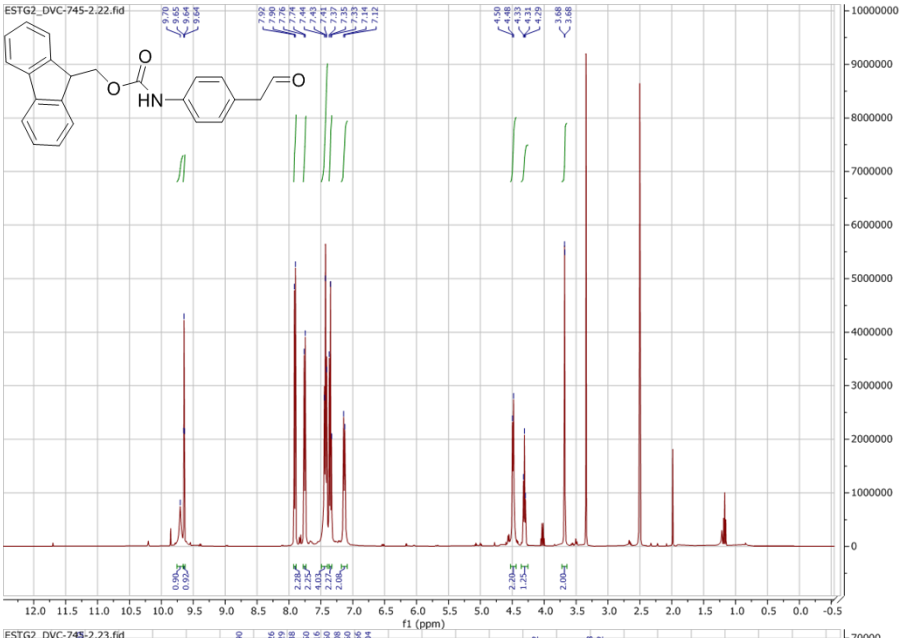

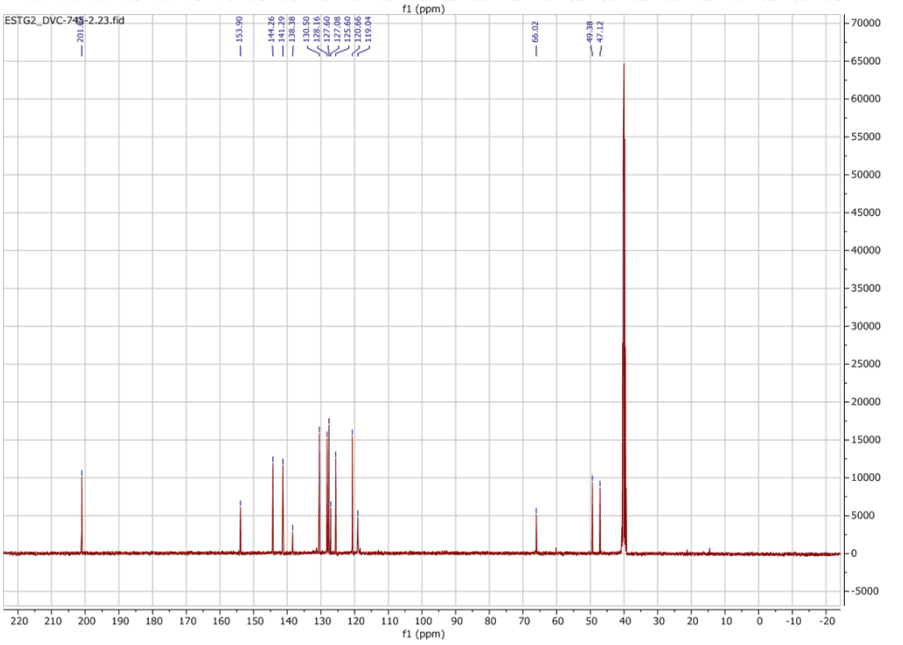

2-(4-nitrophenyl)acetaldehyde (210)

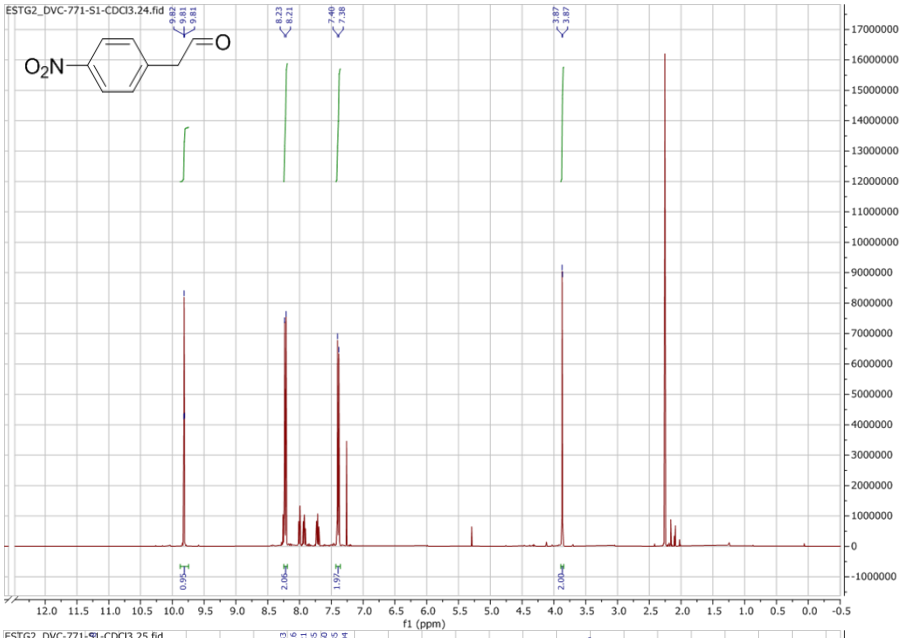

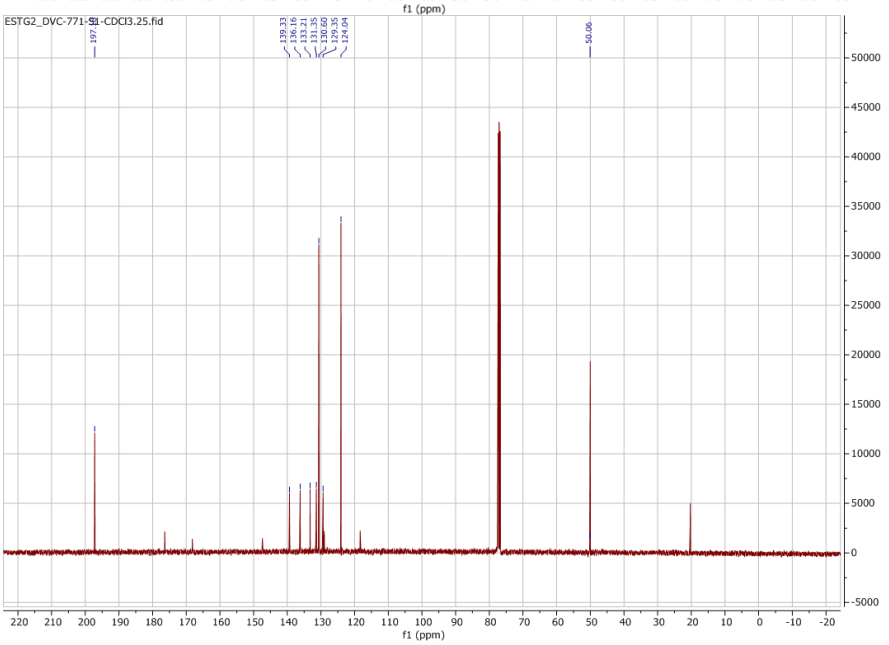

Dibenzyl (2-(4-((tert-butoxycarbonyl)amino)phenyl)ethane-1,1-diyl)dicarbamate (168)

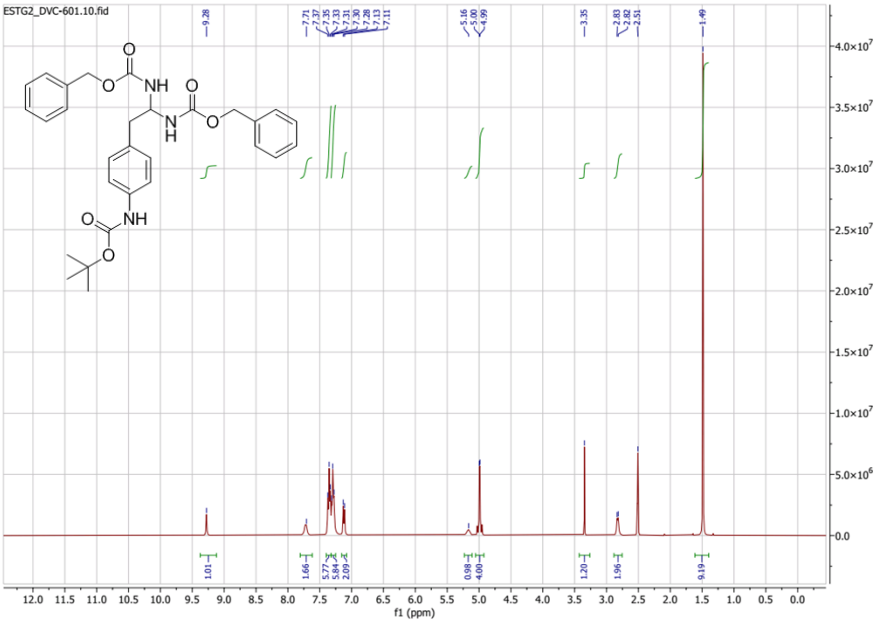

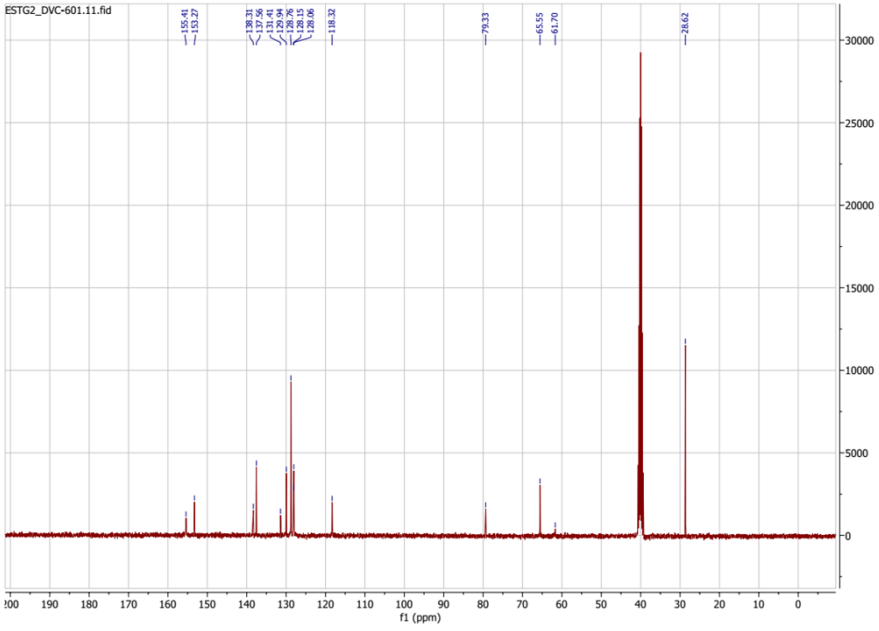

Tris(4-methoxyphenyl) phosphite (183)

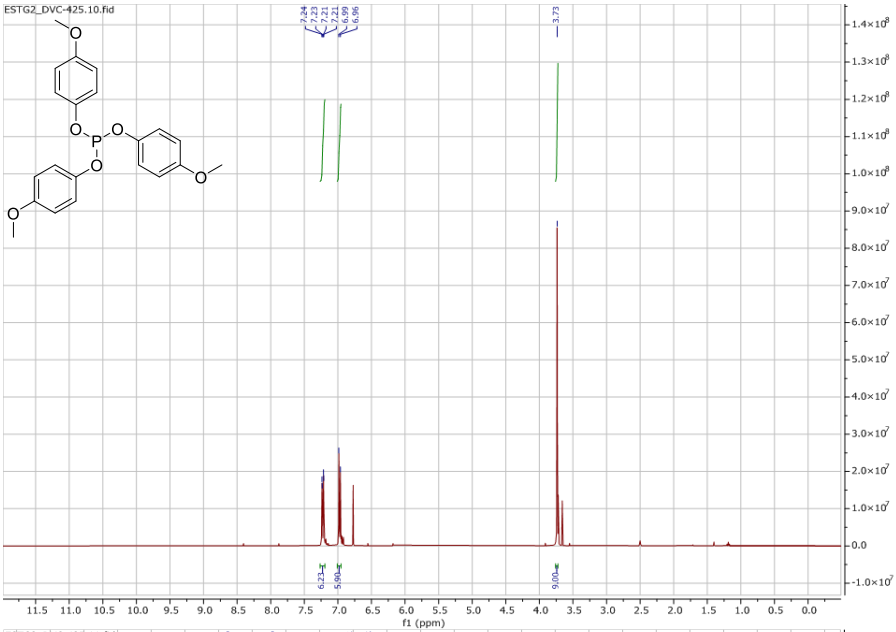

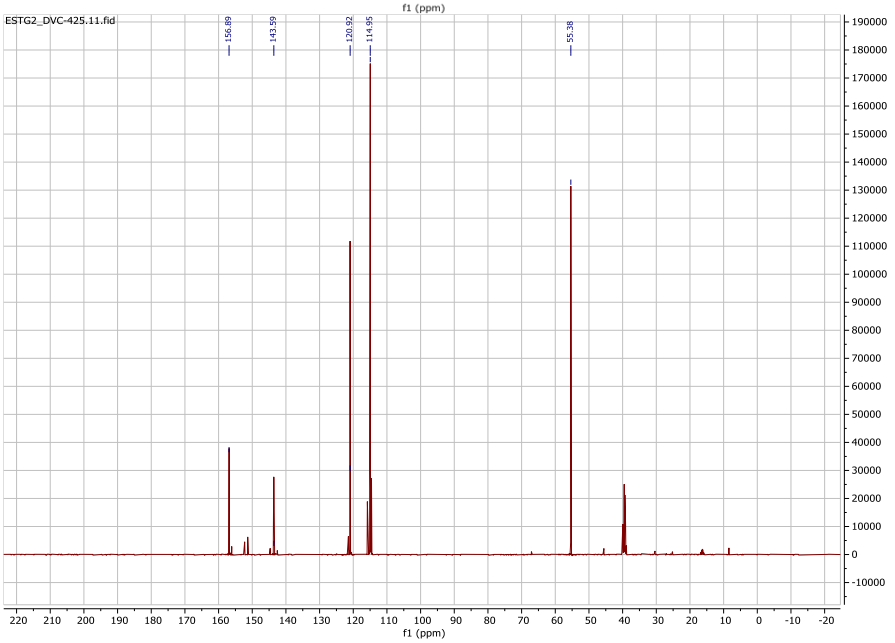

Benzyl ((diphenoxyphosphoryl)(phenyl)methyl)carbamate (16)

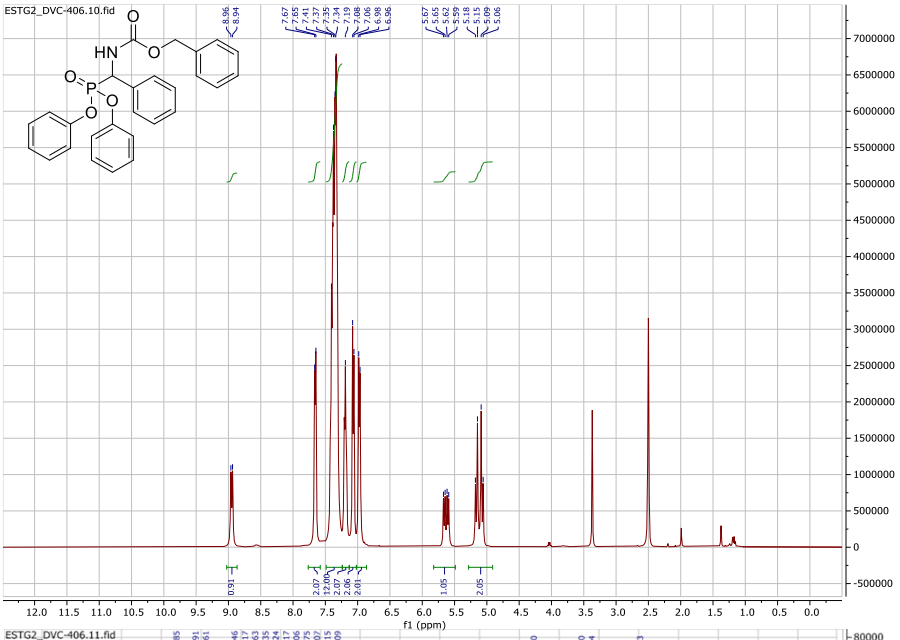

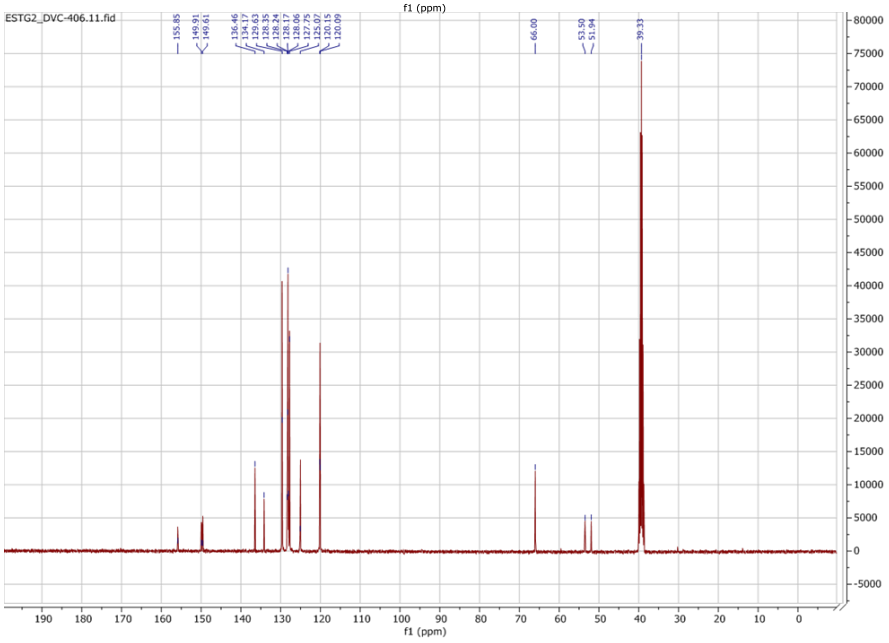

Benzyl((bis(4-methoxyphenoxy)phosphoryl)(phenyl)methyl)carbamate (185a)

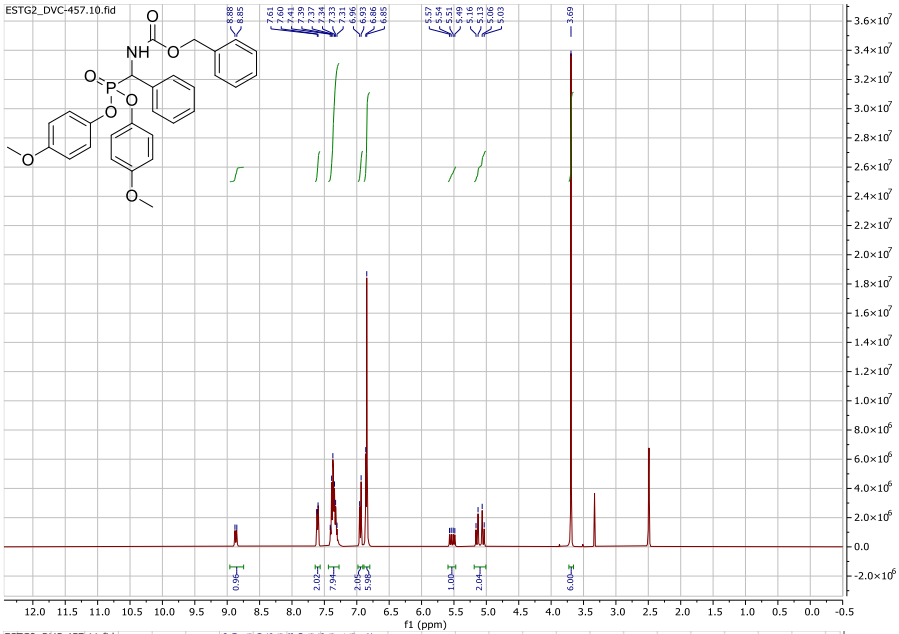

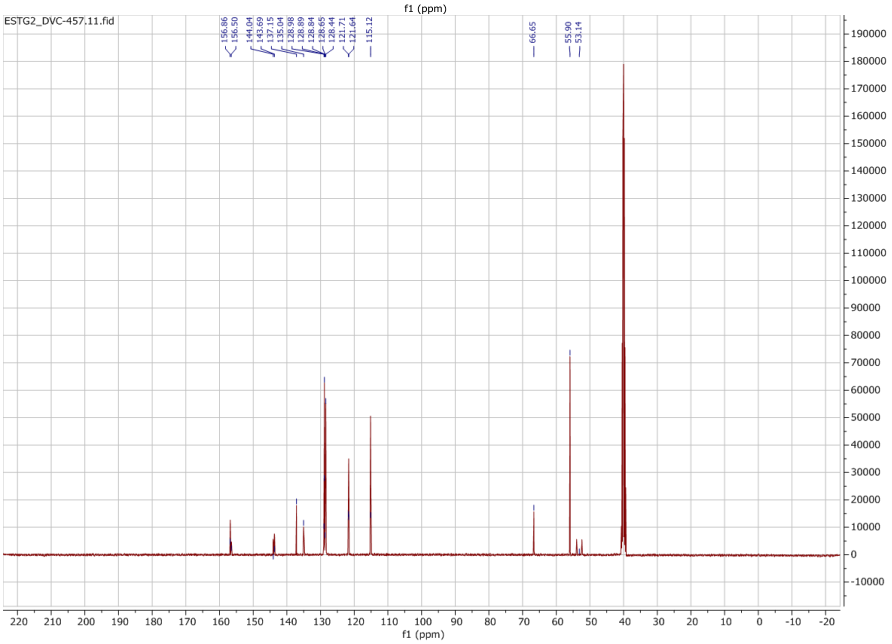

Benzyl ((bis(4-acetamidophenoxy)phosphoryl)(4-chlorophenyl)methyl)carbamate (185b)

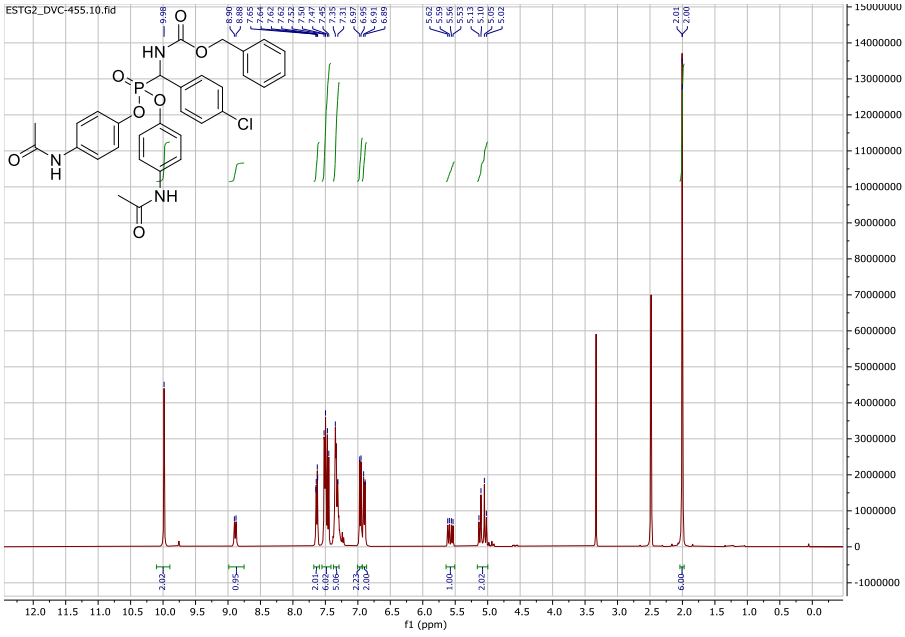

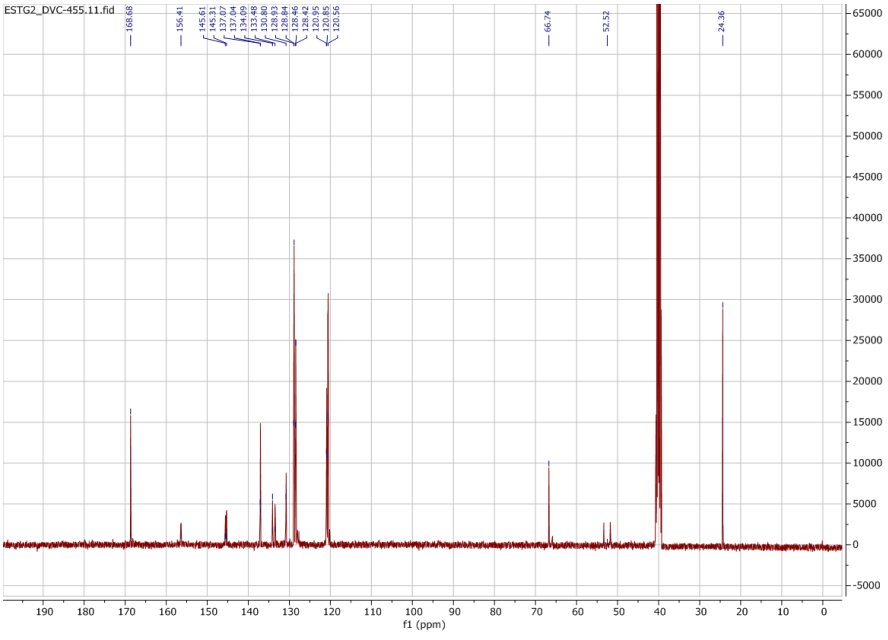

Benzyl (1-(diphenoxyphosphoryl)-2-phenylethyl)carbamate (185c)

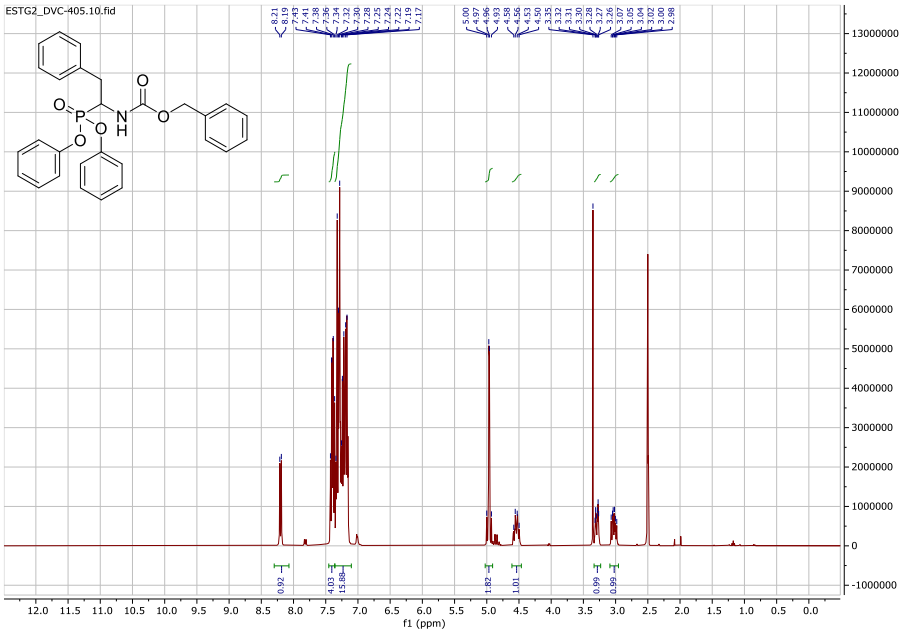

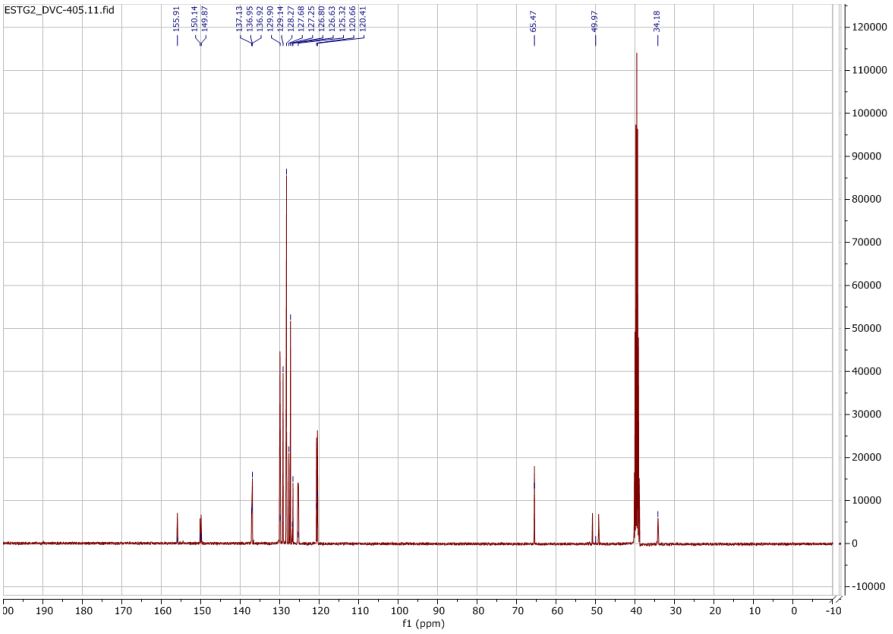

Benzyl(2-(4-((tert-butoxycarbonyl)amino)phenyl)-1-(diphenoxyphosphoryl)ethyl)carbamate (185d)

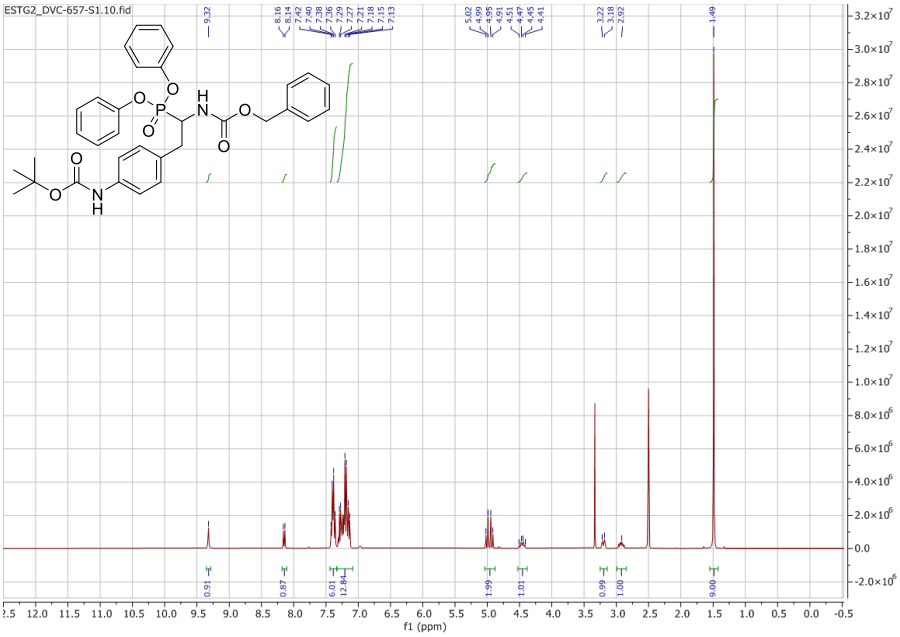

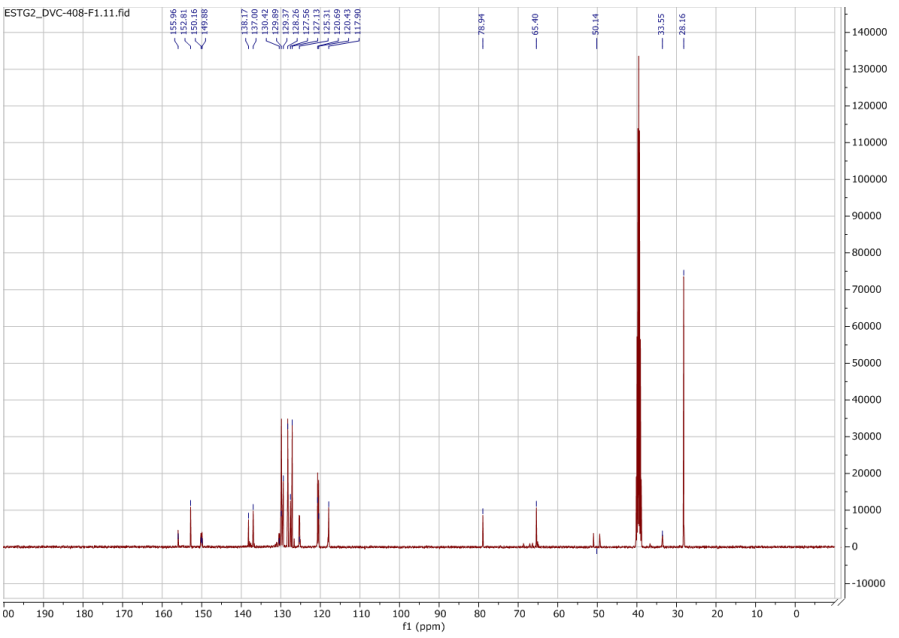

Benzyl ((bis(p-tolyloxy)phosphoryl)(phenyl)methyl)carbamate (185e)

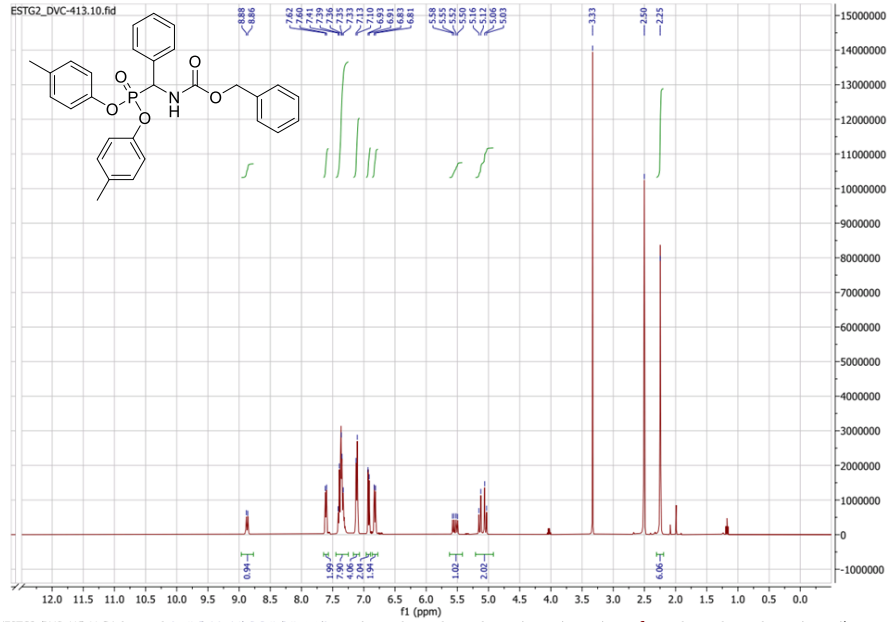

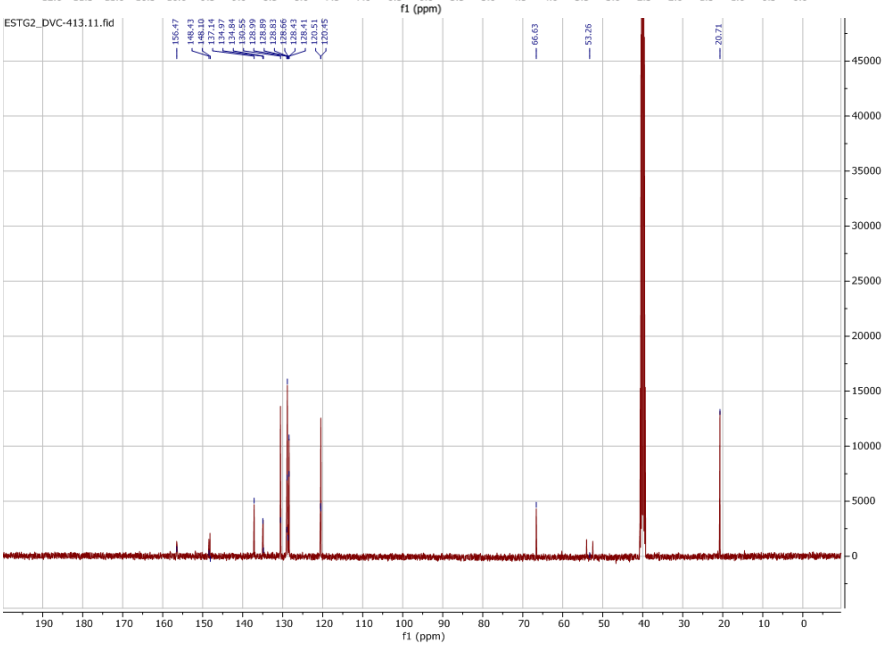

Benzyl ((bis(4-acetamidophenoxy)phosphoryl)(phenyl)methyl)carbamate (185f)

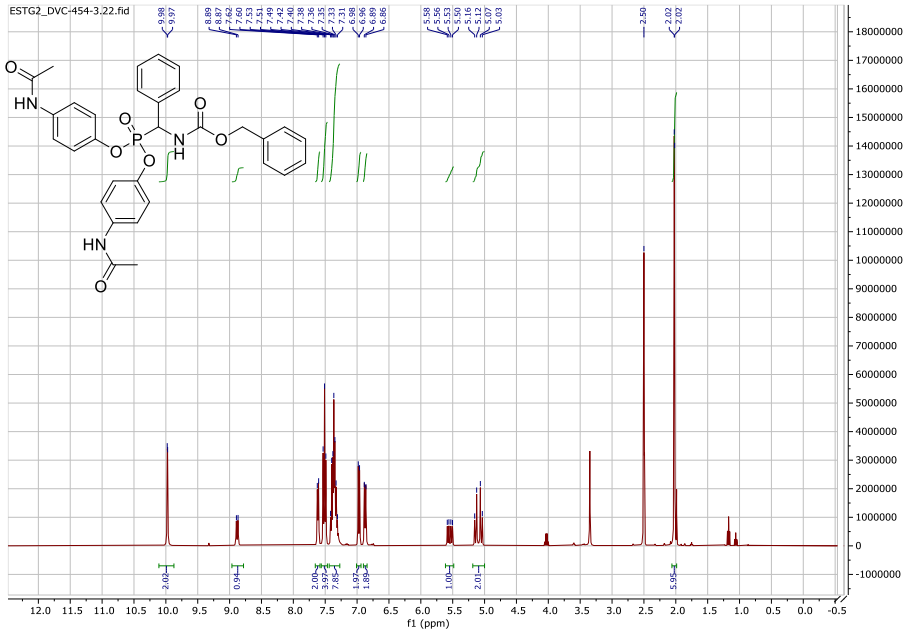

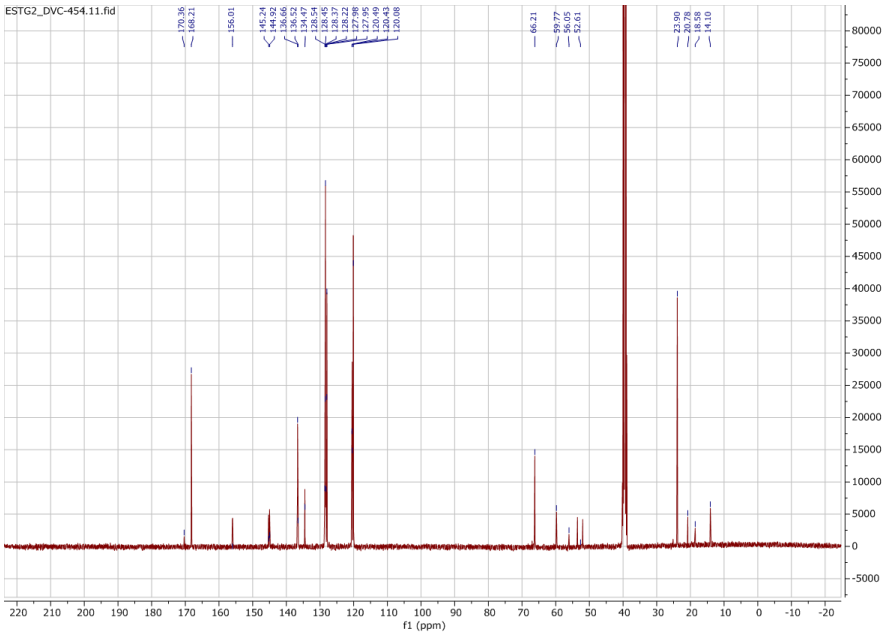

Benzyl ((4-chlorophenyl)(diphenoxyphosphoryl)methyl)carbamate (185g)

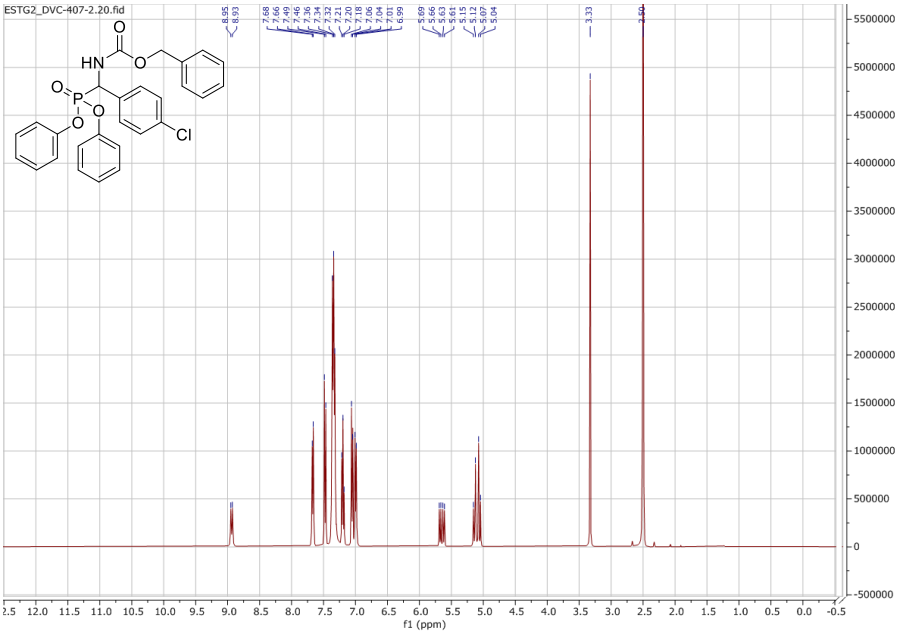

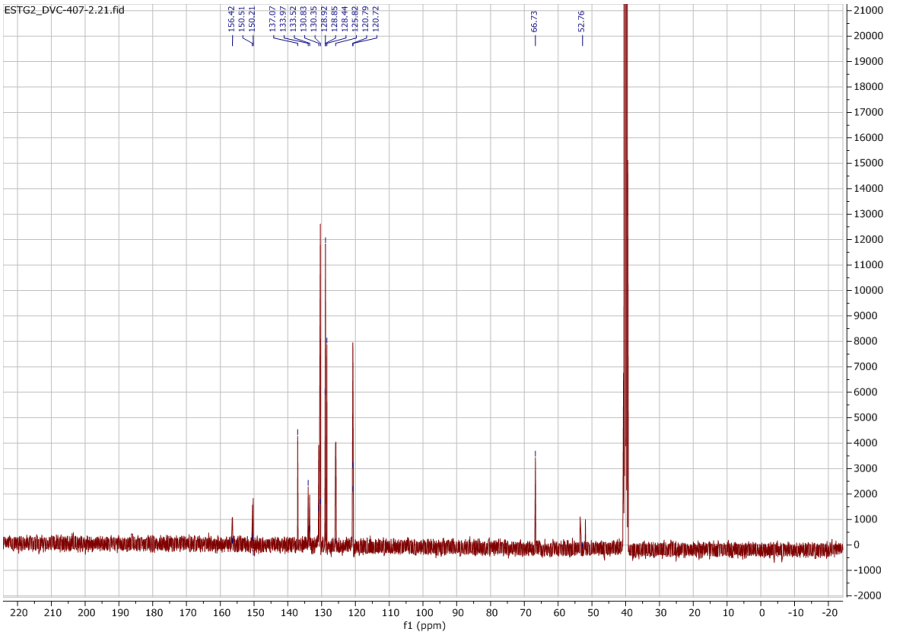

Benzyl ((4-bromophenyl)(diphenoxyphosphoryl)methyl)carbamate (185h)

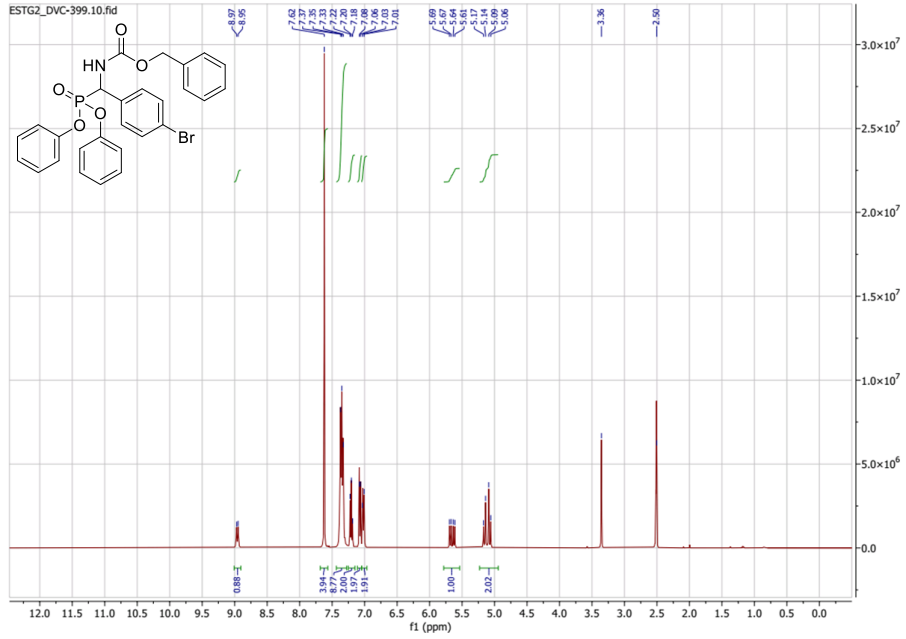

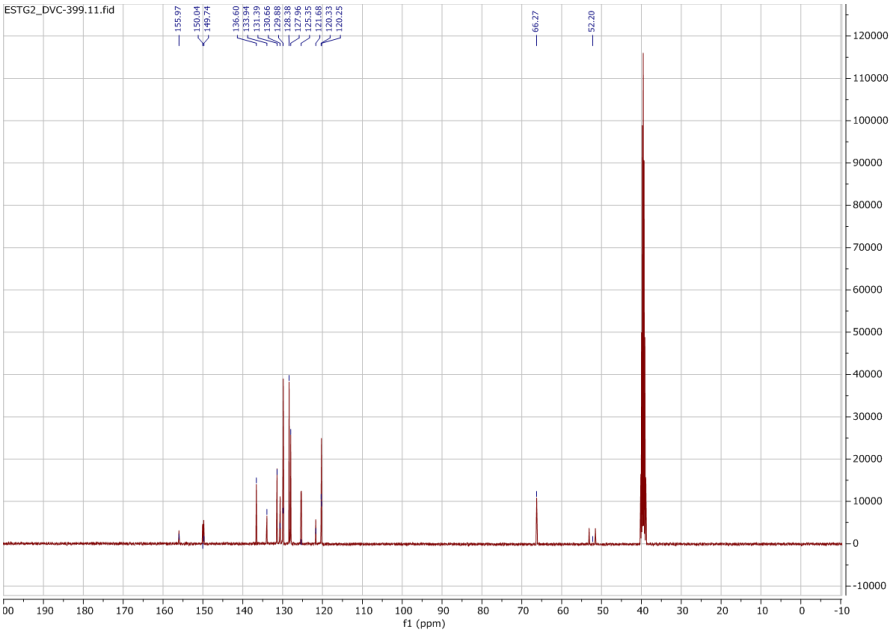

Benzyl((diphenoxyphosphoryl)(4-fluorophenyl)methyl)carbamate (185i)

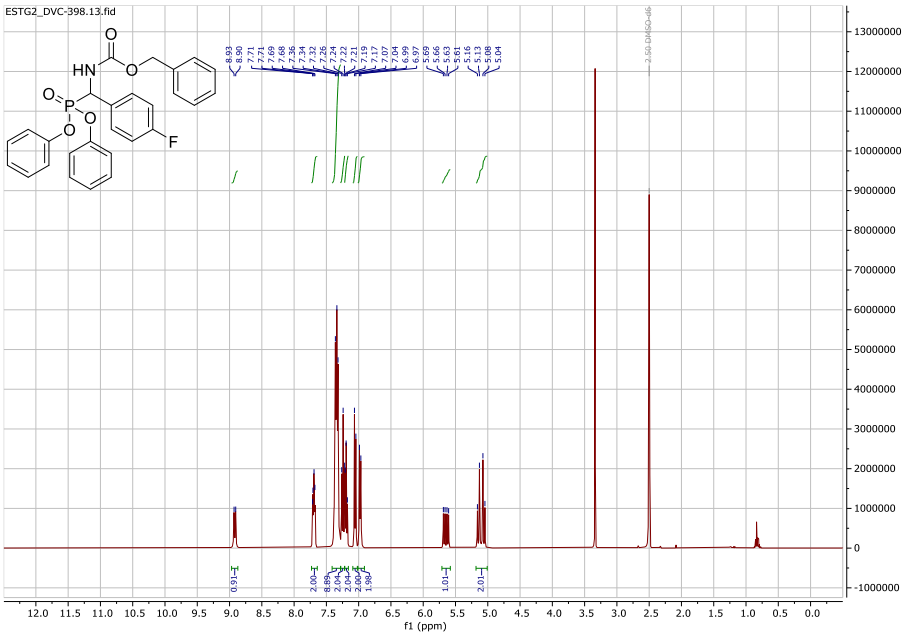

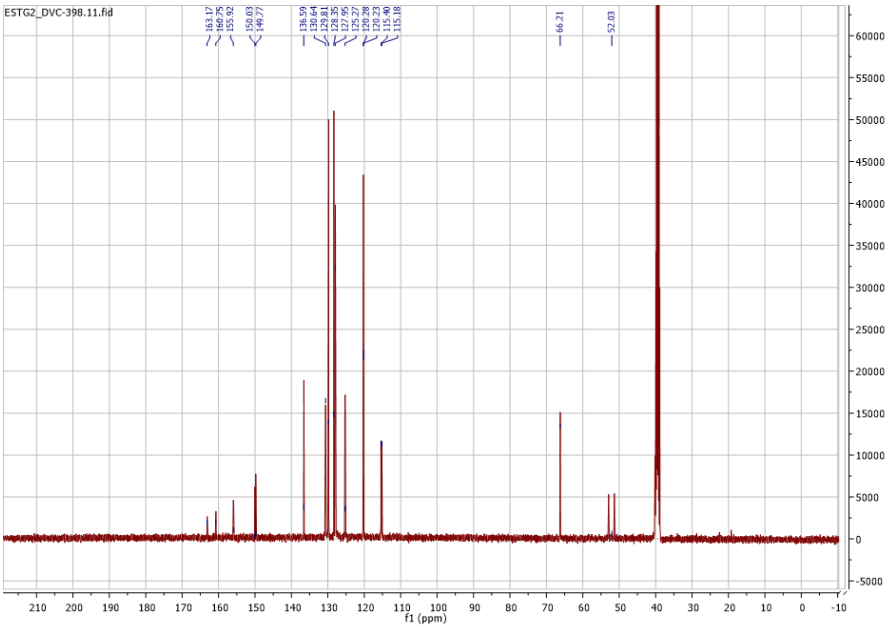

Benzyl ((diphenoxyphosphoryl)(4-iodophenyl)methyl)carbamate (185j)

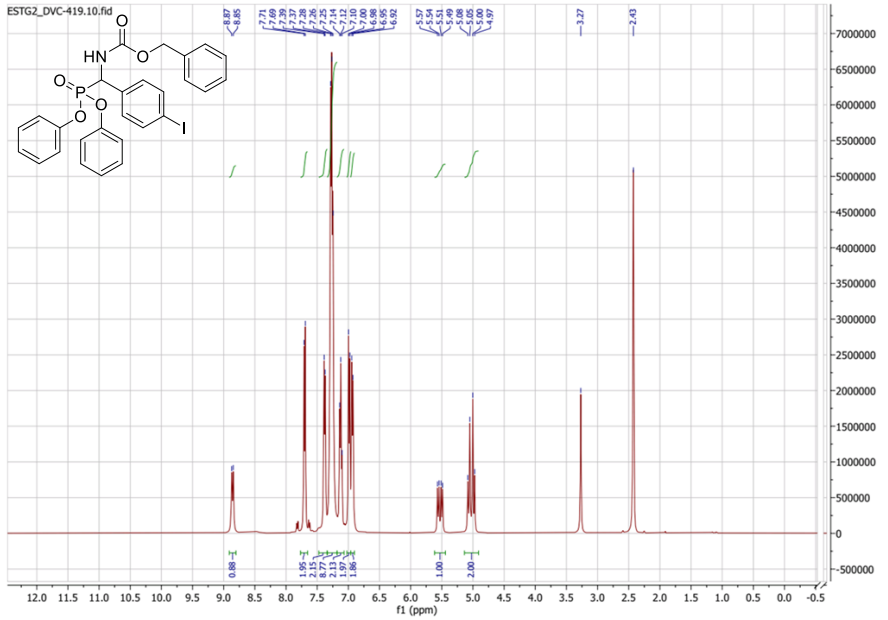

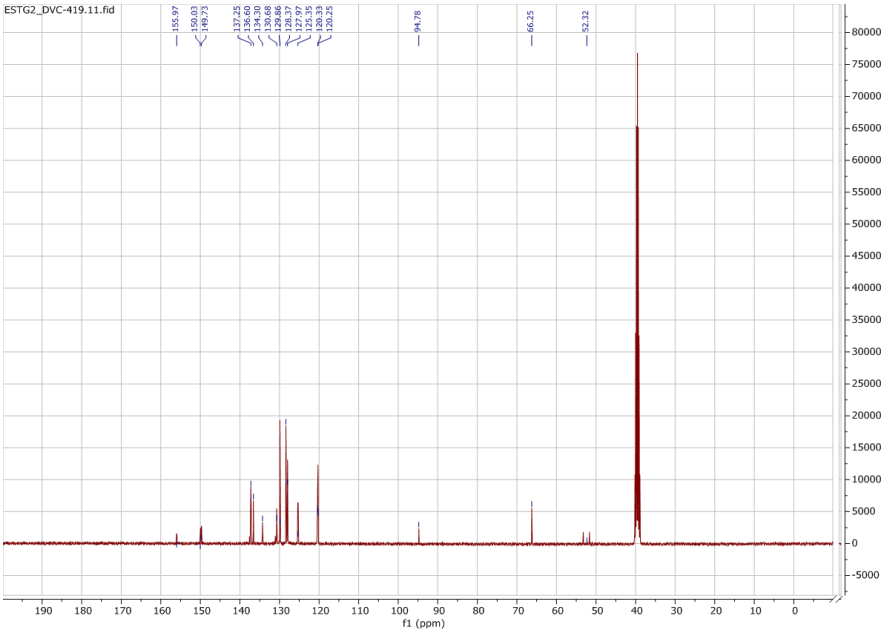

Tert-butyl((diphenoxyphosphoryl)(phenyl)methyl)carbamate (185k)

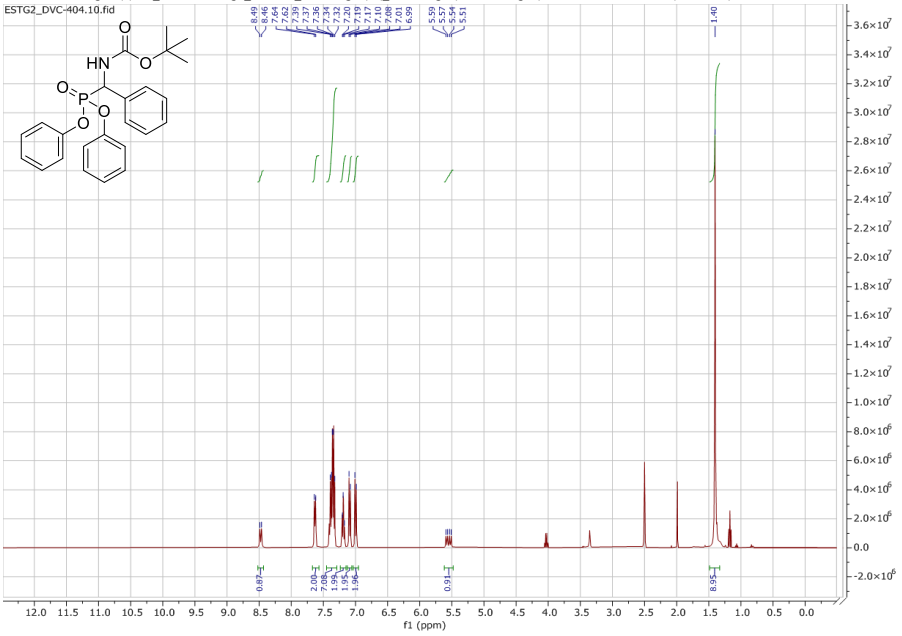

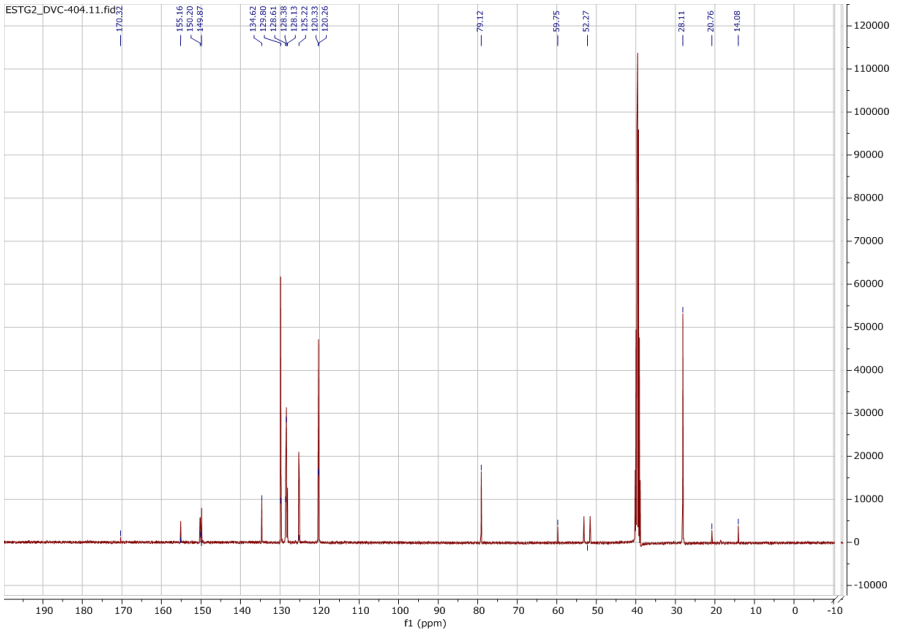

Tert-butyl((diphenoxyphosphoryl)(4-nitrophenyl)methyl)carbamate (185l)

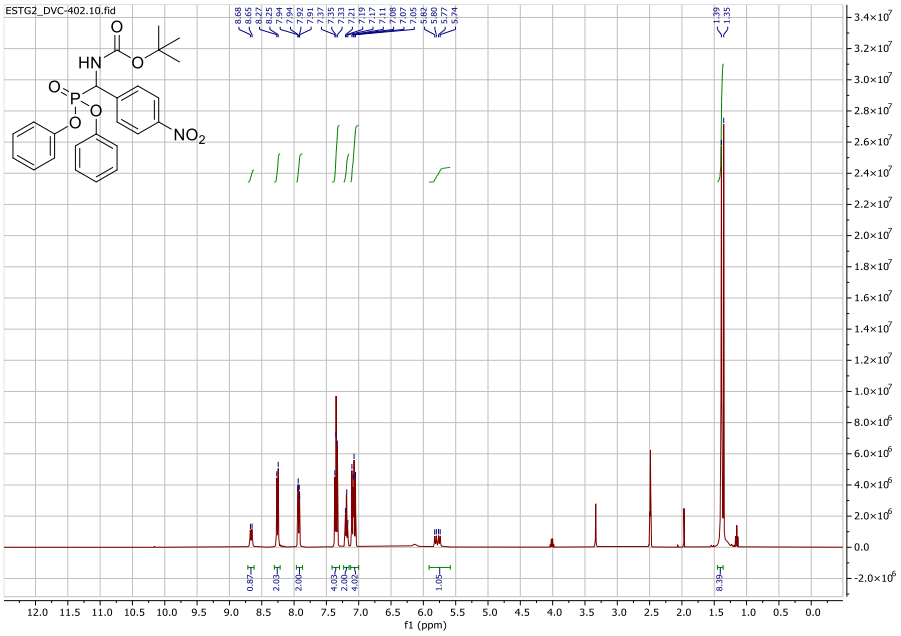

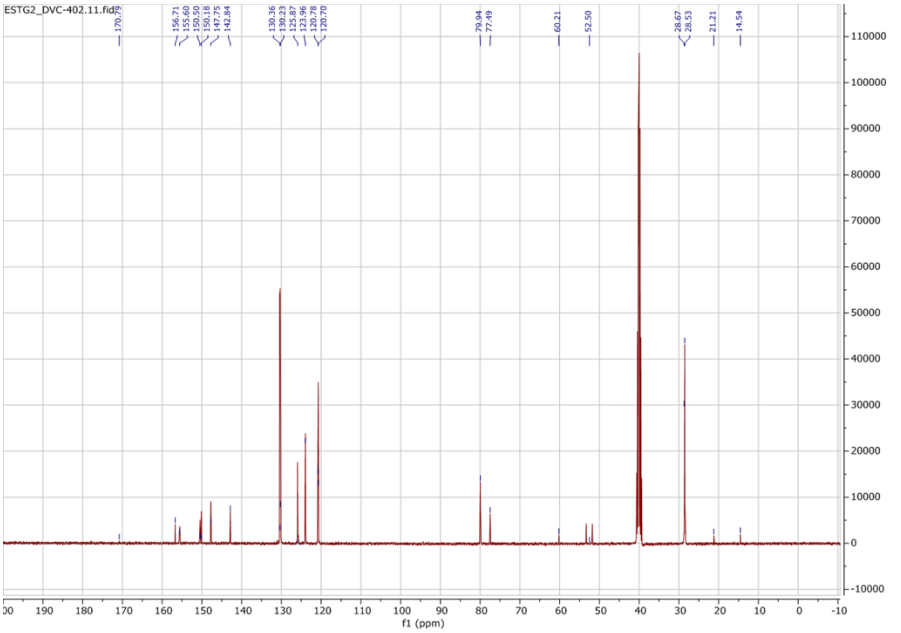

Tert-butyl((diphenoxyphosphoryl)(4-(methylthio)phenyl)methyl)carbamate (185m)

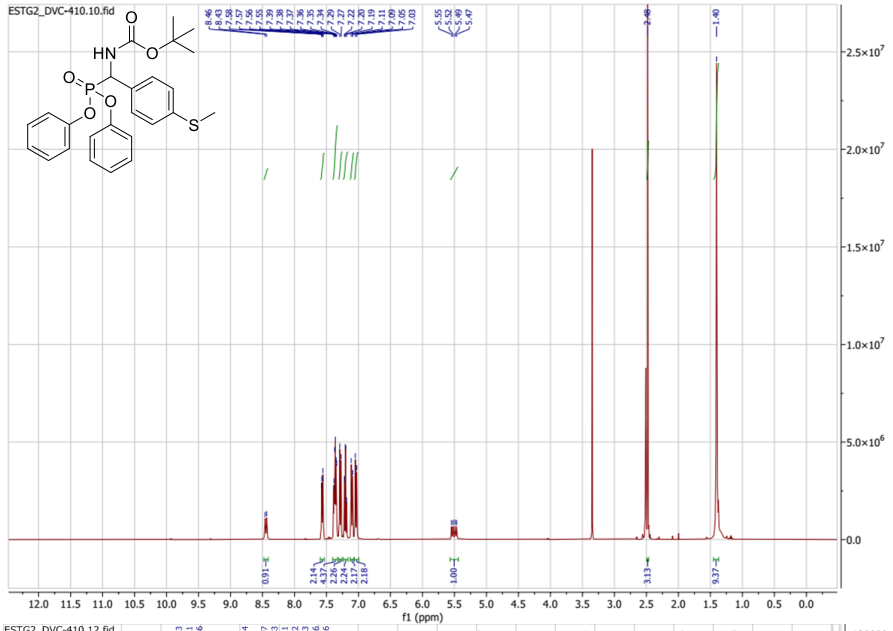

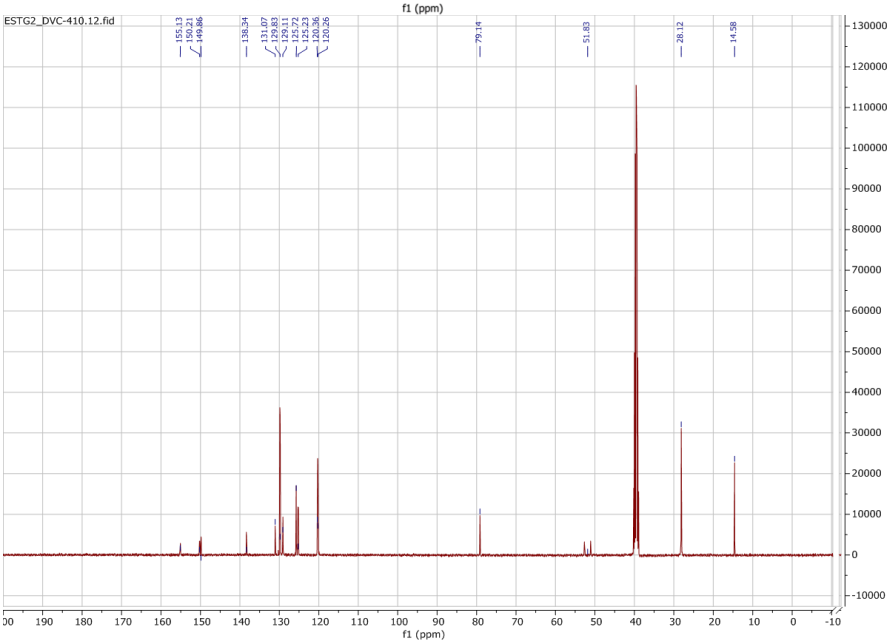

Benzyl((diphenoxyphosphoryl)(4-nitrophenyl)methyl)carbamate (185n)

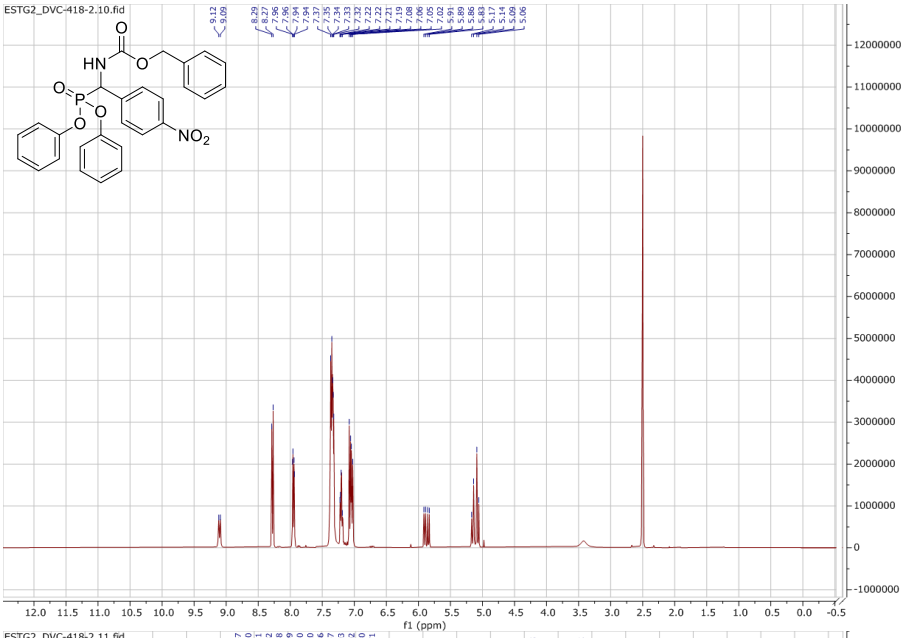

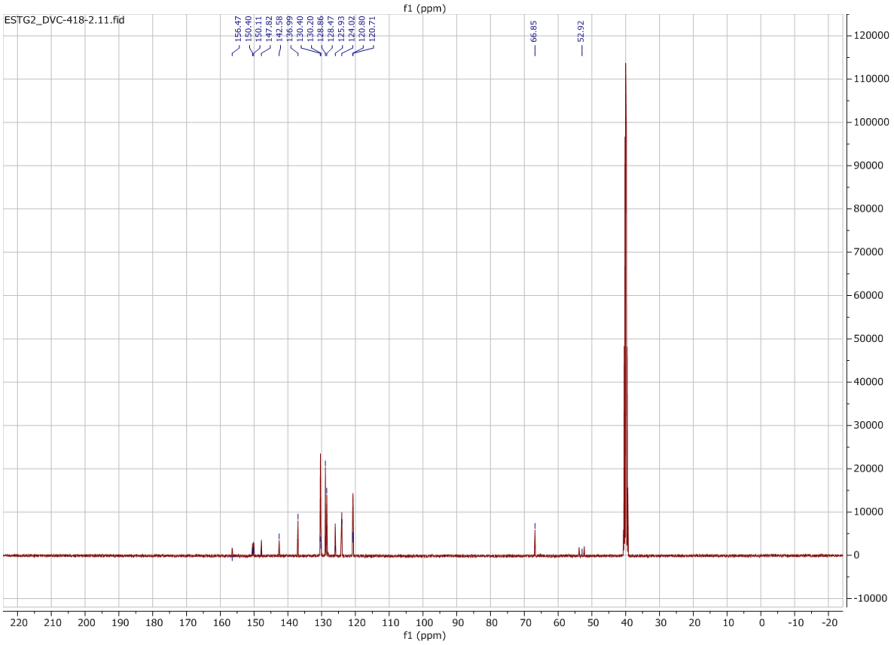

Benzyl ((bis(o-tolyloxy)phosphoryl)(phenyl)methyl)carbamate (185o)

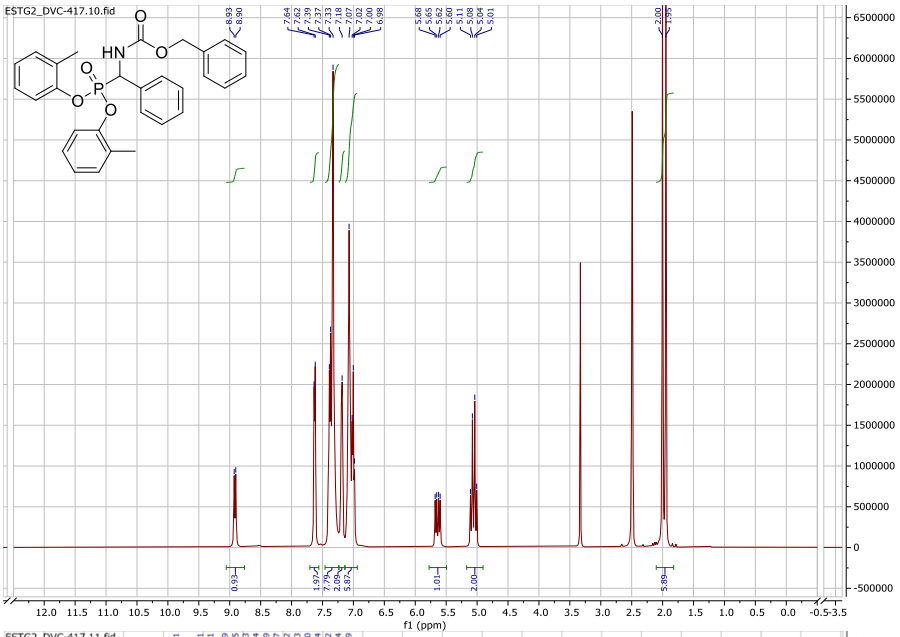

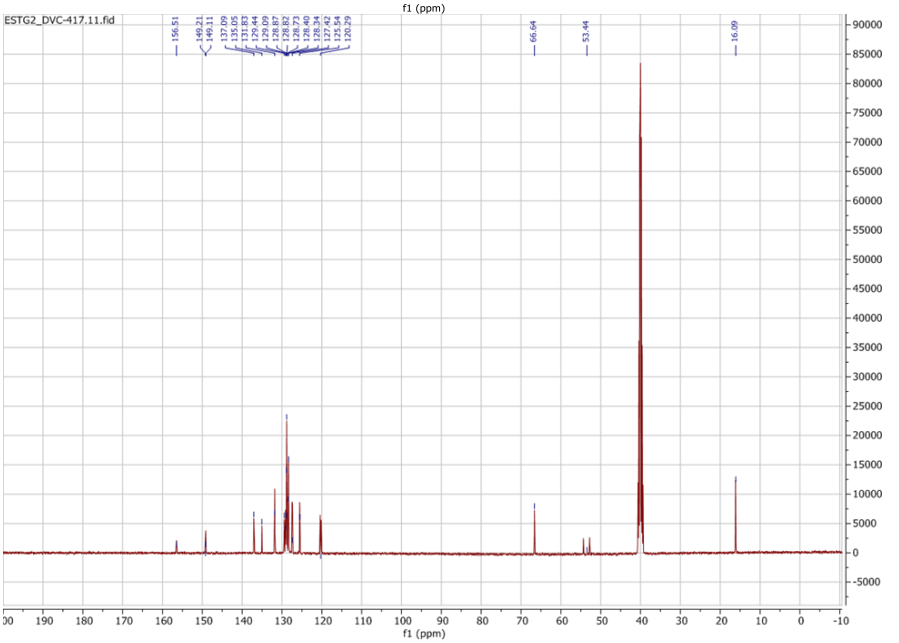

Benzyl ((bis(o-tolyloxy)phosphoryl)(4-chlorophenyl)methyl)carbamate (185p)

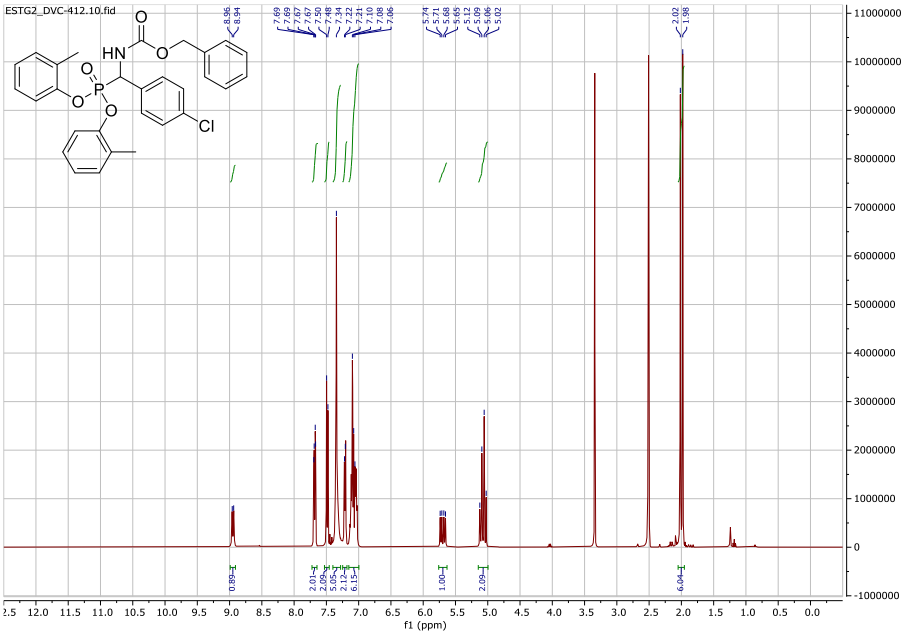

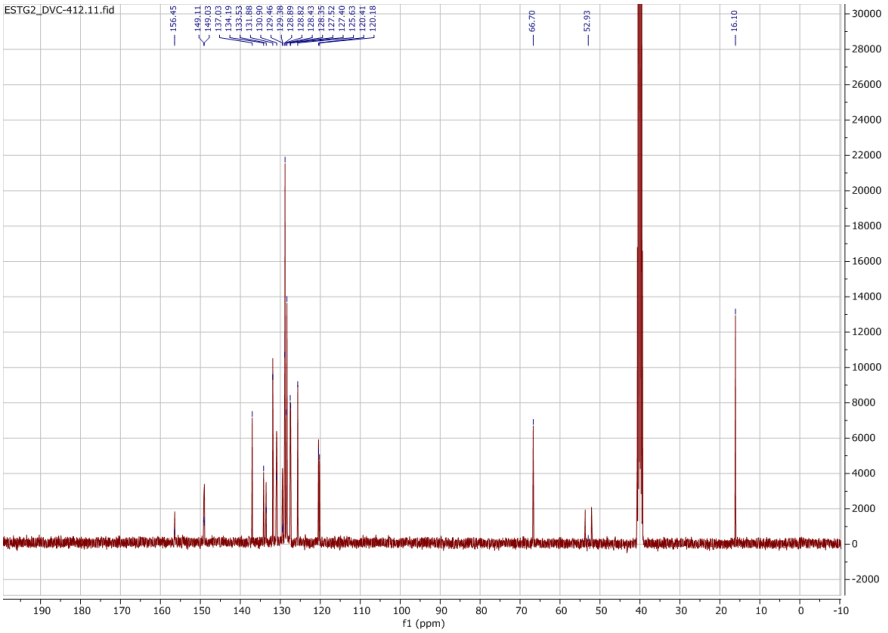

Benzyl ((bis(p-tolyloxy)phosphoryl)(4-chlorophenyl)methyl)carbamate (185q)

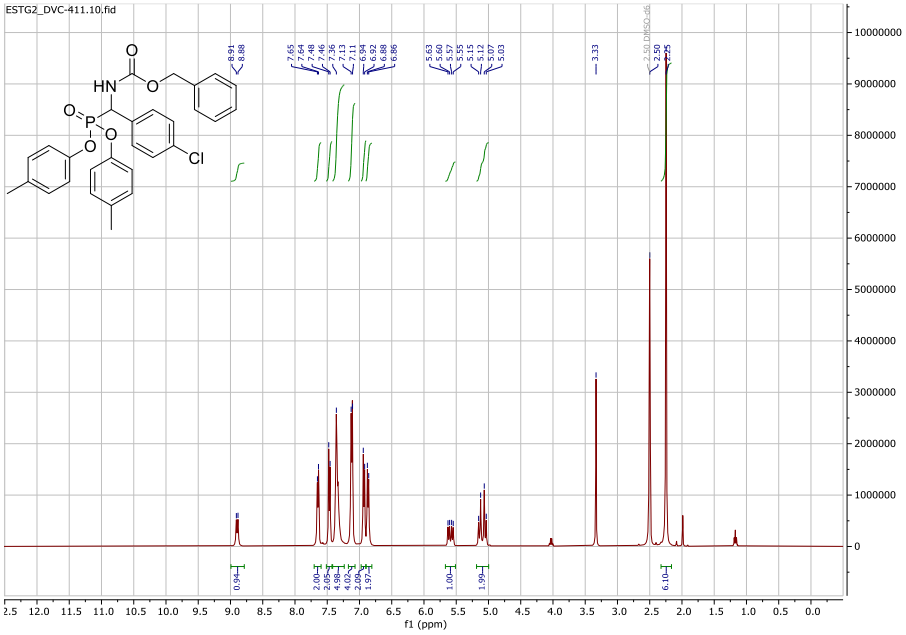

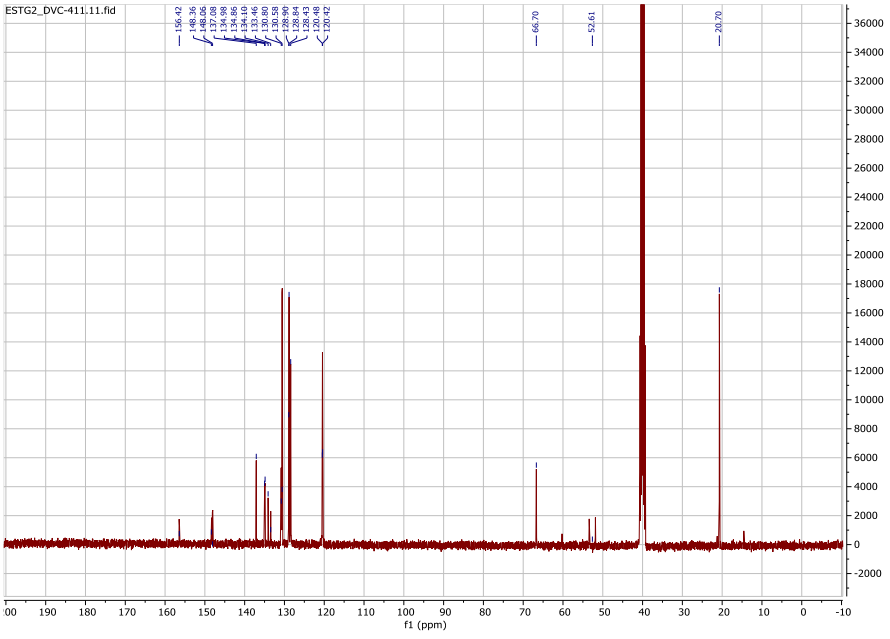

Benzyl ((bis(4-methoxyphenoxy)phosphoryl)(4-chlorophenyl)methyl)carbamate (185r)

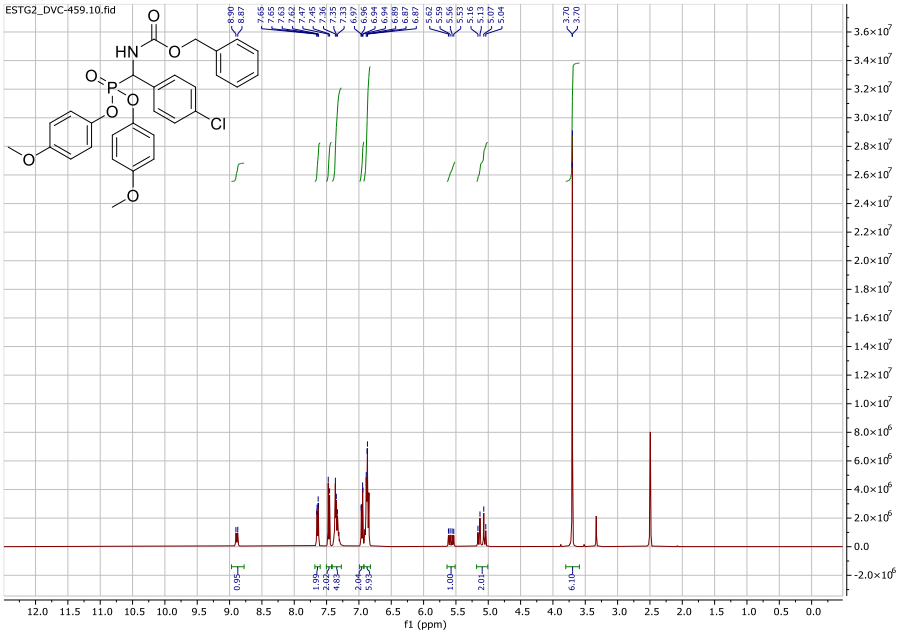

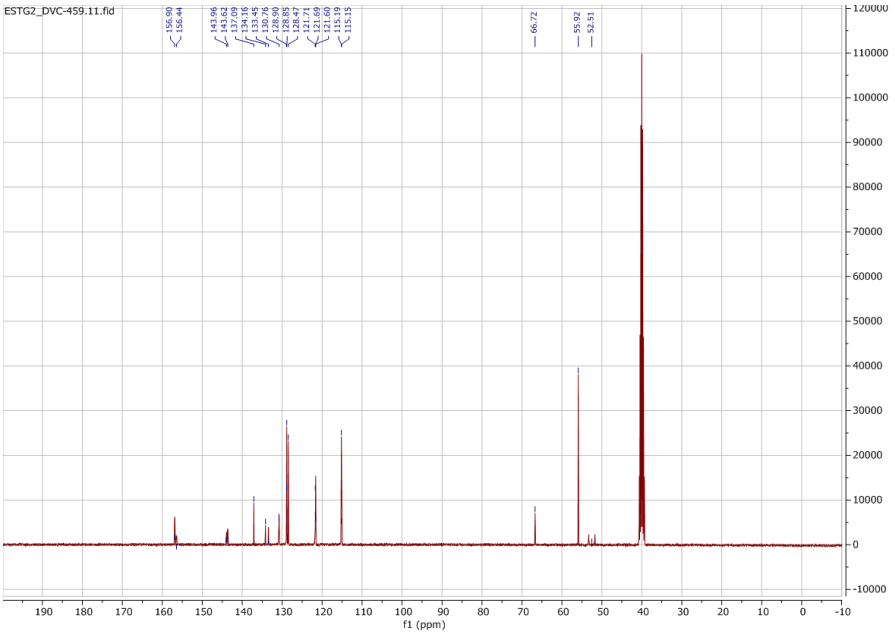

Benzyl((4-cyanophenyl)(diphenoxyphosphoryl)methyl)carbamate (185s)

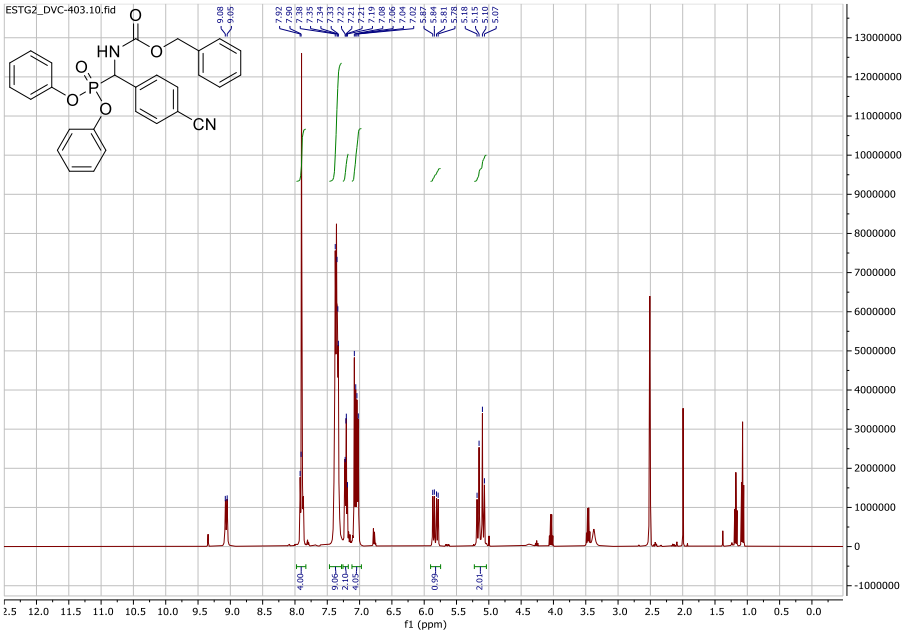

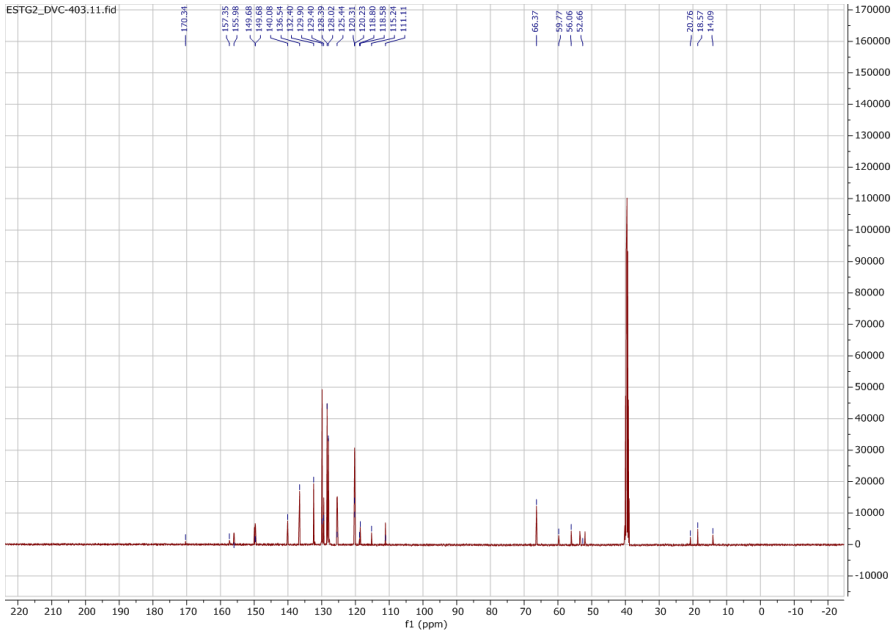

Benzyl((bis(p-tolyloxy)phosphoryl)(4-cyanophenyl)methyl)carbamate (185t)

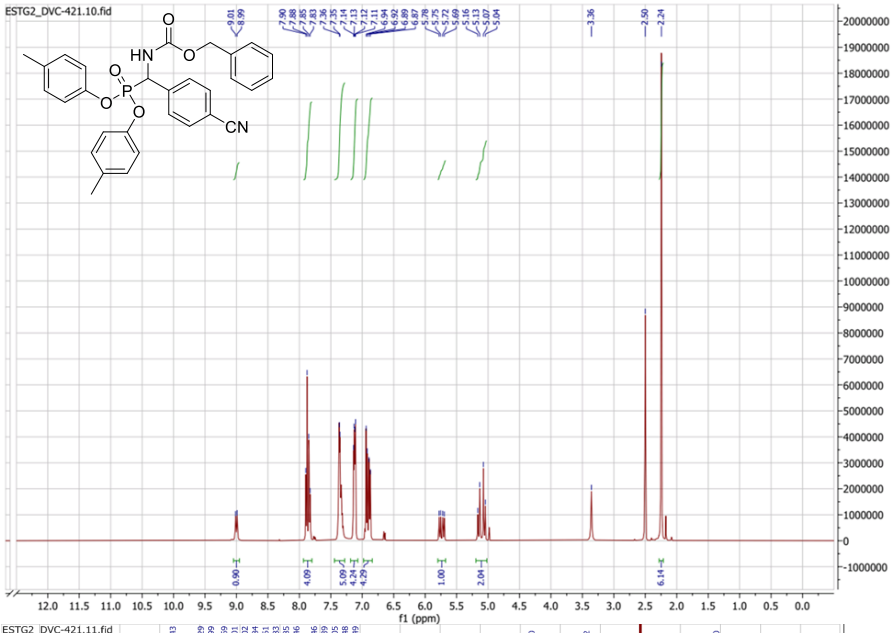

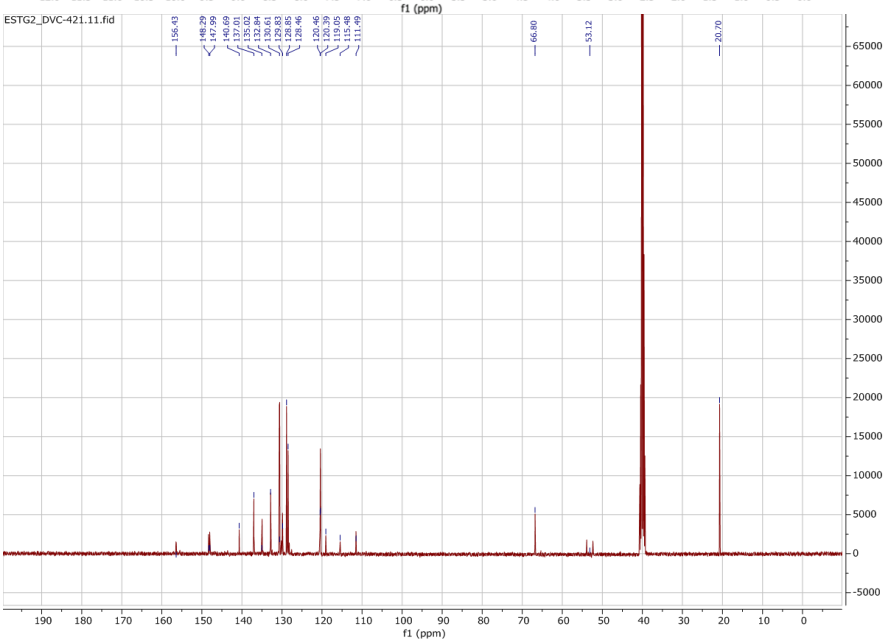

Benzyl ((diphenoxyphosphoryl)(4-hydroxy-3-methoxyphenyl)methyl)carbamate (185u)

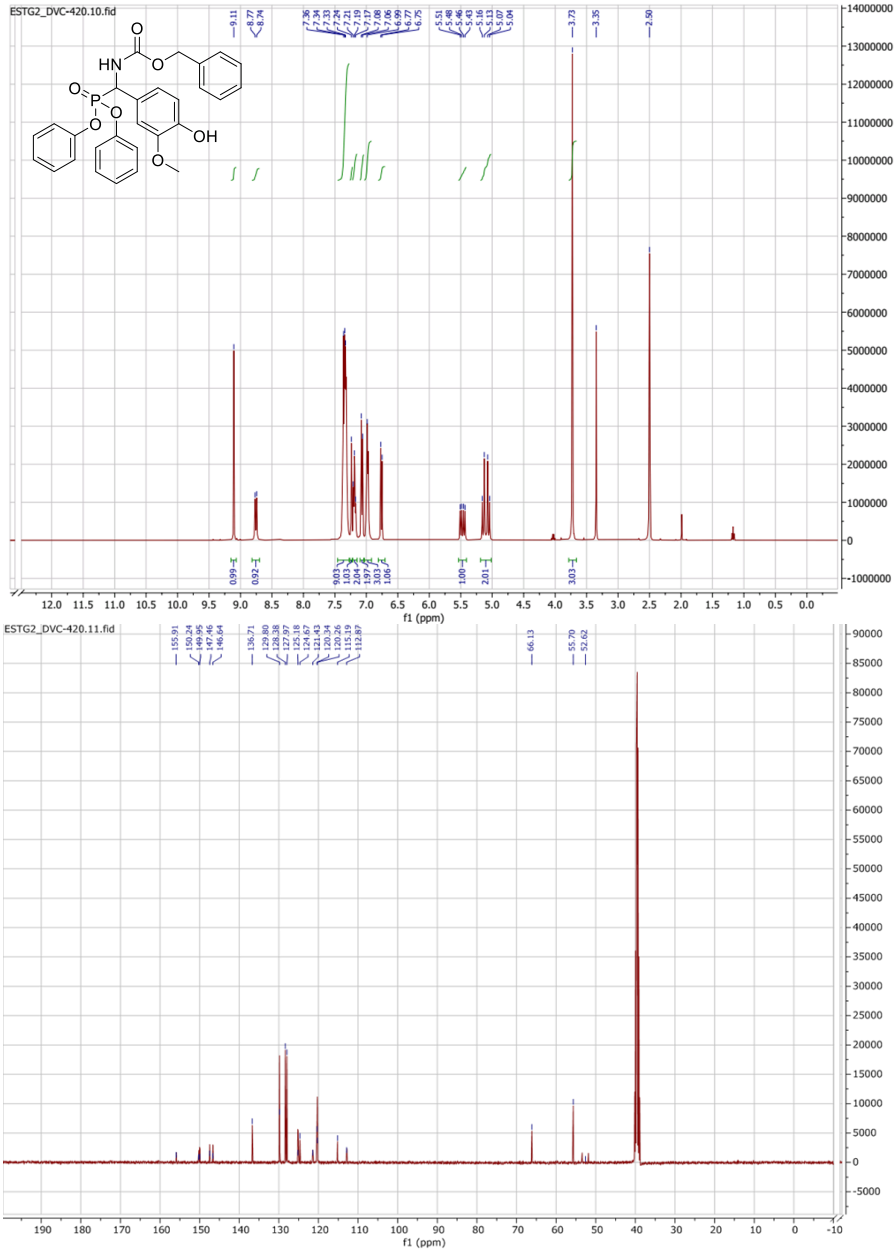

Methyl 4-((((benzyloxy)carbonyl)amino)(diphenoxyphosphoryl)methyl)benzoate (185v)

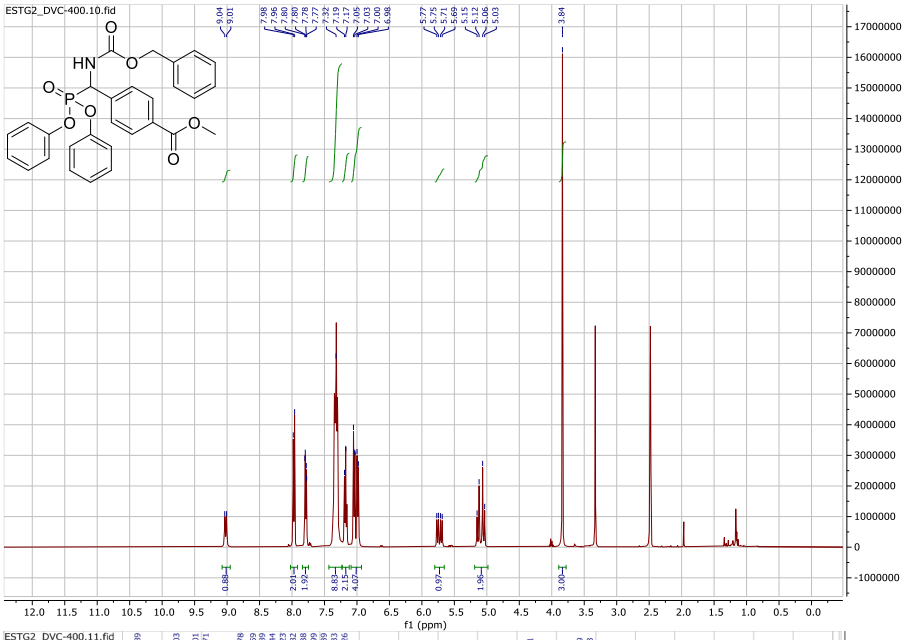

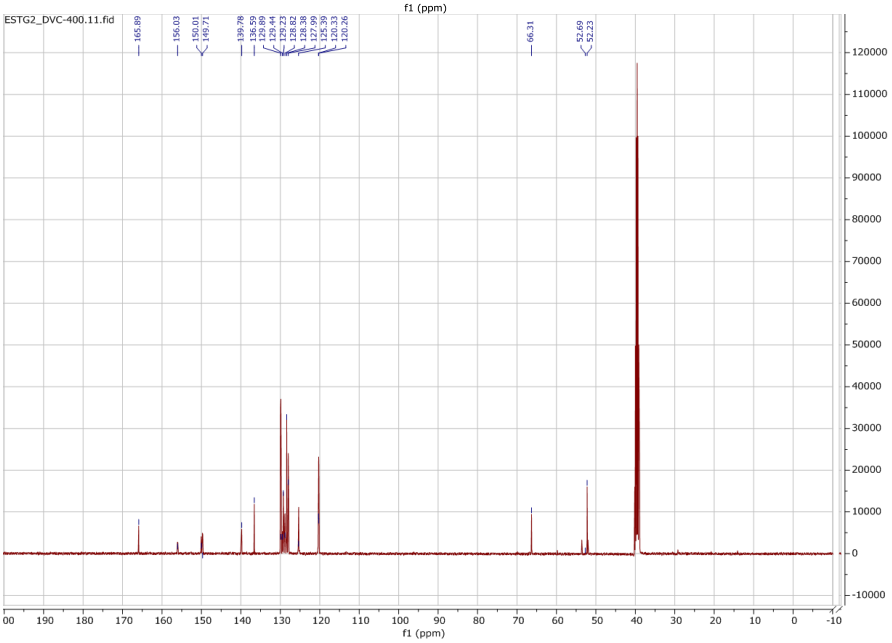

Benzyl ((bis(4-acetamidophenoxy)phosphoryl)(4-((tert-butoxycarbonyl)amino)phenyl)-methyl) carbamate (193)

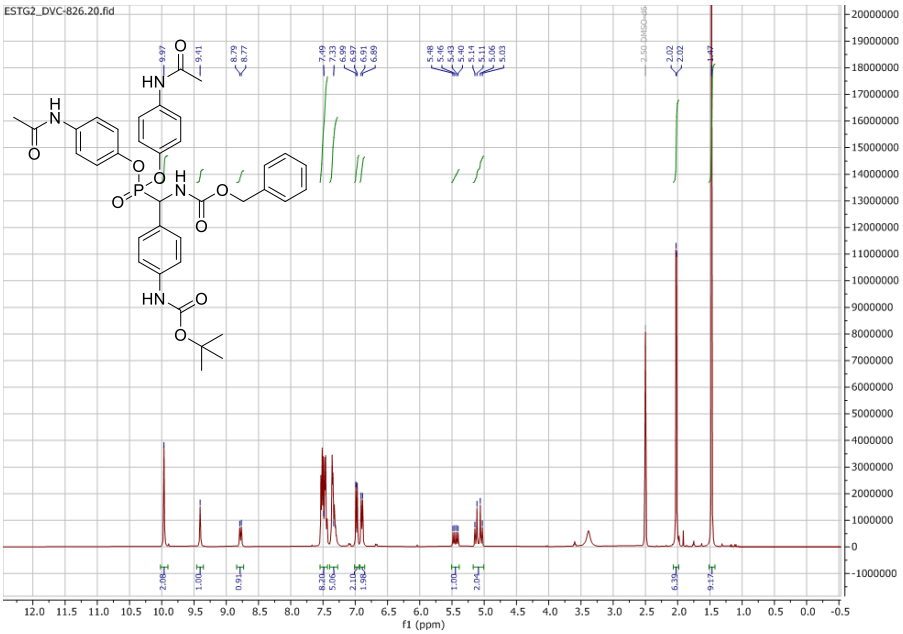

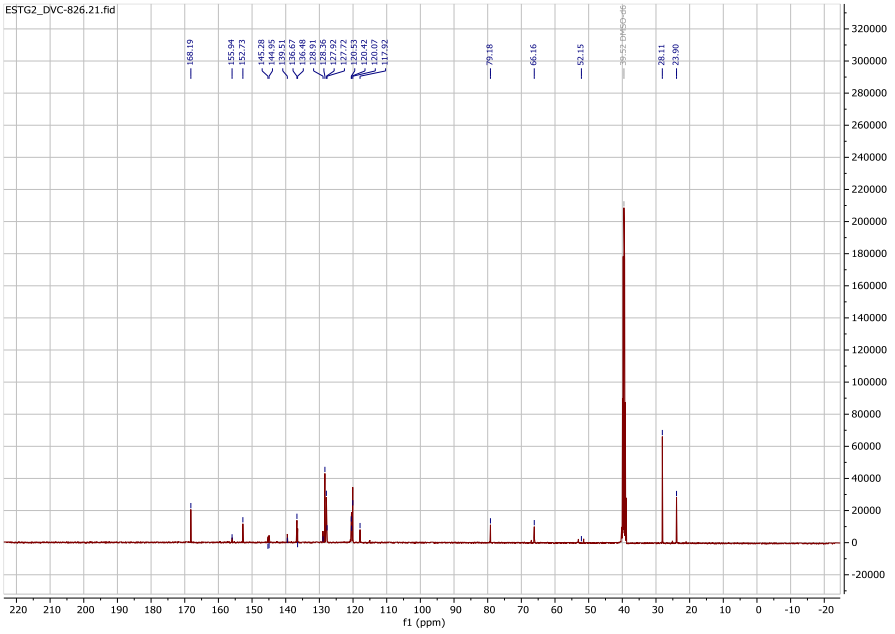

4-((((benzyloxy)carbonyl)amino)(bis(4-acetamidophenoxy)phosphoryl)methyl)benzenaminium trifluoroacetate (194)

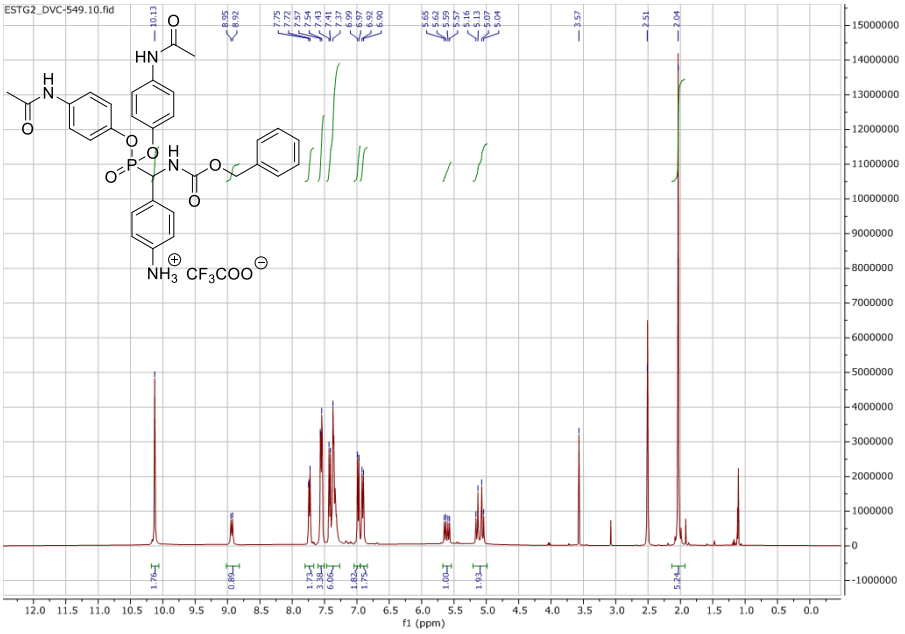

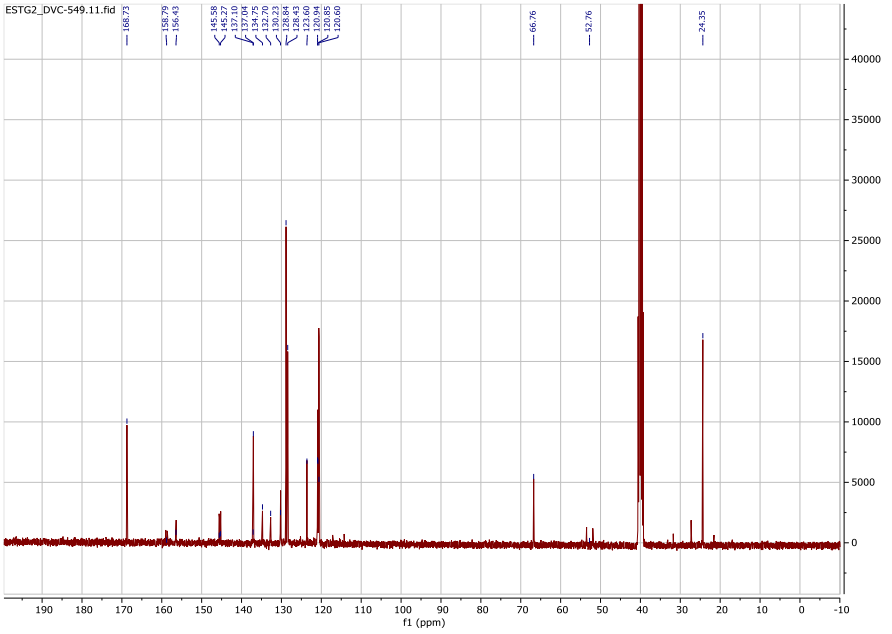

Benzyl(E)-((bis(4-acetamidophenoxy)phosphoryl)(4-(N.N'-bis(tert-butyloxycarbonyl)guanidino)phenyl)methyl)carbamate (196)

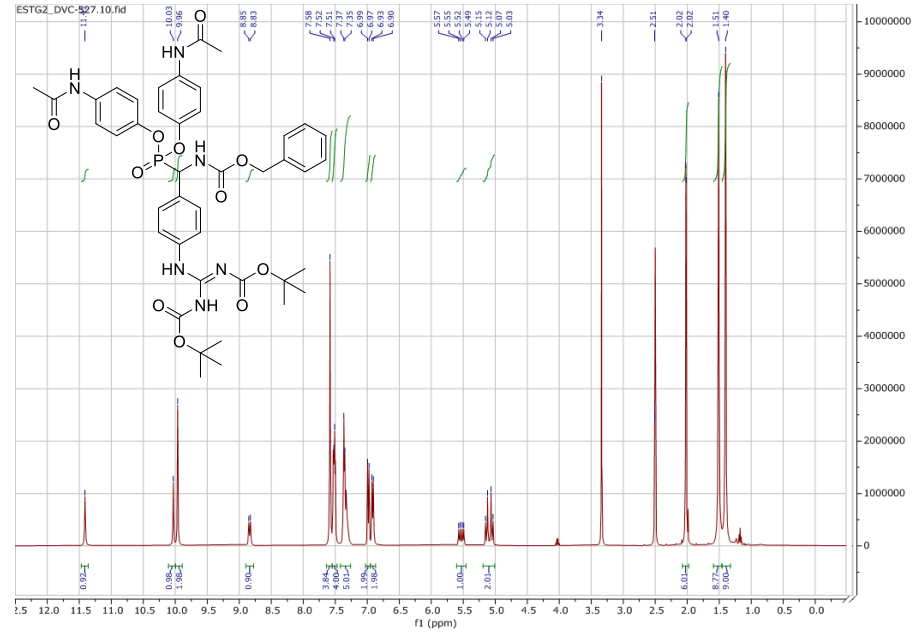

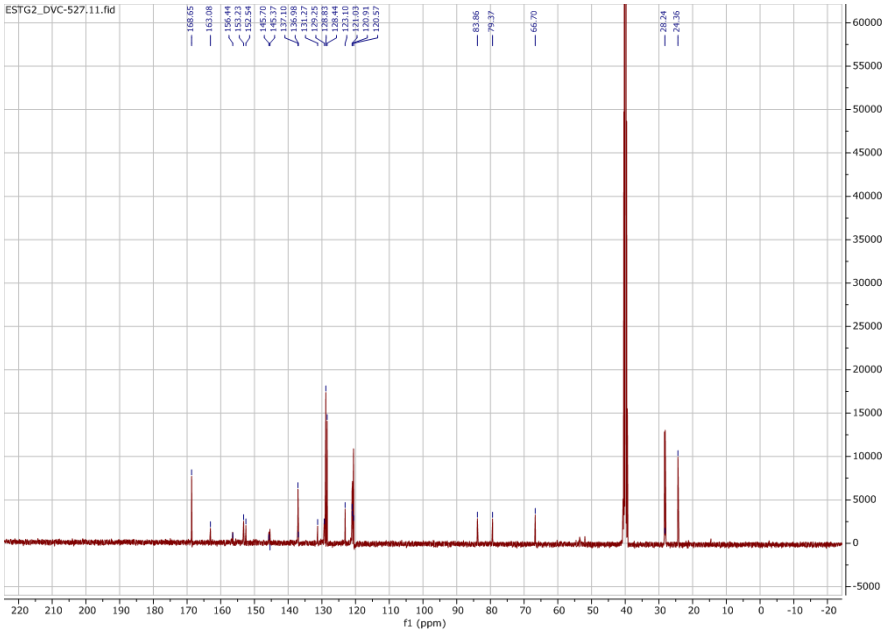

Amino((4-((((benzyloxy)carbonyl)amino)(bis(4-acetamidophenoxy)phosphoryl)methyl)-phenyl) amino)methaniminium trifluoroacetate (197)

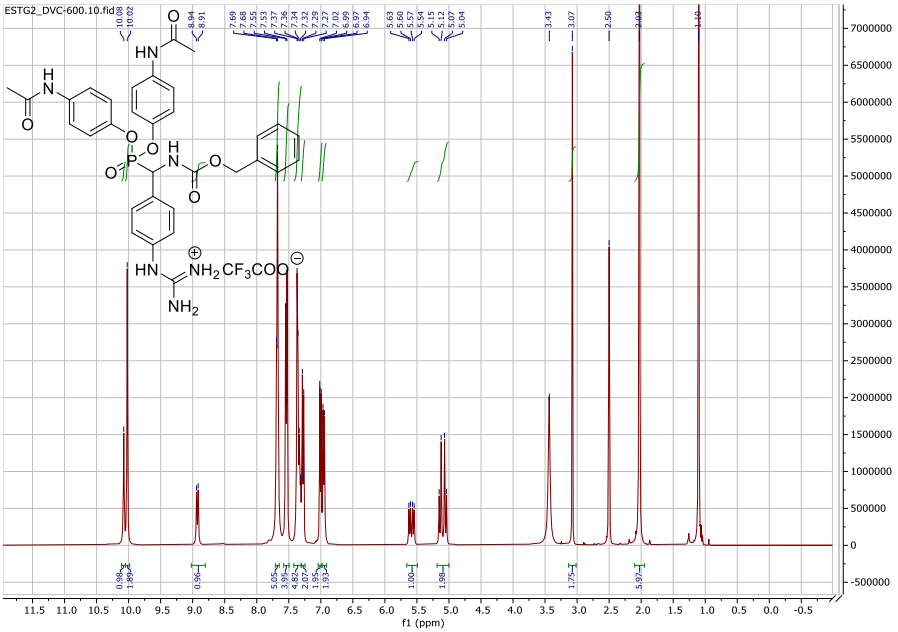

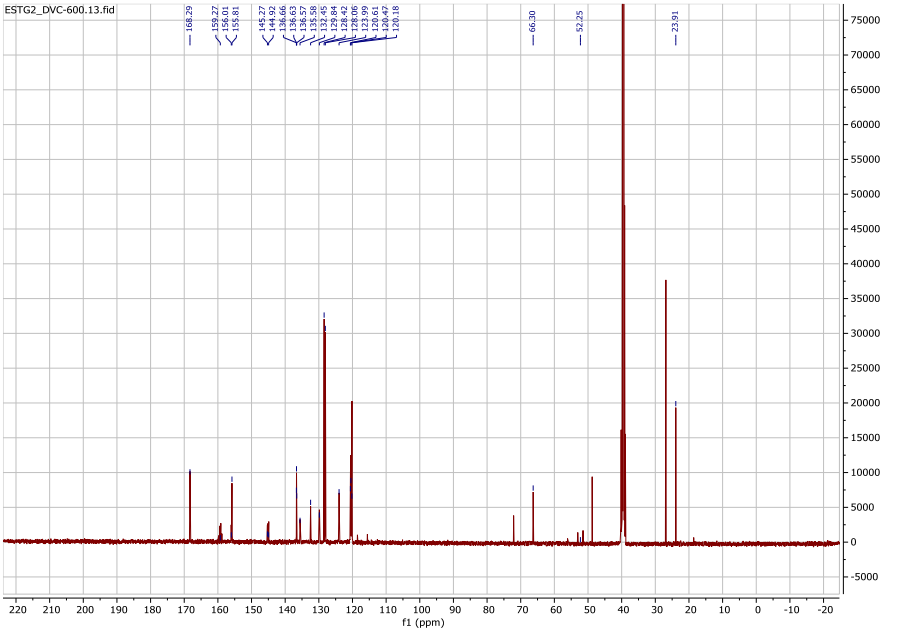

Amino((4-((((benzyloxy)carbonyl)amino)(bis(4-acetamidophenoxy)phosphoryl)methyl)-phenyl) amino)methaniminium chloride (14)

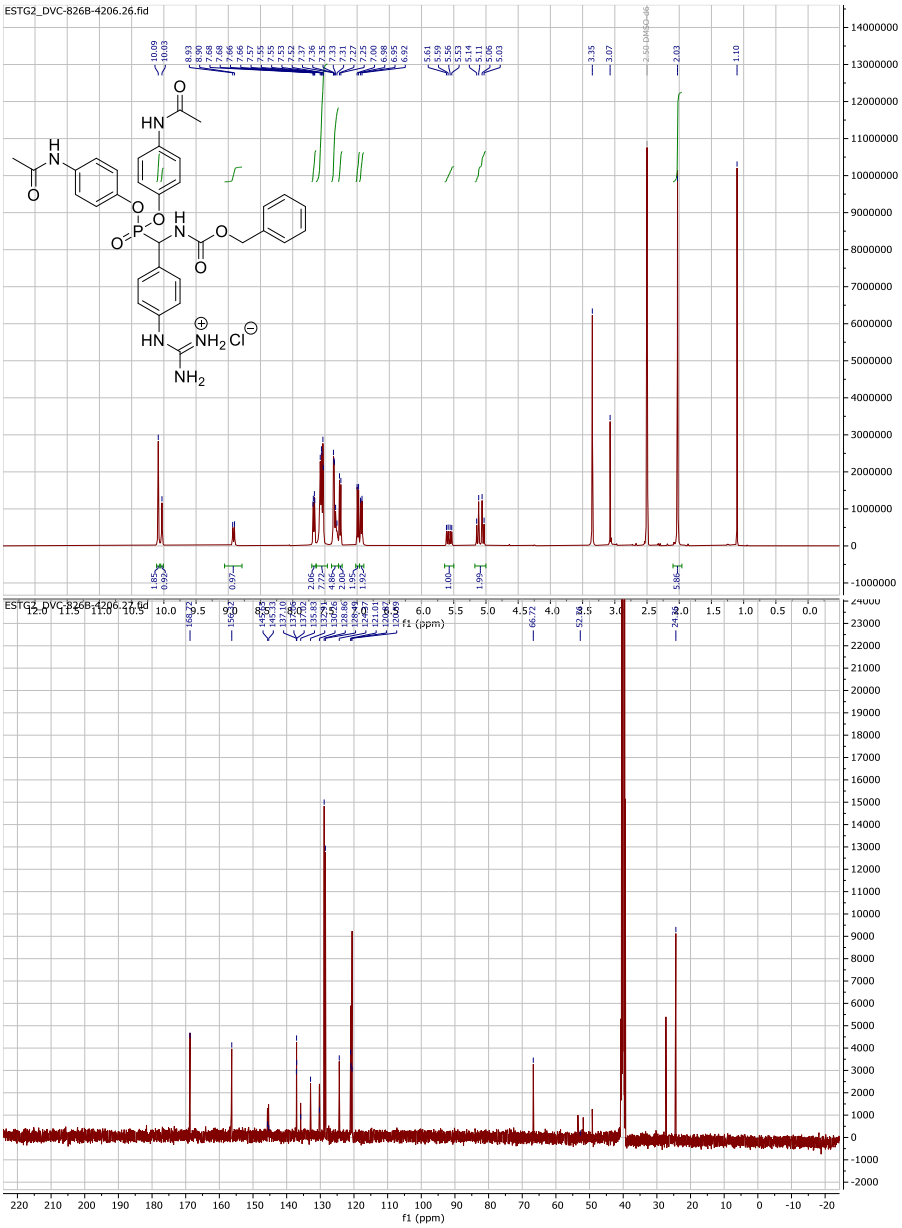

Tris(4-chlorophenyl)phosphite (205)

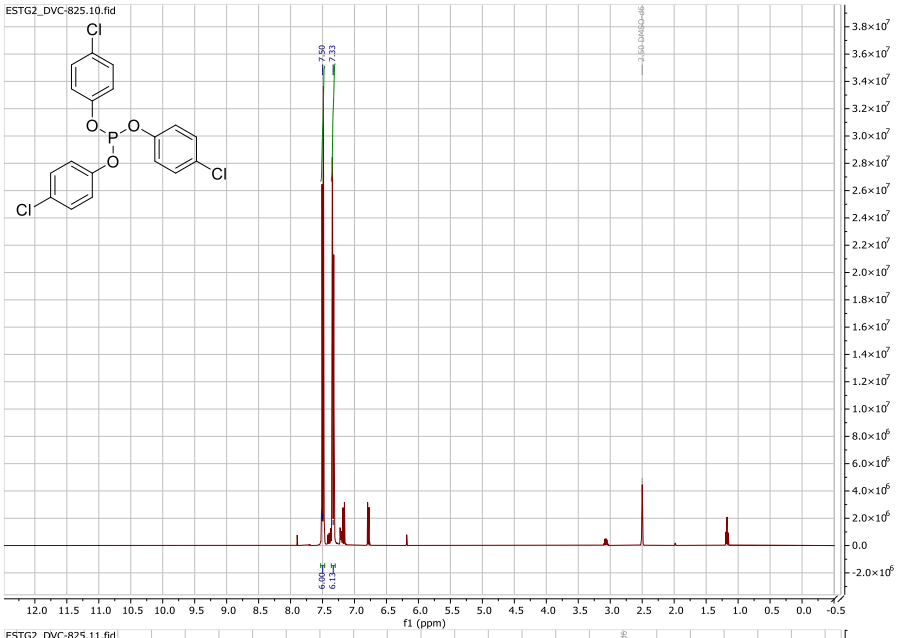

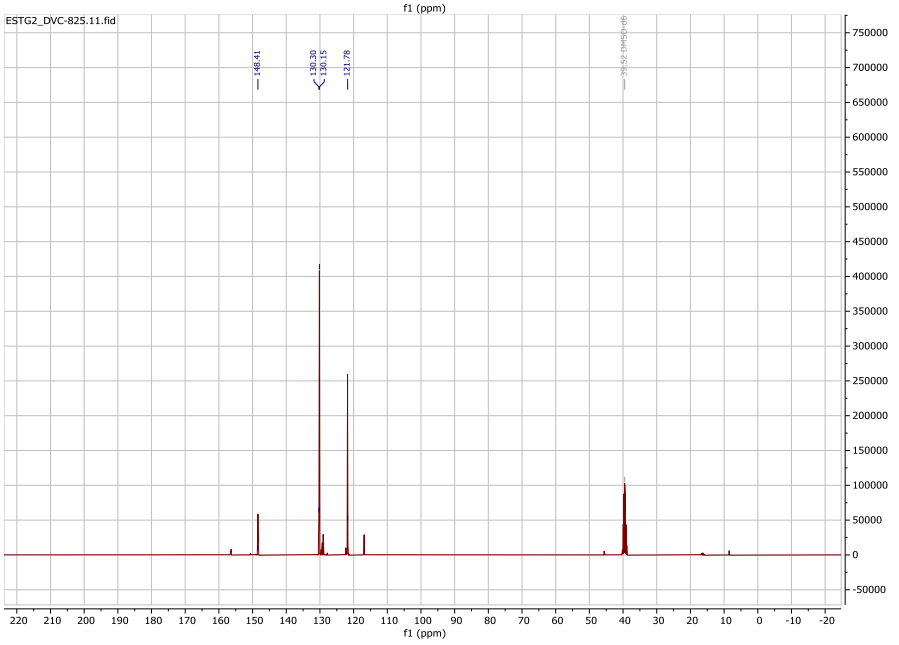

Benzyl((bis(4-chlorophenoxy)phosphoryl)(4-((tert butoxycarbonyl)amino)phenyl)-methyl) carbamate (206)

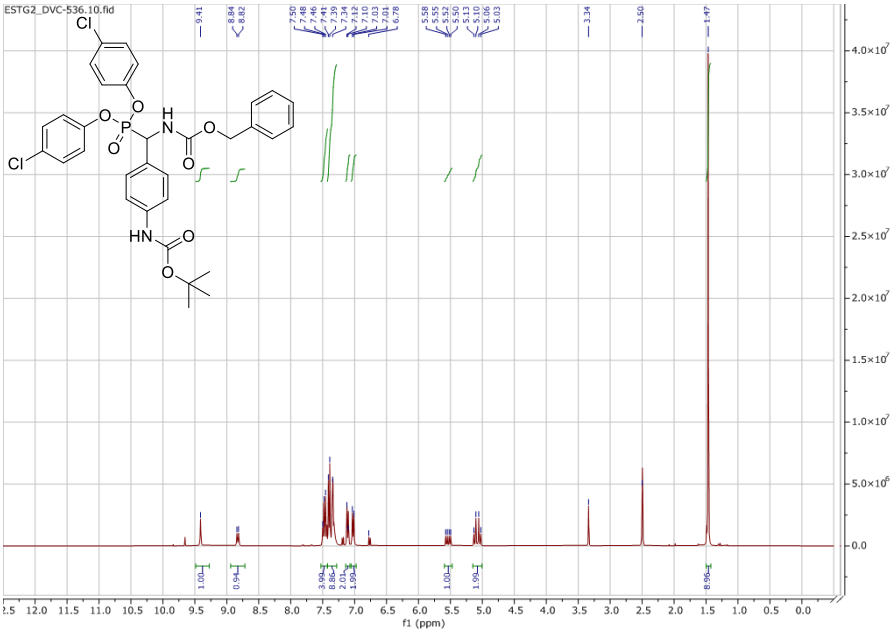

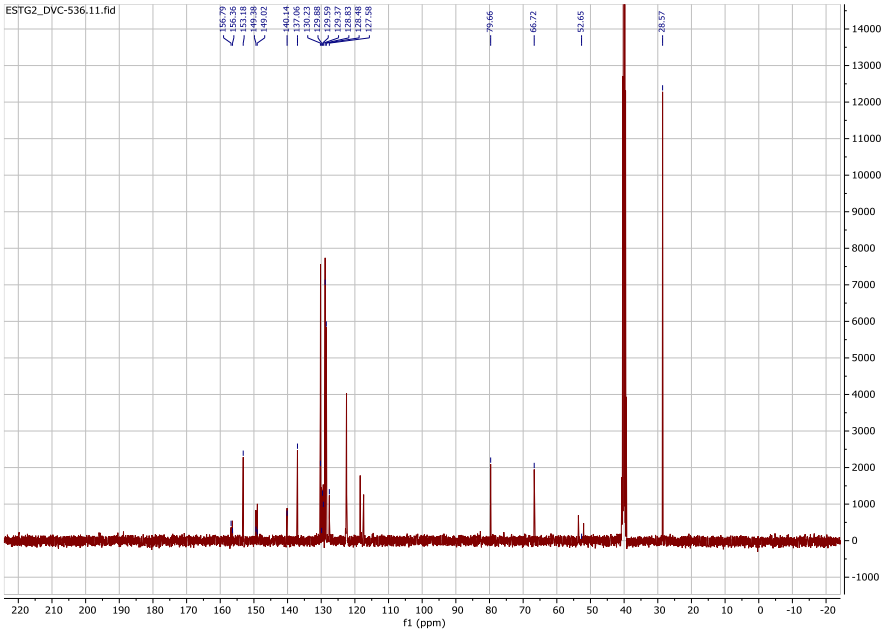

4-((((benzyloxy)carbonyl)amino)(bis(4-chlorophenoxy)phosphoryl)methyl)benzenaminium trifluoroacetate (212)

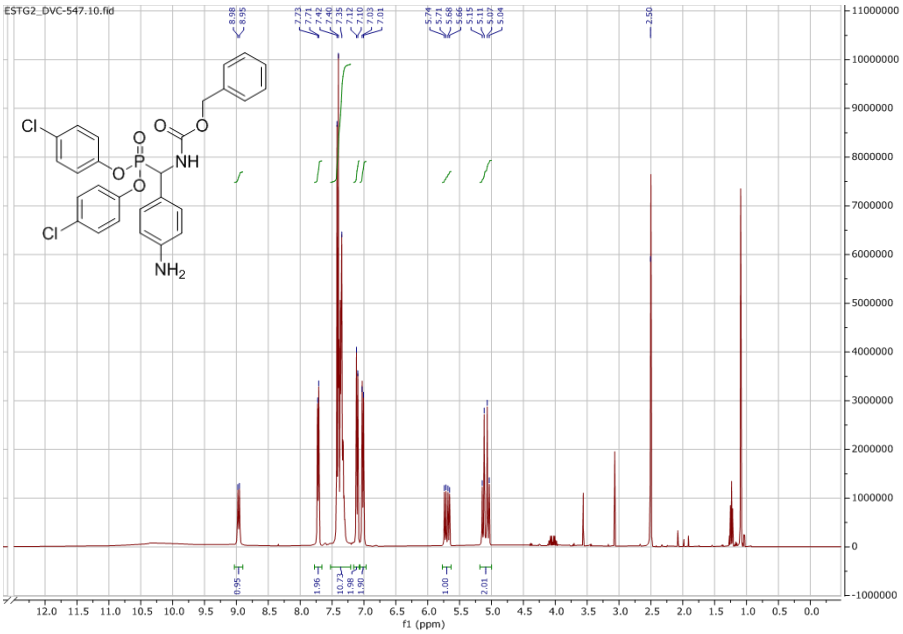

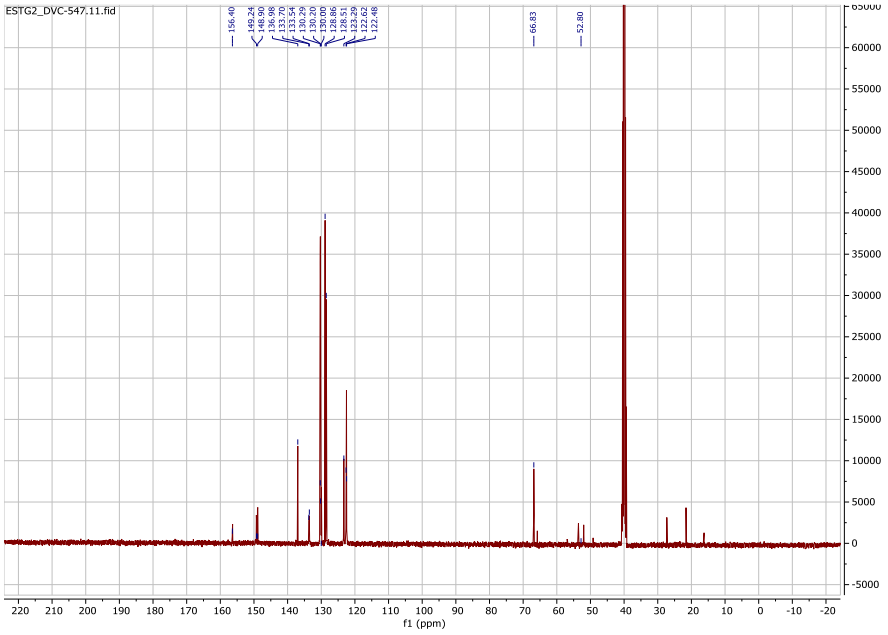

Benzyl(E)-((bis(4-chlorophenoxy)phosphoryl)(4-(N.N'-bis(tert-butyloxycarbonyl)guanidino) phenyl)methyl)carbamate (209)

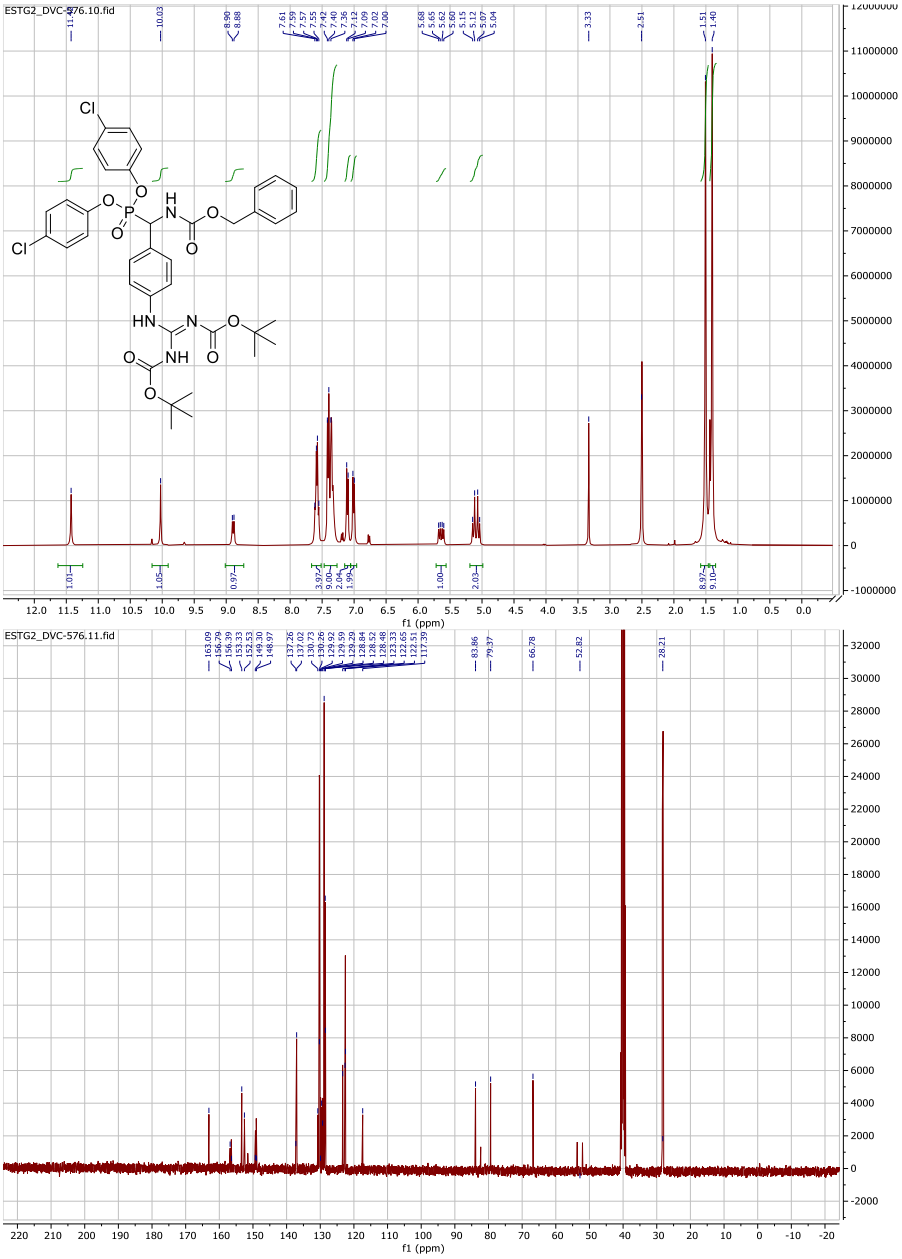

Amino((4-((((benzyloxy)carbonyl)amino)(bis(4-chlorophenoxy)phosphoryl)methyl)phenyl)amino)methaniminium chloride (15)

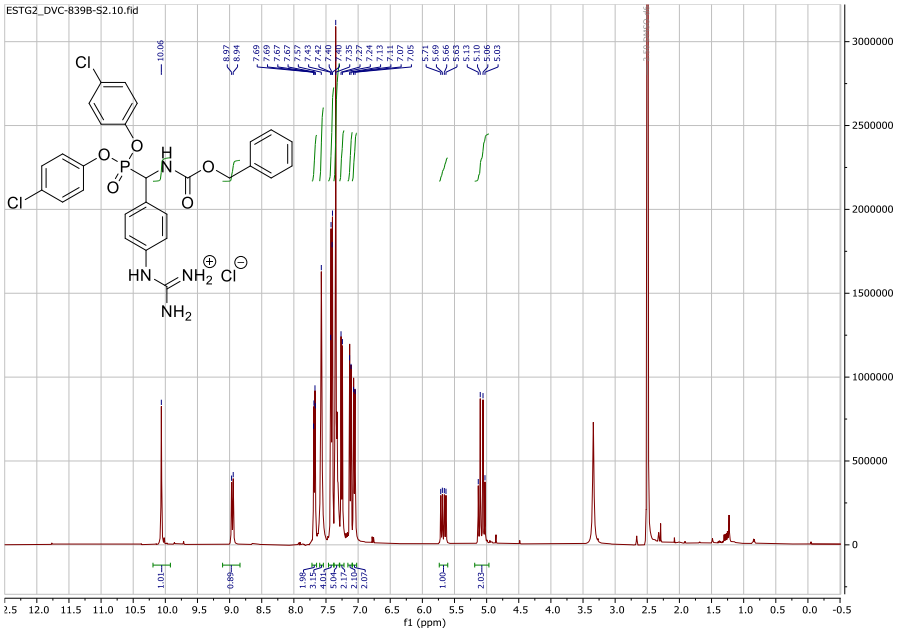

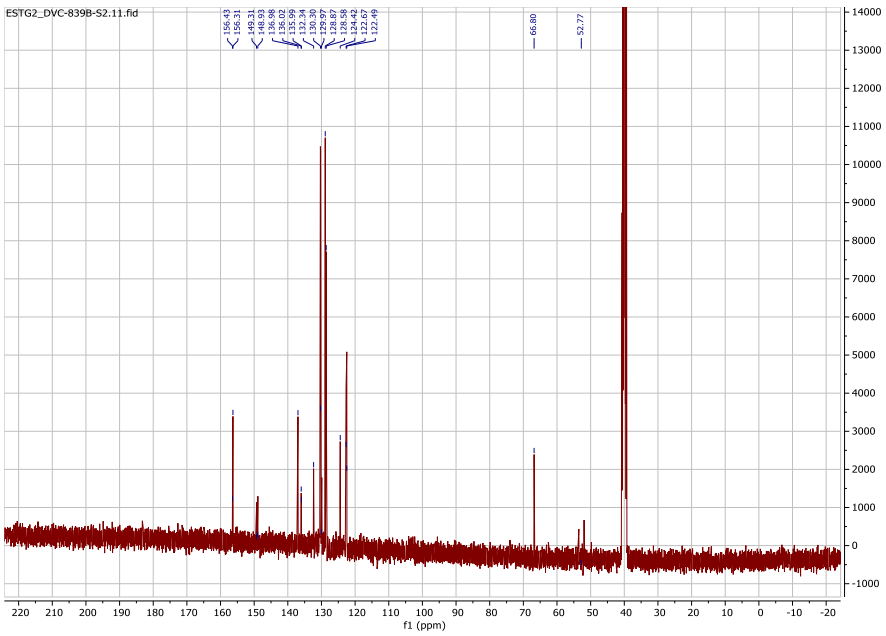

(*S*)-((1*S*,2*R*,4*S*,5*R*)-5-ethylquinuclidin-2-yl)(6-methoxyquinolin-4-yl)methyl carbamate (226)

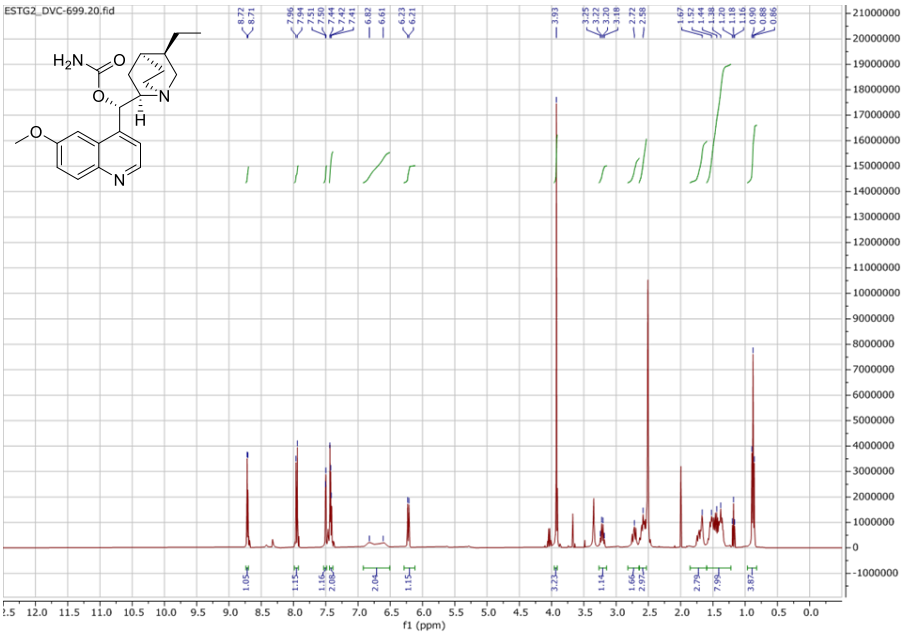

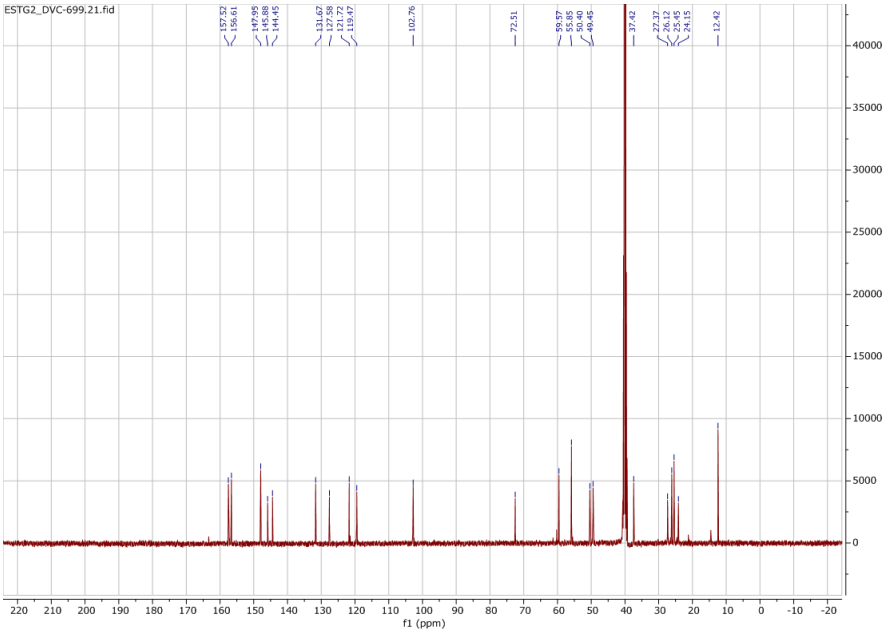

(*R*)-(6-methoxyquinolin-4-yl)((1S,2R,4S,5R)-5-vinylquinuclidin-2-yl)methyl carbamate (227)

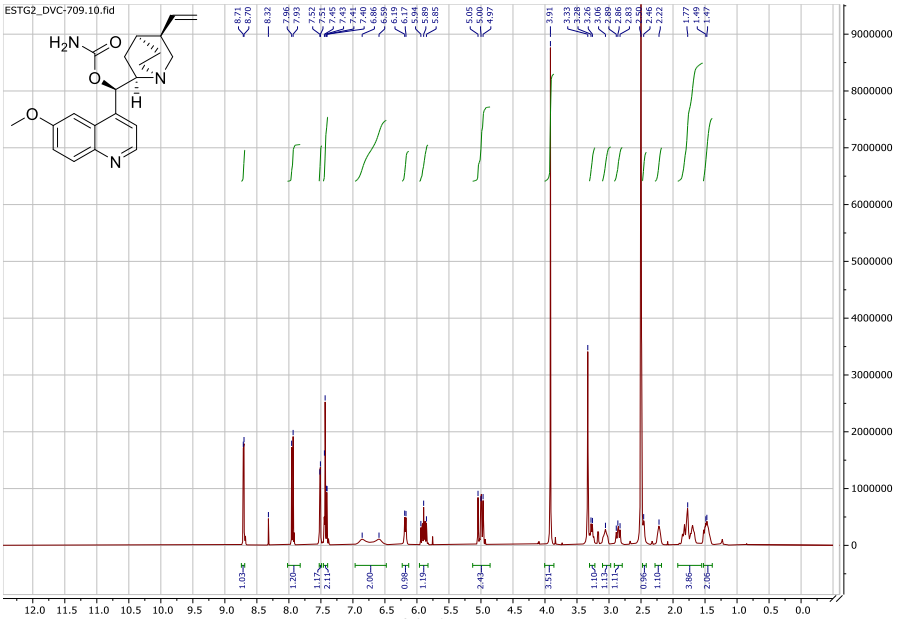

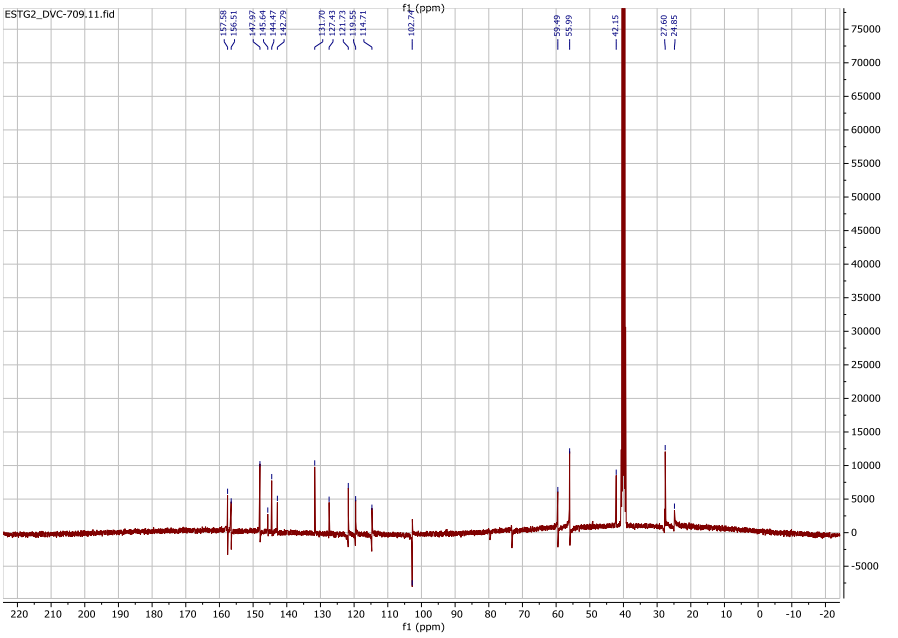

(*R*)-1-(3,5-bis(trifluoromethyl)phenyl)ethyl carbamate (229)

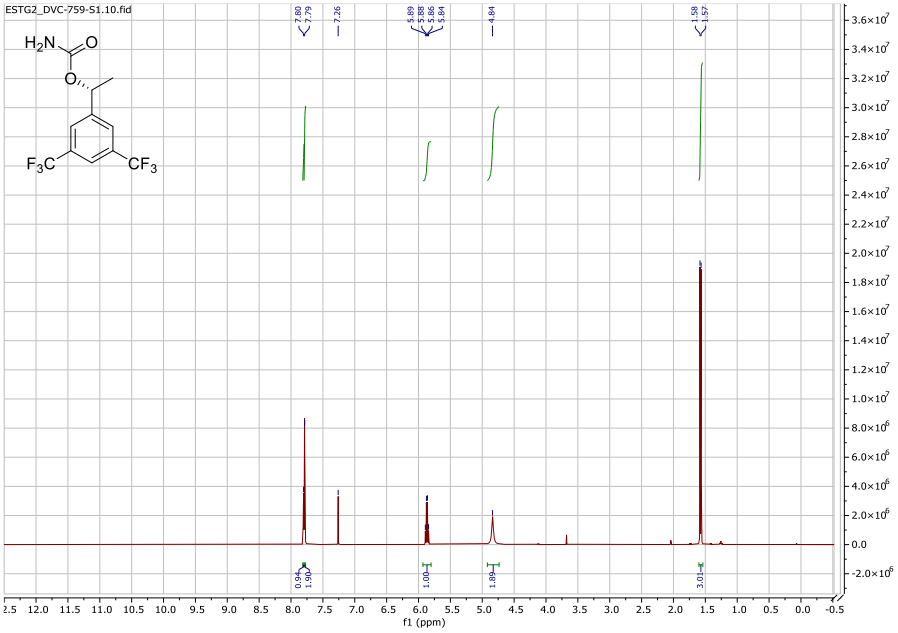

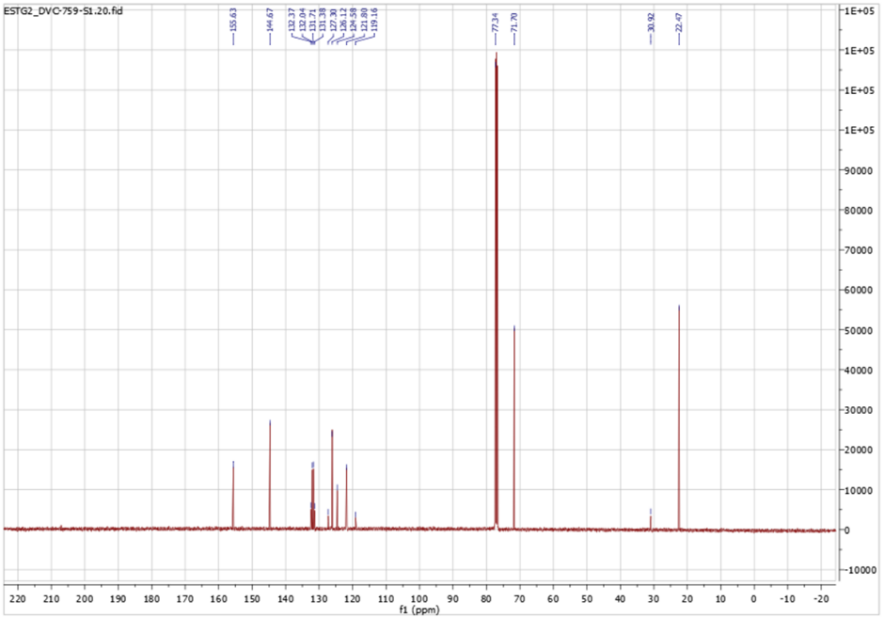

(*S*)-1-phenylethyl carbamate (228)

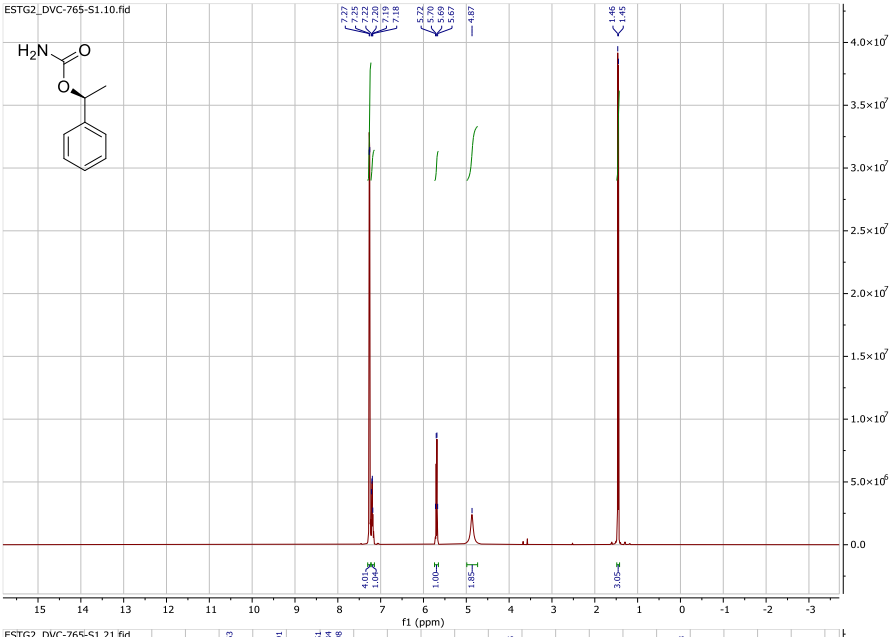

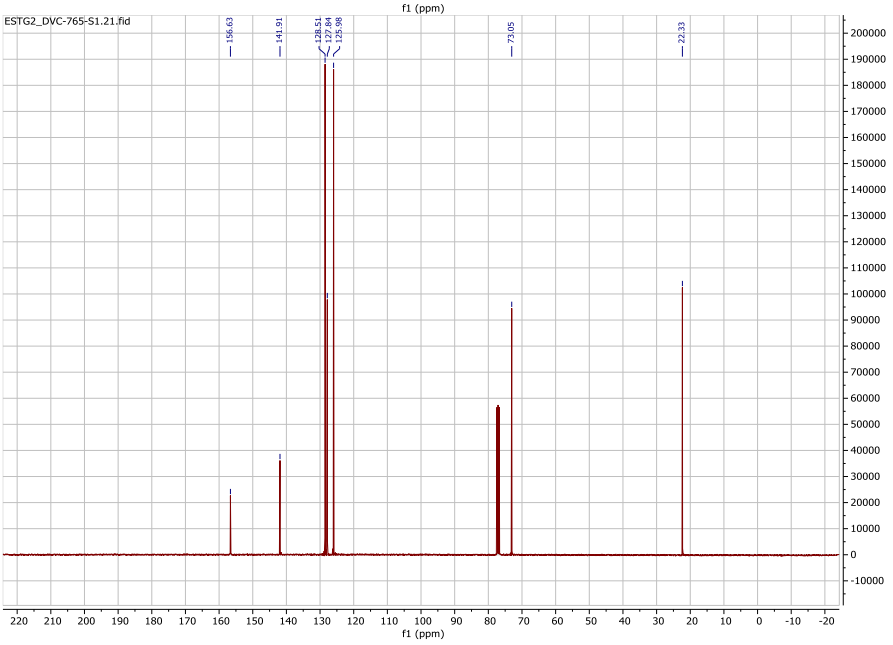

(1*S*,2*R*,4*S*)-1,7,7-trimethylbicyclo[2.2.1]heptan-2-yl carbamate (230)

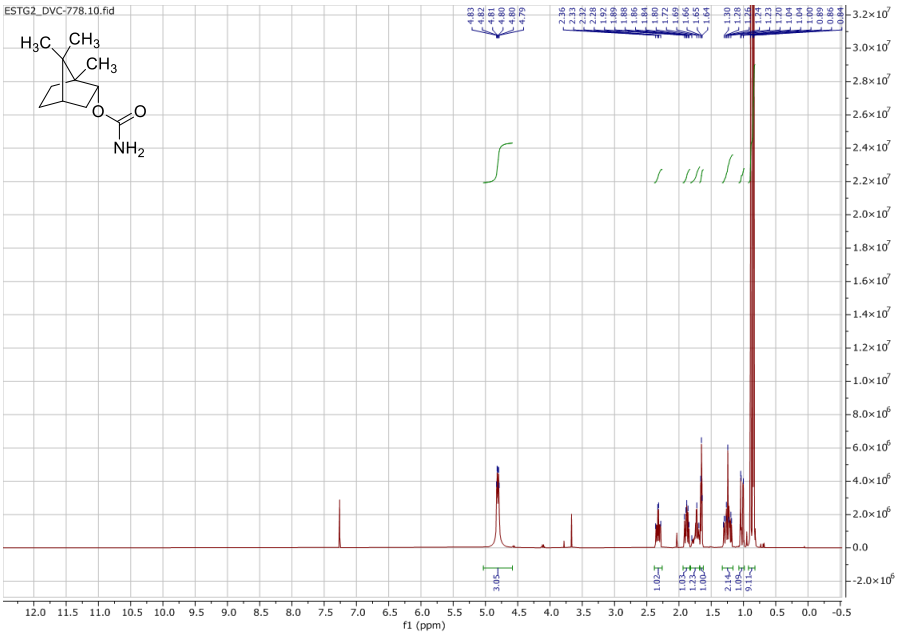

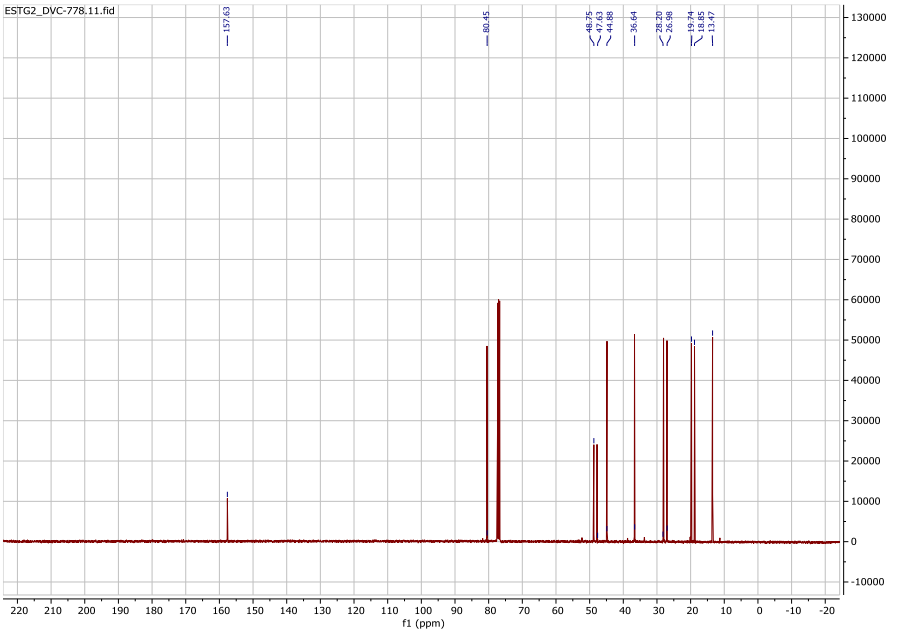

Diphenyl (phenyl(((*S*)-1-phenylethyl)amino)methyl)phosphonate (215)

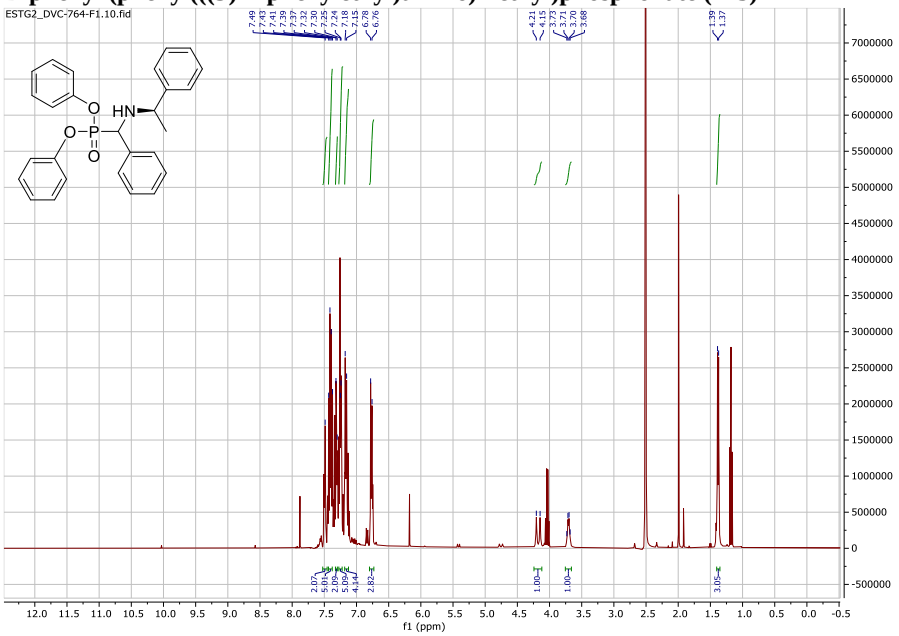

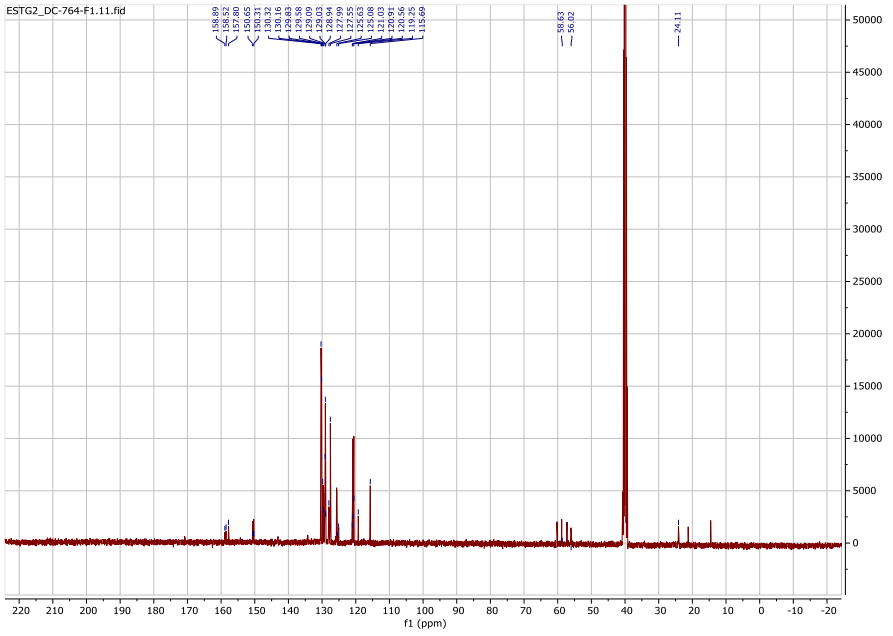

(*R*)-1-(3,5-bis(trifluoromethyl)phenyl)ethyl((diphenoxyphosphoryl)(phenyl)methyl)-carbamate (234)

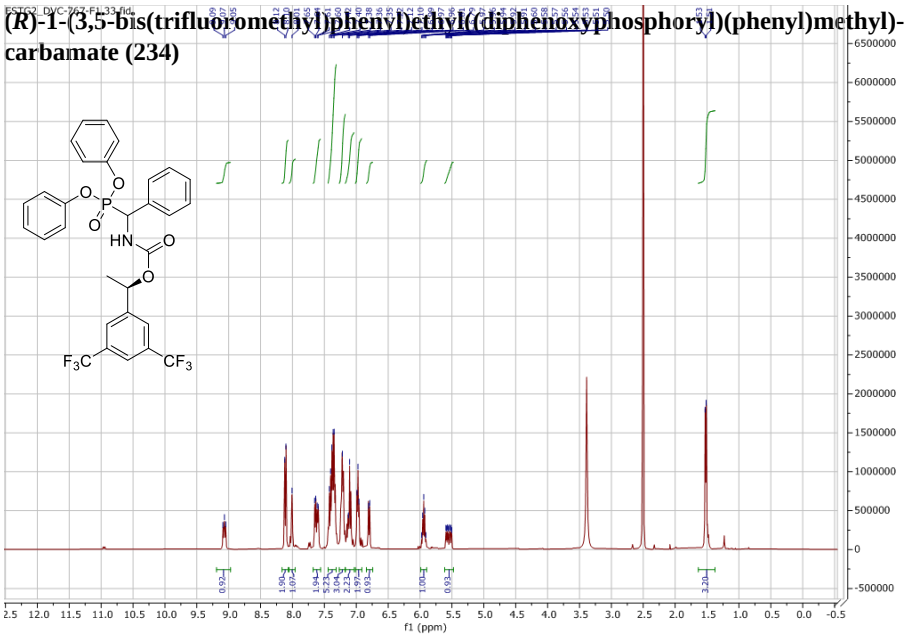

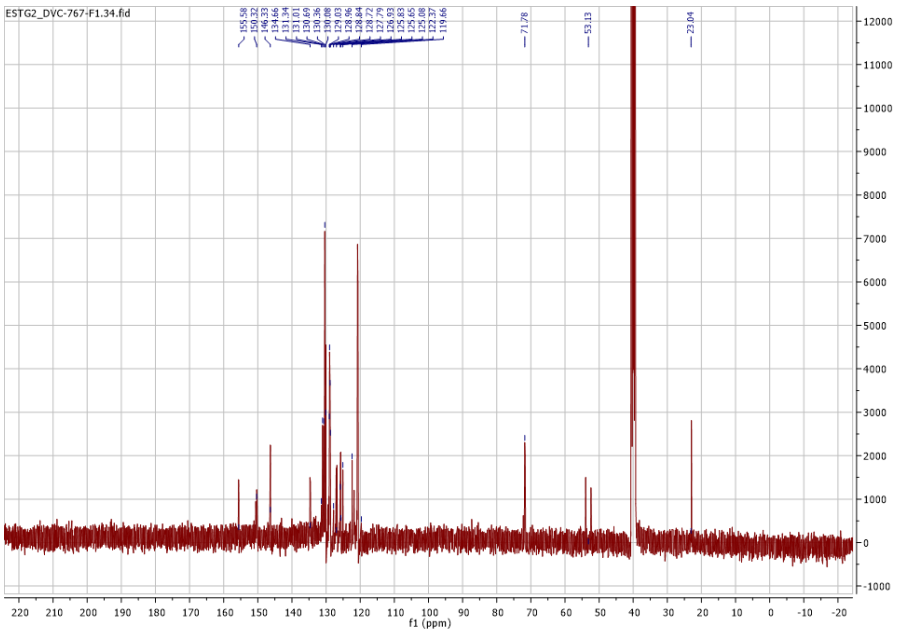

(*S*)-1-phenylethyl ((diphenoxyphosphoryl)(phenyl)methyl)carbamate (233)

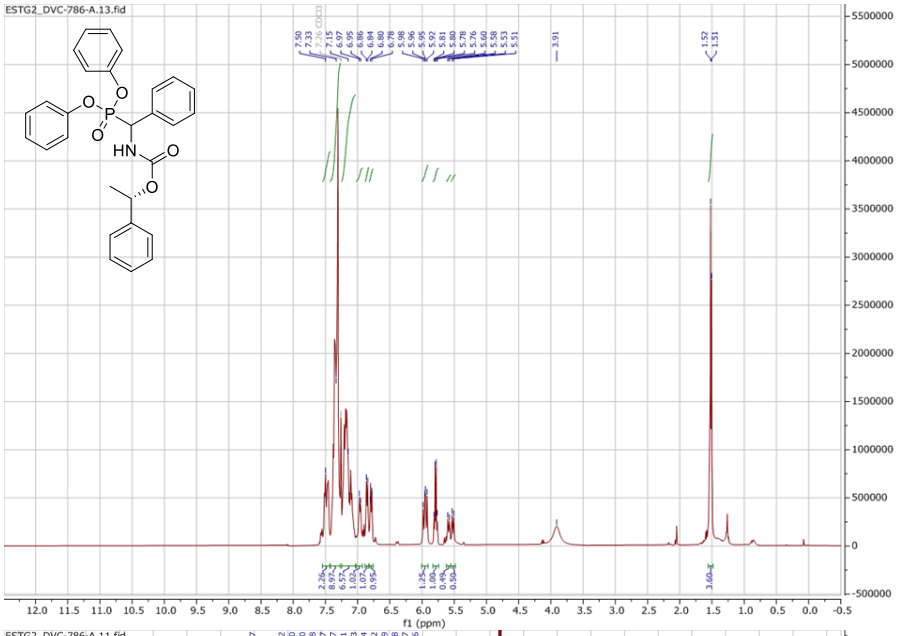

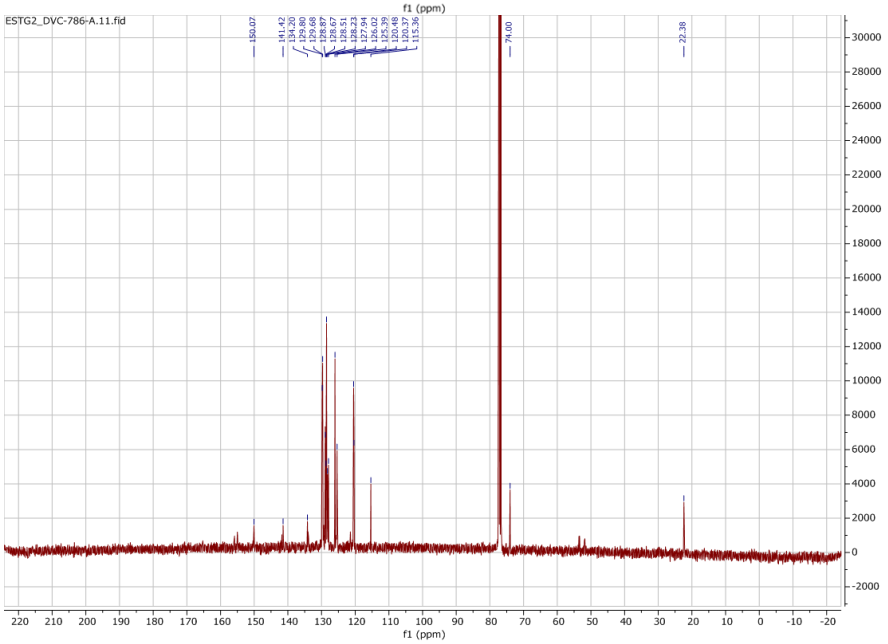

(2*S*)-1,7,7-trimethylbicyclo[2.2.1]heptan-2-yl ((diphenoxyphosphoryl)(phenyl)methyl)-carbamate (235)

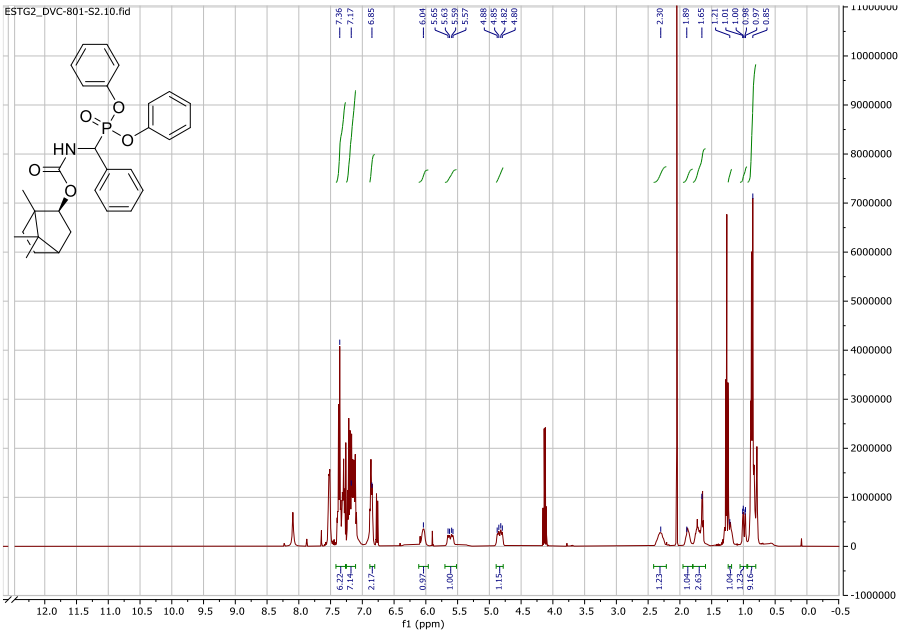

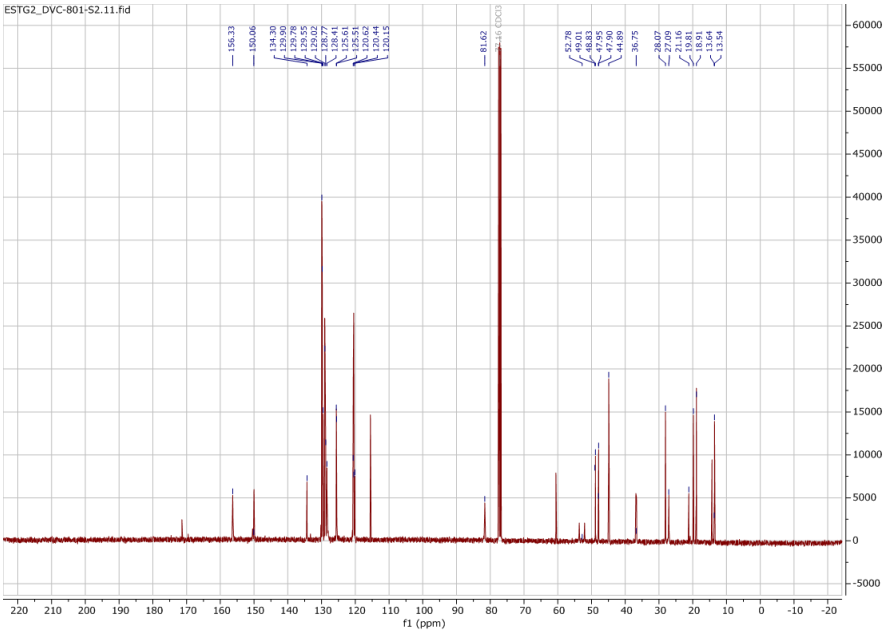

8 Appendix II

Crystal data, data collection and structure refinement details are summarized in Table A1.

Table A1. Experimental details

Crystal data	
Chemical formula	$C_{22}H_{37}N_2O_4$
M_r	393.53
Crystal system, space group	Monoclinic, *I*2
Temperature (K)	293
a, *b*, *c* (Å)	10.71978 (19), 13.6582 (3), 15.7103 (2)
□ (°)	95.5933 (14)
V (Å^3)	2289.25 (7)
Z	4
Radiation type	Cu *K*□
□ (mm^{-1})	0.62
Crystal size (mm)	0.30 × 0.22 × 0.12
Data collection	
Diffractometer	XtaLAB Synergy, Dualflex, HyPix
Absorption correction	Multi-scan *CrysAlis PRO* 1.171.41.123a (Rigaku Oxford Diffraction, 2022) Empirical absorption correction using spherical harmonics, implemented in SCALE3 ABSPACK scaling algorithm.
T_{min}, T_{max}	0.760, 1.000
No. of measured, independent and observed [$I > 2$□(I)] reflections	11174, 3762, 3394
R_{int}	0.025
(sin □/□)$_{max}$ (Å^{-1})	0.630
Refinement	
$R[F^2 > 2$□$(F^2)]$, $wR(F^2)$, S	0.073, 0.245, 1.05

No. of reflections	3762
No. of parameters	268
No. of restraints	1
H-atom treatment	H atoms treated by a mixture of independent and constrained refinement
□ρ_{max}, □ρ_{min} (e Å^{-3})	0.39, -0.22
Absolute structure	Flack x determined using 1186 quotients [(I+)-(I-)]/[(I+)+(I-)] (Parsons, Flack and Wagner, Acta Cryst. B69 (2013) 249-259).
Absolute structure parameter	-0.13 (12)

Computer programs: *CrysAlis PRO* 1.171.41.123a (Rigaku OD, 2022), SHELXT 2014/4 (Sheldrick, 2014), *SHELXL2018*/3 (Sheldrick, 2018).

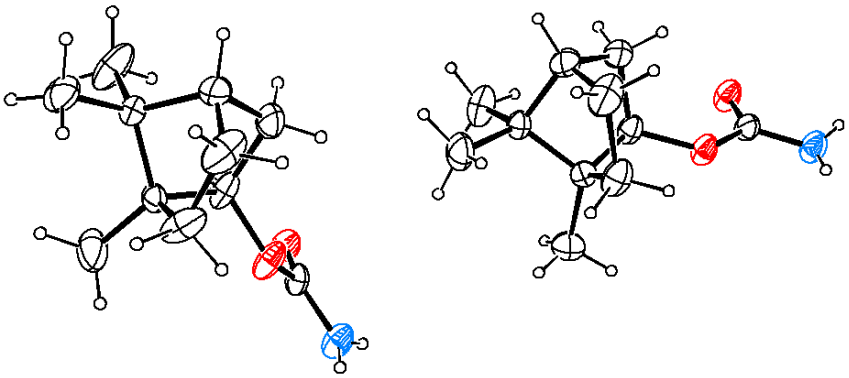

Computing details

Data collection: *CrysAlis PRO* 1.171.41.123a (Rigaku OD, 2022); cell refinement: *CrysAlis PRO* 1.171.41.123a (Rigaku OD, 2022); data reduction: *CrysAlis PRO* 1.171.41.123a (Rigaku OD, 2022); program(s) used to solve structure: SHELXT 2014/4 (Sheldrick, 2014); program(s) used to refine structure: SHELXL2018/3 (Sheldrick, 2018).

Table A2. Crystal data

$C_{22}H_{37}N_2O_4$	$F(000) = 860$
$M_r = 393.53$	$D_x = 1.142$ Mg m^{-3}
Monoclinic, *I*2	Cu *K*□ radiation, □ = 1.54184 Å
a = 10.71978 (19) Å	Cell parameters from 7313 reflections
b = 13.6582 (3) Å	□ = 4.3–76.0°
c = 15.7103 (2) Å	□ = 0.62 mm^{-1}
□ = 95.5933 (14)°	*T* = 293 K
V = 2289.25 (7) Å^3	Block, colourless
Z = 4	0.30 × 0.22 × 0.12 mm

Table A3. Data collection

XtaLAB Synergy, Dualflex, HyPix diffractometer	3394 reflections with $I > 2\square(I)$
Radiation source: micro-focus sealed X-ray tube	$R_{int} = 0.025$
□ scans	$\square_{max} = 76.2°$, $\square_{min} = 4.3°$
Absorption correction: multi-scan *CrysAlis PRO* 1.171.41.123a (Rigaku Oxford Diffraction, 2022) Empirical absorption correction using spherical harmonics, implemented in SCALE3 ABSPACK scaling algorithm.	*h* = -13□9
$T_{min} = 0.760$, $T_{max} = 1.000$	*k* = -16□16
11174 measured reflections	*l* = -19□19
3762 independent reflections	

Table A4. Refinement

Refinement on F^2	H atoms treated by a mixture of independent and constrained refinement
Least-squares matrix: full	$w = 1/[\sigma^2(F_o^2) + (0.1823P)^2 + 0.5831P]$ where $P = (F_o^2 + 2F_c^2)/3$
$R[F^2 > 2\sigma(F^2)] = 0.073$	$(\Delta/\sigma)_{max} = 0.002$
$wR(F^2) = 0.245$	$\Delta\rho_{max} = 0.39$ e Å^{-3}
$S = 1.05$	$\Delta\rho_{min} = -0.22$ e Å^{-3}
3762 reflections	Extinction correction: *SHELXL2018*/3 (Sheldrick 2018), $Fc^*=kFc[1+0.001xFc^2\lambda^3/\sin(2\theta)]^{-1/4}$
268 parameters	Extinction coefficient: 0.0005 (5)
1 restraint	Absolute structure: Flack x determined using 1186 quotients [(I+)-(I-)]/[(I+)+(I-)] (Parsons, Flack and Wagner, Acta Cryst. B69 (2013) 249-259).
Hydrogen site location: mixed	Absolute structure parameter: -0.13 (12)

Special details:

Geometry. All esds (except the esd in the dihedral angle between two l.s. planes) are estimated using the full covariance matrix. The cell esds are taken into account individually in the estimation of esds in distances, angles and torsion angles; correlations between esds in cell parameters are only used when they are defined by crystal symmetry. An approximate (isotropic) treatment of cell esds is used for estimating esds involving l.s. planes.

Table A5. Fractional atomic coordinates and isotropic or equivalent isotropic displacement parameters (Å^2) for (dvc_800_rt)

	x	*y*	*z*	U_{iso}*/U_{eq}
N1	-0.3814 (4)	-0.2918 (4)	-0.0791 (3)	0.0818 (14)
H1A	-0.354406	-0.255745	-0.039787	0.123*
H1B	-0.447 (8)	-0.299 (7)	-0.093 (6)	0.123*
O8	-0.3285 (3)	-0.3617 (3)	-0.1973 (2)	0.0752 (11)

C8	-0.4174 (5)	-0.6262 (6)	-0.8673 (4)	0.098 (2)
H8A	-0.447581	-0.651524	-0.923230	0.118*
H8B	-0.470875	-0.650567	-0.825623	0.118*
O25	-0.1895 (3)	-0.7209 (3)	-0.59662 (19)	0.0709 (9)
O11	-0.1771 (3)	-0.3174 (3)	-0.0958 (2)	0.0802 (11)
C11	-0.2110 (3)	-0.5745 (4)	-0.8850 (3)	0.0566 (9)
O22	-0.3428 (3)	-0.6808 (3)	-0.69924 (18)	0.0785 (12)
C18	-0.2828 (4)	-0.6562 (3)	-0.8435 (2)	0.0611 (10)
C9	-0.2866 (4)	-0.3225 (4)	-0.1214 (3)	0.0653 (11)
C10	-0.2328 (6)	-0.5687 (6)	-0.9825 (3)	0.0915 (17)
H10A	-0.178063	-0.613890	-1.007316	0.110*
H10B	-0.215657	-0.503411	-1.000854	0.110*
H10C	-0.318344	-0.585110	-1.000642	0.110*
C23	-0.3001 (4)	-0.7189 (4)	-0.6239 (2)	0.0584 (10)
C3	-0.2339 (4)	-0.3957 (4)	-0.2521 (3)	0.0672 (12)
H3	-0.166072	-0.430334	-0.218146	0.081*
C4	-0.2930 (5)	-0.4606 (3)	-0.3220 (3)	0.0653 (11)
C27	-0.0684 (5)	-0.5755 (9)	-0.8628 (5)	0.125 (3)
H27A	-0.049736	-0.583694	-0.802164	0.187*
H27B	-0.033619	-0.514757	-0.880122	0.187*
H27C	-0.032648	-0.628696	-0.892089	0.187*
C6	-0.3562 (7)	-0.3205 (6)	-0.4072 (5)	0.116 (3)
H6A	-0.383784	-0.320193	-0.467914	0.139*
H6B	-0.380809	-0.259436	-0.382238	0.139*
C7	-0.2025 (4)	-0.4480 (4)	-0.3913 (3)	0.0589 (10)
C1	-0.2189 (6)	-0.3350 (5)	-0.3925 (4)	0.0868 (16)
H1	-0.170837	-0.301012	-0.433507	0.104*
N2	-0.3935 (4)	-0.7548 (4)	-0.5838 (2)	0.0769 (12)
H2	-0.369657	-0.762917	-0.533080	0.115*
H1D	-0.475 (7)	-0.754 (7)	-0.614 (5)	0.115*
C15	-0.2763 (7)	-0.4947 (5)	-0.8392 (5)	0.107 (2)
H15	-0.250220	-0.427987	-0.852202	0.128*
C20	-0.2560 (8)	-0.5221 (7)	-0.7450 (4)	0.112 (3)

H20A	-0.324732	-0.499654	-0.714190	0.134*
H20B	-0.177961	-0.495511	-0.718264	0.134*
C14	-0.3184 (9)	-0.5645 (6)	-0.2962 (6)	0.125 (3)
H14A	-0.359184	-0.599215	-0.344277	0.188*
H14B	-0.371631	-0.564208	-0.250450	0.188*
H14C	-0.240692	-0.596251	-0.277442	0.188*
C5	-0.4124 (4)	-0.4106 (6)	-0.3617 (3)	0.0870 (17)
H5A	-0.465304	-0.389883	-0.318347	0.104*
H5B	-0.459957	-0.453035	-0.402401	0.104*
C2	-0.1814 (7)	-0.3095 (5)	-0.3005 (5)	0.104 (2)
H2A	-0.218538	-0.247979	-0.285217	0.125*
H2B	-0.091005	-0.305144	-0.289074	0.125*
C13	-0.0694 (6)	-0.4809 (7)	-0.3694 (4)	0.102 (2)
H13A	-0.039779	-0.457744	-0.313353	0.154*
H13B	-0.017590	-0.454890	-0.410488	0.154*
H13C	-0.065833	-0.551143	-0.370320	0.154*
C16	-0.4159 (6)	-0.5179 (6)	-0.8678 (5)	0.112 (3)
H16A	-0.470629	-0.491245	-0.827937	0.134*
H16B	-0.440733	-0.492254	-0.924532	0.134*
C17	-0.2517 (4)	-0.6350 (5)	-0.7493 (3)	0.0714 (14)
C12	-0.2454 (6)	-0.4955 (7)	-0.4778 (4)	0.100 (2)
H12A	-0.244858	-0.565402	-0.471663	0.150*
H12B	-0.189421	-0.476839	-0.519081	0.150*
H12C	-0.328718	-0.473845	-0.496687	0.150*
C28	-0.2551 (13)	-0.7608 (6)	-0.8660 (6)	0.167 (5)
H28A	-0.231232	-0.763625	-0.923234	0.250*
H28B	-0.328608	-0.800104	-0.862044	0.250*
H28C	-0.187934	-0.785317	-0.826882	0.250*

Table A6. Atomic displacement parameters (Å^2) for (dvc_800_rt)

	U^{11}	U^{22}	U^{33}	U^{12}	U^{13}	U^{23}
N1	0.073 (2)	0.114 (4)	0.060 (2)	-0.015 (3)	0.0167 (18)	-0.025 (2)
O8	0.0608 (15)	0.115 (3)	0.0499 (14)	-0.0188 (16)	0.0093 (12)	-0.0268 (16)

C8	0.064 (3)	0.162 (7)	0.066 (3)	-0.036 (3)	-0.012 (2)	0.039 (3)
O25	0.0676 (16)	0.095 (2)	0.0483 (14)	0.0004 (16)	-0.0028 (12)	0.0097 (15)
O11	0.0666 (17)	0.122 (3)	0.0520 (15)	-0.0148 (18)	0.0070 (13)	-0.0212 (18)
C11	0.0560 (19)	0.063 (2)	0.0522 (18)	0.0025 (18)	0.0132 (14)	-0.0006 (18)
O22	0.0573 (15)	0.133 (3)	0.0459 (14)	0.0103 (17)	0.0086 (11)	0.0247 (18)
C18	0.092 (3)	0.052 (2)	0.0405 (17)	-0.003 (2)	0.0141 (17)	-0.0029 (16)
C9	0.067 (2)	0.080 (3)	0.050 (2)	-0.014 (2)	0.0122 (17)	-0.014 (2)
C10	0.110 (4)	0.110 (5)	0.057 (2)	-0.012 (4)	0.017 (2)	0.019 (3)
C23	0.063 (2)	0.077 (3)	0.0350 (15)	0.009 (2)	0.0046 (14)	-0.0028 (17)
C3	0.058 (2)	0.092 (3)	0.0522 (19)	-0.004 (2)	0.0089 (15)	-0.007 (2)
C4	0.074 (2)	0.058 (2)	0.066 (2)	-0.0018 (19)	0.0182 (19)	0.0008 (19)
C27	0.055 (2)	0.223 (10)	0.101 (4)	0.013 (4)	0.028 (2)	0.037 (6)
C6	0.124 (5)	0.122 (6)	0.107 (5)	0.054 (5)	0.040 (4)	0.050 (4)
C7	0.056 (2)	0.071 (3)	0.0502 (18)	0.0040 (18)	0.0051 (15)	-0.0062 (19)
C1	0.112 (4)	0.070 (3)	0.084 (3)	0.002 (3)	0.039 (3)	0.019 (3)
N2	0.070 (2)	0.113 (3)	0.0469 (16)	0.002 (2)	0.0044 (15)	0.015 (2)
C15	0.138 (6)	0.058 (3)	0.137 (6)	-0.012 (3)	0.078 (5)	-0.007 (3)
C20	0.122 (5)	0.135 (6)	0.084 (4)	-0.055 (4)	0.044 (3)	-0.056 (4)
C14	0.175 (7)	0.072 (4)	0.140 (6)	-0.024 (4)	0.073 (6)	0.000 (4)
C5	0.055 (2)	0.131 (5)	0.074 (3)	0.009 (3)	0.0030 (19)	-0.002 (3)
C2	0.110 (4)	0.096 (4)	0.113 (5)	-0.041 (4)	0.048 (4)	-0.037 (4)
C13	0.085 (3)	0.150 (7)	0.073 (3)	0.037 (4)	0.014 (3)	0.000 (3)
C16	0.082 (3)	0.126 (6)	0.134 (6)	0.045 (4)	0.040 (3)	0.061 (5)
C17	0.0474 (17)	0.125 (4)	0.0427 (17)	0.010 (2)	0.0100 (13)	0.012 (2)
C12	0.099 (4)	0.128 (6)	0.074 (3)	-0.009 (4)	0.016 (3)	-0.038 (4)
C28	0.332 (15)	0.061 (3)	0.129 (6)	-0.001 (6)	0.134 (9)	-0.002 (4)

Table A7. Geometric parameters (Å, º) for (dvc_800_rt)

N1—C9	1.335 (6)	C6—H6A	0.9700
N1—H1A	0.8200	C6—H6B	0.9700
N1—H1B	0.72 (8)	C7—C13	1.504 (7)
O8—C9	1.344 (5)	C7—C12	1.534 (7)
O8—C3	1.469 (5)	C7—C1	1.553 (8)

C8—C16	1.481 (12)	C1—C2	1.503 (10)
C8—C18	1.511 (8)	C1—H1	0.9800
C8—H8A	0.9700	N2—H2	0.8200
C8—H8B	0.9700	N2—H1D	0.96 (8)
O25—C23	1.221 (5)	C15—C20	1.521 (11)
O11—C9	1.204 (5)	C15—C16	1.553 (11)
C11—C15	1.514 (7)	C15—H15	0.9800
C11—C10	1.530 (6)	C20—C17	1.544 (11)
C11—C27	1.534 (6)	C20—H20A	0.9700
C11—C18	1.536 (6)	C20—H20B	0.9700
O22—C23	1.333 (5)	C14—H14A	0.9600
O22—C17	1.453 (6)	C14—H14B	0.9600
C18—C28	1.508 (9)	C14—H14C	0.9600
C18—C17	1.513 (6)	C5—H5A	0.9700
C10—H10A	0.9600	C5—H5B	0.9700
C10—H10B	0.9600	C2—H2A	0.9700
C10—H10C	0.9600	C2—H2B	0.9700
C23—N2	1.328 (6)	C13—H13A	0.9600
C3—C4	1.503 (7)	C13—H13B	0.9600
C3—C2	1.538 (9)	C13—H13C	0.9600
C3—H3	0.9800	C16—H16A	0.9700
C4—C14	1.509 (8)	C16—H16B	0.9700
C4—C5	1.529 (7)	C12—H12A	0.9600
C4—C7	1.537 (6)	C12—H12B	0.9600
C27—H27A	0.9600	C12—H12C	0.9600
C27—H27B	0.9600	C28—H28A	0.9600
C27—H27C	0.9600	C28—H28B	0.9600
C6—C1	1.480 (9)	C28—H28C	0.9600
C6—C5	1.572 (10)		
C9—N1—H1A	109.5	C6—C1—C7	104.1 (5)
C9—N1—H1B	125 (7)	C2—C1—C7	101.5 (5)
H1A—N1—H1B	124.4	C6—C1—H1	114.4

C9—O8—C3	117.1 (3)	C2—C1—H1	114.4
C16—C8—C18	105.2 (5)	C7—C1—H1	114.4
C16—C8—H8A	110.7	C23—N2—H2	109.5
C18—C8—H8A	110.7	C23—N2—H1D	117 (5)
C16—C8—H8B	110.7	H2—N2—H1D	132.4
C18—C8—H8B	110.7	C11—C15—C20	104.8 (6)
H8A—C8—H8B	108.8	C11—C15—C16	101.1 (6)
C15—C11—C10	113.9 (5)	C20—C15—C16	105.9 (5)
C15—C11—C27	113.3 (6)	C11—C15—H15	114.5
C10—C11—C27	106.3 (4)	C20—C15—H15	114.5
C15—C11—C18	92.7 (3)	C16—C15—H15	114.5
C10—C11—C18	115.3 (4)	C15—C20—C17	101.9 (4)
C27—C11—C18	115.2 (5)	C15—C20—H20A	111.4
C23—O22—C17	117.3 (3)	C17—C20—H20A	111.4
C28—C18—C8	113.8 (7)	C15—C20—H20B	111.4
C28—C18—C17	112.4 (6)	C17—C20—H20B	111.4
C8—C18—C17	107.7 (4)	H20A—C20—H20B	109.3
C28—C18—C11	118.1 (5)	C4—C14—H14A	109.5
C8—C18—C11	101.8 (4)	C4—C14—H14B	109.5
C17—C18—C11	101.7 (4)	H14A—C14—H14B	109.5
O11—C9—N1	125.5 (4)	C4—C14—H14C	109.5
O11—C9—O8	123.3 (4)	H14A—C14—H14C	109.5
N1—C9—O8	111.2 (4)	H14B—C14—H14C	109.5
C11—C10—H10A	109.5	C4—C5—C6	101.1 (4)
C11—C10—H10B	109.5	C4—C5—H5A	111.6
H10A—C10—H10B	109.5	C6—C5—H5A	111.6
C11—C10—H10C	109.5	C4—C5—H5B	111.6
H10A—C10—H10C	109.5	C6—C5—H5B	111.6
H10B—C10—H10C	109.5	H5A—C5—H5B	109.4
O25—C23—N2	125.2 (4)	C1—C2—C3	102.8 (5)
O25—C23—O22	123.9 (4)	C1—C2—H2A	111.2
N2—C23—O22	110.9 (3)	C3—C2—H2A	111.2
O8—C3—C4	110.4 (4)	C1—C2—H2B	111.2

O8—C3—C2	110.8 (5)	C3—C2—H2B	111.2
C4—C3—C2	103.8 (4)	H2A—C2—H2B	109.1
O8—C3—H3	110.6	C7—C13—H13A	109.5
C4—C3—H3	110.6	C7—C13—H13B	109.5
C2—C3—H3	110.6	H13A—C13—H13B	109.5
C3—C4—C14	115.6 (5)	C7—C13—H13C	109.5
C3—C4—C5	108.2 (5)	H13A—C13—H13C	109.5
C14—C4—C5	111.3 (6)	H13B—C13—H13C	109.5
C3—C4—C7	101.6 (4)	C8—C16—C15	102.3 (4)
C14—C4—C7	116.0 (5)	C8—C16—H16A	111.3
C5—C4—C7	102.9 (4)	C15—C16—H16A	111.3
C11—C27—H27A	109.5	C8—C16—H16B	111.3
C11—C27—H27B	109.5	C15—C16—H16B	111.3
H27A—C27—H27B	109.5	H16A—C16—H16B	109.2
C11—C27—H27C	109.5	O22—C17—C18	110.6 (4)
H27A—C27—H27C	109.5	O22—C17—C20	112.5 (5)
H27B—C27—H27C	109.5	C18—C17—C20	103.2 (5)
C1—C6—C5	104.1 (5)	C7—C12—H12A	109.5
C1—C6—H6A	110.9	C7—C12—H12B	109.5
C5—C6—H6A	110.9	H12A—C12—H12B	109.5
C1—C6—H6B	110.9	C7—C12—H12C	109.5
C5—C6—H6B	110.9	H12A—C12—H12C	109.5
H6A—C6—H6B	109.0	H12B—C12—H12C	109.5
C13—C7—C12	105.8 (5)	C18—C28—H28A	109.5
C13—C7—C4	117.0 (4)	C18—C28—H28B	109.5
C12—C7—C4	115.1 (4)	H28A—C28—H28B	109.5
C13—C7—C1	113.8 (5)	C18—C28—H28C	109.5
C12—C7—C1	112.7 (5)	H28A—C28—H28C	109.5
C4—C7—C1	92.3 (4)	H28B—C28—H28C	109.5
C6—C1—C2	106.7 (6)		

9 Appendix III

M009

PROCESS OPTIMIZATION OF THE SYNTHESIS OF UAMC-00050, A NOVEL uPA INHIBITOR

Davide Ceradini, Kirill Shubin

Aizkraukles Iela 21, Riga, Latvia

The α-aminophosphonate UAMC-00050, a newly developed trypsin-like serine protease inhibitor, has shown promising results for the treatment of dry eye syndrome and ocular inflammation.[1] A laboratory scale synthetic route was initially developed at University of Antwerp. Preparation of larger amounts of UAMC-00050, required in the advanced steps of the project, proved to be difficult, due to the usage of environmentally unfriendly solvents and hazardous reagents. A new process was developed with greener alternatives and less toxic reagents. Every reaction was investigated in order to obtain the maximum yield, all the flash chromatography were replaced with plug filtration and slurry purifications. The overall yield was increased from a 3% of the discovered route to a 33% of the process development route.

References

1) Joossen, C., Baán, A., Moreno-Cinos, C. et al. A novel serine protease inhibitor as potential treatment for dry eye syndrome and ocular inflammation. Sci Rep 10, 17268 (2020).

IT-DED³

Outreach Symposium

2 December 2021

Live Stream

Quinze-Vingts National Ophthalmology Hospital, Paris

EUROPEAN NETWORK ON DRY EYE DISEASE DRUG DEVELOPMENT

Keynote speakers

Prof. Dr. Virginia CALDER, University College London
Prof. Dr. Margarita CALONGE, University of Valladolid

IT-DED³ receives funding from the European Union's Horizon 2020 Research and Innovation Program under grant agreement No 765608

IT-DED³ OUTREACH SYMPOSIUM

MORNING

December 2, 08.30 - 12.00 CET

CHAIRED BY PROF. DR. CHRISTOPHE BAUDOUIN

President of the European Dry Eye Society - EuDES. Professor of Ophthalmology, chairman of department 3 of Ophthalmology in Quinze-Vingts National Ophthalmology Hospital

08.30 - 08.35 *WELCOME NOTE*

Dr. Serge PICAUD, Director of the Vision Insitute

08.35 - 08.50 *INTRODUCTION TO IT-DED³ NETWORK*

Prof. Dr. Koen AUGUSTYNS, Coordinator of IT-DED³
Dean of the Faculty of Pharmaceutical, Biomedical and Veterinary Sciences, Full Professor of Medicinal Chemistry, University of Antwerp

9.00 - 09.30 *KEYNOTE LECTURE*

Prof. Dr. Virginia CALDER, Lecturer in Ocular Immunology
Ophthalmology Institute, University College London
Member of the IT-DED³ External Advisory Board

09.30 - 10.00 *COFFEE BREAK*

10.00 - 12.00 *DRUG DISCOVERY*

Presentations of 20 minutes followed by 10 minutes of Q&A and comments

Chaired by Dr. Amalia ENRIQUEZ-DE-SALAMANCA, Applied Ophthalmology Institute (IOBA), University of Valladolid.

10.00 - Alba RAMOS-LLORCA, University of Antwerp
Design, Synthesis and Biochemical evaluation of novel serine protease inhibitors

10.30 - Camilla SCARPELLINI, University of Antwerp
Design, Synthesis and Biochemical evaluation of novel RIPK1 inhibitors

11.00 - Nikolaos KATSINAS, University of Valladolid
Valorisation of natural compounds and their evaluation as therapeutic agents for ocular surface inflammatory diseases

11.30 - Maha ABDALLAH, Institute of Experimental Biology and Technology - iBET
Extraction of hyaluronic acid and chondroitin sulphate from marine biomass and their evaluation as bioactive polymers in ocular carrier formulation

IT-DED³ OUTREACH SYMPOSIUM

AFTERNOON

December 2, 13.00 - 17.45 CET

13.00 - 13.30 KEYNOTE LECTURE

Prof. Dr. Margarita CALONGE, Full professor in Ophthalmology
Head of Ocular Surface Group at the Institute for Applied Ophthalmobiology (IOBA), University of Valladolid and CIBER-BBN

13.30- 16.00 PRECLINICAL DRUG DEVELOPMENT

Presentations of 20 minutes followed by 10 minutes of Q&A and comments

Chaired by Prof. Dr. Arto URTTI, University of Eastern Finland.

13.30 - Agnese COMPAGNONE, University of Antwerp
Implementation of in-vivo models to identify potential candidates for DED treatment

14.00 - Davide CERADINI, Latvian Insitute of Organic Synthesis
Upscaling of lead compounds from WP1 and enantioselective synthesis of the serine protease inhibitor UAMC-00050

14.30 - Luna KRSTIC, University of Valladolid
Development of new carriers to improve the bioavailability of topic formulations to treat ocular surface inflammatory diseases

15.00- Anusha BALLA, University of Eastern Finland
Drug penetration to ocular surface tissues

15.30 - Bao TRAN GNOC, University Hospital Cologne
Dry eye therapy using cannabinoid ligands in a water-free delivery platform

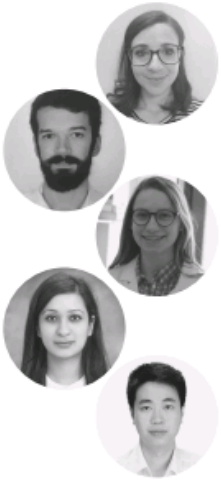

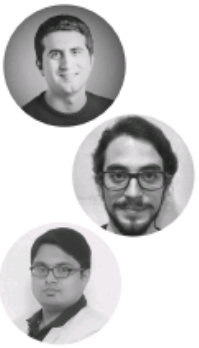

16.00 - 16.15 COFFEE BREAK

16.15 - 17.45 DEVELOPMENT OF CLINICAL DIAGNOSTIC TOOLS

Presentations of 20 minutes followed by 10 minutes of Q&A and comments

Chaired by Dr. Annabelle REAUX-LE-GOAZIGO, the Vision Insitute

16.15 Murat Akkurt, Sorbonne University
Development of new biomarkers for Dry Eye Disease

16.45 Adrián Guerrero-Moreno, Sorbonne University
The nociceptive pathway in dry eye disease and ocular surface pain models

17.15 Md Asif KHAN SETU, University Hospital Cologne
Development of novel diagnostic tools for dry-eye disease using optical coherence tomography (OCT) and confocal microscopy

10 Appendix IV

Chromatogram tier I example

Empower2 software

LC1_ACN

SAMPLE INFORMATION

Sample Name:	#198-Ch-255-DVC-023 LC1 0.1%EA		
Sample Type:	Unknown	Sample Set Name:	13032019 LC1 PO
Vial:	27	Acq. Method Set:	Iz_210_254_F1_100D_25oC
Injection #:	1	Processing Method	LC1_ACN_PO
Injection Volume:	2.00 ul	Channel Name:	W2489 ChA
Run Time:	30.0 Minutes	Proc. Chnl. Descr.:	W2489 ChA 254nm
Date Acquired:	3/13/2019 5:17:11 PM EET	Acquired By:	System
Date Processed:	3/14/2019 8:48:44 AM EET		

Lux Cellulose-1 (1) (4.6x150 mm)
Iz. 0.1% ethanolamine in ACN; F = 1 mL/min; T=25oC

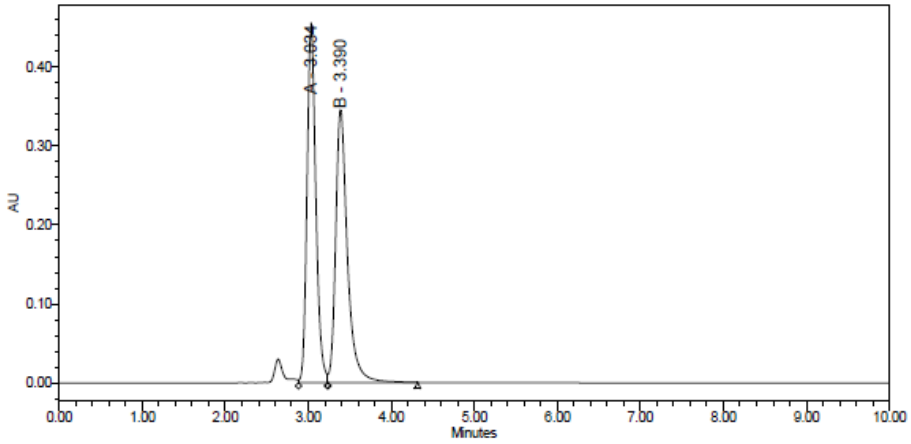

C~1mg/mL (ACN)

	Peak Name	RT	Area	% Area	Height	EP Plate Count	Resolution	Selectivity	Width @ 50%	K Prime
1	A	3.034	3347345	49.57	453704	4109			0.111	0.667
2	B	3.390	3405102	50.43	346649	3218	1.666	1.293	0.141	0.863

Reported by User: System
Report Method: LC1_ACN
Report Method ID6726
Page: 1 of 1

Project Name: Alliance-3_2019
Date Printed:
3/14/2019
9:19:35 AM Europe/Riga

Chromatogram tier II example

Empower 2 software

LC1_ACN

SAMPLE INFORMATION

Sample Name:	#198-Ch-255-DVC-023 LC1 MeCN		
Sample Type:	Unknown	Sample Set Name:	13032019 LC1 PO
Vial:	27	Acq. Method Set:	Iz_210_254_F1_100B_25oC
Injection #:	1	Processing Method	LC1_ACN_PO
Injection Volume:	2.00 ul	Channel Name:	W2489 ChA
Run Time:	30.0 Minutes	Proc. Chnl. Descr.:	W2489 ChA 254nm
Date Acquired:	3/13/2019 3:14:10 PM EET	Acquired By:	System
Date Processed:	3/14/2019 8:49:45 AM EET		

Lux Cellulose-1 (1) (4.6x150 mm)
Iz. 100% ACN; F = 1 mL/min; T=25oC

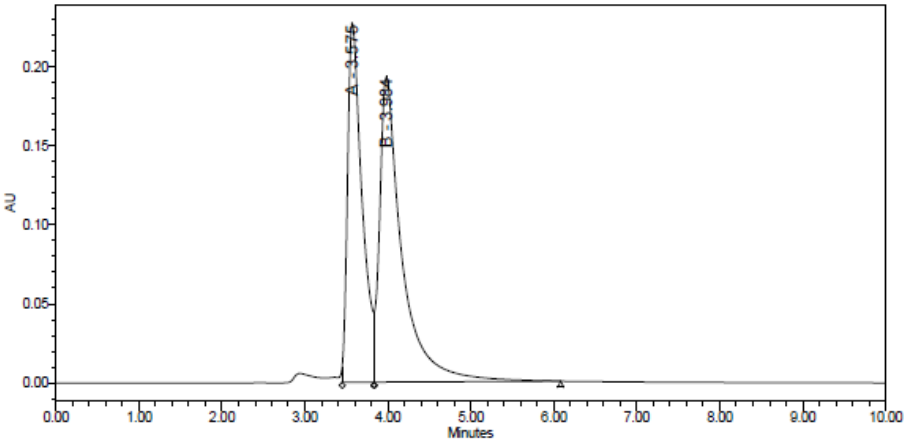

C~1mg/mL (ACN)

	Peak Name	RT	Area	% Area	Height	EP Plate Count	Resolution	Selectivity	Width @ 50%	K Prime
1	A	3.575	2724921	42.91	228860	2143			0.182	0.964
2	B	3.984	3626068	57.09	193282	1527	1.145	1.233	0.240	1.189

Reported by User: System
Report Method: LC1_ACN
Report Method ID6729
Page: 1 of 1

Project Name: Alliance-3_2019
Date Printed:
3/14/2019
9:24:02 AM Europe/Riga

Chromatogram tier III example

Empower 2 software

IB_ACN

SAMPLE INFORMATION

Sample Name:	DVC-045 IB ACN		
Sample Type:	Unknown	Sample Set Name:	18032019 IB PO
Vial:	30	Acq. Method Set:	Iz_210_254_F1_100B_25oC
Injection #:	2	Processing Method	IB_ACN_PO
Injection Volume:	5.00 ul	Channel Name:	W2489 ChA
Run Time:	90.0 Minutes	Proc. Chnl. Descr.:	W2489 ChA 254nm
Date Acquired:	3/18/2019 5:58:55 PM EET	Acquired By:	System
Date Processed:	3/19/2019 9:07:58 AM EET		

Chiralpak IB (4.6x250 mm)
Iz. 100% ACN; F = 1 mL/min; T=25oC

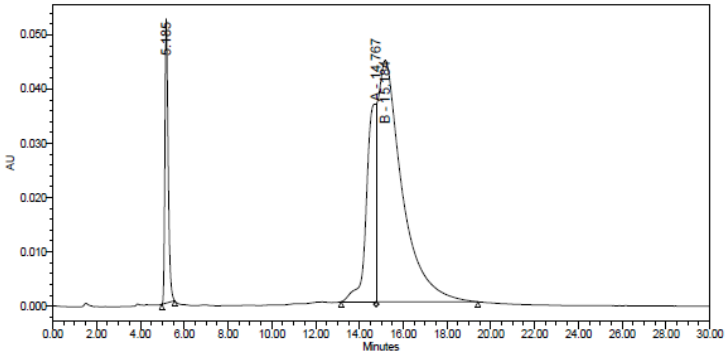

C~1mg/mL (95%ACN+H2O)

	Peak Name	RT	Area	% Area	Height	EP Plate Count	Selectivity	Width @ 50%	K Prime
1		5.185	538211	10.64	52369	6318		0.154	0.591
2	A	14.767	1076590	21.28	36448		5.977		3.530
3	B	15.184	3443852	68.08	44509		1.036		3.658

Reported by User: System
Report Method: IB_ACN
Report Method ID6904
Page: 1 of 1

Project Name: Alliance-3_2019
Date Printed:
3/19/2019
9:08:54 AM Europe/Riga

Chromatogram tier IV example

Empower2 software

IC_ACN_01%PA

SAMPLE INFORMATION

Sample Name:	DVC-023 IC 60%ACN+0.1%PA		
Sample Type:	Unknown	Sample Set Name:	18032019 IC PO
Vial:	27	Acq. Method Set:	Iz_210_254_F1_40A_60B_25oC
Injection #:	1	Processing Method	IC_ACN_01%PA
Injection Volume:	5.00 ul	Channel Name:	W2489 ChA
Run Time:	30.0 Minutes	Proc. Chnl. Descr.:	W2489 ChA 254nm
Date Acquired:	3/19/2019 8:29:52 PM EET	Acquired By:	System
Date Processed:	3/20/2019 8:47:41 AM EET		

Chiralpak IC (4.6x250 mm)
Iz. 60% ACN + 0.1% H3PO4; F = 1 mL/min; T=25oC

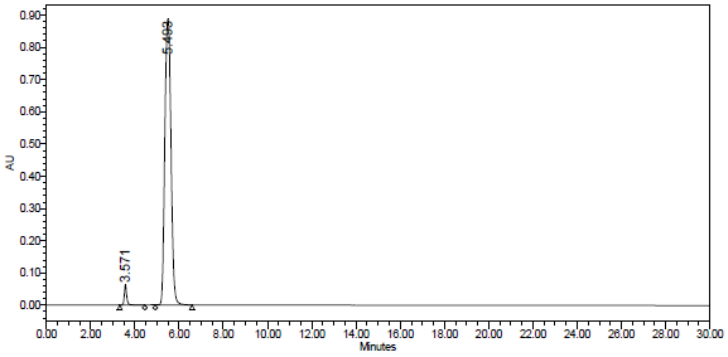

C~1mg/mL (ACN)

	RT	Area	% Area	Height	EP Plate Count	Resolution	Selectivity	Width @ 50%	K Prime
1	3.571	478850	2.72	62716	6230			0.106	0.082
2	5.493	17099583	97.28	888542	1782	5.494	8.086	0.306	0.665

Reported by User: System
Report Method: IC_ACN_01%PA
Report Method ID7048
Page: 1 of 1

Project Name: Alliance-3_2019
Date Printed:
3/20/2019
8:48:57 AM Europe/Riga

Davide Ceradini was born in 1993 in Arzignano, Italy. He obtained his Bachelor's degree in chemistry from the University of Padua in 2015 and a Master's degree in industrial chemistry in 2018. Since 2018, he has been a research assistant at the Latvian Institute of Organic Synthesis. During his stay in Riga, he was working with the IT-DED3 network – a European project for the development of new therapies for Dry Eye Disease. His research interests are mainly green chemistry and quality by design.